Swampland Distance Conjectures and Geometric Flow Equations

Julian Freigang

München 2023

Swampland Distance Conjectures and Geometric Flow Equations

Julian Freigang

Dissertation
an der Fakultät für Physik
der Ludwig–Maximilians–Universität
München

vorgelegt von
Julian Freigang
aus Augsburg

München, den 3.7.2023

Erstgutachter: Prof. Dr. Dieter Lüst
Zweitgutachter: Priv.-Doz. Dr. Ralph Blumenhagen
Tag der mündlichen Prüfung: 26.7.2023

Zusammenfassung

Das Swampland-Programm zielt darauf ab diejenigen effektiven Feldtheorien, die mit Quantengravitation bei hohen Energien vereinbar sind, von denjenigen, welche es nicht sind, zu unterscheiden. Diese Unterscheidung wird mit Hilfe der sogenannten Swampland-Vermutungen gemacht, welche tiefgreifende Einschränkungen auf eine effektive Feldtheorie bewirken können. Diese Vermutungen sind gewöhnlich von allgemeinen Argumenten zu schwarzen Löchern, Holographie oder direkt von der Stringtheorie motiviert. Außerdem sind viele dieser Vermutungen miteinander vernetzt, was auf ein noch unentdecktes grundlegenderes Naturgesetz hindeutet.

Eine der wichtigsten Vermutungen ist die Swampland Distanzvermutung, welche das Kernstück dieser Arbeit bildet. Diese limitiert die Distanz im skalaren Feldraum, welche in einer effektiven Feldtheorie zurückgelegt werden kann, bevor die Theorie aufgrund einer unendlichen Anzahl von Zuständen, die masselos werden, zusammenbricht. Über die letzten Jahre wurde diese Vermutung auf verschiedene Arten verallgemeinert. Es wurde zum Beispiel eine enge Verbindung zu geometrischen Flüssen festgestellt, was etwas Interesse an geometrischen Flüssen innerhalb der Swampland-Gemeinschaft entfacht hat. Desweiteren wird angenommen, dass die Distanzvermutung nur auf Geodäten im Feldraum zutrifft. Allerdings wurde gezeigt, dass sich der Gültigkeitsbereich der Distanzvermutung auch auf Bewegungen, welche keine Geodäten im Feldraum sind, erstreckt.

Diese Arbeit hat zwei Absichten. Zum Einen werden motiviert von der Verbindung zur Distanzvermutung neue geometrische Flüsse konstruiert und untersucht. Dazu gehören eine geometrische Flussgleichung für die Anzahl der Raumzeitdimensionen und eine Erweiterung des Ricci-Flusses, welche die Rückkopplung der Materiefelder mitberücksichtigt. Auf der anderen Seite wird die Distanzvermutung auf das Szenario kosmischer Beschleunigung angewandt, welches immer noch ein offenes und wichtiges Problem in der Physik darstellt. Wie sich herausstellt, ist eine Abweichung von einer Geodäte am Rand des Feldraums begrenzt aufgrund der Übereinstimmung mit der Distanzvermutung.

Abstract

The Swampland Program aims to distinguish between those effective field theories, which can be completed into Quantum Gravity at high energies, and those which can't. The distinction between these two sets is made by the so called Swampland Conjectures which can put severe constraints on an effective field theory. These conjectures are usually motivated by general black hole arguments, holography or directly String Theory. Moreover, many of these seem to be intertwined in a web of conjectures hinting at a more fundamental principle yet to be uncovered.

One of the most important and best studied conjectures is the Swampland Distance Conjecture (SDC) which lies at the heart of this thesis. It limits the scalar field space distance which can be traversed in an effective field theory before the theory has to break down due to an infinite tower of states becoming massless. Over the last years the conjecture was generalized in many different ways. For instance, a close relation to geometric flows has recently been found, which has sparked some interest in geometric flows within the Swampland community. Furthermore, the SDC is supposed to hold for geodesic field space trajectories, but it was shown that the validity of the SDC can be extended to a non-geodesic motion in field space.

The purpose of this thesis now is twofold: On the one hand, motivated by the connection to the SDC new geometric flows are constructed and studied. This includes a geometric flow equation for the number of spacetime dimensions and an extension of Ricci flow which incorporates the backreaction of matter fields. On the other hand, the SDC is applied to the scenario of cosmic acceleration, which is still an open and significant problem in physics. It turns out that the non-geodesicity of trajectories is bounded by consistency with the SDC near the boundary of field space.

Publications

This PhD thesis is based on the work together with Prof. Dr. Dieter Lüst, Dr. Marco Scalisi, Prof. Dr. Toby Wiseman, Davide de Biasio and Nian Guoen. A part of the material was already published [1, 2], whereas the last project [3] was in its final stages at the moment of handing in the PhD thesis. These projects are covered in separate chapters throughout this thesis and there is a declaration at the beginning of each chapter which states on what it is precisely based on.

[1] D. De Biasio, J. Freigang and D. Lüst, *Geometric Flow Equations for the Number of Space-Time Dimensions*, *Fortschritte der Physik Volume* 70 *(2022)*

[2] D. De Biasio, J. Freigang, D. Lüst and T. Wiseman, *Gradient flow of Einstein-Maxwell theory and Reissner-Nordström black holes*, *J. High Energ. Phys. Article* 74 *(2023)*

[3] J. Freigang, G. Nian, D. Lüst and M. Scalisi *Cosmic Acceleration and Turns in the Swampland*, [2306.17217] *(2023)*

Acknowledgements

First and foremost, I would like to thank my supervisor Prof. Dr. Dieter Lüst for giving me the opportunity to write my PhD thesis in his group. His kind guidance and support even through tough periods like CoVid was invaluable. Of course, this also extends to my second supervisor Priv.-Doz. Dr. Ralph Blumenhagen.
I'm also grateful to all my other collaborators, namely Dr. Marco Scalisi, Prof. Dr. Toby Wiseman, Davide de Biasio and Nian Guoen, for some exciting projects and enlightening discussions. I have truly learned a lot these past years.
Furthermore, I would like to thank all the other PhD students of my group and of the IMPRS program for giving me such a great time, especially during the Young Scientist Workshops at Castle Ringberg. All in all, I couldn't have been more happy.
Last but not least, I would like to thank my family for their enduring love and their constant emotional and financial support throughout my entire life, especially my grandmother. Without them this whole PhD wouldn't have been possible for me.

"If string theory is a mistake, it's not a trivial mistake.
It's a deep mistake and therefore kind of worthy."

Lee Smolin

Contents

List of Figures

Chapter 1

Introduction

1.1 History and Motivation

"If string theory is a mistake, it's not a trivial mistake. It's a deep mistake and therefore kind of worthy." In my opinion this quote by Lee Smolin perfectly encapsulates the spirit of the so called *Swampland Program*. But why? To explain that, let's rewind to the beginning of the 20th century.
The last century began with a major revolution in physics. With his discovery of light quanta in 1900 Max Planck paved the way for the development of *Quantum Mechanics* (QM). Even though a lot of physicists were sceptical at first due to its uncommon predictions and implications for our world, it gained more and more traction until it was finally very well established in the 1920s. Some of its key successes were the prediction of the wave-particle duality by Louis de Broglie, the discovery of the Schrödinger equation, which turned out to be one of the central objects in Quantum Mechanics, and the formulation of the uncertainty principle by Werner Heisenberg. However, soon people realized that there were still flaws in the theory. Although it was able to produce some amazing results like the ones just mentioned, it still failed to accurately describe realistic atoms beyond the simplest cases. Moreover, QM was running into problems when applied to massless particles. There was a tension between QM and *Special Relativity* (more on that soon). Paul Dirac started to resolve this tension in the late 1920s with the formulation of his equation which describes electrons including relativistic effects. One very surprising consequence of the Dirac equation was the prediction of antiparticles which was soon after verified by the discovery of the positron. Ultimately, Paul Dirac laid the foundation for the development of *Quantum Field Theory* (QFT). Such theories describe the microscopic world in terms quantum fields, which implies that particles aren't the fundamental objects, but they are merely excitations of the corresponding field. Over the next decades three major QFTs emerged each of them describing one of the fundamental forces

in our universe. The three forces in question are the *electromagnetic force*, the *strong force* and the *weak force*. These are covered by *Quantum Electrodynamics* (QED), *Quantum Chromodynamics* (QCD) and the *Electroweak Theory* (EW Theory) which is a combined formulation of the weak and the electromagnetic force. Some standout contributors to these developments were Richard Feynman, Murray Gell-Mann and Steven Weinberg. However, this list is far from exhaustive and there were many more important contributors. In fact, too many to name them all, hence only a small excerpt was given. It was truly an exciting time period. In the end this evolution culminated in the formulation of the *Standard model* (SM) of particle physics in the mid 1970s which describes our microscopic world with a ridiculous precision to this day and is still one of the greatest achievements of theoretical physics. The SM unifies the previously named three forces in a single theory. In summary, Quantum Mechanics and later Quantum Field Theory revolutionized our understanding of the microscopic world.
But this was only one part of the revolution in physics. In the beginning of the 20th century Albert Einstein published his groundbreaking paper *"On the Electrodynamics of Moving Bodies"* and laid the foundation for the development of his theory of *Special Relativity* (SR). It is based on two principles: there is an universal speed limit, namely the speed of light, and the laws of physics are supposed to be the same in different inertial reference frames. Although these principles seem very simple, the implications are quite profound. In particular, time appears to run slower for objects which are in motion relative to a stationary observer. Over the next decade Albert Einstein pushed his ideas forward and finally constructed his theory of *General Relativity* (GR) which describes gravity as the curvature of spacetime itself. Connecting to the previous example it also states that clocks tick slower in the presence of a strong gravitational field. However, it took several years until it was accepted by the science community after an experimental validation. Then, it quickly dethroned Newton's theory of gravity and became the state of the art gravity theory which holds true to this day. Some predictions of the theory were verified only decades after. So, back then the theory was far ahead of the technological limitations. Some prominent examples here are cosmic inflation, black holes and gravitational waves, which were only detected about a century later. On top of that, our modern life is heavily dependent on GR via the GPS system. The GPS system would become inaccurate within a very short time span if it didn't take GR corrections into account. In total, one can say that GR drastically reshaped our understanding of the world at large scales.
Therefore, there were these two very powerful theories. On the one hand, QM perfectly predicted the microscopic world and, on the other hand, GR reigned over the macroscopic and cosmic scales. Hence, it was very natural that physicists sought out to unify them. After some early attempts the idea of *Quantum Gravity* (QG) gained some traction in the middle of the last century. However, the quantum theory, which had been effortlessly mastering every challenge so far,

suddenly struggled to deal with gravity and produced nonsensical results. All the standard techniques, like canonical quantization or the path integral formalism, couldn't consistently incorporate gravity, which was quite surprising to everybody. Now you might wonder, why did people care or better still care to this day about a theory of Quantum Gravity? As explained so far, these two theories operate at very different length scales. Therefore, they are never needed at the same time, one might object. But that assumption is wrong! Gravity isn't necessarily coupled to large length scales but to large masses and there are certainly very tiny and very heavy objects in the universe, e.g. black holes. Thus, black holes have been the primary object to investigate in the context of QG. Moreover, it is strongly believed that our universe originated from a single point, the big bang, which contained the whole universe and hence was enormously massive. And, lastly, humans always try to push the boundaries of what is possible. So, it is very natural that scientists try to connect two theories, which are known to perfectly work by themselves, even if it would be just for the sake of completeness.
Then, in the 1960s and 1970s a new theory was discovered, mainly by accident: *String Theory*. In an attempt to describe mesonic interactions, Gabriele Veneziano wrote down an amplitude which exhibited some intriguing properties. Subsequently, different physicists including Leonard Susskind realized that the so called Veneziano amplitude could be interpreted as a scattering amplitude of extended objects, namely strings. Soon after that, a new theory of strings was proposed: String Theory. It replaced the fundamental point particle with a tiny vibrating string and the different observed particles correspond to different vibration modes of the strings. This seemingly innocent modification had profound implications for the theory. String Theory turned out to be an inherently UV finite theory since all interactions are smeared out and not point-like, i.e. ultralocal, like in usual QFTs. Moreover, by quantum consistency the theory predicted the number of spacetime dimensions it has to live in, namely Bosonic String Theory demands 26 dimensions and Superstring Theory (the supersymmetric extension of String Theory) 10 dimensions, which is, of course, much more than our observed four spacetime dimensions. This can now be regarded as a feature or a bug of the theory. Either way, String Theory is still the only theory which determines the number of spacetime dimensions [1], whereas other theories need this as an input. Also people soon realized that one can curl up the excess dimensions on tiny geometries, which are too small to be detected. This process is called compactification. But most importantly String Theory's spectrum seemed to contain all so far observed particles and on top of that another particle, which checked all the boxes for a graviton, the mediator particle of gravity. Thus, it became a promising candidate theory for Quantum Gravity. But after some time physicists developed five distinct supersymmetric extensions which seemed incompatible at

[1] There are some possible loopholes to this, like supercritical String Theory.

first. But in the mid 1990s Edward Witten among others showed that these five theories are all related by duality transformations and that they all descend from a 11-dimensional parent theory: *M-Theory*. This was termed the second string revolution. At this point String Theory had gained a lot of traction and many people believed that it is the theory underlying our world. However, in order to show that, one had to compactify the theory down to four dimensions and the 4-dimensional effective theory was dependent on the chosen compactification. Nevertheless, it was widely believed that it was only a matter of time until the right compactification was found. So the years went by and nobody succeeded. Additionally, people realized, how absurdly large the number of possible compactifications is. This lead to a gloomy mood within the String Theory community and more and more theorists began to seriously doubt if String Theory really is the theory of everything. But then a different approach was born in the early 2000s: the *Swampland Program*.
At this point let me emphasise that this brief history of Quantum Gravity and String Theory is not complete. Only a subset was chosen to set the stage for the spirit of the Swampland Program.

1.2 What is the Swampland Program?

The idea of the Swampland Program was introduced in 2005 [4], followed up by [5, 6], as an alternative to the direct search for the correct vacuum which is hidden behind a daunting number of possible string compactifications [7, 8, 9, 10][2]. Instead of just working top-down a systematic exploration of String Theory features was proposed. The goal is to find the properties, that all effective field theories (EFTs), which are derived from String Theory or more generally Quantum gravity, have in common. In fact, from now on the terms String Theory and Quantum Gravity will be used as synonyms because String Theory is, as a matter of fact, a consistent QG theory. It is just not known, if it is the one underlying our world, but it is widely believed that every theory of QG should have the same features [3].
At the core of this search lies theoretical self-consistency [4] [12, 13] which has already proven to be a powerful tool in QFT. An effective theory is only valid up to an energy scale Λ_{QFT} above which it breaks down. At this point usually new degrees of freedom have to be introduced such that the theory can be completed

[2] Actually it took more than 10 years until the idea really became popular among the String Theory community.

[3] There are even some arguments, which suggest that QG is unique and that String Theory is a certain phase of QG [11].

[4] Self-consistency turns out to be much more constraining at higher energy scales, than it is at lower ones, even if gravity is included [12, 13]. Therefore, we have a plethora of consistent effective field theories, but most likely only a unique Quantum Gravity theory.

into the UV. An example would be Fermi theory [14] which is an effective EW Theory. It contains a four-point contact interaction which breaks down at the energy scale of the W-Boson mass. Above this scale the W-Boson needs to be included into the theory, the four-point interaction gets resolved and the theory can be completed into the UV. Now the same concept can be applied to an EFT coupled to gravity. The question, the Swampland Program tries to answer, is, whether such an EFT can be completed into QG and if so, what are the conditions to do so?
Thus, we divide the set of EFTs at a given energy into two categories.

The Swampland and the String Landscape

The set of effective field theories which are consistent with Quantum Gravity is referred to as the *String Landscape*, whereas the set of effective field theories, which cannot be completed into Quantum Gravity in the UV, is defined as the *Swampland* [4, 12, 13].

An illustration of the situation can be found in figure 1.1. One has to emphasise that a theory from the Swampland still is a perfectly fine QFT, it is just not compatible with QG at high energies. Even though the String Landscape is vast, it turns out the Swampland is even bigger. So not everything is possible in String Theory and there are some constraints [13].
The distinction between the Swampland and the Landscape is usually made by the use of so called *Swampland Conjectures* which reflect the just mentioned constraints. In a sense, these determine the border between the Swampland and the Landscape and they are formulated such that they become trivial in the decoupling limit of gravity, that is $M_P \to \infty$. In the best case these conjectures are formulated in the language of the effective theory such that the approach is bottom-up [12]. Hence, one can check, if a given effective theory is compatible with Quantum Gravity, without knowing a specific embedding of the theory into QG. These conjectures represent an UV imprint of QG at much lower energies. This also opens up a new possibility for indirect experimental evidence for String Theory. The energy scale of String Theory lies far beyond the today and in the near future experimentally accessible energy scales, but it is possible to check, if these UV imprints are compatible with current observational data. In fact, there is some progress made in that direction, but we are not yet at a point where we can make strong observational predictions [15, 16, 17, 18, 19, 20].
Probably the three most studied Swampland Conjectures are the *No Global Symmetries Conjecture* [21, 12, 13], the *Weak Gravity Conjecture* [6, 12, 13] and the *Swampland Distance Conjecture* (SDC) [5, 12, 13]. The first one demands the absence of global symmetries in an EFT compatible with QG. People have already argued for this before the Swampland Program using general black hole arguments. Thus, it is well established that this feature should hold in any QG

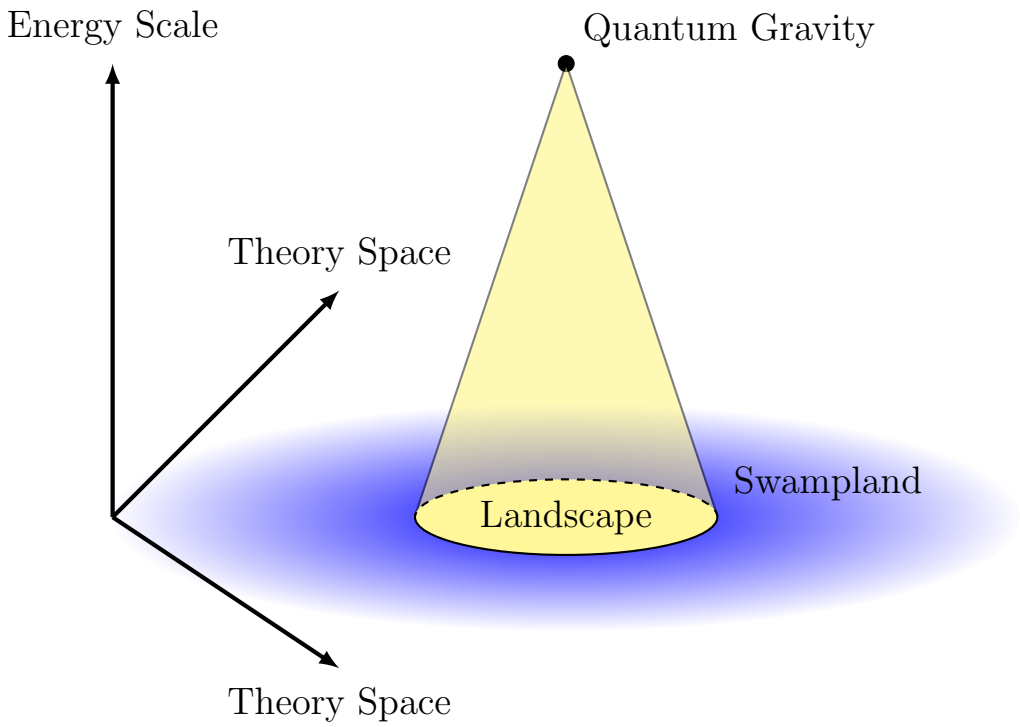

Figure 1.1: An effective theory from the *Landscape* can be completed into Quantum Gravity, whereas a theory from the *Swampland* can't. The set of the Landscape doesn't have to be connected, as it is illustrated here. Also it is believed that we have a unique theory of Quantum Gravity. Hence, it is just a single point in the UV. This figure is inspired by [12].

theory. It was even proven in holographic setups [22, 23]. The Weak Gravity Conjecture essentially requires you to have a particle in your theory for which gravity is the weakest force, e.g. weaker than the electromagnetic force [5]. This translates to a restriction on the spectrum of an effective theory compatible with QG. On the other hand, a Swampland Conjecture can also have implications on the geometry of the internal moduli space. Roughly speaking, the moduli space parametrises the internal geometry on which the QG theory is compactified. From the perspective of the EFT the moduli space represents the possible vacuum expectation values (VEVs) for the scalar fields which are called moduli in this context. Therefore, we have a relation between scalar fields in the effective theory and the internal geometry. This intuition on the moduli space will suffice for the purposes of this thesis and there will also be some explicit examples later. The Swampland Distance Conjecture then states that any infinite distance limit in the moduli space has to be accompanied by an infinite tower of states whose masses drop exponentially with the distance traversed. In the full limit of infinite distance this signals the breakdown of the EFT. Moreover, the SDC even demands that the moduli space of QG has to have these infinite distance points which puts a restriction on the moduli space geometry. Let me mention that there is another class of conjectures, namely conjectures which try to rule out certain gravitational backgrounds. The most prominent example here is the *de Sitter Conjecture* [24] which places a bound on the gradient of potentials in a positive region. Roughly speaking, these are the three big categories of Swampland Conjectures: conjectures that constrain the spectrum, that constrain the internal geometry and that constrain the admissible gravitational backgrounds. Furthermore, all these conjectures have a varying level of rigor and the more rigorous ones tend to be less useful in providing indirect evidence for String Theory [12].

Again, it has to be emphasised that this was just a small subset of the existing conjectures which is enough to highlight the general features. Let me just mention a few more [25, 26, 11, 27, 28, 29]. A good starting point for the interested reader would be [12, 13].

Unlike the No Global Symmetries Conjecture the Weak Gravity Conjecture and the Distance Conjecture are motivated directly by String Theory. However, it was discovered that the Swampland Conjectures are connected via an underlying web and that they are not independent from each other. On the one hand, this hints at a more fundamental principle which is yet to be uncovered. And, on the other hand, this gives another motivation to identify String Theory with Quantum Gravity since the web relates conjectures, which have originated from String Theory, to other conjectures, that were argued for on general QG grounds. Let us highlight one example for this underlying web. There is a nice connection

[5] In fact, this just the electric version of the Weak Gravity Conjecture. The magnetic version provides an upper limit on cut-off scale for the effective theory by the gauge coupling. But we won't comment further on this since it won't be important throughout this thesis.

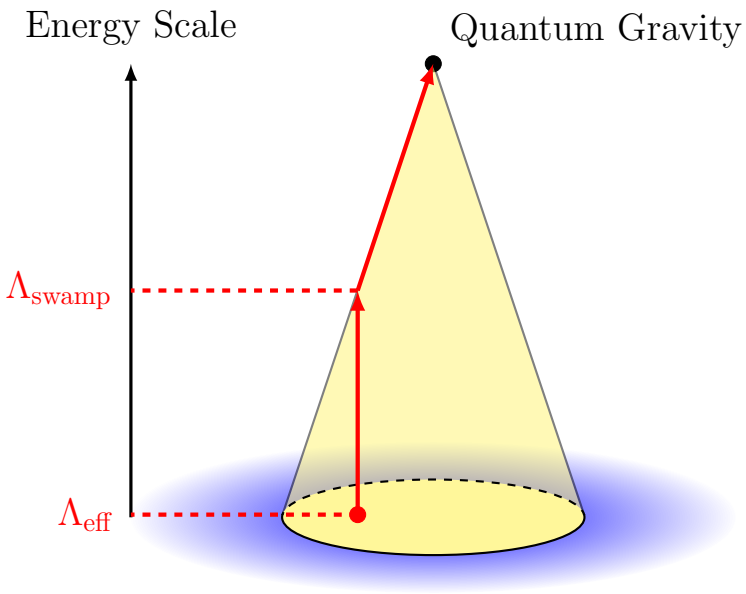

Figure 1.2: If we increase Λ_{eff} in our theory, we reach the boundary of the cone at the scale Λ_{swamp}. At this point we need to modify our theory to be still consistent with Quantum Gravity when further increasing Λ_{eff}. This figure is inspired by [12].

between the No Global Symmetries Conjecture, the Weak Gravity Conjecture and the SDC [30], namely infinite field distances correspond to vanishing gauge couplings. Hence, in these limits global symmetries are restored. So, by the No Global Symmetries Conjecture the breakdown of the EFT is even required.
There is usually the same structure to a Swampland Conjecture [12]. Let's consider some Quantum Field Theory which is evaluated or observed at an energy scale Λ_{eff}. The energy scale Λ_{QFT}, above which the theory becomes inconsistent even without gravity, is assumed to be much higher than the other scales here. If Λ_{QFT} would be low, the theory would become inconsistent before gravity could have an effect on it. Then, this effective QFT gets coupled to gravity which introduces a new energy scale Λ_{swamp}. At this energy scale Λ_{swamp} the theory needs to be modified in order to be consistent with Quantum Gravity in the UV. This modification could be mild, like the introduction of a single particle (see the Weak Gravity Conjecture), or it can be severe, like the introduction of a whole tower of states (see the SDC) [6]. Either way, if Λ_{eff} reaches Λ_{swamp}, this modification has to happen. This situation is illustrated in figure 1.2. However, in a practical theoretical setup the picture is generally slightly different. Instead of increasing Λ_{eff} "by hand" the parameters in the theory are changed. The parameters in question are usually vacuum expectation values of scalar fields parametrising the internal

[6] Also this should be reminiscent of the Fermi theory example.

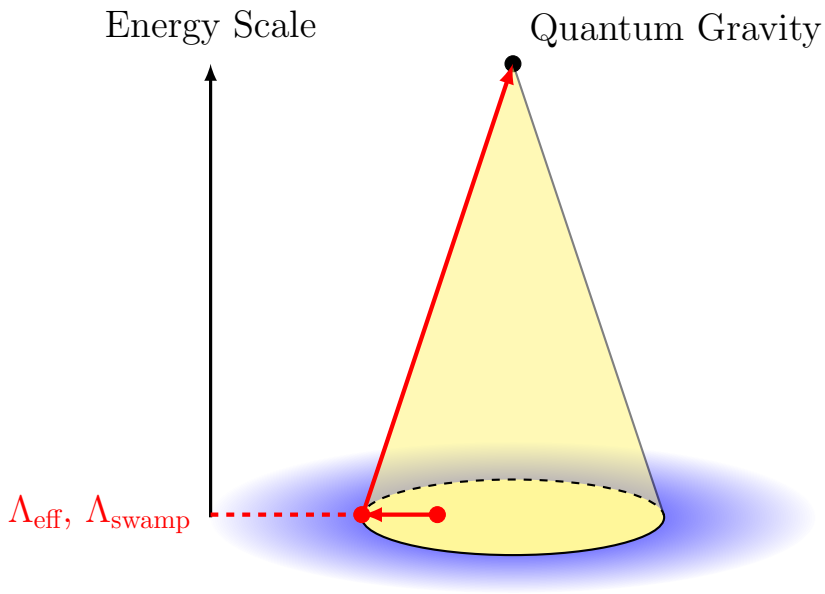

Figure 1.3: By changing the parameters in the theory we move in theory space, until we reach the boundary of the cone. Effectively, this lowers the scale Λ_{swamp} down to Λ_{eff} such that Quantum Gravity effects become relevant already at Λ_{eff}.

geometry. This has the effect that Λ_{swamp} gets lowered until it reaches Λ_{eff} and QG features become relevant directly at Λ_{eff}. This situation is depicted in figure 1.3. Both figures 1.2 and 1.3 are very heuristic and don't depict the situation perfectly accurate. They are merely meant to provide some visual intuition. Also, to be precise, the two illustrations and cases aren't fully decoupled from each other.
To wrap things up, let me come back to the quote by Lee Smolin. The Swampland Program takes a more modest point of view than String Theory, namely it just claims that String Theory is a consistent theory of Quantum Gravity and not that it is directly realized in our world. Hence, even if String Theory is not underlying our world, i.e. it is a "mistake" in the sense of the quote, we can still learn a great deal about QG and nature itself by systematically analyzing it. Thus, in either case String Theory is highly non-trivial and definitely worthwhile exploring.

1.3 Outline of the Thesis

This thesis is organized as follows. In Chapter 2 the theoretical prerequisites from the existing literature are introduced which aim to connect the results in the later chapters of this thesis. In particular, chapter 2 begins with a short introduction into String Theory, which is strongly geared towards the needs of this thesis and is by no means complete. This includes the string spectrum, String Theory compactified on a circle S^1, the string β-functions and the low-energy effective action

of String Theory. In section 2.2 the central connecting piece of this thesis is established, namely the Swampland Distance Conjecture. Moreover, the example of a circle S^1 compactification, which closely follows the presentation in [12], is worked out in much detail such that the main points of the SDC are highlighted. Then, in section 2.3 the SDC is generalized in different ways which closes the gap to the results of this thesis. For instance, the SDC can also be directly applied to the metric instead of massless moduli, which ultimately yields a close relation to geometric flow equations, Ricci flow being the example here. This part is mainly based on [31] and [27]. In order to motivate the results in chapter 3, the reader is further provided with an introduction to the idea of the Swampland Program in the context of large spacetime dimensions D which is largely inspired by [29]. Lastly, the SDC is extended to non-geodesic trajectories. Here the presentation strongly evolves around [32].
In chapter 3 a novel geometric flow equation for the number of spacetime dimensions D is derived on the basis of the two-loop string β-function for the metric. First, this is analyzed in detail for maximally symmetric Einstein spaces, a D-sphere and D-dimensional AdS spacetime. Then, to conclude this chapter, the derived flow is applied to a particular setting, namely the Freund-Rubin compactification, which has already been introduced in chapter 2.
Chapter 4 develops a geometric flow, the Einstein-Maxwell (EM) flow, as a gradient flow, which extends Ricci flow in the sense that it also includes the backreaction of the matter content. In particular, the matter content is given by a Maxwell field. With the application to black hole geometries in mind the well-posedness of the flow is shown in the presence of a non-extremal and an extremal horizon. Finally, the EM flow is performed for the obvious example of Reissner-Nordström black holes, for both its non-extremal and its extremal version. These EM flows are all evaluated numerically, besides the near-horizon flow in the extremal case, which can be solved analytically.
In chapter 5 the allowed non-geodesicity of the SDC is applied to the theory of multi-field cosmic acceleration. As it turns out, infinite-distance trajectories (i.e. trajectories that can extend infinitely such that they are compatible with the SDC) have a bounded turning rate Ω at the boundary of moduli space, namely $\Omega/H < \mathcal{O}(1)\cdot\sqrt{\epsilon}$, where ϵ is the acceleration parameter obeying $\epsilon < 1$. This statement holds even true for trajectories, which are allowed to turn near the boundary of moduli space while staying consistent with the SDC. Moreover, a new tool in the analysis of infinite-distance trajectories was introduced: the swamp cone.
The last chapter, i.e. chapter 6, finally provides a summary of the results in this thesis and an outlook into the future. In the appendix the reader can find some side calculations which have been moved there for the readability of the thesis.
The conventions in this thesis will mostly be chapter-specific which means that different chapters might have different conventions. But everything is thoroughly declared, so there should be no confusion.

Unless otherwise stated, this thesis is formulated in natural units. For instance, the d-dimensional Planck mass $M_{p,d}$ is sometimes reinstated in order to make some Swampland argument. Furthermore, the metric convention is always mostly plus.

Chapter 2

Theoretical Prerequisites

In this chapter the theoretical prerequisites are developed which are important to the rest of this thesis. It starts with a very brief and focused introduction into String Theory. This will be very basic because not a lot is required to follow the later arguments. For a thorough introduction the reader is referred to some well established standard literature [33, 34, 35, 36, 37, 38].
After that the reader is introduced to the Swampland Distance Conjecture which is then applied to the the specific example of a circle S^1 compactification. Moreover, some generalisations of the SDC are presented. For instance, the relation of the SDC to geometric flows is explained and the SDC is extended to non-geodesic trajectories in field space. There is also a short section about the Swampland Program in a large number of spacetime dimensions.

2.1 Brief Introduction into String Theory

The material covered in this section is part of the standard literature and can be found in [35, 36, 38]. There is also a short introduction to String Theory in [12] which we loosely follow here, at least in the choice of topics.

2.1.1 The Spectrum of String Theory

In analogy to a relativistic point-particle, whose action is given by the length of its worldline, one can define the so called *Nambu Goto action* S_{NG} of a relativistic string moving in a flat background in terms of the volume of its worldsheet Σ [39, 40]

$$S_{NG} = -T \int_\Sigma d^2\sigma \sqrt{-\det\left(\frac{\partial X^M}{\partial \sigma^\alpha}\frac{\partial X^N}{\partial \sigma^\beta}\eta_{MN}\right)} \tag{2.1}$$

where $T = \frac{1}{2\pi\alpha'}$ is the string tension. The parameter α' is also called the *Regge Slope* which determines the string mass scale, defined here as $M_s = \frac{1}{2\pi\sqrt{\alpha'}}$. Hence,

the string length is given by $l_S = \frac{1}{\sqrt{\alpha'}}$ in these conventions. The worldsheet Σ is parametrised by coordinates $\sigma^\alpha = (\tau, \sigma)$. The functions $X^M(\sigma^\alpha)$ are maps from the worldsheet into the D-dimensional flat spacetime, so we have $M = 0, \ldots, D-1$. The determinant is taken over the worldsheet coordinates and this action enjoys reparametrisation invariance of the worldsheet and global Poincaré invariance.
The square root in (2.1) makes it notoriously hard to quantize. By introducing an auxiliary metric $h_{\alpha\beta}$ on the worldsheet the Nambu Goto action can be rewritten as

$$S_P = -\frac{T}{2} \int_\Sigma d^2\sigma \sqrt{-h} h^{\alpha\beta} \partial_\alpha X^M \partial_\beta X^N \eta_{MN} \tag{2.2}$$

where $h \equiv \det h_{\alpha\beta}$ and $\frac{\partial}{\partial\sigma^\alpha} \equiv \partial_\alpha$. This action is called the *Polyakov action* [41, 42] [1]. The equation of motion for $h_{\alpha\beta}$ turn into the following constraint on the energy-momentum tensor $T_{\alpha\beta}$ on the worldsheet

$$T_{\alpha\beta} = 0. \tag{2.3}$$

Among the previous symmetries the Polyakov action has an additional rescaling symmetry of $h_{\alpha\beta}$ which is labelled *Weyl symmetry* [2]. Moreover, Weyl invariance makes $T_{\alpha\beta}$ traceless, even without the equation of motion. That statement always holds classically, but can fail at the quantum level. These symmetries can be used to completely fix the auxiliary metric to be the flat metric on the worldsheet, i.e. $h_{\alpha\beta} = \eta_{\alpha\beta}$. This choice is called the *conformal gauge*[3]. At this point the standard route is to introduce light-cone coordinates on the worldsheet as follows

$$\sigma^\pm = \tau \pm \sigma. \tag{2.4}$$

From here on we focus on closed strings which obey a periodicity condition [4]

$$X^M(\tau, \sigma) = X^M(\tau, \sigma + 2\pi). \tag{2.5}$$

However, the open string is treated the same way except for a few minor differences. Here we refer the reader again to the standard literature [33, 35, 36, 38]. In conformal gauge the equation of motion for X^M becomes a wave equation such that X^M can be split into

$$X^M(\tau, \sigma) = X_L^M(\sigma^+) + X_R^M(\sigma^-) \tag{2.6}$$

where these terms correspond to a left- and right-moving wave on the closed string. Both parts can now be separately expanded into Fourier modes α_n^M for the right-moving sector and $\bar{\alpha}_n^M$ for the left-moving sector. The exact expansions aren't

[1] It turns out the Polyakov action was already introduced earlier in [43, 44, 45]

[2] This is where String Theory is special. This symmetry only works for 1d extended objects.

[3] This doesn't fix the gauge completely. There is still some residual gauge symmetry left which leaves $\eta_{\alpha\beta}$ invariant.

[4] We choose the length of the string to be $l = 2\pi$.

important here, so we refrain from giving them.
In principle the theory defined by (2.2) is easy to quantize, but we also need to take care of the constraints (2.3). But before dealing with that the Fourier modes α_n^M get promoted to operators at the quantum level such that they obey the following commutation relations

$$\left[\alpha_m^M, \alpha_n^N\right] = m\delta_{m+n,0}\ \eta^{MN} \tag{2.7}$$

and the same holds true for $\bar{\alpha}_n^M$. The mixed commutators are vanishing, i.e. the two sectors are independent of each other. The commutation relations (2.7) are just the standard commutation relations of the harmonic oscillator. Modes α_n^M with $n > 0$ are the annihilation operators of the vacuum and modes with $n < 0$ are creation operators. Since we demand that X^M is hermitian, the modes are related as $\left(\alpha_n^M\right)^\dagger = \alpha_{-n}^M$. It turns out that α_0^M is proportional to the momentum p^M of the string. Also α_0^M commutes with every other mode. Hence, the vacuum gets another label by the momentum p^M, i.e. $|0, p\rangle$. Now the constraints (2.3) can be employed via the *Virasoro generators* which are given by

$$L_n = -\frac{1}{2\pi}\int_0^{2\pi} d\sigma\ e^{-in\sigma} T_{--} = \frac{1}{2}\sum_{m=-\infty}^{\infty} \alpha_{n-m}^M \alpha_m^N\ \eta_{NM} \tag{2.8}$$

where T_{--} is a component of the energy-momentum tensor in worldsheet light-cone coordinates. There is an analogous expression for the left-moving sector. In the classical theory the constraints (2.3) are equivalent to demanding $L_n = 0 = \bar{L}_n$, but at the quantum level things are more subtle. There is an ordering ambiguity for L_0 and $\bar{L}_0$ in the sum of (2.8) which ultimately results in a normal ordering constant a[5]. Thus, all physical states in the spectrum need to fulfill

$$L_n\,|phys\rangle = 0 \quad \text{for } n > 0 \tag{2.9}$$

$$(L_0 + a)\,|phys\rangle = 0. \tag{2.10}$$

The same applies to the left-moving sector. Furthermore, there is a level-matching constraint which forces the number of right- and left- moving creation operators to be the same

$$(L_0 - \bar{L}_0)\,|phys\rangle = 0. \tag{2.11}$$

This is one of the only ways the two sectors are connected. Moreover, at the quantum level the generators (2.8) fulfill the following famous *Virasoro commutation relations*

$$[L_n, L_m] = (m-n)L_{m+n} + \frac{c}{12}m(m^2-1)\delta_{m+n,0} \tag{2.12}$$

[5]In Minkowski space the normal ordering constant from the right- and left- moving sector coincide, i.e. $a = \bar{a}$

where c is the so called *central charge*. The second term is a quantum effect which corresponds to a quantum breaking of the Weyl invariance, i.e. the trace of the energy-momentum tensor acquires a contribution proportional to c. It turns out that each bosonic field contributes a value of 1 to c such that c is given by the number of fields. Each spacetime coordinate has its own map X^M which corresponds to a bosonic field. Thus, we find $c = D$.
This quantization procedure is called *old covariant quantization*. However, due to the constraints one has to impose on the physical states it is very difficult to find the spectrum of the theory. There are two other quantization schemes. On the one hand, there is the *path integral quantization* and, on the other hand, there is the *light-cone quantization*. The former is the cleaner way of dealing with the situation but there are a lot of technicalities involved. Therefore, we focus on the latter which provides a shortcut to the spectrum. The main idea of light-cone quantization is to fix the residual gauge freedom and to solve the constraints (2.3) explicitly before the quantization. As the name suggests, we introduce light-cone coordinates for the the fields X^M in the following way

$$X^{\pm} = \frac{1}{\sqrt{2}} \left(X^0 \pm X^1 \right). \tag{2.13}$$

First, we use the residual gauge freedom to set all oscillators in the "+"-direction to 0 such that we get

$$X^+ = \alpha' p^+ \tau \tag{2.14}$$

where p^+ is defined analogously. Furthermore, we have set the center of mass position to 0. Then the constraints (2.3) can be used to relate X^- to the transverse coordinates X^i for $i = 2, \ldots, D-1$, namely we find

$$\partial_{\pm} X^- = \frac{1}{\alpha' p^+} \left(\partial_{\pm} X^i \right)^2. \tag{2.15}$$

Hence, only the transverse oscillators α_n^i are independent degrees of freedom because there are no oscillators in the "+"-direction and the oscillators in the "-"-direction are given in terms of the transversal ones by (2.15). All physical states can now be built by acting with different combinations of the transverse oscillators α_n^i and $\bar{\alpha}_n^i$ for $n < 0$ on the vacuum state $|0, p\rangle$ which allows us to directly read off the spectrum. The states of the spectrum follow the mass formula

$$\alpha' M^2 = 2(N^{\perp} + \bar{N}^{\perp} - 2) \tag{2.16}$$

where a normal ordering constant was fixed by criticality, i.e. the absence of quantum anomalies[6], and $N^{\perp}$ ($\bar{N}^{\perp}$) counts the number of oscillators in the right (left)-moving sector. Moreover, the level-matching condition demands $N^{\perp} = \bar{N}^{\perp}$.

[6] This fixes the spacetime dimension to be 26 for the bosonic string.

Another way to infer the normal ordering constant is by considering the little group of massless states which is $SO(d-2)$. It turns out that the state at the first excited level perfectly decomposes into irreducible representations of that group. So, it has to be massless which then fixes the normal ordering constant. At the first excited level [7] there is one state $\alpha^i_{-1}\bar{\alpha}^j_{-1}|0,p\rangle$. This state contains a symmetric traceless part, an antisymmetric part and a trace part. Thus, there is a symmetric, transverse, traceless excitation g_{ij} in the spectrum which can be associated with the *graviton*. This is precisely the reason String Theory is a consistent theory of Quantum Gravity. Moreover, there is also the antisymmetric tensor field B_{ij} which is called the *Kalb-Ramond field*. Lastly, the trace part is a scalar field named the *dilaton*. The dilaton governs the string coupling strength. All states with $N^\perp = \bar{N}^\perp > 1$ are massive string states of the order M_s. These are in general also important ingredients of String Theory. But these states can never be excited in a low-energy effective theory because M_s is much higher than the energy scale of the effective theory Λ_{eff}. Therefore, we don't consider them further.
This introduction was only concerned with Bosonic String Theory which is enough for the purpose of this thesis. The interested reader is again referred to the literature [33, 34, 35, 37] for a treatment of Superstring Theory.

2.1.2 String Theory on a circle S^1

Let's consider a closed bosonic string with mapping functions $X^M(\tau,\sigma)$ in flat spacetime which corresponds to a metric

$$ds^2 = \eta_{MN} dX^M dX^N. \tag{2.17}$$

The simplest possible compactification is on a circle S^1 of radius R, which means we take a spatial coordinate X^d with $d \in \{1,\dots,D-1\}$ and make the identification

$$X^d \sim X^d + 2\pi R\omega \tag{2.18}$$

for $\omega \in \mathbb{Z}$. This identification relaxes the periodicity condition (2.5) of the closed string in the following way

$$X^d(\tau,\sigma) = X^d(\tau,\sigma) + 2\pi R\omega \tag{2.19}$$

again for an integer ω, the so called winding number. So the compact dimension opens up the possibility for the closed string to wind around it which would not be possible for a point-particle. The winding number ω of the string is also conserved which means that the string can't be unwound without breaking it. The wave function translating X^d around the string has to be single-valued [35]

$$e^{ip^d(X^d+2\pi R\omega)} \stackrel{!}{=} e^{ip^d X^d} \tag{2.20}$$

[7] We skip the tachyonic groundstate because it gets projected out in the Superstring Theory.

which forces the momentum along the circle direction to have discrete values

$$p^d = \frac{n}{R} \tag{2.21}$$

where $n \in \mathbb{Z}$. From the mode expansion of $X^d(\tau,\sigma) = X^d_R(\tau-\sigma) + X^d_L(\tau+\sigma)$ one can then infer

$$p^d_R = \frac{1}{2}\left(\frac{n}{R} - \frac{\omega R}{\alpha'}\right) \tag{2.22}$$

$$p^d_L = \frac{1}{2}\left(\frac{n}{R} + \frac{\omega R}{\alpha'}\right) \tag{2.23}$$

such that the mass m in the $D-1$ non-compact dimensions is given by

$$\alpha' m^2 = \alpha' \frac{n^2}{R^2} + \frac{1}{\alpha'}\omega^2 R^2 + 2(N_L + N_R - 2) \tag{2.24}$$

where N_L counts the number of left-moving oscillators and N_R the number of right-moving oscillators. In the above the first term accounts for the momentum along the circle direction and the second term represents the energy contribution due to the string winding ω times around the compact dimension. Moreover, the level-matching condition gets relaxed to

$$N_R - N_L = n\omega. \tag{2.25}$$

The spectrum in the non-compact $D-1$ dimensions also gets new contributions, even for $n = 0 = \omega$, because there are now two distinct sets of oscillator modes, namely the ones along the compact direction $\alpha^d_n, \bar{\alpha}^d_n$ and the ones living in the non-compact spacetime $\alpha^M_n, \bar{\alpha}^M_n$ for $M \neq d$. For more details on the spectrum one should consider e.g. [35, 36, 38].
However, there is an interesting feature of the spectrum (2.24). It is invariant under

$$R \leftrightarrow \frac{\alpha'}{R}, \qquad n \leftrightarrow \omega \tag{2.26}$$

which is an example of a duality transformation called *T-duality*. Thus, no matter, if the compact circle is small or large, the spectrum of the compactified string looks the same. This will become important later when we consider the Swampland Distance Conjecture. But T-duality isn't just a symmetry of the mass spectrum, in fact, it can be shown to be a symmetry of the full (free) theory, i.e. including the mode expansions etc. Furthermore, the radius $R = \sqrt{\alpha'}$ is a fixed point of this transformation. At this fixed point some vector fields, which were introduced by the compactification, become massless and their gauge symmetry gets enhanced. More details on that can be found in [35, 36, 38] Before concluding this section let us emphasise that T-duality is a deeply stringy effect which works only due to the extension of the string.

2.1.3 The String one-loop β-functions

So far the discussion has only been about strings in flat space with metric η_{MN}. Now we will consider a string in a general curved background, namely we will replace $\eta_{MN} \to G_{MN}(X)$. Even more generally, the string can further be consistently coupled to an antisymmetric tensor field B_{MN} and a scalar field Φ. These are the Kalb-Ramond field and the dilaton which were previously introduced. Together with the spacetime metric G_{MN} they form the massless bosonic closed string spectrum. Therefore, the Polyakov action (2.2) gets modified by these non-trivial background fields to be [35]

$$S_P = -\frac{T}{2}\int_\Sigma d^2\sigma\sqrt{-h}\left(h^{\alpha\beta}\partial_\alpha X^M \partial_\beta X^N G_{MN} + \epsilon^{\alpha\beta}\partial_\alpha X^M \partial_\beta X^N B_{MN} + \alpha'\Phi R^{(2)}\right) \tag{2.27}$$

where $\epsilon^{\alpha\beta}$ is the totally antisymmetric tensor and $R^{(2)}$ is the Ricci scalar of the 2d worldsheet [8]. From the worldsheet point of view the functions G_{MN}, B_{MN} and Φ are couplings, which means they acquire a running behavior at the quantum level. As it is also common in Quantum Field Theory, the β-functions are expanded in loop orders. This corresponds here to an expansion in α' or, intuitively, we expand the worldsheet theory around small curvature backgrounds. The one-loop β-functions are given by [12, 35, 36]

$$\beta^G_{MN} = \alpha'\left(R_{MN} + 2\nabla_M\nabla_N\Phi - \frac{1}{4}H_M{}^{LK}H_{NLK}\right) + \mathcal{O}(\alpha'^2) \tag{2.28}$$

$$\beta^B_{MN} = \alpha'\left(-\frac{1}{2}\nabla_K H^K{}_{MN} + H^K{}_{MN}\nabla_K\Phi\right) + \mathcal{O}(\alpha'^2) \tag{2.29}$$

$$\beta^\Phi = \alpha'\left(-\frac{1}{2}\nabla^2\Phi + \nabla_K\Phi\nabla^K\Phi - \frac{1}{24}H_{MNK}H^{MNK}\right) + \mathcal{O}(\alpha'^2) \tag{2.30}$$

where R_{MN} is the spacetime Ricci tensor, ∇_M is the spacetime covariant derivative and H_{MNK} is the field strength of B_{MN}, namely $H_{MNK} = \nabla_{[M}B_{NK]}$. Now for the flat background, i.e. with only η_{MN} like in (2.2), quantum conformal invariance, which is equivalent to Weyl symmetry, forces the spacetime dimension to be critical. The critical dimension of the bosonic string is 26, whereas it is 10 for the superstring. In the non-trivial background above the β-functions of the couplings have to vanish to ensure conformal invariance, so we get

$$\beta^{G,B,\Phi} = 0. \tag{2.31}$$

These conditions are also called the string equations of motion which can also be derived from an action. This action corresponds to the low-energy effective

[8] In fact, the dilaton term breaks classical Weyl invariance. It should be considered with the other one-loop corrections to the couplings. Then, the classical Weyl symmetry is restored by cancellations [35].

action of String Theory because it only involves the massless string fields, e.g. for Type IIA/IIB Superstring Theory the low-energy effective action is IIA/IIB supergravity. For instance, the low-energy effective action, which has (2.31) as its equations of motion, is given by [12, 35, 36]

$$S = 2\pi M_s^{D-2} \int d^D X \sqrt{-G} e^{-2\Phi} \left(R_D - \frac{1}{12} H_{MNK} H^{MNK} + 4\partial_M \Phi \partial^M \Phi \right) \quad (2.32)$$

where $D = 10$ for the superstring and $D = 26$ for the bosonic string. Moreover, R_D is the D-dimensional spacetime Ricci scalar. The action (2.32) is in the so called *string frame* because the Ricci scalar has a prefactor depending on the dilaton, namely $e^{-2\Phi}$. This will be important when comparing String Theory results to field theory results for point-particles because the latter are usually given in the *Einstein frame*. In the Einstein frame the Ricci scalar has no prefactor except for the D-dimensional Planck mass.

2.2 Swampland Distance Conjecture

In this section the Swampland Distance Conjecture in its standard form is introduced and explained. Its features are further highlighted in a specific example, namely the circle S^1 compactification.

2.2.1 Definition and Explanation

The *Swampland Distance Conjecture* (SDC) was originally introduced in [5] and it constrains the field space geometry of the scalar fields without potential, called *moduli*, consistent with Quantum Gravity. The field space described by the moduli is called *moduli space* $\mathcal{M}$. Consider a d-dimensional effective theory of some scalars ϕ^i minimally coupled to gravity

$$S = \int d^d X \sqrt{-g} \left(\frac{R_d}{2} - \frac{1}{2} G_{ij}(\phi^k) \partial_\mu \phi^i \partial^\mu \phi^j + \dots \right) \quad (2.33)$$

where the d-dimensional Planck mass $M_{P,d} \equiv 1$, R_d is the d-dimensional spacetime Ricci scalar and G_{ij} is the field space metric on $\mathcal{M}$. The dots $\dots$ indicate that there might be further ingredients in this effective theory, but these aren't important for the SDC. The scalar fields are canonically normalized, if $G_{ij} = \delta_{ij}$. The SDC now consists of two main parts and can be formulated as follows [5, 12, 13].

Swampland Distance Conjecture

- Starting from any point $P \in \mathcal{M}$ there exists always another point $Q \in \mathcal{M}$ such that the geodesic distance between P and Q denoted by $\Delta(P,Q)$ is infinite, i.e. $\mathcal{M}$ is non-compact.
- At each infinite distance limit, i.e. $\Delta(P,Q) \to \infty$, there exists an infinite tower of states scaling as

$$M(Q) \sim M(P)\, e^{-\lambda \Delta(P,Q)}$$

where λ is a positive constant of $\mathcal{O}(1)$.

The first statement gives the intuitive picture that a moduli space consistent with QG has a bulk and one or several infinite distance points [12]. Moreover, this is precisely what constrains the geometry of $\mathcal{M}$, in the sense that it has to have these infinite distance points.
The second part characterises the limit to these infinite distance points. It is important to note here that the exponential scaling is tied to the distance being infinite which means that there is no exponential scaling for a finite distance. Furthermore, the geodesic distance is given by [12]

$$\Delta(P,Q) = \int_\gamma \sqrt{G_{ij} \frac{\partial \phi^i}{\partial \xi} \frac{\partial \phi^j}{\partial \xi}}\, d\xi \tag{2.34}$$

where γ is the shortest geodesic distance between P and Q which is parametrised by ξ. It gets determined by the geodesic equation on the field space

$$\ddot{\phi}^i + \Gamma^i_{jk} \dot{\phi}^j \dot{\phi}^k = 0 \tag{2.35}$$

where the dot $\dot{}$ denotes differentiation with respect to ξ and Γ^i_{jk} are the Christoffel symbols of G_{ij}. In practice one tends to work with canonically normalised fields such that (2.35) becomes trivial and the shortest distance is just given by the fields themselves because the field space is flat. Moreover, since the SDC is a statement about infinite field distance, the starting point P doesn't matter. Hence, it is often omitted and the distance is just labelled Δ without any arguments.
The exponential in the second part of the SDC further contains this positive constant $\lambda \sim \mathcal{O}(1)$ which governs the rate of the exponential. It isn't further characterised by the SDC which is certainly unsatisfying. However, there has to be a lower bound on λ, because otherwise the exponential scaling of the mass tower gets spoiled. Some concrete bounds have been proposed in the literature [26, 46, 47, 48], but so far there is no full explanation from first principles or directly from the EFT data [13].
The second statement of the SDC also has severe consequences for the EFT. In the

infinite distance limit[9] one has to include an infinite amount of massless particles to be consistent with QG. But this renders the EFT useless and it breaks down which means there is no field theory description in that limit. So, in a sense, the consistency with QG leads to its own demise and the effective description can only be valid for a finite field distance traversed. In particular, if we identify the QG cut-off scale Λ_{swamp} with the first state in the infinite tower[10], we get

$$\Lambda_{\text{swamp}} \sim e^{-\lambda\Delta} \tag{2.36}$$

such that Λ_{swamp} gets exponentially lowered with the distance traversed. As soon as Λ_{swamp} hits the scale Λ_{eff}, the full tower has to be included. This resembles the situation depicted in figure 1.3 pretty well, since the distance is associated with the change of some VEVs in the theory. But that will be made even more clear in the next section.
Lastly, there is also a refined version of the SDC [51, 52] which sharpens it and extends it to also include moduli with a potential. However, since this isn't further needed in the thesis, we omit it here.

2.2.2 Example: Compactification on a Circle S^1

In this part we closely follow the presentation of [12]. This includes the conventions and the calculations, although significantly more details are provided here.
Consider a D-dimensional theory of pure gravity, where $D = d + 1$. The action then reads

$$S = \int d^D X \sqrt{-G}\, \frac{R_D}{2} \tag{2.37}$$

where R_D is the D-dimensional Ricci scalar. We employ again units such that the d-dimensional Planck mass $M_{P,d}$ is set to 1 which will directly translate to $M_{P,D} = 1$, as will be shown soon. Now we compactify the d-th spatial coordinate X^D on a compact circle S^1 of radius R such that we identify

$$X^D \simeq X^D + 1 \tag{2.38}$$

where picked our units such that the periodicity is set to 1. In fact, such circle compactifications were first introduced and studied by Kaluza [53] and Klein [54]. In this setup the metric can be written as

$$ds^2 = G_{MN} dX^M dX^N = e^{2\alpha\phi} g_{\mu\nu} dX^\mu dX^\nu + e^{2\beta\phi} \left(dX^d\right)^2 \tag{2.39}$$

where $M = 0, \ldots, d$ and $\mu = 0, \ldots, d-1$. Furthermore, $g_{\mu\nu}$ and ϕ, which can be seen as a d-dimensional scalar field, only depend on the external coordinates

[9] To be precise, this full limit is actually discontinuous.
[10] This isn't fully correct. Usually Λ_{swamp} is associated with the species scale Λ_{sp} [49, 50], but for us this distinction isn't important here since the two only differ marginally [13].

X^μ and not on X^d. Using the Ansatz (2.39), the D-dimensional Ricci can be decomposed as

$$R_D = e^{-2\alpha\phi}\left(R_d - C_1\partial_\mu\phi\partial^\mu\phi - C_2\partial^\mu\partial_\mu\phi\right) \tag{2.40}$$

where R_d is the d-dimensional Ricci scalar and the constants C_1 and C_2 are given by

$$C_1 = (d-1)(d-2)(\alpha-\beta)^2 + 2\beta d(d-2)(\alpha-\beta) + d(d-1)\beta^2 \tag{2.41}$$
$$C_2 = 2\left((d-1)(\alpha-\beta) + \beta d\right). \tag{2.42}$$

The full derivation of this decomposition can be found in appendix A. Since this is under a spacetime integral, we can directly drop the last term in (A.11) as a total derivative (after going to Einstein-frame). Thus, the action becomes

$$S = \int d^dX\sqrt{-g}\;\; e^{((d-2)\alpha+\beta)\phi}\left(\frac{R_d}{2} - \frac{C_1}{2}\partial_\mu\phi\partial^\mu\phi\right) \tag{2.43}$$

where the integral over X^d is normalised to 1 in our conventions. By demanding that we are in the Einstein frame, we get

$$\beta = -(d-2)\alpha. \tag{2.44}$$

Moreover, ϕ should be canonically normalised, i.e. $C_1 = 1$, which then gives

$$\alpha^2 = \frac{1}{(d-1)(d-2)}. \tag{2.45}$$

Hence, the action finally reads

$$S = \int d^dX\sqrt{-g}\;\left(\frac{R_d}{2} - \frac{1}{2}\partial_\mu\phi\partial^\mu\phi\right) \tag{2.46}$$

which is an example of (2.33) with a 1-dimensional moduli space. The prefactor of the action wasn't changed at all during this calculation such that $M_{P,d} \equiv 1$ directly implies $M_{P,D} \equiv 1$, as promised. The field ϕ is related to the radius R of the circle in the following way

$$2\pi R = \mathcal{V}_{S^1} = \int_0^1 dX^d\sqrt{G_{dd}} = e^{\beta\phi} = e^{-\sqrt{\frac{d-2}{d-1}}\phi} \tag{2.47}$$

where $\mathcal{V}_{S^1}$ denotes the volume of the circle. So, interestingly, the radius R becomes dynamical in the lower dimensional theory and varying the scalar field ϕ corresponds to changing the radius of the internal circle. In particular, the limit $\phi \to \infty$ means the radius shrinks to 0, i.e. $R \to 0$, and the limit $\phi \to -\infty$ corresponds to the decompactification limit $R \to \infty$ in which the compact dimension

opens up. By these considerations the moduli space $\mathcal{M}$ of ϕ is given by the real line

$$\mathcal{M} = \mathbb{R}. \tag{2.48}$$

Obviously, this has, as demanded by the SDC, two infinite distance points, namely $\pm\infty$. Any point in between, which would correspond to the "bulk" here, is infinitely far away from these points.
Next, the geodesic equation is trivial for a 1d field space which is also canonically normalised, so one can directly consider the distance (2.34). This gives

$$\Delta(P, Q) = \phi_Q - \phi_P \tag{2.49}$$

where ϕ_Q is the value of ϕ at the point Q and respectively for ϕ_P. Again, we are interested in infinite distance limits, so we can safely drop the finite contribution ϕ_P. Then, people usually write (dropping the Q-label)

$$\Delta \sim \phi. \tag{2.50}$$

Therefore, the geodesic field distance is given by the field itself, which is a general feature of canonically normalised fields. Please note that the distance is logarithmic in the radius R because the kinetic term in R isn't canonically normalised.
In order to identify the tower of states, we need to introduce another massless D-dimensional scalar Ψ to (2.37), namely

$$S = \int d^D X \sqrt{-G} \, \left(\frac{R_D}{2} - \frac{1}{2} \partial_M \Psi \partial^M \Psi \right). \tag{2.51}$$

The scalar field Ψ now also depends on X^d. However, since X^d is periodic, the scalar field also has to be periodic in X^d. Thus, it can be decomposed into modes ψ_n as

$$\Psi\left(X^M\right) = \sum_{n=-\infty}^{\infty} \psi_n(X^\mu) e^{2\pi i n X^d} \tag{2.52}$$

such that the periodicity along X^d is enforced and the momentum along the circle direction is quantized like for the string in section 2.1.2. The modes ψ_n only depend on the external coordinates X^μ. Because Ψ is real, the modes satisfy $\psi_n^\dagger = \psi_{-n}$. Then, using

$$\int_0^1 dX^d e^{2\pi i (n+m) X^d} = \delta_{n+m,0} \tag{2.53}$$

the kinetic term of Ψ decomposes as

$$-\frac{1}{2} \int d^D X \sqrt{-G} \, \partial_M \Psi \partial^M \Psi =$$

$$\int d^dX\sqrt{-g}\left(-\frac{1}{2}\partial_\mu\psi_0\partial^\mu\psi_0-\sum_{n=1}^{\infty}\left(\partial_\mu\psi_n\partial^\mu\psi_n^\dagger+(2\pi n)^2e^{2\sqrt{\frac{d-1}{d-2}}\phi}\psi_n\psi_n^\dagger\right)\right). \tag{2.54}$$

Hence, there is a massless real zero-mode ψ_0 and infinitely many complex scalars ψ_n with masses

$$M_n = 2\pi n \;\; e^{\sqrt{\frac{d-1}{d-2}}\phi} \tag{2.55}$$

in d dimensions. This mass tower is commonly named KK-tower M_{KK} after Kaluza and Klein, the inventors of the circle compactification. Thus, there is a mass tower scaling like [11]

$$M_{KK} \sim e^{\lambda\Delta} \tag{2.56}$$

where

$$\lambda = \sqrt{\frac{d-1}{d-2}} \tag{2.57}$$

which is an $\mathcal{O}(1)$ constant. The masses in this KK-tower drop to 0 in the limit $\phi \to -\infty$ which corresponds to the decompactification limit of the circle. In fact, such KK-towers, which become massless in the large volume limit of the internal geometry, are ubiquitous even in more complicated higher-dimensional compactifications.

However, what about the other limit $\phi \to \infty$, i.e. $R \to 0$? This is also an infinite distance limit and it should be accompanied with an infinite tower of states becoming massless according to the SDC. It obviously can't be the KK-tower, so there has to be another tower of states. The mass spectrum, that we supplemented by the addition of Ψ, corresponds to a point-particle. Instead we will use now the mass spectrum of a string on circle (2.24) which is a Quantum Gravity mass spectrum. To better relate the two cases, we assume that the d-dimensional metric is flat, i.e. $g_{\mu\nu} = \eta_{\mu\nu}$, and that there is no contribution from the oscillators. Hence, the spectrum reads

$$m^2 = \frac{n^2}{R^2} + \frac{1}{\alpha'^2}\omega^2R^2. \tag{2.58}$$

A few steps have to be performed to compare this to the results from the field theory calculation, namely we need to go from the string frame in (2.32) to the Einstein frame. First, the metric (2.39) contains additional factors $e^{2\alpha\phi}$ and $e^{2\beta\phi}$ compared to the metric (2.17). The d-dimensional mass spectrum contains a factor of the inverse d-dimensional metric which results in [12]

$$m^2 = -\eta^{\mu\nu}p_\mu p_\nu \quad \to \quad m^2 = -e^{-2\alpha\phi}\eta^{\mu\nu}p_\mu p_\nu. \tag{2.59}$$

[11] Usually the geodesic distance in the SDC is defined with an absolute value such that the structure in the exponential stays the same for limits to $\pm\infty$. That is why the minus sign is missing in this example.

To compensate this change, the mass spectrum (2.58) gets multiplied by $e^{2\alpha\phi}$ and it is then given in the Einstein frame. But this isn't the full story. We need to make another change, namely there is a dilaton factor $e^{-2\Phi}$ multiplying the action (2.32). Let's consider the effective d-dimensional dilaton Φ_d defined by [12]

$$e^{-2\Phi_d} = e^{-2\Phi} e^{\beta\phi} M_s. \tag{2.60}$$

We perform variations of the internal radius R that leave Φ_d invariant which implies the following scaling for the D-dimensional dilaton

$$e^{-2\Phi} \sim \frac{e^{-\beta\phi}}{M_s}. \tag{2.61}$$

From the string effective action we can read off the d-dimensional Planck mass

$$\frac{1}{2} M_{p,d}^{d-2} = 2\pi M_s^{D-2} e^{-2\Phi}. \tag{2.62}$$

But in our units we have set $M_{p,d} \equiv 1$ such that by (2.61) the string scale M_s has to scale like

$$M_s \sim e^{\frac{\beta}{d-2}\phi}. \tag{2.63}$$

Thus, we find that in this scenario α' isn't constant, namely it behaves like

$$\alpha' = \alpha'_0 \; e^{-\frac{2\beta}{d-2}\phi} \tag{2.64}$$

where we specified the dimensionful proportionality constant here to be α'_0. This change affects the winding modes in the mass spectrum (2.58) such that we get

$$m^2 = M_{KK}^2 + M_{wind}^2 = (2\pi n)^2 \; e^{2\sqrt{\frac{d-1}{d-2}}\phi} + \frac{\omega^2}{(2\pi)^2 \alpha'_0} \; e^{-2\sqrt{\frac{d-1}{d-2}}\phi} \tag{2.65}$$

where we reinstated the values for α and β. It is remarkable that we exactly recover the KK-tower M_{KK} from the slightly naive field theory calculation before. But there is another tower which is associated with the winding modes of the string. This winding tower M_{wind} is the contribution coming from Quantum Gravity, since these winding states are a purely stringy effect, and it is precisely this tower which becomes massless in the limit $\phi \to \infty$, i.e. $R \to 0$. In the field theory this limit wasn't accompanied by a tower becoming massless. Thus, we see that the SDC is only fully fulfilled in a QG setup. In total, we have two inversely scaling towers

$$M_{KK} \sim e^{\lambda\Delta} \tag{2.66}$$

$$M_{wind} \sim e^{-\lambda\Delta} \tag{2.67}$$

where $\lambda = \sqrt{\frac{d-1}{d-2}} \sim \mathcal{O}(1)$. Thus, in each infinite distance limit a tower becomes massless and invalidates the EFT[12], as it is demanded by the SDC. It is even conjectured by the *Emergent String Conjecture* that these are the two leading types of towers becoming massless in an infinite distance limit [55]. In a more general setup there can also be other extended objects, which can wind internal cycles, such as *D-branes*, which serve as endpoints for open strings [56, 57].
Moreover, the KK-tower and the winding tower are exchanged by T-duality which was introduced in section 2.1.2. Remember that T-duality relates the limits of small and large circles which is precisely what happens to the two towers. The SDC is sometimes also referred to as a *duality conjecture* in the sense that it is predicting the existence of a duality at every infinite distance limit such that the infinite tower provides the new fundamental (weakly coupled) degrees of freedom of the dual description [13].
Finally, one has to say that the SDC and all of its implications were extensively tested in String Theory scenarios and they are pretty well established in the community [30, 58, 59, 60, 55, 61, 62, 63]. Hence, in practice the verification isn't usually done and people just know that there are these KK-towers and winding towers, as soon as infinite field distance limits are encountered.

2.3 Generalizations of the SDC

In this section the SDC is generalized in several different ways such that we nicely connect to the results of this thesis. This includes the *Generalized Distance Conjecture* [25], which is related to geometric flows [27], the *Large Dimension Conjecture* [29] and the extension to non-geodesic trajectories [32]. However, there are also other extensions like the *Black Hole Entropy Distance Conjecture* [28], just to highlight another example.

2.3.1 Generalized Distances and Geometric Flows

The Swampland Distance Conjecture was originally formulated for scalar fields [5]. It is hence very natural to ask the question, if the SDC also holds for different fields. Furthermore, the scalar fields in the EFT usually have their origin in different places, like the spacetime metric. So it was proposed in [25] that there exists a general version of the SDC, the so called *Generalized Distance Conjecture* (GDC), which should apply to all fields. The field space metric G [13] for an arbitrary field $\mathcal{O}_{M_1 \dots M_n}$ with n spacetime indices gets naturally determined by the

[12] Remarkably, this only happens in the lower dimensional theory, whereas the full higher dimensional theory is completely fine in these limits [12].

[13] In abuse of notation we will use G for the general field space metric and not just for the scalar field space as before.

kinetic term

$$\mathcal{L}_{kin} = -G^{M_1\ldots M_n N_1\ldots N_n}\mathcal{D}\mathcal{O}_{M_1\ldots M_n}\mathcal{D}\mathcal{O}_{N_1\ldots N_n} \tag{2.68}$$

where $\mathcal{D}$ is some differential operator. This motivates to formulate the following distance

$$\Delta_{\mathcal{O}} = \int_\gamma \left(\left\langle G^{M_1\ldots M_n N_1\ldots N_n} \frac{\partial \mathcal{O}_{M_1\ldots M_n}}{\partial \xi} \frac{\partial \mathcal{O}_{N_1\ldots N_n}}{\partial \xi} \right\rangle \right)^{\frac{1}{2}} d\xi \tag{2.69}$$

where γ is a geodesic path through field space parametrized by ξ. The angled brackets denote an averaging over the spacetime manifold $\mathcal{M}$

$$\left\langle G^{M_1\ldots M_n N_1\ldots N_n} \frac{\partial \mathcal{O}_{M_1\ldots M_n}}{\partial \xi} \frac{\partial \mathcal{O}_{N_1\ldots N_n}}{\partial \xi} \right\rangle = \frac{1}{\mathcal{V}_{\mathcal{M}}} \int_{\mathcal{M}} G^{M_1\ldots M_n N_1\ldots N_n} \frac{\partial \mathcal{O}_{M_1\ldots M_n}}{\partial \xi} \frac{\partial \mathcal{O}_{N_1\ldots N_n}}{\partial \xi} \tag{2.70}$$

where $\mathcal{V}_{\mathcal{M}}$ is the (infinite) spacetime volume of $\mathcal{M}$. This is necessary because in general the field VEVs depend on the spacetime coordinates. In the case of constant VEVs the spacetime volume cancels out. Moreover, the generalized distance (2.69) nicely reduces to (2.34) for scalar fields.
Then the Generalized Distance Conjecture says that any infinite distance limit of $\Delta_{\mathcal{O}}$ is accompanied by a light tower of masses scaling like [25]

$$m \sim e^{-\lambda \Delta_{\mathcal{O}}} \tag{2.71}$$

where λ [14] is a constant of $\mathcal{O}(1)$. In [25] the Generalized Distance Conjecture was originally formulated for setups in which the external non-compact is an Einstein space. However, it isn't completely far fetched that it should hold for more general setups. Moreover, in [25] the conjecture was also extended to situations where more than one field $\mathcal{O}_{M_1\ldots M_n}$ is evolving in its field space.
Probably the most obvious choice for the Generalized Distance Conjecture would be the spacetime metric itself, as it is a crucial ingredient of a theory of Quantum Gravity. Applying the just described procedure to transverse traceless metric variations g_{MN}, we get [25]

$$\Delta_g = c \int_{\xi_i}^{\xi_f} \left(\frac{1}{\mathcal{V}_{\mathcal{M}}} \int_{\mathcal{M}} \sqrt{g} g^{MN} g^{OP} \frac{\partial g_{MO}}{\partial \xi} \frac{\partial g_{NP}}{\partial \xi} \right)^{\frac{1}{2}} d\xi \tag{2.72}$$

where $c \sim \mathcal{O}(1)$ is dimensionful constant parameter. The path γ is parametrized by ξ which ranges from ξ_i to ξ_f. Intuitively, the metric $g_{MN}(\xi)$ describes a family of metrics in a *generalized moduli space* [15]. However, this notion of distance in a metric field space isn't new, namely it has already appeared in [64, 65]. Although this was derived for transverse traceless metric variations, the distance (2.72) also

[14] Of course, the exponential rate λ is different depending on the field. This is just abuse of notation.

[15] It is generalized in the sense that it goes beyond scalar fields.

holds for general metric variations [27]. Thus, for an infinite distance Δ_g we expect a mass tower becoming light like

$$m \sim e^{-\lambda \Delta_g} \tag{2.73}$$

where $\lambda \sim \mathcal{O}(1)$.
A straightforward application of (2.72) are Weyl rescalings of the form

$$\tilde{g}_{\mu\nu} = e^{2\xi} g_{\mu\nu} \tag{2.74}$$

which results in a collapse of the distance formula to [25, 27]

$$\Delta_g \simeq \xi_f - \xi_i \simeq \xi. \tag{2.75}$$

Here we are considering a lower d-dimensional effective metric $g_{\mu\nu}$, hence the different indices. This can further be applied to a family of AdS metrics parametrized by a cosmological constant $\Lambda(\xi)$ ranging from $\Lambda_i = \Lambda(\xi_i)$ to $\Lambda_f = \Lambda(\xi_f)$. The cosmological constant behaves under Weyl rescalings as [25, 27]

$$\Lambda(\xi) = -\frac{1}{2}(d-1)(d-2)e^{-2\xi} \tag{2.76}$$

such that the distance becomes

$$\Delta_g \simeq \xi_f - \xi_i \simeq \ln\left(\frac{\Lambda_i}{\Lambda_f}\right) \simeq \ln \Lambda. \tag{2.77}$$

In combination with the Generalised Distance Conjecture this leads to the *AdS Distance Conjecture* (ADC) [25]. In an AdS space described by a cosmological constant Λ the ADC predicts in the limit $\Lambda \to 0$ a mass tower scaling like

$$m \sim |\Lambda|^{\alpha} \tag{2.78}$$

where α is positive and $\mathcal{O}(1)$. In general, one expects $\alpha \geq \frac{1}{2}$ where the threshold $\alpha = \frac{1}{2}$ is called the strong ADC [25, 27]. Moreover, the dual limit $\Lambda \to \infty$ is far less clear here since it corresponds to super-Planckian curvatures. But there is some evidence from String Theory constructions that hints at a mass tower becoming light even in that limit [27].
In [27] it was then observed that there is a close relation between geometric flow equations in General Relativity and the Generalised Distance Conjecture. For instance, they considered *Ricci Flow* which was introduced in [66] [16]. It is one of the prototypical examples of geometric flow equations and it was famously used by Perelman in his proof of the Poincaré Conjecture [70, 71]. Other examples of

[16] We will not provide a full introduction to Ricci flow here. For reviews on Ricci Flow consider [67, 68, 69]. There will also be more details and some more context in chapter 4.

geometric flows are the *Ricci-Bourguignon Flow* [72, 73] or the *Calabi Flow* [74]. For a family of metrics $g_{\mu\nu}(\tau)$ on a d-dimensional manifold Ricci flow is given as [66]

$$\frac{\partial}{\partial\tau}g_{\mu\nu}(\tau) = -2R_{\mu\nu}(\tau) \tag{2.79}$$

where $R_{\mu\nu}$ is the Ricci tensor associated with $g_{\mu\nu}$. Here τ is the flow parameter of mass dimension -2 along which we want to evaluate the distance. Ricci flow is a partial differential equation (PDE) since $R_{\mu\nu}$ involves second order derivatives of $g_{\mu\nu}$. Intuitively, Ricci flow can be seen as a set of heat equations which means that the geometry gets smoother along the flow. Moreover, (2.79) can be derived as a gradient flow from the Einstein Hilbert action, but more on that in chapter 4.
Of particular interest are the fixed points $g_{\mu\nu}(\tau_*)$ of (2.79) [27]

$$\frac{\partial}{\partial\tau}g_{\mu\nu}(\tau)\Big|_{\tau=\tau_*} = 0 \tag{2.80}$$

which are given by flat space with vanishing Ricci tensor

$$R_{\mu\nu}(\tau) = 0. \tag{2.81}$$

It was already shown above that a vanishing cosmological constant, i.e. flat space, lies at infinite distance (2.72) for Weyl rescalings. This motivates us to investigate Ricci flow for Einstein spaces, which have the following property

$$R_{\mu\nu} = \Lambda g_{\mu\nu}, \tag{2.82}$$

where Λ is the cosmological constant of the space, i.e. it is negative for AdS spaces and positive for dS spaces. As a consequence of (2.79) the Ricci scalar $R(\tau)$ behaves as follows [27]

$$\frac{\partial}{\partial\tau}R = \nabla^2 R + 2R_{\mu\nu}R^{\mu\nu}. \tag{2.83}$$

If we consider Einstein spaces with (2.82), this provides a shortcut to the behavior of $\Lambda(\tau)$, namely we get

$$\frac{\mathrm{d}\Lambda}{\mathrm{d}\tau} = 2\Lambda^2. \tag{2.84}$$

Here we only have an ordinary differential equation (ODE) because Λ is independent of the spacetime coordinates. In fact, each equation in (2.79) gives (2.84) leading to a consistent collapse of the set of PDEs to a single ODE. Moreover, it is obvious that the fixed point is characterized by $\Lambda = 0$. The solution of (2.84) is [27]

$$\Lambda(\tau) = \frac{\Lambda_0}{1 - 2\Lambda_0(\tau - \tau_0)} \tag{2.85}$$

where we defined $\Lambda_0 = \Lambda(\tau_0)$. The main focus here are AdS spaces with $\Lambda_i < 0$. These will flow to $\Lambda = 0$ from below as $\tau \to \infty$ which is a fixed point at infinite flow time. We have already learned that according to (2.76) the cosmological constant scales under canonical Weyl rescalings like

$$\Lambda(\xi) = \Lambda_i e^{-2\xi} \tag{2.86}$$

where $\Lambda_i = \Lambda(\xi_i)$ as before. Now comparing (2.85) with (2.86) we observe the following relation between τ and ξ [27]

$$\xi = \frac{1}{2} \ln \left(1 - 2\Lambda_0(\tau - \tau_0)\right). \tag{2.87}$$

Since we are interested in $\xi > 0$ with $\xi \to \infty$, we need to have $\tau - \tau_0 > 0$ with $\tau \to \infty$ in accordance with the above. Thus, the path defined by the Ricci flow is just a reparametrisation of the path defined by the Weyl rescalings. This gets further supported by the distance along the path. Plugging the solution to the Ricci flow (2.85) into the distance formula (2.72) we get [27]

$$\Delta_g = c\sqrt{d} \ln \left(1 - 2\Lambda_0(\tau - \tau_0)\right) = 2c\sqrt{d}\, \xi \simeq \xi \tag{2.88}$$

So even the distance along a path given by Ricci flow diverges in the same way as the distance by the GDC. This leads to the following *Ricci flow conjecture* [27].

Ricci Flow Conjecture

Consider Quantum Gravity on a family of d-dimensional metrics $g_{\mu\nu}(\tau)$ satisfying the Ricci flow

$$\frac{\partial}{\partial \tau} g_{\mu\nu}(\tau) = -2R_{\mu\nu}(\tau).$$

Then, there exists an infinite tower of states, which becomes massless, when following the flow to a fixed point $g_{\mu\nu}(\tau_*)$ at infinite distance.

The origin of the mass tower needs a little explanation and motivation. In general, the d-dimensional spacetime $\mathcal{M}_{d,\tau}$ is only part of the full spacetime D-dimensional spacetime $\mathcal{M}_D$ due to compactification. So the generic situation looks like

$$\mathcal{M}_D = \mathcal{M}_{d,\tau} \times K_{D-d,\tau} \tag{2.89}$$

where $K_{D-d,\tau}$ is the compact space and the index τ denotes evolution under Ricci flow. Of course, the full D-dimensional theory has to be Ricci flat to fulfill the string β-functions (2.31). So usually we apply Ricci flow to an effective spacetime $\mathcal{M}_{d,\tau}$ which implies that the internal space $K_{D-d,\tau}$ has to compensate this behavior such that the full theory stays Ricci flat. For a concrete example consider

external AdS spacetime and an internal sphere. If the external spacetime flows to flat space, the sphere has to also flow to flat space, i.e. the sphere has to blow up, giving rise to a KK-tower [27].
There is further a close relation between Ricci flow and the renormalization group flow of the string β^G-function (2.28), namely Ricci flow is basically given by the right-hand side of (2.28) for vanishing dilaton and Kalb-Ramond field. This was studied in [75, 76]. Moreover, this relation was also investigated in the context of the Swampland Program [77].
In [27] the Ricci Flow Conjecture was further extended to a conjecture about the Ricci scalar and to distances in terms of entropy functionals which can also involve scalar fields on top of the metric. However, neither of these are needed in the following, so the interested reader is invited to check out the original work.
Now one might wonder, if this is just tied to Einstein manifolds, but there are several other examples in [27] to further strengthen their key observation, namely that the generalized distance for metrics is directly related to the distance along Ricci flow. So geometric flows in general can be seen as an alternative or even a complementary formulation of the Generalized Distance Conjecture in this context. Instead of changing the on-shell fields "by hand" to infinite distance limits, as it is usually done for the different distance conjectures, geometric flows introduce a new flow parameter τ which determines then the evolution of the fields via the corresponding flow equation. In general, such geometric flows put your fields off-shell which can lead to other difficulties. However, there were also some attempts to formulate an on-shell version of geometric flows [78].
All of this strongly motivates to investigate geometric flows beyond the example described here. It is then very natural to extend this to other examples like black holes, preferably extremal black holes which admit a supersymmetric description. This feeds directly into one of the main results of this thesis. In chapter 4 the framework for geometric flows of extremal black holes is developed and applied to a Reissner-Nordström black hole [2].

2.3.2 Swampland Distance Conjecture at large D

The limit of a large spacetime dimension D isn't a novelty in gravitational theories. For instance, it was already studied in the context of General Relativity in [79], see [80] for a more recent review. Moreover, this idea was then applied to the Swampland Program in [29] which was followed up by [81]. For instance a new duality, called *D-Duality*, was proposed in [81] which relates Quantum Gravity compactifications of different dimensions.
Before moving on to the main results of [29] let's briefly talk about large dimensions D in String Theory. As already mentioned, String Theory has a critical dimension, namely $D = 10$ for the superstring and $D = 26$ for the bosonic string. However, there are attempts to generalize String Theory to an arbitrary dimen-

sion, like the *linear dilaton background* which cancels the Weyl anomaly by an additional contribution to the energy-momentum tensor [82, 83, 84, 85]. But their full quantum consistency isn't settled yet [29].
The main idea of [29] was to consider the Swampland Program for large dimensions D and to ask the question, whether large D Quantum Gravity belongs to the Swampland. One of the main analysis tools is the Swampland Distance Conjecture which gets extended to distances between different spacetime dimensions. In particular, this means that one has to extend the parameter space to include D such that the field space distance Δ gets promoted to have a D-dependency, i.e.

$$\Delta \to \Delta(D). \tag{2.90}$$

This might then imply constraints on the spacetime dimension D. These possible constraints were formulated in a conjecture, the so called *Large Dimension Conjecture* (LDC). For a given mass tower M_i the LDC demands that the associated distance $\Delta_i(\phi_j, D)$ is a positive function of the EFT fields ϕ_j and of D, namely

$$\Delta_i(\phi_j, D) \geq 0, \tag{2.91}$$

unless there is a dual tower $\tilde{M}_i$, such that the dual distance $\tilde{\Delta}_i(\phi_j, D)$ becomes positive, when $\Delta_i(\phi_j, D)$ changes its sign and takes negative values [29]. A particular example for these dual towers M_i and $\tilde{M}_i$ are the KK-tower M_{KK} and the winding tower M_{wind} (2.66) for the circle compactification. For $\Delta \sim \phi \geq 0$ the tower becoming massless is the winding tower M_{wind}, as described in section 2.2.2. But if Δ becomes negative, there is the dual tower M_{KK} becoming massless in perfect agreement with the LDC.
But in terms of the large D limit the circle compactification isn't really interesting. Hence, we turn to a different example, namely the *Freund-Rubin compactification*, which is a non-warped product manifold of a d-dimensional AdS space and a d'-dimensional sphere, i.e. $\mathcal{M}_D = AdS_d \times S^{d'}$ with $D = d + d'$. We will follow the conventions of [29] here. This is obtained as a solution to the D-dimensional Einstein field equations without cosmological constant in the presence of a d-form field strength localised on the AdS space [17]

$$F_{\mu_1 \dots \mu_d} = \frac{\epsilon_{\mu_1 \dots \mu_d}}{\sqrt{-g_A}} f \tag{2.92}$$

where f is a constant with units of mass squared and g_A is the determinant of the AdS metric.
The presence of the field strength modifies the Ricci scalar of the AdS space R_A and the Ricci scalar of the sphere R_S to

$$R_A \ = -\tfrac{d(d'-1)}{D-2} f^2 \tag{2.93}$$

[17] In fact, one can also move the form field to the d'-sphere via Hodge duality [29].

$$R_S \quad = \tfrac{d'(d-1)}{D-2} f^2. \tag{2.94}$$

This also implies the following correlation between the AdS radius r_A and the sphere radius r_S

$$(d-1)r_S = (d'-1)r_A. \tag{2.95}$$

The KK-tower in this setup is given in terms of the AdS cosmological constant Λ_d [18] [29]

$$m_{KK}^2 \sim -2\frac{(d-1)d'}{(d-2)(d'-1)^2}\Lambda_d \tag{2.96}$$

which immediately tells us that the strong ADC is fulfilled for arbitrary dimensions d and d'. From (2.96) one can infer the distance by inverting the exponential scaling of the Swampland Distance Conjecture, i.e.

$$\Delta \sim -\frac{1}{\lambda}\ln m_{KK} \sim -\ln m_{KK} \tag{2.97}$$

for a decay rate λ of $\mathcal{O}(1)$. We keep the sign here explicit since it is important for the LDC. In our example the distance will correspond to the AdS distance Δ_{AdS} but we will suppress that label here.
There are now several possibilities to build the large $D = d + d'$ limit. First, we fix the dimension d' of the sphere and take $d \sim D \to \infty$. In that limit the KK-tower (2.96) and the distance (2.97) become apparently independent of the spacetime dimension $d \sim D$

$$m_{KK}^2 \sim -\frac{d'}{(d'-1)^2}\Lambda_d \sim -\Lambda_d \tag{2.98}$$

$$\Delta \sim -\frac{1}{2}\ln(-\Lambda_d). \tag{2.99}$$

But in this limit the cosmological constant Λ_d can be expressed in terms of the AdS radius r_A and d as follows

$$\Lambda_d \sim -\frac{D^2}{r_A^2}. \tag{2.100}$$

such that the distance becomes

$$\Delta \sim \ln\left(\frac{r_A}{D}\right). \tag{2.101}$$

So we need to further specify, if we want to keep Λ_d or r_A constant in the limit of $d \sim D \to \infty$. For instance, let's choose the latter case. Thus, the distance becomes negative for $D > r_A$. If there is no dual tower to m_{KK} in this theory,

[18] Keep in mind that $\Lambda_d < 0$.

then the LDC forces the spacetime dimension to a smaller value than a critical value D_0 given by

$$D \leq D_0 = r_A. \tag{2.102}$$

In the region $D > r_A$ all the KK-states are above the Planck mass [19], i.e. super-Planckian, which results in a breakdown of the notion of spacetime since curvatures become large. So, if there is no dual tower, the KK-tower must be below the Planck mass [29]. However, these large curvature regimes aren't under good control. Thus, there might some strong gravitational corrections which interfere with this argument [29].
Moreover, let's also consider the limit $d' \sim D \to \infty$ for fixed d and r_A. This directly implies that Λ_d is also fixed. The KK-tower (2.96) and the distance (2.97) get a non-trivial scaling for a very large $d' \sim D$

$$m_{KK}^2 \sim -\frac{\Lambda_d}{D} \tag{2.103}$$

$$\Delta \sim \frac{1}{2} \ln\left(\frac{D}{-\Lambda_d}\right) \tag{2.104}$$

such that the KK-tower becomes massless and the distance diverges in the full limit $d' \sim D \to \infty$. Now it is obvious from (2.95) that r_S has to also diverge here in order to keep r_A fixed. Thus, it is precisely the modulus associated with the volume of the d'-dimensional sphere which gives rise to this massless tower. So this case is nothing else than the SDC in disguise. Furthermore, we can't learn anything from the LDC in this limit since it is always fulfilled [29].
Motivated by the relation between geometric flows and the GDC a geometric flow equation for the number of spacetime dimensions D is derived in chapter 3 [1] which will provide a mechanism for the large D limit. This flow then also gets applied to the large d' limit in the Freund-Rubin compactification.

2.3.3 Non-Geodesic Trajectories

The Swampland Distance Conjecture was originally formulated only for geodesic distances. However, it was observed in [32] that this can be relaxed and that we can also move on non-geodesic trajectories, while still being consistent with the SDC when approaching infinite distance points in moduli space. In particular, this non-geodesicity corresponds to a lower bound on the exponential decay rate λ of the mass tower becoming massless. Having a lower bound for the decay rate is nothing new [26, 46, 47, 48] but so far it has never been tied to a non-geodesicity of a trajectory.
For instance, this deviation from a geodesic can be achieved by adding a potential

[19] In the limit $d \sim D \to \infty$ we have $M_{p,D} = M_{p,d}$. So there is no need to differentiate between the two Planck masses here [29].

V such that we move in a valley, i.e. a flat direction, of the potential. To be more precise, the SDC is formulated for exactly massless moduli but it is expected to also hold in the presence of a scalar potential, as long as the masses and energies, which are induced by it, are below the cut-off Λ_{swamp} of the EFT. This means we have a *pseudomoduli space* [32]. This also means that the valley of the potential doesn't have to be perfectly flat but only flat enough such that the relevant energies are below the cut-off Λ_{swamp} [32]. Now these valleys of the potential V in the pseudomoduli space don't necessarily have to align with the geodesic directions in the moduli space without the potential V. This then implies that, since it is strongly expected that the SDC holds in both cases, there may be deviations from a geodesic compatible with the SDC. Such scenarios involving a potential have already been studied in the context of string flux compactifications [52, 86, 87] but we will take a model-independent bottom-up approach as presented in [32].
For instance, we consider, as in [32], a simple hyperbolic plane and products thereof because these occur as the asymptotic boundary geometry of various Calabi-Yau (CY) compactifications, see for example [30, 88, 89]. And the boundary of the moduli space is precisely where the physics relevant to the SDC happens. So, having motivated the choice, we start with just a single hyperbolic plane, namely we assume that the moduli field space of an EFT is given by an hyperbolic plane. The metric of the field space then reads [20]

$$d\Delta^2 = \frac{n^2}{s^2}(ds^2 + d\phi^2) \tag{2.105}$$

where this covers the upper half-plane $s > 0$ and n is related to the Ricci scalar, i.e. the curvature, as [32]

$$R = -\frac{2}{n^2}. \tag{2.106}$$

We take the field s to be along the vertical axis in field space, whereas ϕ is along the horizontal direction. The field s is commonly referred to as the *saxion* and ϕ as the *axion*. Moreover, the axion ϕ is in principle a periodic scalar. But, as pointed out in [32], the periodicity is generally spontaneously broken by axion monodromy potentials [90, 91], which is also usually the case in string flux compactifications [92, 93], so we will assume henceforth that ϕ is not periodic and can take any real values.
As explained and derived in appendix B, the geodesics of the hyperbolic plane, that reach the boundary of moduli space $s = \infty$, are vertical lines with constant axion $\phi = \phi_0 = const$, which also directly means that the geodesic distance Δ_{geo}

[20] We have chosen to label the line element with $d\Delta^2$ instead of ds^2 here in order to avoid any confusion with the field s.

[21] is purely given by s. In particular, we get

$$\Delta_{geo} \sim n \ln s. \tag{2.107}$$

where n is assumed to be positive from here on. In the spirit of the SDC we now *postulate* a mass tower M_s along the s-direction [32]

$$M_s \sim s^{-a} \tag{2.108}$$

with $a > 0$ such that this tower becomes massless in the infinite distance limit. This is the minimum requirement by the SDC but, in general, there are a plethora of mass towers in a real String Theory setting. Moreover, let us emphasise that there is no dual tower postulated here, namely for $s \to 0$, since we interpret this moduli space as the asymptotic limit of a CY compactification, meaning we are only concerned with large values of s. Using the SDC, namely

$$M_s \sim e^{-\lambda_g \Delta_{geo}}, \tag{2.109}$$

together with (2.107) and (2.108) we can infer the geodesic decay rate λ_g in this setup to be

$$\lambda_g = \frac{a}{n}. \tag{2.110}$$

As explained above, we may now deviate from a geodesic by e.g. the introduction of a potential in the EFT. This then means that the distance can also get contributions from ϕ which isn't forced to be constant anymore. However, we still require the trajectory to reach the boundary of moduli space $s = \infty$. For instance, the non-geodesic distance Δ is given by [22]

$$\Delta = n \int \sqrt{1 + \left(\frac{d\phi}{ds}\right)^2} \ \frac{ds}{s} \tag{2.111}$$

where we have chosen to parametrise ϕ in terms of s, i.e. we have $\phi(s)$. This parametrisation eliminates the necessity for a parameter along the trajectory and guarantees an infinite distance for $s \to \infty$. To ensure compatibility with the SDC, it was found in [32] that we can approach the infinite distance point $s = \infty$ at most by a constant tangent vector (this is ultimately tied to a non-vanishing decay rate in the limit $s \to \infty$), corresponding to the largest possible deviation from a geodesic at the boundary of moduli space, i.e. $s = \infty$ [23]. A constant tangent

[21] We will give the geodesic distance here the extra label "geo" to stress the difference to a non-geodesic distance Δ. Moreover, we will do the same for the decay rate, namely the geodesic decay rate is given by λ_g and the non-geodesic one by λ.

[22] This also motivates the choice in (2.105) a posteriori, as the distance is given by the integral over the square root of the line element.

[23] In fact, as we will also see in chapter 5, the tangent vector for our parametrisation is given by $T^a = (1, d\phi/ds)$.

vector in the (s, ϕ)-plane directly implies that s and ϕ are linearly related, namely

$$\frac{d\phi}{ds} = \beta = const. \tag{2.112}$$

For $\beta = 0$ we clearly recover the geodesic case. Moreover, because the hyperbolic plane is conformally flat, we can translate this straightforwardly into an angle as follows

$$\tan\theta = \beta. \tag{2.113}$$

In that case the non-geodesic distance Δ becomes

$$\Delta \sim n\sqrt{1+\beta^2}\ \ln s = \frac{n}{\cos\theta}\ln s \tag{2.114}$$

By choosing the non-geodesic decay rate λ to be

$$\lambda = \frac{\lambda_g}{\sqrt{1+\beta^2}} = \lambda_g \cos\theta, \tag{2.115}$$

we still perfectly fulfill the SDC for the mass tower M_s in the sense that

$$\lambda\Delta = \lambda_g \Delta_{geo}. \tag{2.116}$$

According to [32] we term this situation the *critical case*. Thus, the critical case corresponds to a constant deviation from the geodesic distance Δ_{geo} and a constant deviation from the geodesic decay rate λ_g. Whereas the distance gets longer, the decay rate is reduced. But, as it was pointed out earlier, the decay rate is expected to have a lower bound λ_0 translating to a bound on the non-geodesicity of the trajectory. So the important object, which constrains the situation, is the decay rate.
This can be also seen in other ways. For instance, consider taking $\beta \to \infty$, i.e. $\theta \to \pi/2$, then we could delay the mass tower M_s indefinitely, which would clearly violate the SDC in the sense that we could traverse an infinite field distance without a massless tower appearing. Hence, this case was called *swampy* in [32]. Furthermore, if such a critical trajectory is realized by a potential, we can determine an effective field living in the flat valley of the potential. For such a field the pseudomoduli space would be 1-dimensional [24] and the non-geodesic distance from the (s, ϕ)-plane would correspond to a geodesic distance in this pseudomoduli space, as it is flat and 1-dimensional. However, the non-geodesic decay rate λ corresponding to the mass tower M_s would also directly descend to this effective field theory in the valley, meaning that we suddenly fulfill a SDC with a lower decay rate (than in the original parent theory). Obviously, this demands a bound on the deviation from a geodesic trajectory in the (s, ϕ)-plane, because otherwise

[24] Because we only consider the upper half of the hyperbolic plane, this 1-dimensional pseudomoduli space is only the positive real line.

the decay rate could become so low the exponential behavior in the valley theory gets spoiled, even though the distance would be geodesic from that perspective. The main point here is that, depending on the perspective, a distance can be geodesic or not but the decay rate is the same in both cases, confirming that the decay rate is the more fundamental object.
Next, let us point out that the geodesic equation enjoys a reflection symmetry of the axion, i.e. $\phi \to -\phi$. This is also shown in appendix B. This means we can also consider a negative β corresponding to a negative θ. Moreover, the change in the decay rate isn't affected by that.
Now we extend our moduli space to a product of two hyperbolic planes which has the following metric

$$d\Delta^2 = \frac{n^2}{s^2}(ds^2 + d\phi^2) + \frac{m^2}{u^2}(du^2 + d\psi^2) \tag{2.117}$$

where we have two saxions s, u and two axions ϕ, ψ. All the previous comments about the periodicity of the axions still apply here. At this point we also have to introduce a mass tower along the second saxionic direction u, meaning that we have two mass towers

$$M_s \sim s^{-a}, \quad M_u \sim u^{-b} \tag{2.118}$$

for $a, b > 0$, such that we meet the minimum requirements of the SDC. In general, M_s and M_u could also combine to give new towers but this would be highly model-dependent and we won't consider this possibility in this thesis [32]. Moreover, the geodesics for this geometry are also derived in appendix B. Thus, a geodesic corresponds to a movement in the (s, u)-plane with constant axions, i.e. $\phi = \phi_0 = const$ and $\psi = \psi_0 = const$.
Like for the single hyperbolic plane, we want to investigate non-geodesic trajectories which approach infinite distance points. These infinite distance points are $s \to \infty$ and $u \to \infty$, which imply $M_s \to 0$ and $M_u \to 0$ respectively. Since the simultaneous limit of both going to infinity is very subtle [25], we will only approach one infinite distance point at a time. The situation is symmetric in s and u, so we can choose either field. For instance, we pick the s-direction again. This is obviously also a geodesic in the product case as long as we keep u fixed, i.e. $u = u_0 = const$. Then, there are two possibilities to extend this to a non-geodesic trajectory, namely the two axionic directions. On the one hand we can fix ψ such that both u, ψ are constant but this just reproduces the result from the single hyperbolic plane. And on the other hand we keep both ϕ and u constant which

[25] First, as it is shown in appendix B, this situation is geodesic. But, more importantly, the tower structure usually gets more complicated because the two towers are generally expected to combine is some way which is highly model-dependent. In the simultaneous infinite distance limit this then becomes relevant. We will comment some more on that later.

is a new case. Thus, we will focus on this one. The distance is then given by

$$\Delta = n \int \sqrt{1 + \left(\frac{m}{n}\frac{s}{u_0}\frac{d\phi}{ds}\right)^2} \ \frac{ds}{s} \tag{2.119}$$

where we have chosen to parametrise ψ in terms of s for the same reasons as before. Now remember that the tangent vector approaching $s = \infty$ can at most be constant which directly implies a constant change in the distance compared to the geodesic case. It turns out the same holds here [32]. Then, from (2.119) we can directly infer

$$s\frac{d\psi}{ds} = \gamma = const \tag{2.120}$$

such that the decay rate for the mass tower M_s gets modified like

$$\lambda = \frac{\lambda_g}{\sqrt{1 + \left(\frac{m}{n}\frac{\gamma}{u_0}\right)^2}} \tag{2.121}$$

to be perfectly consistent with SDC. All of this is completely analogous to the previous case with a single hyperbolic plane. Again we recover the geodesic case by setting $\gamma = 0$ but here we can't directly employ an angle, since we aren't conformally flat anymore. Nevertheless, we will comment more about an angle formulation in chapter 5. This is again the critical case in the sense that it represents the maximum deviation from a geodesic when approaching an infinite distance point. But there is still the lower bound on the decay rate λ_0 which we also have to respect in this case, as this lower bound is tied to the mass tower M_s and not to a specific trajectory.

In summary, we have seen that it is possible to deviate from a geodesic, still being consistent with the SDC. The maximum deviation in the asymptotic limit is called the critical case in which the decay rate and the distance get modified by a constant factor. In practice, the conditions for the critical case, namely the relation between the fields like (2.112) and (2.120), are derived in the fastest way by demanding that the geodesic distance gets changed by a constant.

In chapter 5 these concepts are applied to the scenario of cosmic acceleration. There we will further extend the concepts to trajectories which involve multiple fields up to an arbitrary number N. Moreover, we even consider trajectories which have a non-constant deviation from a geodesic and only in the full limit to the boundary of moduli space this deviation will become constant, as demanded by the SDC.

Chapter 3

Geometric Flow Equations for the Number of Spacetime Dimensions

This whole chapter is based on a collaboration with Davide de Biasio [1]. Some parts were adjusted in this thesis but the general result stays the same. Moreover, the conventions in this chapter differ from the previous ones but everything is declared properly, so there should be no confusion.

On the one hand, there was some recent interest in the limit of large dimensions within the Swampland Program [29, 81], as outlined in section 2.3.2. One promotes the number of dimensions D to an independent parameter in Quantum Gravity and then investigates the behavior of different Swampland Conjectures. On the other hand, there is the close relation between geometric flow equations and the Generalised Distance Conjecture, as motivated in section 2.3.1. In this chapter we try to combine these concepts to derive new geometric flow equations which describe the variation of spacetime geometries under the change of their dimensions. To the best of our knowledge this flow with respect to D, denoted by *D-flow*, was not discussed before in the literature and introduces a new territory in the field of geometric flow equations in gravity. Schematically, D-flow has the following structural form

$$\frac{\partial f_1(g_{\mu\nu})}{\partial D\,(\lambda)} = f_2(R) \tag{3.1}$$

where λ is a flow parameter analogous to the one usually introduced when studying Ricci flow. Here f_1 is a certain function of the spacetime metric $g_{\mu\nu}$ and f_2 is a function of the curvature invariants of the geometry, denoted collectively by R here. As we will discuss soon, the function f_1 will be closely related to the D-dependent volume of the spacetime manifold, whereas f_2 will be determined by linear and quadratic curvature invariants in the simplest cases. The appearance of quadratic curvature invariants in the flow equation for D is directly related to the two-loop graviton β-function in String Theory. Finally, note that in the

D-flow equations we are treating D as a continuous parameter, as it is done in the dimensional regularization scheme for example.

3.1 Derivation of the Flow

The standard procedure of deriving the low-energy graviton equations of motion emerging from String Theory is to compute the associated β^G-function up to a certain power in α' and to impose it to be zero such that the conformal symmetry of the original theory is restored. This was widely explored, for example, in [94, 95, 96, 97, 98, 99, 100, 101]. So we turn the *two-loop* expression [1]

$$\beta^G_{\mu\nu} = \alpha' R_{\mu\nu} + \frac{(\alpha')^2}{2} R_{\mu\alpha\sigma\gamma} R_\nu{}^{\alpha\sigma\gamma} + \mathcal{O}(\alpha'^3) \tag{3.2}$$

into the *geometric flow* equation

$$\frac{\partial g_{\mu\nu}}{\partial \lambda} \equiv -2\beta^G_{\mu\nu} = -2\alpha' R_{\mu\nu} - (\alpha')^2 R_{\mu\alpha\sigma\gamma} R_\nu{}^{\alpha\sigma\gamma} \tag{3.3}$$

which can be regarded as an extension of the standard Ricci flow (2.79). But here the α'-dependence is kept explicit in contrast to what is usually done with Ricci flow. This is due to the fact that it can't be removed by a simple rescaling of the flow parameter λ. This choice has two main advantages. First, it allows us to quantitatively study how rapidly the flow gets switched off as the string contributions get smaller, for example by expressing the flow equations in terms of the ratio between $\sqrt{\alpha'}$ and a typical length scale of the manifold. Secondly, it gives us the possibility to properly address the flow of Ricci flat spacetime metrics for which the two-loop term becomes the leading contribution such that it sources a non-trivial evolution in λ. Clearly, there is no known nor direct way to turn the equation (3.3) into a flow equation for the dimension D of the manifold. Therefore, keeping our final purpose in mind we want to recast it in a suitable form and then proceed with *promoting* D to a λ-dependent quantity. Our first step, starting from (3.3), is to observe that it implies the following flow behaviour for the square root of the metric determinant

$$\frac{\partial \sqrt{g}}{\partial \lambda} = \frac{1}{2\sqrt{g}} \frac{\partial g}{\partial \lambda} \tag{3.4}$$

where we have chosen to work with Euclidean signature for the equations to be properly defined. For a profound discussion of the many mathematical subtleties that underlie the analysis of geometric flow equations, specifically concerning their

[1] To capture more types of manifolds, it is beneficial to go beyond the one-loop expression here. This means we include terms up to $\mathcal{O}(\alpha'^2)$.

parabolicity, the reader is strongly encouraged to look at the standard references like [67, 68, 69]. Using the well-known *Jacobi's formula*

$$\frac{d}{dt}\det A(t) = \mathrm{tr}\left(\mathrm{adj}(A(t))\,\frac{dA(t)}{dt}\right) \tag{3.5}$$

for the derivative of the determinant of a matrix we get

$$\frac{\partial\sqrt{g}}{\partial\lambda} = \frac{1}{2\sqrt{g}}\,\mathrm{Tr}\left(g g^{\alpha\mu}\frac{\partial g_{\mu\nu}}{\partial\lambda}\right) = \frac{\sqrt{g}}{2}\,\mathrm{Tr}\left(g^{\alpha\mu}\frac{\partial g_{\mu\nu}}{\partial\lambda}\right). \tag{3.6}$$

By plugging the flow equation (3.3) into (3.6), we are left with

$$\frac{\partial\sqrt{g}}{\partial\lambda} = -\alpha'\sqrt{g}R - \frac{(\alpha')^2}{2}\sqrt{g}K \tag{3.7}$$

with R being the *Ricci scalar* and K being the *Kretschmann scalar* corresponding to $g_{\mu\nu}$. Combining all the metric components into a single equation is surely a step ahead towards our goal, but it is still not enough: to achieve a good definition of a flow equation for D and to promote D to a continuous modulus of the theory, it is clear that any explicit dependence on the spacetime coordinates, whose number is precisely D, must be *factored out*. This can straightforwardly be done by integrating both sides of (3.7) over the spacetime manifold on which $g_{\mu\nu}(\lambda)$ is defined as a family of Riemannian metrics. We obtain the following

$$\int\frac{\partial\sqrt{g}}{\partial\lambda} = -\alpha'\int\sqrt{g}R - \frac{(\alpha')^2}{2}\int\sqrt{g}K. \tag{3.8}$$

When dealing with a *non-compact* spacetime manifold the integrals are intended to be properly regularised. For example, we might be required to introduce appropriate cut-offs on some coordinates in order to make both sides of the equation finite. At this point we want to manipulate the left-hand side of (3.8) and express it in a more convenient form. In order to do so, we must first stress that, despite the fact that we will then try to generalise our discussion to a setting in which the manifold's dimension itself can change along the flow, we are still working with the standard form (3.3) at a fixed value of D. Hence, taking the λ-derivative out of the integral only accounts to the appearance of a *boundary term* which can be safely dropped. Therefore, we are left with

$$\frac{\partial\mathcal{V}}{\partial\lambda} = -\alpha'\int\sqrt{g}R - \frac{(\alpha')^2}{2}\int\sqrt{g}K \tag{3.9}$$

where the volume $\mathcal{V}$ is defined as

$$\mathcal{V} \equiv \int\sqrt{g}. \tag{3.10}$$

At this point we observe that

$$\mathcal{S}_1 \equiv \int \sqrt{g} R \tag{3.11}$$

is nothing more than the standard *Einstein-Hilbert* action in Euclidean signature, while

$$\mathcal{S}_2 \equiv \frac{1}{2} \int \sqrt{g} K \tag{3.12}$$

is a higher order correction of the former, as previously mentioned. Now we can see that the final form

$$\frac{\partial \mathcal{V}}{\partial \lambda} = -\alpha' \mathcal{S}_1 - (\alpha')^2 \mathcal{S}_2 \tag{3.13}$$

of the flow equation can be meaningfully generalised to a scenario in which the dimension D of the manifold is not forced to be fixed along the flow since neither explicit components of the metric nor coordinate-dependent quantities appear in it. This is precisely the route that we will follow. Inspired by (3.13), we *postulate* the flow equation for $D(\lambda)$ to be

$$\frac{dD}{d\lambda} \equiv -\left(\frac{\partial \mathcal{V}}{\partial D}\right)^{-1} \left[\alpha' \mathcal{S}_1 + (\alpha')^2 \mathcal{S}_2\right]. \tag{3.14}$$

It must be highlighted that (3.13) and (3.14) are *not precisely equivalent*. Namely, if we want to reduce (3.14) back to (3.13), we must assume the D-derivative of $\mathcal{V}$ to be *finite*, in order to bring it to left-hand side and apply the *chain rule*. As we will see, this is not always the case. Therefore, (3.13) must be regarded as a special case of (3.14). Furthermore, it is clear that the D-dependence of $\mathcal{V}$ will descend from our choice of the explicit form of the metric at any given value of D which is *not fixed* by the flow itself. That, in a sense, will be the *input information* allowing us to fix the flow behaviour of the dimension. Such a choice is usually extremely *natural*, like for the example in which the manifold is taken to always be a D-sphere along the flow. Once we have chosen a specific family of metric tensors at different values of D and we have computed the associated scalars $\mathcal{S}_1(D)$ and $\mathcal{S}_2(D)$, we can turn the number of dimensions into a continuous parameter. Then, (3.14) must be interpreted as to tool allowing us to find the correct $D(\lambda)$ such that the D-behaviour assumed for $\mathcal{V}$ can be reconciled with (3.13).

3.2 Maximally Symmetric Spaces

A D-dimensional Riemannian manifold is said to be *maximally symmetric*, if it possesses the highest allowed number of *Killing vectors*, namely $D(D+1)/2$.

This straightforwardly implies that the associated Riemann curvature tensor gets reduced to the simple form

$$R_{\mu\nu\alpha\beta} = \frac{R}{D(D-1)} \left(g_{\mu\alpha} g_{\nu\beta} - g_{\mu\beta} g_{\nu\alpha} \right). \tag{3.15}$$

Therefore, it can be shown that

$$K = \frac{2R^2}{D(D-1)}. \tag{3.16}$$

Because of that the *volume flow* equation in Euclidean signature becomes

$$\frac{\partial \mathcal{V}}{\partial \lambda} = - \int \sqrt{g} \left(\mathcal{R} + \frac{\mathcal{R}^2}{D(D-1)} \right) \tag{3.17}$$

where $\mathcal{R} \equiv \alpha' R$.

3.3 D-Sphere

Starting from the standard expression for the metric on a D-sphere with radius ρ, which is indeed a maximally symmetric space, we can straightforwardly derive the expression

$$R\left(D\right) = \frac{D\left(D-1\right)}{\rho^2} \tag{3.18}$$

for the Ricci scalar and the formula

$$\mathcal{V}\left(D\right) = \frac{2\pi^{\frac{D+1}{2}} \rho^D}{\Gamma\left(\frac{D+1}{2}\right)} \tag{3.19}$$

for the D-dependence of the volume which is plotted in figure 3.1.
At this point we can proceed towards enforcing the flow equation (3.14). As was widely discussed in the previous section, an explicit solution for $D\left(\lambda\right)$ can only be achieved by specifying from the start a D-dependent family of metric tensors. In this example $g_{\mu\nu}\left(D\right)$ will be nothing more than the metric for a D-sphere with radius ρ for any *natural* value of D. It must be stressed that we do not need, nor it would have made sense, to specify the form of the metric for any *real* value of D. As a matter of fact, it is more than sufficient to turn D into a continuous function $D\left(\lambda\right)$ of the flow parameter, after we have computed $\mathcal{V}\left(D\right)$, $R\left(D\right)$ and $K\left(D\right)$ as functions of D, since all our efforts in rephrasing the flow equation differently were precisely aimed towards allowing us to make D continuous in a consistent way. Therefore, we can now derive the following form for (3.14)

$$\frac{dD}{d\lambda} = -\frac{D(D-1)}{\mu^2} \left(1 + \frac{1}{\mu^2} \right) \left(\frac{\partial \log \mathcal{V}}{\partial D} \right)^{-1} \tag{3.20}$$

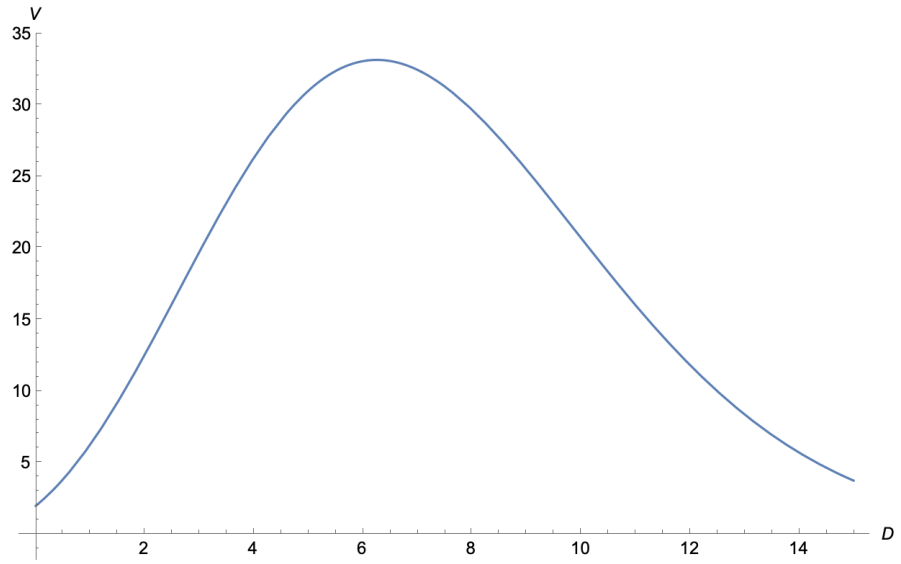

Figure 3.1: Graph of the volume $\mathcal{V}$ of a D-sphere as the number of dimensions D is promoted to a continuous variable.

where

$$\mu \equiv \frac{\rho}{\sqrt{\alpha'}} \tag{3.21}$$

is defined as the ratio between the sphere radius and the length scale of a string. It is important to highlight the presence of a *deformation* factor

$$Z\left(\mu\right) \equiv \frac{1}{\mu^2}\left(1+\frac{1}{\mu^2}\right) \tag{3.22}$$

on the right-hand side of the equation (3.20) accounting for the rescaling of the flow produced by the *significance* of stringy effects with respect to the size of the sphere. Therefore, plotting $Z\left(\mu\right)$ allows us to observe how rapidly the λ-evolution gets switched off as string effects get negligible, namely as $\sqrt{\alpha'}$ gets much smaller than ρ. This can be seen in figure 3.2. Given the above considerations, we can now *absorb* $Z(\mu)$ into the flow parameter λ, defining a new, rescaled, flow parameter

$$\xi \equiv Z(\mu)\lambda \tag{3.23}$$

and obtaining the following flow equation

$$\begin{aligned}\frac{dD}{d\xi} =& -D(D-1)\left(\frac{\partial \log \mathcal{V}}{\partial D}\right)^{-1} = \\ =& 2D(1-D)\left[\log\left(e\rho^2\pi\right) - \psi_0\left(\frac{D+1}{2}\right)\right]^{-1}\end{aligned} \tag{3.24}$$

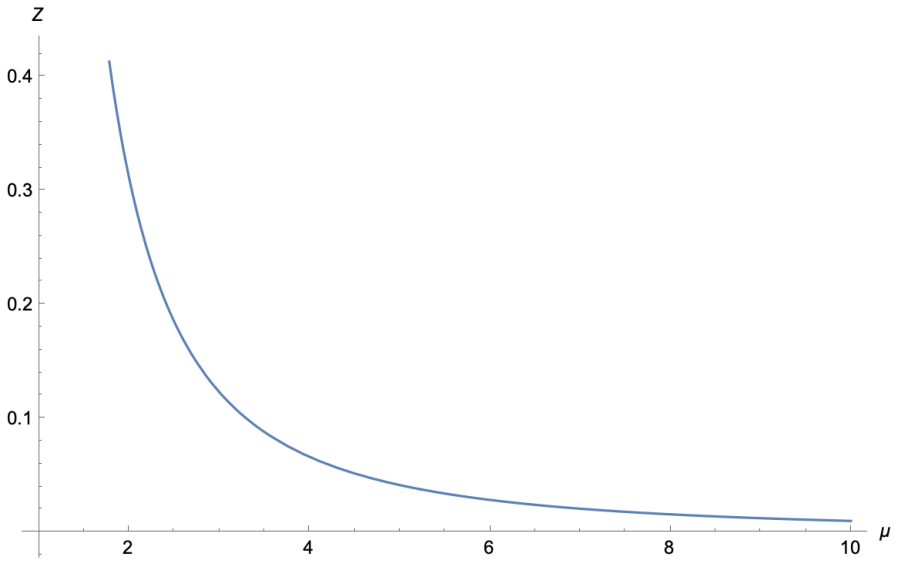

Figure 3.2: Graph of the deformation factor Z as the scale ratio μ grows, namely as the sphere radius gets much bigger than the length of a string.

where ψ_0 is the *Polygamma* function. Clearly, when writing down the explicit form of the volume $\mathcal{V}$, a dependence on ρ reappears independently from $\sqrt{\alpha'}$. Nevertheless, it is still remarkable that the flow equation, when $\mathcal{V}$ is implicit and taken as a variable by itself, only depends on the ratio μ.

3.3.1 Large D Behaviour

In this section we want to study the flow equation at a large number of dimensions D, in order to build a better intuition of its asymptotic behaviour. In particular, the explicit form of the volume can be approximated by

$$\mathcal{V}(D) \approx \sqrt{2}e \left(\rho\sqrt{\frac{2\pi e}{D}}\right)^{D}. \tag{3.25}$$

Therefore, the flow for $D(\xi)$ can be obtained from

$$\frac{dD}{d\xi} = 2D(1-D)\left(\log\frac{2e\pi\rho^2}{D}\right)^{-1} \approx -2D^2\left(\log\frac{\sigma}{D}\right)^{-1} \tag{3.26}$$

where $\sigma \equiv 2e\pi\rho^2 > 0$. By rescaling the flow parameter as $\tau \equiv 2\xi\sigma$ and by defining the quantity

$$X \equiv \frac{\sigma}{D} \tag{3.27}$$

the above equation gets simplified for very small values of X as

$$\frac{dX}{d\tau} = \frac{1}{\log X}. \tag{3.28}$$

Therefore, we can simply integrate it

$$\tau - \tau_0 = X\,(\log X - 1) - X_0\,(\log X_0 - 1) \approx X \log X - X_0 \log X_0 \tag{3.29}$$

and solve for X. Starting from a small value of X_0, corresponding to a large D, it is unavoidable to flow towards $X = 0$. Indeed, this means that the flow equation forces us to flow towards $D = \infty$.

3.3.2 Fixed Points

In the following section we will look for *fixed points* of the flow. For instance, we will solve the equation

$$\frac{dD}{d\xi} = D(1 - D)\left(\frac{\partial \log \mathcal{V}}{\partial D}\right)^{-1} = 0 \tag{3.30}$$

in order to find values of D for which the right-hand side of the flow equation is zero. Then we will study the stability of such points in detail. Indeed, by plugging in the explicit form of $\mathcal{V}$, it can be shown that (3.30) admits two, distinct solutions: $D_a = 0$ and $D_b = 1$. Concerning the *stability* of the fixed point D_a we investigate the *local* behaviour at D_a in the following figure 3.3.

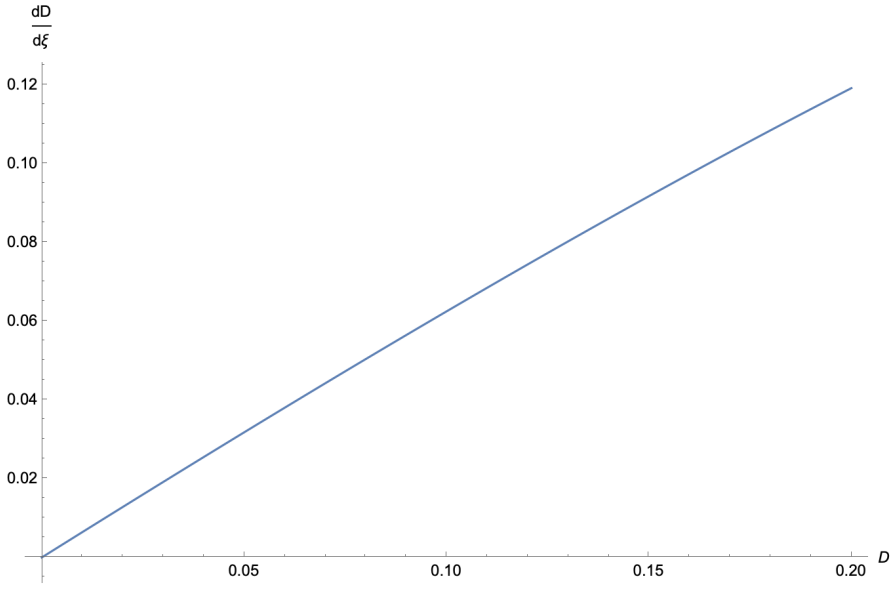

Figure 3.3: $dD/d\xi$ around D_a with $\rho = 1$

Therefore, D_a is an *unstable* fixed point of the flow. This is due to the fact that $dD/d\xi$ is positive for D slightly bigger than 0 [2]. So any perturbation is *magnified*

[2] It makes no sense to consider a negative dimension D.

by the flow and brings us far away from D_a.
Concerning on the other hand the *stability* of the fixed point D_b, we observe the *local* behaviour at D_b in the following plot 3.4.

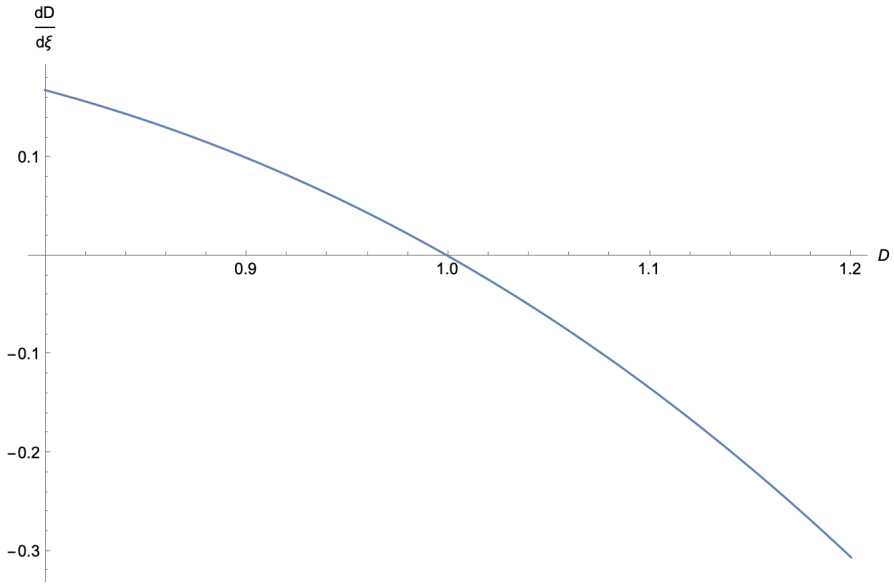

Figure 3.4: $dD/d\xi$ around D_b with $\rho = 1$

Hence, D_b is a *stable* fixed point of the flow. This is due to the fact that $dD/d\xi$ is negative for D slightly bigger than 1 and positive for D slightly smaller than 1. So any perturbation is *compensated* by the flow and we are lead back to D_b. Focusing on $D \in (0, 1+\varepsilon)$, with $0 < \varepsilon \ll 1$, we can turn back to the *equivalent* flow equation for the volume $\mathcal{V}$

$$\frac{d\mathcal{V}}{d\lambda} = \frac{dD}{d\lambda}\frac{d\mathcal{V}}{dD} = D(1-D)\mathcal{V}. \tag{3.31}$$

Here the chain rule can only be applied since we are in a region where $\mathcal{V}$ is *monotonic* in D. Now we can ask ourselves whether the stability of the fixed point is affected by our change of perspective. For that it is enough to study the sign of $d\mathcal{V}/dD$ and we can straightforwardly observe that we are working in an interval where $d\mathcal{V}/dD > 0$. Thus, this *confirms* the fact that D_b is a *stable* fixed point for the volume flow, while D_a is *unstable*.

3.3.3 Singularities

At this point our aim is to locate and study *singular* points along the flow. Namely, there are values $\bar{D}_a$ of the dimension for which

$$\frac{d\mathcal{V}}{dD} = 0. \tag{3.32}$$

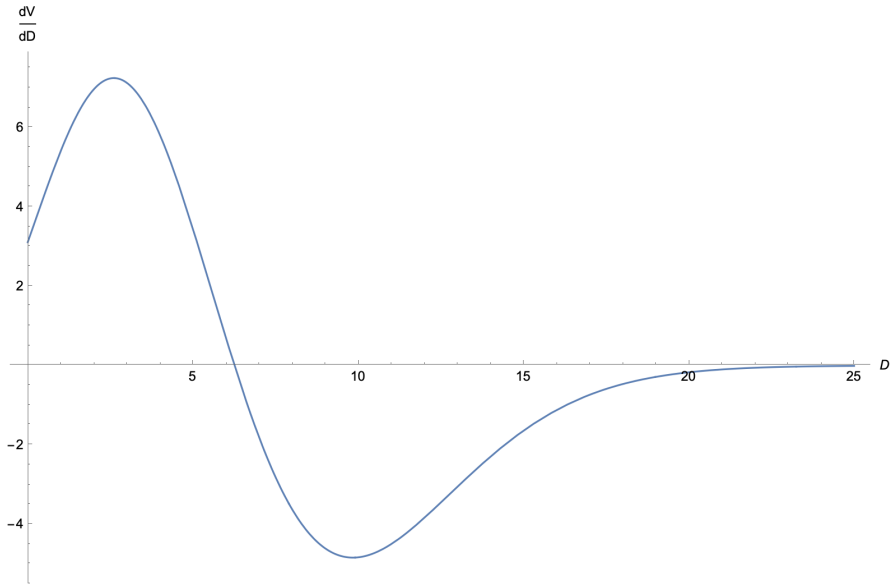

Figure 3.5: $d\mathcal{V}/dD$ for $\rho = 1$ in terms of D.

At these points the derivative $d\mathcal{V}/dD$ blows up to infinity leading to a *singularity*. Indeed, it can be easily observed from the plot presented in Figure 3.5 that there are two values of D for which the flow gets singular. That is, two *extremal points* of $\mathcal{V}$, when intended explicitly as a function of D. The first one, which we choose to name $\bar{D}_a$, sits at a finite value of D. It is approximately equal to 6.26. The second one, in contrast, corresponds to the $D \to \infty$ limit which can be consistently referred to as $\bar{D}_b$. While the presence of the former is manifest, the existence of the latter might still be a little bit obscure. In order to dispel any doubts, the limit can be taken by exploiting the large D approximation of $\mathcal{V}$ producing

$$\lim_{D\to\infty} \frac{d\mathcal{V}}{dD} \approx \lim_{D\to\infty} \left(\frac{2e\pi\rho^2}{D}\right)^{\frac{D}{2}} \log 2 = 0. \tag{3.33}$$

Therefore, it is now clear that the flow equation for $D(\xi)$ presents two *singular points*. The one at infinity is almost harmless. The one at $\bar{D}_a$, however, is definitely less trivial and requires further attention. In particular, the flow can not be *extended* along the whole real line $\mathbb{R}$ where D is allowed to take its values. When the initial point D_0 is taken to belong to the $(0, \bar{D}_a)$ interval, $D(\xi)$ is confined there, too. Analogously, choosing D_0 in $(\bar{D}_a, \infty)$ imposes $D(\xi)$ not to decrease below $\bar{D}_a$. The *stability* of such a singularity under small perturbations can be studied by analysing the sign of $dD/d\xi$ in its neighbourhood. The situation is depicted in figure 3.6. If D_0 is chosen to be slightly smaller than $\bar{D}_a$, the flow brings $D(\xi)$ back towards $D_b = 1$. On the other hand, if D_0 is bigger than $\bar{D}_a$, $D(\xi)$ flows towards the singular point $\bar{D}_b$ at infinity. Hence, $\bar{D}_a$ is *repulsive*, while $\bar{D}_b$ is *attractive*.

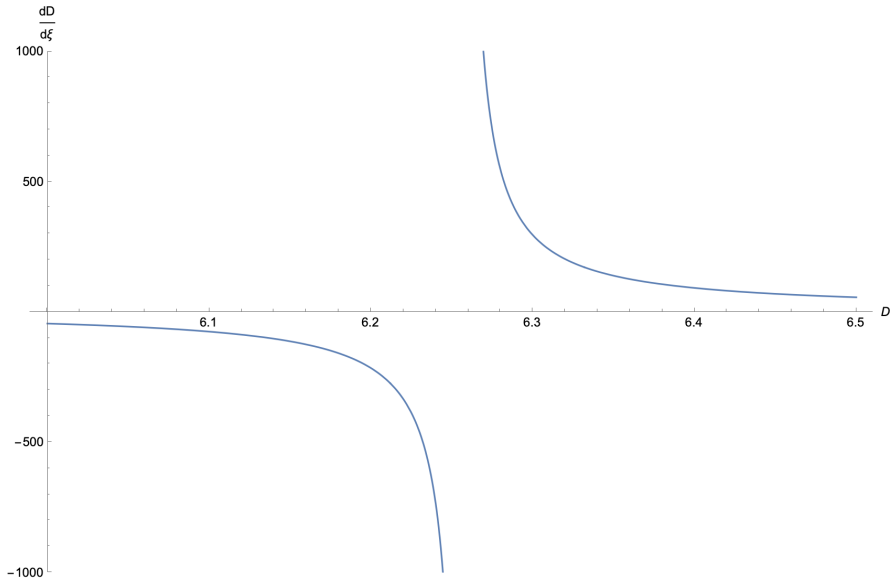

Figure 3.6: $dD/d\xi$ for $\rho = 1$ around $\bar{D}_a$.

3.4 D-dimensional AdS

In this section we compute the D-Flow for the case of AdS spaces. For instance, we have

$$\mathrm{d}s^2 = -\left(1+\frac{r^2}{\alpha^2}\right)\mathrm{d}t^2 + \left(1+\frac{r^2}{\alpha^2}\right)^{-1}\mathrm{d}r^2 + r^2\mathrm{d}\Omega_{D-2}^2 \tag{3.34}$$

and

$$R = \frac{D(1-D)}{\alpha^2}. \tag{3.35}$$

This directly implies that $D > 2$. Since we are working with a maximally symmetric space, we further have

$$K = \frac{2R^2}{D(D-1)} = \frac{2D(D-1)}{\alpha^4}. \tag{3.36}$$

At this point we introduce a radial cut-off Λ and compute the volume enclosed into a sphere with radius Λ centred at $r = 0$. Moreover, we remove the time integral because it will just cancel in the D-flow. So, the volume $\mathcal{V}$ reads

$$\mathcal{V}(D|\Lambda) = \int_0^\Lambda \mathrm{d}r r^{D-2}\int_{S_{D-2}}\mathrm{d}\Omega_{D-2} = \frac{\Lambda^{D-1}}{D-1}\frac{2\pi^{\frac{D-1}{2}}}{\Gamma\left(\frac{D-1}{2}\right)}. \tag{3.37}$$

As a simplification we take $\Lambda = \alpha$ and arrive at

$$\frac{dD}{d\lambda} = \frac{D(D-1)}{\sigma^2}\left(1-\frac{1}{\sigma^2}\right)\left(\frac{\partial\log\mathcal{V}}{\partial D}\right)^{-1} \tag{3.38}$$

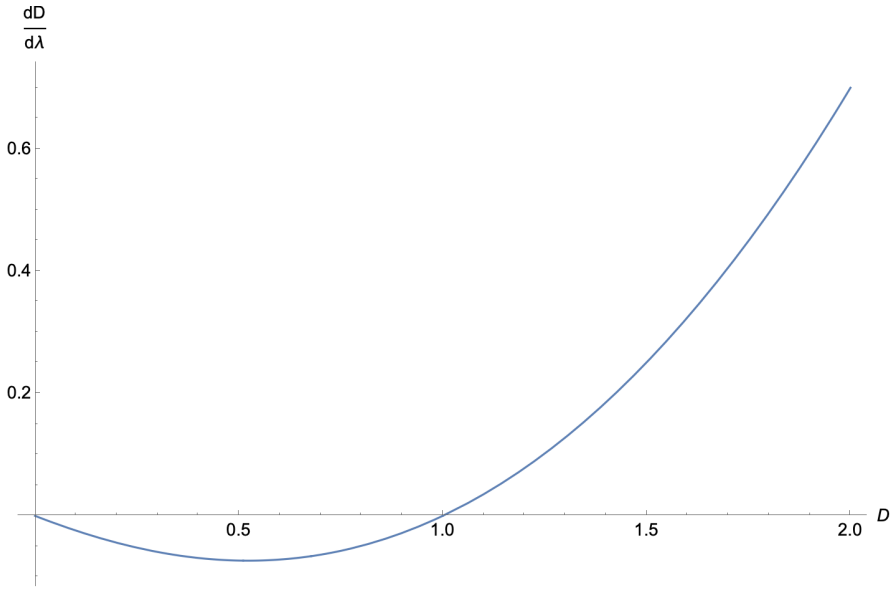

Figure 3.7: $dD/d\lambda$ in terms of D for $\alpha = 1$.

with

$$\sigma \equiv \frac{\alpha}{\sqrt{\alpha'}}. \tag{3.39}$$

Hence, the deformation factor $Z(\sigma)$ is slightly different from the one we had for the sphere, namely here we have

$$Z(\sigma) \equiv \frac{1}{\sigma^2}\left(1 - \frac{1}{\sigma^2}\right). \tag{3.40}$$

Besides large σ, the flow gets now also weak when approaching $\sigma \sim 1$. This is specifically due to the sign of the Ricci scalar R. In order to better investigate the shape of Z, it can be interesting to include even higher order terms.
Since we have worked out the sphere case in full detail, we will be much quicker in the analysis here. The steps are precisely the same and the interesting behavior for us is mainly the fixed point structure. By reabsorbing the σ-dependent factor into the flow equation, we find fixed points at $D = 0$ and at $D = 1$. However, both of these lie outside the range of validity for D. By visual inspection of figure 3.7 we further notice that the fixed point at $D = 1$ is *repulsive*. Thus, for any valid starting point D_0 we are always pushed towards $D = \infty$.

3.5 Freund-Rubin Compactification

In this section we consider a particular setting for Superstring Theory compactification on a sphere, namely we analyse the Freund-Rubin compactification, as

presented in [29], and write down its associated D-Flow equation. Although this has already been introduced in section 2.3.2, we will briefly recap everything and match the notation to this chapter.
Since we are dealing with a non-warped product manifold

$$\mathcal{M}_D = AdS_d \times S^{d'} \tag{3.41}$$

with $D = d + d'$, we will be left with an evolution equation for D which will have to be translated into a flow for d and/or one for d'. In order to do so, our *underdetermined* system forces us to impose a further condition on either d or d'. Since the low-energy effective field theory description we are interested in is expected to live on the AdS spacetime, the most natural choice is to assume its dimension to be fixed and move the whole flow dependence to the compact manifold dimension d'.

3.5.1 Description of the Setup

As just given, the Freund-Rubin compactification is of the form $\mathcal{M}_D = AdS_d \times S^{d'}$ with $D = d + d'$ where G is the metric of the full spacetime $\mathcal{M}_D$, g_A is the metric of the AdS part and g_S is the metric of the sphere. It is a solution to the D-dimensional Einstein equations without cosmological constant in the presence of a d-form field strength localised on the AdS spacetime

$$F_{\mu_1 \dots \mu_d} = \frac{\epsilon_{\mu_1 \dots \mu_d}}{\sqrt{-g_A}} f \tag{3.42}$$

where f is a constant with units of mass squared.
Due to the presence of the field strength, the Ricci scalars of the AdS space $\mathcal{R}_A$ and the Ricci scalar of the sphere $\mathcal{R}_S$ are modified to be

$$\mathcal{R}_A = -\tfrac{d(d'-1)}{D-2} f^2 \tag{3.43}$$

$$\mathcal{R}_S = \tfrac{d'(d-1)}{D-2} f^2. \tag{3.44}$$

This results in a correlation between the AdS radius R_A and the sphere radius R_S

$$(d-1)R_S = (d'-1)R_A. \tag{3.45}$$

Furthermore, the coordinates of the two subspaces do not mix. Hence, the volume just factorises as

$$\mathcal{V}_D = \int_{\mathcal{M}_D} \sqrt{-G} = \int_{AdS_d} \sqrt{-g_A} \int_{S^{d'}} \sqrt{g_S} = \mathcal{V}_{AdS_d} \mathcal{V}_{S^{d'}} \tag{3.46}$$

and the total Ricci scalar is just the sum of the Ricci scalars of the subspaces

$$\mathcal{R}_D = \mathcal{R}_A + \mathcal{R}_S = \frac{f^2(d-d')}{D-2}. \tag{3.47}$$

3.5.2 D-Flow

Constructing the D-Flow equation for this example we only focus on the first order contribution in α' since we already get a non-trivial flow behavior at one-loop order. Hence, α' can be directly absorbed into the flow parameter λ. Because the Ricci scalar does not depend on the coordinates, the D-Flow equation simply reduces to

$$\frac{d}{d\lambda}D(\lambda) = -\mathcal{R}_D \left(\frac{\partial \log \mathcal{V}_D}{\partial D}\right)^{-1} . \tag{3.48}$$

As it was previously discussed, we now impose d to be fixed and move the whole flow dependence to d'. Hence, we consider $\mathcal{V}$ as a function of d' and obtain the following expression

$$\frac{d}{d\lambda}d'(\lambda) = -\mathcal{R}_D \left(\frac{\partial \log \mathcal{V}_D}{\partial d'}\right)^{-1} \tag{3.49}$$

where

$$\mathcal{V}_{S^{d'}} = \frac{R_S^{d'} 2\pi^{\frac{d'+1}{2}}}{\Gamma\left(\frac{d'+1}{2}\right)} \tag{3.50}$$

$$\frac{\partial \log \mathcal{V}_D}{\partial d'} = \frac{\partial \log \mathcal{V}_{S^{d'}}}{\partial d'} = \frac{1}{2}\left(\log(\pi R_S^2) - \psi_0\left(\frac{d'+1}{2}\right)\right). \tag{3.51}$$

The resulting flow equation for d' then becomes

$$\frac{d}{d\lambda}d'(\lambda) = -\frac{2f^2(d-d')}{d+d'-2}\frac{1}{\log(\pi R_S^2) - \psi_0\left(\frac{d'+1}{2}\right)} . \tag{3.52}$$

It must be stressed that the above derivation assumes both R_S and R_A to be fixed along the flow, unavoidably violating the condition expressed in (3.45). Otherwise, we can choose to impose (3.45) which allows one of the radii to change with d'. This option will be discussed later. First of all, it can be straightforwardly observed that the above expression has two fixed points: one at $d' = d$ and one at $d' = \infty$. By studying the sign of the right-hand side of (3.52) we can analyse the character of such points. In particular, we find the following:

- $d' = d$ is an *unstable* fixed point. By taking d' slightly smaller than d we get pushed to 0. By taking, on the other hand, d' slightly larger than d we get pushed to ∞.

- $d' = \infty$ is a *stable* fixed point. By taking $d' > d$, we always get pushed to ∞.

Fixed AdS Radius

In the following discussion, we assume the radius R_A of the AdS spacetime to be fixed, impose (3.45) and introduce a λ-dependence in the sphere radius R_S. In particular, we have

$$R_S(\lambda) = \frac{d'(\lambda) - 1}{d - 1} R_A. \tag{3.53}$$

This unavoidably alters the flow equation for d' which takes now the form

$$\frac{d}{d\lambda} d'(\lambda) = -\frac{2f^2(d - d')}{d + d' - 2} \frac{1}{2\frac{d'}{d'-1} + \log\left(\pi R_S(\lambda)^2\right) - \psi_0\left(\frac{d'+1}{2}\right)}. \tag{3.54}$$

The expression for $R_S(\lambda)$ is presented directly above. As can be clearly observed, a new term has been introduced in the denominator. But it doesn't alter the unstable behaviour of the fixed point at $d' = d$, nor the stability of the one at $d' = \infty$. Nevertheless, it introduces a further *stable* fixed point at $d' = 1$. The sphere radius, in correspondence to the three fixed points, assumes three peculiar values:

- At $d' = 1$, the sphere turns into a 1-dimensional circle. Hence, the whole computation of the curvature breaks down and the flow gets pathological.
- At $d' = d$, R_S is equal to R_A.
- At $d' = \infty$, R_S grows towards ∞. Hence, KK states are expected to produce a tower of massless states.

The picture, emerging when both the AdS dimension d and the radius R_A are kept fixed, while varying the internal sphere dimension d' and size, can be summarised as follows. We have an unstable fixed point at $d = d'$, with $R_A = R_S$, where the theory seems to be consistent. As soon as a small perturbation of the sphere dimension is introduced, we get either pushed towards $d' = 1$, where our flow equations get pathological, or towards $d' = \infty$, where an infinite tower of states is expected to appear in the spectrum. The specific scaling behaviour of KK-modes was presented in [29] as

$$m^2_{KK}(l = 1) = -2\frac{(d - 1)d'}{(d - 2)(d' - 1)^2}\Lambda_d \tag{3.55}$$

where l labels the KK momentum. The cosmological constant Λ_d of the AdS effective field theory was chosen to not to vary along the flow, as the whole λ-dependence was moved to parameters of the internal dimensions and R_A stays constant. Therefore, it can be clearly observed that such states get asymptotically massless, when we flow towards $d' = \infty$. In particular, following the standard

discussions of the Swampland Distance Conjecture, we expect the flow to be provided with an appropriate notion of distance $\Delta(\lambda_0, \lambda)$, so that we asymptotically have

$$m_{KK}^2(\lambda) \sim m_{KK}^2(0)\, e^{-\alpha\Delta(\lambda_0,\lambda)} \tag{3.56}$$

where α labels now the decay rate in the mass tower. Furthermore, these KK-states are associated to the growing sphere, as discussed in section 2.3.2. In our example, focusing on the $d' = \infty$ limit, this would then translate into identifying the asymptotic behaviour of the distance with

$$\alpha\Delta(\lambda_0, \lambda) \sim \log \frac{m_{KK}^2(0)}{m_{KK}^2(\lambda)} = \log \frac{d'_0(d'_\lambda - 1)^2}{d'_\lambda(d'_0 - 1)^2} \sim \log d'_\lambda. \tag{3.57}$$

This clearly doesn't uniquely fix an appropriate notion of Δ, since it only regards its long distance behaviour. Nevertheless, it fits the standard expectation that the distance should grow proportionally to the logarithm of the dimension and it allows us to observe that $d' = \infty$ is at infinite distance from the unstable fixed point at $d' = d$. It would certainly be interesting to fully work out a proper distance Δ for this, because we can't really use the typical distances like (2.72). Moreover, D-flow has provided a mechanism here for the $d' \to \infty$ limit. For instance, in section 2.3.2 this limit was performed "by hand", whereas here it was a result of D-flow. So this further hints at a close relation between geometric flows and the SDC even in an exotic setup like here.

Chapter 4

Gradient Flow of Einstein-Maxwell Theory

This whole chapter is based on a collaboration with Prof. Toby Wiseman and Davide de Biasio [2]. In particular, my contribution was the construction of the flow and the analysis of the near horizon flow. The latter was performed in close collaboration with Davide de Biasio. All the numerical simulations were performed by Prof. Wisenman himself. In particular, this includes the whole section 4.4 and the subsection 4.5.3. However, these parts are still included here for completeness, as I was also involved in the interpretation of the results. But all the numerical details are omitted and only the results and plots are kept here. The interested reader is invited to check out the full paper. Moreover, this chapter has its own conventions but everything is declared properly, so there should be no confusion.

As it was motivated in section 2.2.2 there is a close relation between geometric flow equations like Ricci flow and the Generalized Distance Conjecture. So it makes sense to generalise Ricci flow such that it can be applied to more scenarios. In particular, we are interested in extremal black holes like the Reissner-Nordström solution. Since this chapter will be more concerned with the general and mathematical features of such an extension, we will first provide a small review on some properties of Ricci flow applied to black hole geometries.
Ricci flow may be regarded as a natural gradient flow of the Euclidean signature Einstein-Hilbert action with respect to the DeWitt metric [102, 103], and provides a way to study both the stability of saddle points in the canonical ensemble, as well as the global structure of the space of solutions. An example is gravity in a box with spherical spatial symmetry and fixed boundary radius. Describing this at finite temperature using a Euclidean continuation, the saddle points of the action are the small and large black holes, as well as "hot" flat space, and being Ricci flat, these are fixed points of Ricci flow. The small black hole is always thermodynamically unstable in the canonical ensemble [104] and there is an analog

of the Hawking-Page phase transition between the large black hole and hot flat space [105]. This thermodynamic instability of the small black hole results in a negative mode of the Lichnerowicz operator [106, 107, 108, 109, 110], which drives an instability under Ricci flow [102]. A very interesting recent study of the Wick rotation from Lorentzian signature finds that mode stability about a fixed point in the semiclassical Euclidean path integral is directly related to the stability under Ricci flow [111].

This instability implies a relevant deformation of the small black hole that generates two flows away from it. In [102] it was found these flows connect to the other two stable fixed points, the large black hole, and hot flat space, the latter requiring a surgery to resolve a singularity along the flow. This is intriguingly qualitatively similar to the behaviour of real time evolution of a small black hole surrounded by a bath of radiation at its Hawking temperature. Removing the box by taking it to infinite size, the small black hole tends to the usual Schwarzschild solution and the large black hole is removed with the box. Since the unstable mode is localized about the horizon, the instability under Ricci flow persists. One of the two flows from Schwarzschild then again tends to flat spacetime (after resolving a singularity at finite flow time that changes the spacetime topology). The other "eats up" spacetime indefinitely as there is now no large black hole for it to flow to.

As previously mentioned, these Ricci flows of the Schwarzschild black hole can be thought of as RG flow of a sigma model [112]. However it is also possible that the off-shell geometries that the flow passes through may have significance in the gravitational path integral [102].

The above discussion was for Euclidean signature. In fact Ricci flow is not well defined for Lorentzian spacetimes in general. However, restricting to static or stationary metrics it is well posed and preserves smooth non-extremal Killing horizons [102, 113, 114], the surface gravity and angular velocities of these being constant along the flow. Furthermore, the Euclidean negative mode discussed above preserves the Euclidean $U(1)$ isometry, and hence can be Wick rotated to an instability of the Ricci flow of static black hole spacetimes. Thus, the unstable flows of Euclidean Schwarzschild can be Wick rotated to give flows of static spacetimes away from Lorentzian Schwarzschild.

Further motivated by these considerations it is interesting to consider the flow of a gravitational system with matter. Here we will consider the simple setting of gravity coupled to a Maxwell field. There is a natural family of flows that are gradient flows of the Einstein-Maxwell action with respect to a natural metric on the superspace. These flows couple the metric and Maxwell vector potential. The flow of the metric is similar to Ricci flow but with an extra contribution from the Maxwell stress tensor. The flow of the Maxwell field is given by the Yang-Mills flow in the background of the metric. We call this combined gradient flow the Einstein-Maxwell flow (EM flow). The non-trivial fixed points of the flow are

then the Reissner-Nordström (RN) solutions.

4.1 Einstein-Maxwell Theory

4.1.1 Setup

Since we are concerned with a natural gradient geometric flow of the static Einstein-Maxwell system, we will briefly review the 4-dimensional Einstein-Maxwell system and its RN black hole solutions. We will also introduce convenient coordinates for the later discussion. The theory contains the metric $g_{\mu\nu}$ and a gauge field A_μ and the classical solutions solve the Einstein-Maxwell equations

$$\begin{aligned} R_{\mu\nu} &= 2F_{\mu\alpha}F_{\nu}{}^{\alpha} - \frac{1}{2}F^2 g_{\mu\nu} \\ \nabla^\mu F_{\mu\nu} &= 0 \end{aligned} \tag{4.1}$$

which derive from the action

$$S = \frac{1}{16\pi G}\int d^4x\sqrt{-g}\left(R - F^2\right). \tag{4.2}$$

We note that we have chosen to use a gravitational normalization for the Maxwell field. The static vacuum solutions to this are the Reissner-Nordström black holes. The metric may be written as

$$\begin{aligned} ds^2 &= -f(r)dt^2 + \frac{dr^2}{f(r)} + r^2 d\Omega^2 \\ f(r) &= \left(1 - \frac{r_+}{r}\right)\left(1 - \frac{r_-}{r}\right) \end{aligned} \tag{4.3}$$

with $d\Omega^2 = d\theta^2 + \sin^2\theta d\phi^2$ and the magnetically and electrically charged solutions have gauge potentials

$$\begin{aligned} A_{mag} &= -\sqrt{r_+ r_-}\cos\theta d\phi \\ A_{elec} &= \sqrt{r_+ r_-}\left(\frac{1}{r_+} - \frac{1}{r}\right)dt \end{aligned} \tag{4.4}$$

respectively.[1] The mass M and the magnetic or electric charge Q (in appropriate units) of the solutions are

$$2GM = r_+ + r_-$$

[1] One may also source the RN solution with a mixed electromagnetic solution of the form $A = \alpha\left(\frac{1}{r_+} - \frac{1}{r}\right)dt + \beta\cos\theta d\phi$ for appropriate α, β. Here, as stated earlier, we will only be concerned with purely electric or magnetic solutions as generally mixed fields will produce a Poynting energy flux whose backreaction is not compatible with the static symmetry of the metric. In the case of these spherical solutions a static solution with both electric and magnetic charge is allowed since the spherical symmetry ensures the electric and magnetic fields are parallel, being radially directed, and hence the Poynting vector vanishes.

$$Q = \sqrt{r_+ r_-} \tag{4.5}$$

so that $GM \geq |Q|$. We may also consider the negatively charged solutions by reversing the signs of the gauge potentials above but here we just consider the positively charged case for simplicity. Regarding r_+ as the outer horizon position and r_- as the inner horizon position implies $r_+ > r_-$.

4.1.2 Thermodynamics

The solutions obey a First Law of black hole mechanics

$$dM = TdS + \mu dQ \tag{4.6}$$

where the Hawking temperature T, the Bekenstein-Hawking entropy S and the potential μ associated to the charge Q of the non-extremal solutions are given by

$$\begin{aligned} T = \frac{\kappa}{2\pi} &= \frac{r_+ - r_-}{4\pi r_+^2} \\ S &= \frac{\pi r_+^2}{G} \\ \mu &= \frac{1}{G}\sqrt{\frac{r_-}{r_+}}. \end{aligned} \tag{4.7}$$

Here κ is the surface gravity. We note that for the electric RN one can see from writing $A_{elec} = -\psi\, dt$ that $G \cdot \mu$ corresponds to the potential difference from the horizon to that at infinity, i.e. $\psi_{r_+} - \psi_\infty$, noting that the potential at the horizon vanishes. The extremal limit corresponds to taking $r_- \to r_+$, so that the surface gravity (and hence the temperature) vanishes, and corresponds to taking the charge $|Q| \to GM$. The specific heat capacity at constant charge c_Q and the capacitance at fixed temperature ϵ_T are

$$\begin{aligned} c_Q &= T\left.\frac{\partial S}{\partial T}\right|_Q = -\frac{2\pi r_+^2}{G}\frac{r_+ - r_-}{(r_+ - 3r_-)} \\ \epsilon_T &= \left.\frac{\partial Q}{\partial \mu}\right|_T = \frac{G r_+ (r_+ - 3r_-)}{r_+ - r_-} \end{aligned} \tag{4.8}$$

respectively. We note that c_Q is negative for small charges and becomes positive for $r_+ \geq r_- > \frac{1}{3}r_+$, so for charges $|Q| > \frac{\sqrt{3}GM}{2} = Q_{crit}$, whereas ϵ_T has precisely the opposite sign to c_Q. If we work at fixed temperature T and charge Q, the relevant ensemble is the canonical ensemble and, as discussed in [115, 116], then thermodynamic stability is simply governed by the positivity of c_Q. Thus at fixed temperature and charge, the canonical ensemble is unstable for $|Q| < Q_{crit}$ but

becomes stable for sufficient charges $|Q| > Q_{crit}$. If we instead choose to work at fixed temperature T and potential μ, then we must use the grand canonical ensemble and the condition for stability, namely that the corresponding Gibbs potential has a local minimum, is then given by positivity of *both* c_Q as well as ϵ_T (see for example [117]). Now we see from their explicit expressions that c_Q and ϵ_T have opposite sign, and hence the grand canonical ensemble is unstable for all values of temperature and potential.

The work of [109, 110] related the negative mode of the Euclidean continuation of the Schwarzschild black hole to its negative specific heat capacity and hence thermodynamic instability. The magnetic RN solution can also be analytically continued to a smooth Euclidean solution in the same manner. Monteiro and Santos [115] have shown it also has a Euclidean negative mode for charges where the specific heat at constant charge is negative, and hence the canonical ensemble is unstable, and this mode disappears as the charge is increased to $|Q| = Q_{crit}$ (see also [118]).

Whereas, for electric RN, one fixes A_{elec} at infinity and therefore this is naturally related to the ensemble with fixed electric potential. This is therefore associated to the grand canonical ensemble which is unstable in any case. But the static Lorentzian electric RN solution cannot straightforwardly be analytically continued to a (real) Euclidean solution, due to the electric gauge field whose potential would naively become imaginary.

Interestingly, however, we will find later that the stability of the static EM flows about RN do reflect these behaviours in the sense that the flow of the magnetically charged fixed point becomes stable for sufficient charge, but that of the electric fixed point does not. This is particularly interesting in light of the recent links between the stability of the canonical ensemble for Schwarzschild in a box and its stability under Ricci flow [111]. So this suggests a generalization which includes charge.

We will find our geometric flows preserve surface gravity of a horizon and hence we will be interested in the set of solutions at a fixed temperature in order to understand possible end-points of the flow. Furthermore, we will see that the magnetic flow preserves magnetic charge, and the electric flow preserves the electric potential difference between the horizon and infinity. From the expressions above it follows that for magnetic RN solutions at a given fixed magnetic charge Q the temperature T is given in terms of r_+ as

$$T(r_+) = \frac{1}{4\pi} \frac{r_+^2 - Q^2}{r_+^3} \tag{4.9}$$

which has a maximum

$$T_{max} = \frac{1}{6\sqrt{3}\pi|Q|} \tag{4.10}$$

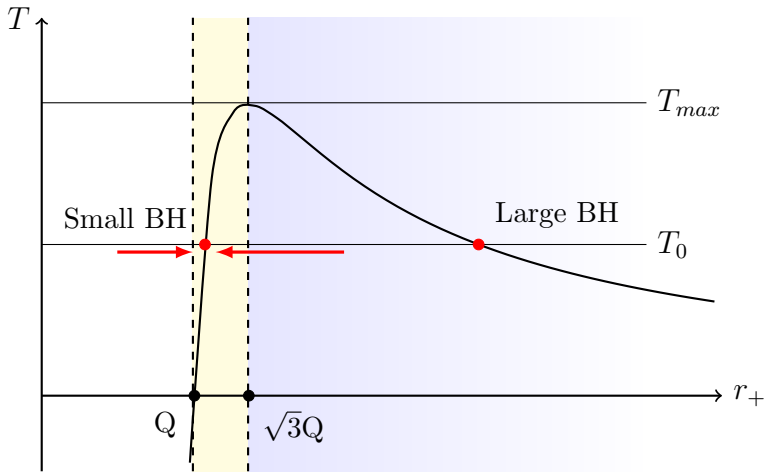

Figure 4.1: This plot shows the temperature $T(r_+)$ of a magnetic RN solution at fixed (sufficiently large) charge Q. For a temperature $T_0 < T_{max}$ there are two solutions: a small BH and a large BH. The small BH, with smaller r_+, is stable since $c_Q > 0$ (indicated by the yellow shading), whereas the large BH, with bigger r_+, is unstable since $c_Q < 0$ (indicated by the blue shading). Moreover these two BHs merge into a marginally stable one at $r_+ = \sqrt{3}|Q|$ which corresponds to $T_0 = T_{max}$. The red arrows already indicate the flow behavior which we will observe later. The extremal BH lies at $r_+ = Q$ with vanishing temperature.

at $r_+ = \sqrt{3}|Q|$. This arises since for fixed charge there is a minimum mass, given by the BPS bound $M \geq |Q|$, and a unique solution exists for all greater masses. Then for $M \to |Q|$ the temperature vanishes, but for very large $M \gg |Q|$ the temperature also becomes small, so by continuity in between there is a maximum. Assuming one takes a temperature $T_0 < T_{max}$ there are then two magnetic RN solutions. In analogy with Hawking-Page we may think of these as a small and large black hole. Now the smaller one, with mass $M < \frac{2|Q|}{\sqrt{3}G}$, is thermodynamically stable (with no Euclidean negative mode), and the larger one has a greater horizon size and mass $M > \frac{2|Q|}{\sqrt{3}G}$, and is thermodynamically unstable (with a Euclidean negative mode). Given a charge, then increasing the temperature to its critical value, T_{max}, these two solutions merge to a single marginally stable solution. For greater temperatures there are no RN black hole spacetimes. This situation is summarized in figure 4.1.
For electric RN solutions, then fixing the electric potential μ the situation is different. The temperature T in terms of r_+ now reads

$$T(r_+) = \frac{1 - G^2\mu^2}{4\pi} \frac{1}{r_+}. \tag{4.11}$$

For a given potential there exists a single black hole for every temperature T_0 and these solutions are always thermodynamically unstable since c_Q and ϵ_T have

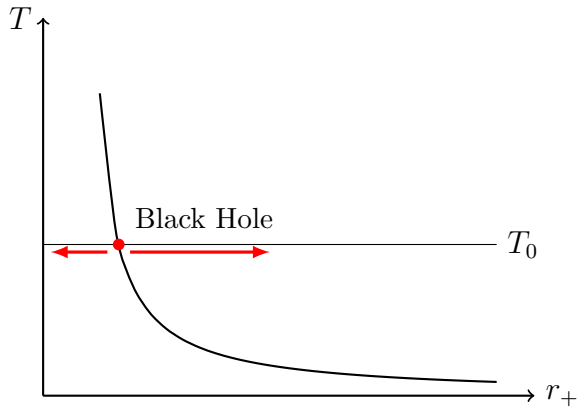

Figure 4.2: This plot shows the temperature $T(r_+)$ of an electric RN solution at constant electric potential μ. For any temperature T_0 there is only a single BH solution which is always unstable. The red arrows indicate the flow behavior which will be shown later.

precisely opposite signs. Figure 4.2 shows a depiction of this case.

4.1.3 Convenient Units and Coordinates

When considering a RN fixed point of the flow we will find it convenient to choose units such that $r_+ = 1$, i.e. the outer horizon is a unit sphere, and the exterior spacetime is $r > 1$. In this case a useful radial coordinate we will use later is ρ, related to r by

$$r = \frac{1}{1-\rho^2} \tag{4.12}$$

which maps the infinite range $r \in [1, \infty)$ to the interval $\rho \in [0, 1)$. Then the RN metric (in these units, so $r_+ = 1$) becomes

$$\begin{aligned} ds^2 &= -\rho^2 F(\rho) dt^2 + 4r(\rho)^4 \frac{d\rho^2}{F(\rho)} + r(\rho)^2 d\Omega^2 \\ F(\rho) &= 1 - r_- + r_- \rho^2 \end{aligned} \tag{4.13}$$

with the magnetic Maxwell potential as above (with $r_+ = 1$) and the electric one being

$$A_{elec} = \sqrt{r_-}\rho^2 dt. \tag{4.14}$$

Taking $r_- \to 0$ yields the uncharged Schwarzschild black hole solution, whereas taking $r_- \to 1$ gives the extremal RN black holes. In this extremal limit we

introduce a new coordinate

$$\rho' = \rho^2 \tag{4.15}$$

such that again $\rho' \in [0, 1)$. The extremal metric then reads

$$\begin{aligned} ds^2 &= -\rho'^2 dt^2 + r(\rho')^4 \frac{d\rho'^2}{\rho'^2} + r(\rho')^2 d\Omega^2 \\ r(\rho') &= \frac{1}{1-\rho'} \end{aligned} \tag{4.16}$$

which is supplemented by either an electric or a magnetic potential

$$\begin{aligned} A_{elec} &= \rho' dt \\ A_{mag} &= -\cos\theta d\phi \end{aligned} \tag{4.17}$$

where we assumed positively charged solutions. Taking $\rho' \to 0$, so that $r \to 1$, we directly recognise the near horizon geometry as $AdS_2 \times S^2$.

4.2 Gradient Flows

Given an action S, which is a functional of some fields Ψ^A, then the variation $\delta S/\delta\Psi^A$ is a covector on the space of fields, the "superspace". Here the label "A" collectively denotes spacetime indices and coordinates. As discussed in [102], given a metric on superspace, G_{AB}, which is also a functional of the fields Ψ^A, the expression $\delta S/\delta\Psi^A$ may be converted into a vector and a gradient flow can be defined as

$$\frac{d}{d\lambda}\Psi^A = G^{AB}\frac{\delta S}{\delta \Psi^B}. \tag{4.18}$$

The simplest such local superspace metrics will only depend on the fields and not their derivatives. If G_{AB} is a positive definite metric, then this is a gradient descent of the action which monotonically decreases along the flow. Different choices of superspace metric will yield different flow equations.

4.2.1 Gradient Flow of the Einstein-Hilbert Action

For instance, let us consider the Einstein-Hilbert action in this context

$$S_{EH} = \frac{1}{16\pi G}\int d^4x\sqrt{-g}R. \tag{4.19}$$

We may associate Ψ^A with the metric $g_{\mu\nu}(x)$, such that the abstract index A is enumerating both the metric components and coordinate position. A natural metric on superspace is given by the DeWitt$_k$ metric (using the notation of [111])

$$(h_{\mu\nu}, \tilde{h}_{\alpha\beta}) = \frac{1}{32\pi G}\int d^4x\sqrt{-g}h_{\mu\nu}G^{\mu\nu\alpha\beta}\tilde{h}_{\alpha\beta}, \tag{4.20}$$

where $h_{\mu\nu}$ and $\tilde{h}_{\alpha\beta}$ are two perturbations of the metric $g_{\mu\nu}$, and

$$G^{\mu\nu\alpha\beta} = \frac{1}{2}\left(g^{\mu\alpha}g^{\nu\beta} + g^{\mu\beta}g^{\nu\alpha} + kg^{\mu\nu}g^{\alpha\beta}\right) \tag{4.21}$$

for a real k. Then, rearranging the gradient flow equation (4.18) as

$$G_{AB}\frac{d\Psi^A}{d\lambda}\delta\Psi^B = \delta S \tag{4.22}$$

with δS given by the variation $\delta\Psi^B$, explicitly gives

$$\left(\frac{d}{d\lambda}g_{\mu\nu}, \delta g_{\alpha\beta}\right) = \delta S_{EH} = -\frac{1}{16\pi G}\int d^4x\sqrt{-g}\delta g_{\alpha\beta}\left(R^{\alpha\beta} - \frac{1}{2}g^{\alpha\beta}R\right). \tag{4.23}$$

We will focus on the case $k = -1$. So the flow equation becomes

$$\frac{d}{d\lambda}g_{\mu\nu}(x) = -2R_{\mu\nu} \tag{4.24}$$

which is simply the Ricci flow. An important point is that since the DeWitt$_{-1}$ metric is not positive definite, the Einstein-Hilbert action does not generally vary monotonically along Ricci flows. For example a monotone functional is famously given by the Perelmann entropy [69].
The fixed points of Ricci flow are ones so that $\dot{g}_{\mu\nu} = 0$ where the dot indicates a flow time derivative, i.e. $\dot{} = d/d\lambda$. Thus, the fixed points are Ricci flat metrics. However, one may also consider solutions to the Ricci soliton equation

$$R_{\mu\nu} = \nabla_{(\mu}\xi_{\nu)} \tag{4.25}$$

to be geometric fixed points of the flow, since for these we have $\dot{g}_{\mu\nu} = -\text{Lie}_\xi g_{\mu\nu}$. For non-vanishing ξ the metric is clearly varying, but the geometry it represents is not. Thus, a Ricci soliton represents a geometric fixed point of the flow, so the geometry doesn't flow, but the coordinates it is presented in do.
Ricci flow is itself diffeomorphism invariant. By performing a flow time dependent diffeomorphism

$$\begin{aligned} x^\mu &\rightarrow x^\mu + v^\mu(\lambda, x) \\ \frac{d}{d\lambda}v^\mu &= \xi^\mu \end{aligned} \tag{4.26}$$

we generate a new flow of the metric

$$\frac{d}{d\lambda}g_{\mu\nu} = -2R_{\mu\nu} + \mathrm{Lie}_\xi g_{\mu\nu} \tag{4.27}$$

where we may write $\mathrm{Lie}_\xi g_{\mu\nu} = 2\nabla_{(\mu}\xi_{\nu)}$. The flows $g_{\mu\nu}(\lambda)$ for the Ricci flow and the above flow are the same geometrically, but the two metrics will differ by a coordinate transformation at any given λ, i.e. depending on the flow time.
Due to its diffeomorphism invariance, Ricci flow is not well-posed as a PDE for initial data at some starting flow time λ. However, following DeTurck [119], we may make the choice that

$$\xi^\mu = g^{\alpha\beta}\left(\Gamma^\mu{}_{\alpha\beta} - \bar{\Gamma}^\mu{}_{\alpha\beta}\right) \tag{4.28}$$

given a smooth fixed (i.e. flow time independent) reference connection $\bar{\Gamma}^\mu{}_{\alpha\beta}$ on the manifold. Then the principle part (meaning the second derivative terms) of the flow is

$$\frac{d}{d\lambda}g_{\mu\nu} =_{PP} g^{\alpha\beta}\partial_\alpha\partial_\beta g_{\mu\nu}. \tag{4.29}$$

For Riemannian metrics this is now parabolic. For Lorentzian signature metrics this is generally not well-posed, as timelike perturbations "anti-diffuse". However, following [113, 114], we may restrict to the space of static or stationary metrics, and then the flow is indeed parabolic, thus well-posed.
Let us take the reference connection $\bar{\Gamma}^\mu{}_{\alpha\beta}$ to be the Levi-Civita connection of a static reference metric, $\bar{g}_{\mu\nu}$. Then the flow obviously preserves staticity of the metric, namely starting with a static metric it will remain static. If the metric is static, we may generally write it locally as

$$g_{\mu\nu}(x) = \begin{pmatrix} -N(x^k) & 0 \\ 0 & h_{ij}(x^k) \end{pmatrix} \tag{4.30}$$

with $N \geq 0$ and $\det(h_{ij}) > 0$ in coordinates $x^\mu = (t, x^k)$ adapted to the static symmetry. Note that in these static coordinates N may vanish at black hole horizons but away from these it should be positive. We may always choose coordinates locally so that the spatial metric h_{ij} is a smooth Riemannian metric. Then since $g_{\mu\nu}$ has no explicit time dependence, the principle part becomes

$$\frac{d}{d\lambda}g_{\mu\nu} =_{PP} h^{ij}\partial_i\partial_j g_{\mu\nu} \tag{4.31}$$

which is indeed a parabolic diffusion-like flow for the metric components on the curved space h_{ij}.

4.2.2 Gradient Flow of the Einstein-Maxwell Action

We now consider the gradient flow of the Einstein-Maxwell action

$$S = \frac{1}{16\pi G}\int d^4x\sqrt{-g}\left(R - F^2\right) \tag{4.32}$$

with $F_{\mu\nu} = 2\partial_{[\mu}A_{\nu]}$. Now, schematically, our field space Ψ^A is composed of the metric $g_{\mu\nu}(x)$ together with the gauge field $A_\mu(x)$. A natural superspace metric is then given by

$$\begin{aligned}(h_{\mu\nu}, \tilde{h}_{\alpha\beta}) &= \frac{1}{32\pi G}\int d^4x\sqrt{-g}h_{\mu\nu}G^{\mu\nu\alpha\beta}_{(g)}\tilde{h}_{\alpha\beta}\\ (u_\mu, \tilde{u}_\alpha) &= \frac{1}{16\pi G}\int d^4x\sqrt{-g}u_\mu G^{\mu\alpha}_{(A)}\tilde{u}_\alpha\end{aligned} \tag{4.33}$$

where, as above, $h_{\mu\nu}$ and $\tilde{h}_{\alpha\beta}$ are metric perturbations, whereas u_μ and $\tilde{u}_\alpha$ are perturbations to the gauge field A_μ. Moreover, for the superspace metrics we take

$$\begin{aligned}G^{\mu\alpha}_{(A)} &= \frac{4}{\tau}g^{\mu\alpha}\\ G^{\mu\nu\alpha\beta}_{(g)} &= \frac{1}{2}\left(g^{\mu\alpha}g^{\nu\beta} + g^{\mu\beta}g^{\nu\alpha} - g^{\mu\nu}g^{\alpha\beta}\right)\end{aligned} \tag{4.34}$$

for a constant τ. Furthermore, we take $(h_{\mu\nu}, u_\alpha) = 0$ so that the metric and gauge perturbations are orthogonal. We may regard the parameter τ as determining the speed of the flow of the gauge field relative to that of the metric and later we will focus on the case $\tau = 1$. We see that this superspace metric is constructed only from the metric (so doesn't involved the gauge field) and that its restriction to the metric simply gives the DeWitt$_{-1}$ superspace metric.
Then we obtain the following gradient flow equations

$$\begin{aligned}\frac{d}{d\lambda}g_{\mu\nu} &= -2R_{\mu\nu} + 4F_{\mu\alpha}F_{\nu}{}^{\alpha} - F^2 g_{\mu\nu}\\ \frac{d}{d\lambda}A_\mu &= \tau\nabla^\alpha F_{\alpha\mu}.\end{aligned} \tag{4.35}$$

We will call this system the Einstein-Maxwell flow (EM flow) and its fixed points, $\dot{g}_{\mu\nu} = 0 = \dot{A}_\mu$, are solutions of the Einstein-Maxwell equations.
The EM flow is both diffeomorphism and gauge invariant. Thus, we may consider the analog of Ricci solitons, so field configurations where the geometry and the gauge field flow only up to diffeomorphisms and gauge transformations

$$\begin{aligned}\dot{g}_{\mu\nu} &= -\mathrm{Lie}_\xi g_{\mu\nu}\\ \dot{A}_\mu &= -\mathrm{Lie}_\xi A_\mu - \partial_\mu\Lambda\end{aligned} \tag{4.36}$$

with ξ generating the flow dependent diffeomorphism and Λ the gauge transformation of the Maxwell field along the flow. We may explicitly modify the EM flow to add such a flow time dependent diffeomorphism ξ and gauge transformation Λ as

$$\begin{aligned} \frac{d}{d\lambda} g_{\mu\nu} &= \mathrm{Lie}_\xi g_{\mu\nu} - 2R_{\mu\nu} + 4F_{\mu\alpha}F_\nu{}^\alpha - F^2 g_{\mu\nu} \\ \frac{d}{d\lambda} A_\mu &= \mathrm{Lie}_\xi A_\mu + \partial_\mu \Lambda + \tau \nabla^\alpha F_{\alpha\mu} \end{aligned} \tag{4.37}$$

such that we get the same flow up to diffeomorphisms and gauge transformations. The analog of Ricci solitons can then be thought of as the fixed points of this modified flow.
As for Ricci flow, the Einstein-Maxwell flow is not parabolic, even when restricted to static field configurations. In a linearization of the flow the two derivative terms vanish on linear perturbations that are diffeomorphisms or gauge transformations of the gauge field. In order to obtain a well-posed flow, we take the modified flow above in equation (4.37) and choose ξ as the DeTurck vector in equation (4.28) and further take

$$\Lambda = \tau \nabla^\alpha A_\alpha. \tag{4.38}$$

Now, choosing the reference metric to be static, the flow truncates to the space of static metrics and gauge fields. From here on we will focus on the case $\tau = 1$ such that the principle part of the flow on static metrics and gauge fields then becomes

$$\begin{aligned} \frac{d}{d\lambda} g_{\mu\nu} &=_{PP} h^{ij}\partial_i\partial_j g_{\mu\nu} \\ \frac{d}{d\lambda} A_\mu &=_{PP} h^{ij}\partial_i\partial_j A_\mu. \end{aligned} \tag{4.39}$$

Since h_{ij} is a smooth Riemannian metric, the character of the flow is governed by the components of $g_{\mu\nu}$ and A_μ diffusing on the spatial geometry h_{ij}, and hence is parabolic. If we take $\tau \neq 1$, we would get another contribution, which is a second order derivative of the metric components, to the gauge field equation in (4.39). However, this wouldn't spoil the parabolicity of A_μ but it just hints at a preferred canonical choice of $\tau = 1$.
We have written this static flow for a general gauge potential A_μ compatible with the static symmetry. However, as emphasized earlier, in general a static potential will have a stress tensor that is only stationary, but not static due to a Poynting energy flux being generated when both (static) electric and magnetic fields are present. Thus, here we take the Maxwell potential to be either purely electric, i.e. $A = -\psi dt$, or purely magnetic, so $A = A_i dx^i$. These electric or magnetic forms are consistently preserved by the flow for the DeTurck choice of ξ and the gauge choice in equation (4.38).

From this point on we will term the parabolic Einstein-Maxwell flow in (4.37) of a static spacetime with either magnetic or electric Maxwell field and DeTurck vector ξ and gauge choice Λ as the "magnetostatic or electrostatic Einstein-Maxwell (EM) flow".

4.3 Static EM Flows of Black Hole Spacetimes

We now consider the EM flow on static black hole spacetimes. While the flow is parabolic away from horizons, it isn't clear that it will preserve the smooth structure of a horizon and this is what we aim to demonstrate here. Furthermore, in the extremal case we will see the nice property that the flow of the near horizon geometry decouples from the flow of the exterior of the horizon, as one might expect from extremal black holes.

4.3.1 Static non-extremal black hole spacetimes

The EM flow of static non-extremal black holes is very simple to consider, being similar to the discussion for Ricci flow. In fact, for Ricci flow one may simply perform a Euclidean continuation of a static metric, identifying the period of the Euclidean time coordinate so that the Euclidean manifold becomes smooth at the horizon. Since Ricci flow of this Euclidean geometry preserves the $U(1)$ isometry associated to the static symmetry, it is obvious that the smoothness of the horizon is preserved.
However, in the case of the EM flow a gauge field with electric potential component cannot generally be analytically continued to Euclidean time. Hence, we will use a different argument, namely that of [113, 114], which exploits the similarity between a static Killing horizon and the origin of a polar coordinate system. Following [113, 114] the most general smooth static symmetric metric with a Killing horizon associated to the surface gravity κ (with respect to the Killing vector $\partial/\partial t$) can be written in coordinates $x^\mu = (t, r, x^a)$ adapted to the static symmetry and horizon as

$$ds^2 = -r^2 V dt^2 + U(dr + rU_a dx^a)^2 + h_{ab} dx^a dx^b \tag{4.40}$$

where $r = 0$ is the horizon. Moreover, V, U, U_a, h_{ab} are all smooth functions of r^2 and of x^a with $V, U > 0$ and h_{ab} is a Riemannian metric. At the horizon there is the additional condition that

$$\big(V - \kappa^2 U\big)\big|_{r=0} = 0. \tag{4.41}$$

Then making the coordinate transformation $\alpha = r \sinh \kappa t$, $\beta = r \cosh \kappa t$ (analogous to that going from polar to Cartesian coordinates) one finds a metric tensor

with smooth components and non-vanishing determinant.
The most general symmetric two-tensor, that is also smooth on the Killing horizon, takes a similar form, although with different component functions V, U, U_a and h_{ab} compared to the metric above. These must obey the same smoothness conditions, so being smooth functions of r^2 and of x^a and also satisfying (4.41). But they don't need to have the positivity of V and h_{ab} doesn't have be a Riemannian metric.
Now consider a covector ω. The most general form compatible with the symmetry $\mathrm{Lie}_{\partial/\partial t}\omega = 0$ and with smoothness at the Killing horizon can be written as

$$\omega = r^2\Phi\, dt + rW dr + \omega_a dx^a \tag{4.42}$$

where now Φ, W and the components ω_a are again smooth functions of r^2 and of x^a. We may see this by writing a general smooth vector in the coordinates α and β, introduced above, as

$$\omega = \omega_\alpha d\alpha + \omega_\beta d\beta + \omega_a dx^a \tag{4.43}$$

where ω_α, ω_β, ω_a are smooth functions of α, β and x^a. Then transforming back to t and r coordinates we obtain

$$\omega = \kappa r\left(\omega_\alpha \cosh\kappa t + \omega_\beta \sinh\kappa t\right) dt + \left(\omega_\alpha \sinh\kappa t + \omega_\beta \cosh\kappa t\right) dr + \omega_a dx^a. \tag{4.44}$$

In order to have the static symmetry, we see that these components should have no explicit t dependence. Noting that a smooth function f of α and β, which obeys $\partial_t f = 0$, must be a function of $\beta^2 - \alpha^2 = r^2$. Then we see the behaviour of ω_α and ω_β is constrained to go as

$$\begin{aligned} \omega_\alpha &= -\alpha W(r^2, x^a) + \frac{1}{\kappa}\beta\Phi(r^2, x^a) \\ \omega_\beta &= -\frac{1}{\kappa}\alpha\Phi(r^2, x^a) + \beta W(r^2, x^a) \end{aligned} \tag{4.45}$$

for $\Phi(r^2, x^a)$, $W(r^2, x^a)$ smooth functions of r^2 and x^a which yields the form in equation (4.42) above.
Then a gauge field A, which is purely electric, compatible with the static symmetry and smooth on the Killing horizon, will take the form

$$A = r^2\Phi\, dt \tag{4.46}$$

(after a gauge transformation to remove any spatial components). In the purely magnetic case, it will take the form

$$A = rW dr + \omega_a dx^a. \tag{4.47}$$

We take the reference metric to be some smooth spacetime with a coinciding Killing horizon at $r = 0$ with the same surface gravity, so

$$\bar{g}_{\mu\nu}dx^\mu dx^\nu = -r^2\bar{V}dt^2 + \bar{U}(dr + r\bar{U}_a dx^a)^2 + \bar{h}_{ab}dx^a dx^b \tag{4.48}$$

such that $\bar{V}$, $\bar{U}$, $\bar{U}_a$ and $\bar{h}_{ab}$ obey the same conditions as the corresponding component functions of the metric. Being static, then staticity with respect to $\partial/\partial t$ is preserved by the flow. Likewise the electric or magnetic form of the gauge potential is also preserved.[2]

Translating to α and β coordinates, all the tensors are smooth in the coordinates α, β, x^a and compatible with the symmetry $\partial/\partial t$. Now consider the flow equations. The tensors derived from the metric, the reference metric and the gauge field, the curvature and the field strengths and the various Lie derivative and gauge transform terms will also all be smooth and respect the symmetry. Combining these into the right-hand sides of the flow equations will again yield a smooth symmetric two tensor and a smooth symmetric covector. Since these respect the static symmetry and are smooth in α, β, then returning to t, r, x^a coordinates, they will take the smooth forms discussed above, and thus the smooth form of the metric and gauge field will be preserved by the flow. In particular, the constant surface gravity κ with respect to $\partial/\partial t$ will be preserved by the flow which directly implies that the temperature associated to the black hole remains unchanged.

4.3.2 Conserved charges under EM flow

Since black holes can carry charges, we may wonder whether any charges or potentials are conserved by the static EM flow. Let us consider first the electric flow in asymptotically flat spacetimes. We take the asymptotic boundary condition that the metric and the reference metric tend to Minkowski space and the non-vanishing component of the vector field A^t tends to a constant Φ_∞. Thus we have

$$\begin{aligned} ds^2 &\to -dt^2 + dr^2 + r^2\left(d\theta^2 + \sin^2\theta d\phi^2\right) \\ A^t &\to \Phi_\infty \end{aligned} \tag{4.49}$$

as $r \to \infty$. We may interpret Φ_∞ as the electric potential difference of the spacetime, since we have seen that $A^t \to 0$ at black hole horizons. Thus, we see that for black hole spacetimes the electric static EM flow preserves the electric potential difference μ since it is fixed by the asymptotic boundary conditions.

One may ask, does it also preserve the charge? Working to higher order in powers of $1/r$, given a potential of the form

$$A^t = \Phi_\infty + \frac{1}{r}f(\theta,\phi) + O\big(\frac{1}{r^2}\big) \tag{4.50}$$

[2]We note that there is no mixing between these electric and magnetic components since they transform differently under the static $t \to -t$ symmetry.

then the electric charge is

$$Q = \frac{1}{4\pi}\int_{S^2_\infty} \star F = \frac{1}{4\pi}\int d\theta d\phi \sin\theta f(\theta,\phi) \tag{4.51}$$

where the integral is taken over the 2-sphere at infinite radius. Naively it appears that this electric charge is also fixed in flow time since one may simply show that

$$\dot{A}^t = O\left(\frac{1}{r^2}\right). \tag{4.52}$$

and thus the leading $1/r$ term in A^t is not affected by the flow. This is similar to the observation in [120] that the ADM mass of a static spacetime is invariant under Ricci flow since again the leading asymptotic fall-off is not corrected.
While technically correct, we argue that this is not physically the correct picture. A counter example in our context that we discussed earlier is that we may Ricci flow from the Schwarzschild black hole to flat spacetime (via a topology change). So clearly we should physically expect that the mass changes.[3] The resolution is that there are different ways to compute charges or masses during a flow. Charges are defined far away from the system of interest and, thus, there are two limits we are concerned with, namely large radius and large flow times. Depending on the ordering of these limits we may obtain a definition of charge that doesn't vary with flow time or one that does. If we define charge at fixed finite flow time and infinite radius, we don't allow the charge to vary in a finite flow time as information from the interior of the system cannot propagate out to infinity. On the other hand, if we define charges on a very large but formally finite sphere, these charges may vary at sufficiently late times in the flow. This is analogous to the discussion in [120] where, although the ADM mass is fixed during Ricci flow, quasi-local masses do evolve.
This may be precisely illustrated with a simple example given by the following exact solution to diffusion in flat Euclidean 3d space

$$F(\lambda,\vec{x}) = \frac{1}{|\vec{x}|}\int_0^\infty d\omega \tilde{F}(\omega) e^{-\omega\lambda}\sin\left(|\vec{x}|\sqrt{\omega}\right) \tag{4.53}$$

where $\vec{x}$ are the usual Euclidean coordinates, λ is diffusion flow time and $\tilde{F}(\omega)$ is the integral transform of the initial data at $\lambda = 0$. We consider an initial profile given by

$$\tilde{F}(\omega) = \begin{cases} \frac{1}{\pi\omega} & \omega < 1/L \\ 0 & \omega \geq 1/L \end{cases} \tag{4.54}$$

[3] One might be tempted to say that this is associated to the surgery required to change topology, but this is not the case as the surgery is local to the region in the interior where the singularity develops as the horizon shrinks and does not affect the asymptotics at all.

and then the p-th flow time derivative at $\lambda = 0$ is

$$\left.\frac{d^p}{d\lambda^p}F(\lambda,\vec{x})\right|_{\lambda=0} = \begin{cases} \frac{1}{r} + O\left(1/r^2\right) & p = 0 \\ -\frac{1}{r^2}\frac{2(-1)^p \cos\left(r/\sqrt{L}\right)}{\pi\sqrt{L}^{2p-1}} + O\left(1/r^3\right) & p > 0. \end{cases} \tag{4.55}$$

Since $F(0,\vec{x}) \sim 1/r$, but $\left.\frac{d^p}{d\lambda^p}F(\lambda,\vec{x})\right|_{\lambda=0} \sim 1/r^2$ for any $p > 0$, we see that the asymptotic $\sim 1/r$ behaviour persists unchanged at finite flow time, so that $F(\lambda,\vec{x}) \sim 1/r$. However, it is quite evident that pointwise, so at any fixed position $\vec{x}$, we have $F(\lambda,\vec{x}) \to 0$ as $\lambda \to \infty$. In diffusion we know that it will take a diffusion time $\lambda \sim r^2$ to effect a change on the scale r. Thus, while formally at finite flow time the $1/r$ coefficient will remain unchanged, if we actually look at some very large, but finite fixed radius, and ask how the diffusion field looks at late flow times, it will tend to zero, as will all its spatial derivatives. Formally for any point $\vec{x}$ we have

$$\lim_{\lambda\to\infty} \partial_{i_1}\partial_{i_2}\ldots\partial_{i_n}F(\lambda,\vec{x}) = 0 \tag{4.56}$$

for any number of derivatives $n \geq 0$.
Let us return to the context of the electric static EM flow. The charge is fixed for finite flow times if we compute it from the formula above (i.e. from the $1/r$ fall-off). However, if instead we compute it as the charge inside some very large radius R

$$Q = \frac{1}{4\pi}\int_{S^2_{r=R}} \star F, \tag{4.57}$$

this will closely approximate the charge computed with the original definition for early times, $\lambda \ll R^2$, but then will change and deviate from this definition if we wait for a sufficiently long flow time, $\lambda \sim R^2$. With this more physical definition of charge, we conclude that for the electric static EM flow the electric potential is fixed as a boundary condition and the charge will vary with flow time.
The converse holds for the magnetic static EM flow. Here we asymptotically have the boundary condition that

$$A_a \to A_a(\theta,\phi) \tag{4.58}$$

for large r, where $x^a = (\theta,\phi)$ and $A_a(\theta,\phi)$ is a fixed covector field on the 2-sphere at infinity. We may regard this as a "Dirichlet" boundary condition for the magnetic potential as $r \to \infty$. The magnetic charge is now computed as

$$Q_{mag} = \frac{1}{4\pi}\int_{S^2_\infty} F = \frac{1}{4\pi}\int d\theta d\phi \left(\partial_\theta A_\phi - \partial_\phi A_\theta\right) \tag{4.59}$$

and thus it is fixed by the asymptotic data A_a. As it is the leading behaviour of A_a that determines this magnetic charge in the large r limit, we emphasize that

this remains fixed independent of whether we evaluate the charge integral strictly in the infinite radius limit or instead at some very large but finite radius R.
Thus, in summary, the electrostatic EM flow preserves the electric potential as a boundary condition (but not electric charge), and the magnetostatic EM flow preserves the magnetic charge as a boundary condition. Both flows preserve the surface gravity. We will return to this point later when drawing an analogy between the behaviour of these flows starting with an RN black hole and the thermodynamic stability of the RN solution.

4.3.3 Static extremal black hole spacetimes

Already for Ricci flow it is far less obvious that the flow is compatible with preserving a static smooth extremal horizon. We begin our discussion by considering the flow of the metric. Then, we will consider adding the gauge field, which is either purely electric or purely magnetic.
Following [121] a general static extremal horizon can be written as

$$ds^2 = -r^2 e^T dt^2 + e^R \left(\frac{dr}{r} + r\omega_a dx^a \right)^2 + \gamma_{ab} dx^a dx^b \tag{4.60}$$

where $r = 0$ is the horizon and crucially T, R, ω_a and γ_{ab} are smooth functions of r and x^a there. Furthermore, T and R obey

$$\begin{aligned} (T-R)|_{r=0} &= 0 \\ \partial_r (T-R)|_{r=0} &= \psi \end{aligned} \tag{4.61}$$

where ψ is some constant depending on the geometry. The near horizon geometry is then given by the limit as $r \to 0$

$$ds^2_{NH} = e^T \left(-r^2 dt^2 + \frac{dr^2}{r^2} \right) + \gamma_{ab} dx^a dx^b \tag{4.62}$$

which is a (warped) product of AdS_2 with the horizon 2-geometry γ_{ab}. Suppose we flow the metric by a symmetric tensor $A_{\mu\nu}$ so that

$$\frac{d}{d\lambda} g_{\mu\nu} = A_{\mu\nu}. \tag{4.63}$$

Then we should have that the form above is preserved. In order for this to hold, the tensor $A_{\mu\nu}$ must have an analogous form to that of the metric, namely

$$A_{\mu\nu} = \begin{pmatrix} -r^2 \hat{A}_{tt} & 0 & 0 \\ & \frac{1}{r^2} \hat{A}_{rr} & \hat{A}_a \\ & & \hat{A}_{ab} + r^2 \hat{A}_a \hat{A}_b \end{pmatrix} \tag{4.64}$$

so that the component functions $\hat{A}_{tt}, \hat{A}_{rr}, \hat{A}_a, \hat{A}_{ab}$ are smooth in r and x^a. Then to preserve the metric smoothness conditions (4.61), we further require

$$\begin{aligned} \left(\hat{A}_{tt} - \hat{A}_{rr}\right)\Big|_{r=0} &= 0 \\ \partial_r(\hat{A}_{tt} - \hat{A}_{rr})\Big|_{r=0} &= \psi\, \hat{A}_{tt}\Big|_{r=0}. \end{aligned} \tag{4.65}$$

This tensor is now also smooth on the Lorentzian spacetime. Linearly combining such tensors satisfying (4.65) with the same value of ψ yields again smooth symmetric tensors (also with the same value of ψ) and contracting their indices with the metric gives also a smooth function of r and x^a.
The near horizon limit of this smooth tensor exists and is given as

$$A^{NH}_{\mu\nu} = \begin{pmatrix} -r^2 A^{NH}(x^a) & 0 & 0 \\ & \frac{1}{r^2} A^{NH}(x^a) & 0 \\ & & A^{NH}_{ab}(x^a) \end{pmatrix} \tag{4.66}$$

where the components are defined from those of the original tensor at $r = 0$ as

$$\begin{aligned} A^{NH}(x^a) &= \hat{A}_{tt}(r, x^a)\Big|_{r=0} \\ A^{NH}_{ab}(x^a) &= \hat{A}_{ab}(r, x^a)\Big|_{r=0} \end{aligned} \tag{4.67}$$

and may be thought of as a scalar and symmetric 2-tensor respectively, defined on the 2-dimensional near horizon spatial geometry γ_{ab}.
The static EM flow updates both the metric and gauge field by the sum of several terms and we now consider these individually, showing that smoothness is preserved.

Ricci Tensor Term

We now show that the Ricci tensor of this geometry is smooth. This implies that flowing the metric by the Ricci tensor preserves smoothness. This analysis is simplified by noting that we may use residual coordinate freedom to choose ω_a to vanish in the metric (4.60). Explicitly we may write (4.60) as

$$\begin{aligned} ds^2 = &- r^2 e^T dt^2 + e^R \left(1 - r^2 w_a w^a e^R\right) \frac{dr^2}{r^2} \\ &+ \gamma'_{ab} \left(dx^a + e^R w^a dr\right) \left(dx^b + e^R w^b dr\right) \end{aligned} \tag{4.68}$$

where $\gamma'_{ab} = \gamma_{ab} + e^R r^2 w_a w_b$ and w^a is defined by $w_a = \gamma'_{ab} w^b$. We now take a new coordinate $y^a(r, x)$ which obeys the following linear differential equation

$$\partial_r y^a = e^R w^b \partial_b y^a. \tag{4.69}$$

This may be solved by taking boundary conditions $y^a = x^a$ at $r = 0$ and then integrating in r starting from the surface $r = 0$. Since the components of $e^R w^a$ are smooth in r and x^a, this will have smooth solutions and the inverse transformation $y^a \to x^a$ will also exist (at least locally near $r = 0$). These coordinates then yield a metric of our desired form

$$\begin{aligned} ds^2 &= -r^2 e^T dt^2 + e^{R'} \frac{dr^2}{r^2} + \gamma''_{ab} dy^a dy^b \\ \gamma''_{ab} &= \gamma'_{cd} \left.\frac{\partial x^c}{\partial y_a}\right|_r \left.\frac{\partial x^d}{\partial y_b}\right|_r \end{aligned} \tag{4.70}$$

where $e^{R'} = e^R \left(1 - r^2 w_a w^a e^R\right)$. An important fact we will use later is that, since $y^a \simeq x^a$ near $r = 0$, the near horizon metric is unchanged by this transformation. Furthermore, the near horizon form of any other smooth tensor is also unchanged. Now proceeding we will assume we have taken the above coordinates so that our extremal metric can be written as

$$ds^2 = -r^2 e^T dt^2 + e^R \frac{dr^2}{r^2} + \gamma_{ab} dx^a dx^b \tag{4.71}$$

without the off-diagonal w_a terms. Then by direct calculation one can obtain the Ricci tensor

$$R_{\mu\nu} = \begin{pmatrix} -r^2 \hat{R}_{tt} & 0 & 0 \\ & \frac{1}{r^2}\hat{R}_{rr} & \hat{R}_a \\ & & \hat{R}_{ab} + r^2 \hat{R}_a \hat{R}_b \end{pmatrix}. \tag{4.72}$$

We define $K_{ab} = \partial_r \gamma_{ab}$ and $K = \gamma^{ab} K_{ab}$. For fixed r then γ_{ab} is a 2-metric, whose covariant derivative we denote as $\tilde{\nabla}$ and whose Ricci tensor we write as $R^{(\gamma)}_{ab}$. Moreover, we decompose the following expressions covariantly over this r-dependent 2-geometry γ_{ab} and emphasise that Latin indices are raised/lowered with respect to γ_{ab}. Then we may write

$$\begin{aligned} \hat{R}_{tt} &= e^{T-R}\left(e^R Q_0 + r Q_1 + r^2 Q_2\right) \\ \hat{R}_{rr} &= \left(e^R W_0 + r Q_1 + r^2 W_2\right) \\ \hat{R}_a &= \frac{1}{r}\left(U^0_a + r U^1_a\right) \\ \hat{R}_{ab} + r^2 \hat{R}_a \hat{R}_b &= e^{-R}\left(e^R V^0_{ab} + r V^1_{ab} + r^2 V^2_{ab}\right) \end{aligned} \tag{4.73}$$

where

$$\begin{aligned} Q_0 &= -\frac{1}{2}\tilde{\nabla}^2 T - \frac{1}{4}(\tilde{\nabla} T)^2 - \frac{1}{4}\tilde{\nabla}_a T \tilde{\nabla}^a R - e^{-R} \\ W_0 &= -\frac{1}{2}\tilde{\nabla}^2 R - \frac{1}{4}(\tilde{\nabla} R)^2 - \frac{1}{4}\tilde{\nabla}_a T \tilde{\nabla}^a R - e^{-R} \end{aligned}$$

$$U^0_a = -\frac{1}{2}\tilde{\nabla}_a(T-R) \tag{4.74}$$

and

$$\begin{aligned} Q_1 &= -\frac{3}{2}\partial_r T + \frac{1}{2}\partial_r R - \frac{1}{2}K \\ U^1_a &= -\frac{1}{2}\partial_r \tilde{\nabla}_a T - \frac{1}{4}\partial_r T\tilde{\nabla}_a(T-R) + \frac{1}{4}K\tilde{\nabla}_a R \\ &\quad + \frac{1}{4}K_{ab}\tilde{\nabla}^b(T-R) - \frac{1}{2}\tilde{\nabla}_a K + \frac{1}{2}\tilde{\nabla}^b K_{ab} \end{aligned} \tag{4.75}$$

and where

$$\begin{aligned} Q_2 &= -\frac{1}{2}\partial_r^2 T - \frac{1}{4}(\partial_r T)^2 + \frac{1}{4}(\partial_r T)(\partial_r R) - \frac{1}{4}(\partial_r T)K \\ W_2 &= -\frac{1}{2}\partial_r^2 T - \frac{1}{4}(\partial_r T)^2 + \frac{1}{4}(\partial_r T)(\partial_r R) + \frac{1}{4}(\partial_r R)K - \frac{1}{2}\partial_r K - \frac{1}{4}K_{ab}K^{ab} \end{aligned} \tag{4.76}$$

and then finally

$$\begin{aligned} V^0_{ab} &= R^{(\gamma)}_{ab} - \frac{1}{2}\tilde{\nabla}_a\tilde{\nabla}_b T - \frac{1}{2}\tilde{\nabla}_a\tilde{\nabla}_b R - \frac{1}{4}\tilde{\nabla}_a T\tilde{\nabla}_b T - \frac{1}{4}\tilde{\nabla}_a R\tilde{\nabla}_b R \\ V^1_{ab} &= -K_{ab} \\ V^2_{ab} &= -\frac{1}{2}\partial_r K_{ab} + \frac{1}{4}KK_{ab} - \frac{1}{4}K_{ab}\partial_r(T-R) + \frac{1}{4}\gamma_{ab}\left(K^{cd}K_{cd} - K^2\right). \end{aligned} \tag{4.77}$$

First, one can check that $\hat{R}_a$ is in fact a smooth function of r, even though naively it appears to go as $O(1/r)$, due to the fact that $T = R$ at $r = 0$ so U^0_a vanishes at $r = 0$. The other components $\hat{R}_{tt}$, $\hat{R}_{rr}$, $\hat{R}_{ab}$ are then clearly smooth in r and x^a. Secondly, one can explicitly confirm that the smoothness conditions (4.65) indeed hold by virtue of the behaviour of the metric functions.
Furthermore, we see that the near horizon geometry of the Ricci tensor is given by

$$R^{NH}_{\mu\nu} = \begin{pmatrix} -r^2 R^{NH} & 0 & 0 \\ & \frac{1}{r^2}R^{NH} & 0 \\ & & R^{NH}_{ab} \end{pmatrix} \tag{4.78}$$

where

$$\begin{aligned} R^{NH} &= e^T\left(-\frac{1}{2}\tilde{\nabla}^2 T - \frac{1}{2}(\tilde{\nabla}T)^2 - e^{-T}\right) \\ R^{NH}_{ab} &= R^{(\gamma)}_{ab} - \tilde{\nabla}_a\tilde{\nabla}_b T - \frac{1}{2}\tilde{\nabla}_a T\tilde{\nabla}_b T. \end{aligned} \tag{4.79}$$

Clearly the near horizon geometry only depends on the intrinsic geometry and not on any r derivatives at the horizon $r = 0$. Thus, we see that the Ricci tensor term in our EM flow equation for the metric indeed preserves the extremal horizon structure.

DeTurck Diffeomorphism Term

Now we consider the diffeomorphism term $\nabla_{(\mu}\xi_{\nu)}$ in the metric flow equation. In order to keep the metric static and preserve $g_{tr} = g_{ta} = 0$ during the flow, the diffeomorphism vector field must have $\xi^t = 0$ and the remaining components cannot depend on t. Additionally, for the diffeomorphism to preserve the extremal horizon we find that it must take the form

$$\xi^\mu = \left(0, r^2 f, v^a\right) \tag{4.80}$$

where f and v^a are smooth functions of r and x^a. The vanishing ξ^r component at $r = 0$ implies that the position of the horizon is not changed in the flow, as one would expect. Perhaps less obvious is that this component must vanish quadratically in r as the following expressions show

$$\nabla_{(\mu}\xi_{\nu)} = \begin{pmatrix} -r^2\hat{A}_{tt} & 0 & 0 \\ & \frac{1}{r^2}\hat{A}_{rr} & \hat{A}_a \\ & & \hat{A}_{ab} + r^2\hat{A}_a\hat{A}_b \end{pmatrix} \tag{4.81}$$

where we have

$$\begin{aligned} \hat{A}_{tt} &= e^T\left(\frac{1}{2}v^a\tilde{\nabla}_a T + rf + \frac{1}{2}r^2 f\partial_r T\right) \\ \hat{A}_{rr} &= e^R\left(\frac{1}{2}v^a\tilde{\nabla}_a R + rf + r^2\left(\frac{1}{2}f\partial_r R + \partial_r f\right)\right) \\ \hat{A}_a &= \frac{1}{2}e^R\tilde{\nabla}_a f + \frac{1}{2}\gamma_{ab}\partial_r v^b \\ \hat{A}_{ab} + r^2\hat{A}_a\hat{A}_b &= \tilde{\nabla}_{(a}v_{b)} + \frac{r^2}{2}fK_{ab}\ . \end{aligned} \tag{4.82}$$

In particular, $\hat{A}_a$ would be singular, going as $\sim 1/r$ if $\xi^r \sim r$ rather than quadratically in r.[4] One can check that this indeed obeys the smoothness conditions (4.65). The near horizon form is then

$$\left(\nabla_{(\mu}\xi_{\nu)}\right)^{NH} = \begin{pmatrix} -r^2 A^{NH} & 0 & 0 \\ & \frac{1}{r^2}A^{NH} & 0 \\ & & A^{NH}_{ab} \end{pmatrix} \tag{4.83}$$

[4]We note that while a general behaviour $\xi^r = rf(r, x^a)$ for f smooth in its arguments would be singular, it seems possible to have $\xi^r = rc + r^2 f(r, x^a)$ with c a constant. However, as we discuss shortly, the DeTurck vector component ξ^r does not have such a linear in r leading behaviour. Thus, we drop this contribution.

with

$$\begin{aligned} A^{NH} &= \frac{1}{2} e^T v^a \tilde{\nabla}_a T \Big|_{r=0} \\ A^{NH}_{ab} &= \tilde{\nabla}_{(a} v_{b)} \Big|_{r=0} \end{aligned} \tag{4.84}$$

and we see this only depends on v^a and not on f. We may check that the DeTurck choice of diffeomorphism indeed gives the above form for ξ^μ in (4.80). Recall that

$$\xi^\mu = g^{\alpha\beta} \left(\Gamma^\mu_{\ \alpha\beta} - \bar{\Gamma}^\mu_{\ \alpha\beta} \right) \tag{4.85}$$

with the reference connection being the Levi-Civita connection of a smooth static reference metric

$$d\bar{s}^2 = -r^2 e^{\bar{T}} dt^2 + e^{\bar{R}} \left(\frac{dr}{r} + r\bar{\omega}_a dx^a \right)^2 + \bar{\gamma}_{ab} dx^a dx^b \tag{4.86}$$

where $\bar{T}$, $\bar{R}$, $\bar{\omega}_a$ and $\bar{\gamma}_{ab}$ obey the same restrictions as their counterparts in the actual metric. In particular, we also need to have $\psi = \bar{\psi}$ in order to obtain a smooth extremal horizon when adding up tensors composed from the actual and the reference metric. We emphasize that while we have chosen to use our coordinate freedom to eliminate the $drdx^a$ terms in the metric for these calculations, this generally will not eliminate those terms in the reference metric.
One then finds the DeTurck vector field indeed has the form required for a diffeomorphism that preserves the extremal horizon, as in equation (4.80). It may explicitly be checked that $\xi^t = 0$ and that the component ξ^r goes as

$$\xi^r = r e^{-R} \left(\frac{e^{\bar{T}-\bar{R}}}{e^{T-R}} - 1 \right) + O(r^2). \tag{4.87}$$

This naively looks to only vanish as $\sim r$ rather than $\sim r^2$ at the horizon. However, due to the smoothness of the metric and reference metric, and hence $T - R = \bar{T} - \bar{R} = 0$ at $r = 0$, this expression actually goes as $O(r^2)$, as in equation (4.80). Finally one finds that

$$\begin{aligned} \xi^a = &- \frac{1}{2} \gamma^{ab} \tilde{\nabla}_b (T + R) + \frac{1}{2} e^{\bar{T}-T} \bar{\gamma}^{ab} \tilde{\nabla}_b \bar{T} \\ &+ \frac{1}{2} e^{\bar{R}-R} \bar{\gamma}^{ab} \tilde{\nabla}_b \bar{R} + \gamma^{bc} \left(\tilde{\Gamma}^a_{\ bc} - \bar{\tilde{\Gamma}}^a_{\ bc} \right) + O(r) \end{aligned} \tag{4.88}$$

where $\tilde{\Gamma}^a_{\ bc}$ and $\bar{\tilde{\Gamma}}^a_{\ bc}$ are the (Levi-Civita) connections of the horizon 2-metric γ_{ab} and reference metric $\bar{\gamma}_{ab}$ respectively. Moreover, let us emphasise that indices are raised/lowered with respect to γ_{ab} and not $\bar{\gamma}_{ab}$.

Hence, on the horizon $r = 0$ the 2d vector inducing the near horizon diffeomorphism is

$$v^a = e^{\bar{T}-T}\bar{\gamma}^{ab}\tilde{\nabla}_b\bar{T} - \gamma^{ab}\tilde{\nabla}_b T + \gamma^{bc}\left(\tilde{\Gamma}^a{}_{bc} - \bar{\tilde{\Gamma}}^a{}_{bc}\right). \tag{4.89}$$

Having discussed the Ricci tensor and DeTurck diffeomorphism terms for a static extremal horizon and shown they give smooth tensors we now see that DeTurck-Ricci flow will preserve the smooth structure of a static extremal horizon. Moreover, we may take the near horizon limit of the flow to obtain a geometric flow of the near horizon geometry. This near horizon flow will be independent of the details of the geometry away from the horizon depending only on the intrinsic geometry of the horizon itself.
Now we turn to the remaining parts in the static EM flow. These are the Maxwell field and its flow and also its backreaction terms in the metric flow equation. We will consider the purely electric and magnetic cases separately.

The electric Maxwell field

A purely electric potential is preserved under the EM flow. We find that smoothness for the Maxwell field on the static extremal horizon geometry implies that a pure electric potential takes the form,

$$A = r\Phi(r, x^a)dt \tag{4.90}$$

where the potential function Φ is smooth in r and x^a. Note that the electric potential vanishes at the horizon which is necessary for the vector field A^μ to have finite norm. Further, as we will see, in order for the field strength $F_\mu{}^\alpha F_{\nu\alpha}$ term in the flow to preserve the extremal metric we require

$$\tilde{\nabla}_a\Phi\Big|_{r=0} = 0 \tag{4.91}$$

so that Φ is constant over the horizon. The right-hand side of the Maxwell field equation in the static EM flow (for a diffeomorphism of the form (4.80)) can be decomposed as

$$\begin{aligned}
\nabla^\mu F_{\mu t} + \mathrm{Lie}_\xi A_t &= rQ_0 + r^2 e^{-R}Q_1 + r^3 e^{-R}Q_2 \\
Q_0 &= \tilde{\nabla}^2\Phi - \frac{1}{2}\tilde{\nabla}^a(T-R)\tilde{\nabla}_a\Phi + v^a\tilde{\nabla}_a\Phi \\
Q_1 &= 2\partial_r\Phi + \frac{1}{2}\Phi\left(K - \partial_r(T+R)\right) + e^R f\Phi \\
Q_2 &= \partial_r^2\Phi + \frac{1}{2}\left(K - \partial_r(T+R)\right)\partial_r\Phi + e^R f\partial_r\Phi
\end{aligned} \tag{4.92}$$

with the r- and a-components vanishing. Note that these terms preserve the form of the electric potential. In particular, the condition (4.91) is perfectly consistent

with the above. Hence, the value of Φ on the horizon will be constant over the 2-geometry and will remain unchanged in flow time. Then taking the near horizon limit, the electric gauge potential is just given by

$$A^{NH} = r\Phi^{NH}dt \tag{4.93}$$

for constant $\Phi^{NH} = \Phi(0, x^a)$ and is fixed along the flow. It thus generates a constant radially directed electric field F^{NH}_{tr} on the horizon. The charge enclosed by the horizon is then simply proportional to its horizon area.
We note that the flow gauge transformation term $\partial_\mu\Lambda$ is trivial here because $\Lambda = \nabla_\alpha A^\alpha$ (remember $\tau = 1$) vanishes for a static electric potential.
Finally, the Maxwell field backreacts on the metric flow via the symmetric tensor $F_\mu{}^\alpha F_{\nu\alpha}$ and its trace. We find

$$F_\mu{}^\alpha F_{\nu\alpha} = \begin{pmatrix} -r^2\hat{A}_{tt} & 0 & 0 \\ & \frac{1}{r^2}\hat{A}_{rr} & \hat{A}_a \\ & & \hat{A}_{ab} + r^2\hat{A}_a\hat{A}_b \end{pmatrix} \tag{4.94}$$

where

$$\begin{aligned} \hat{A}_{tt} &= -\tilde{\nabla}_a\Phi\tilde{\nabla}^a\Phi - e^{-R}\partial_r(r\Phi)\partial_r(r\Phi) \\ \hat{A}_{rr} &= -e^{-T}\partial_r(r\Phi)\partial_r(r\Phi) \\ \hat{A}_a &= -\frac{1}{r}e^{-T}\partial_r(r\Phi)\tilde{\nabla}_a\Phi \\ \hat{A}_{ab} + r^2\hat{A}_a\hat{A}_b &= -e^{-T}\tilde{\nabla}_a\Phi\tilde{\nabla}_b\Phi. \end{aligned} \tag{4.95}$$

Note we see the previously claimed condition (4.91) is required for $(\hat{A}_{tt} - \hat{A}_{rr})$ to vanish on the horizon and one can directly check then that the remaining smoothness constraint in equation (4.65) holds.
Since $F_\mu{}^\alpha F_{\nu\alpha}$ is smooth, its trace with respect to the metric will be too, and so will be the backreaction term $F_\mu{}^\alpha F_{\nu\alpha} - \frac{1}{4}g_{\mu\nu}F^2$ in the metric equation of the EM flow.

The magnetic Maxwell field

Now we turn to the purely magnetic case. We assume our magnetic Maxwell field to take the following form

$$A = b_r(r, x^a)dr + b_a(r, x^a)dx^a \tag{4.96}$$

where b_r and b_a are smooth functions in r and x^a. Now also remember that we took the choice $\tau = 1$, as it seems to be the preferred choice. The form for the magnetic Maxwell field is preserved by the flow equations which are given by

$$\tau\nabla^\mu F_{\mu r} + \mathrm{Lie}_\xi A_r = Q_0 + rQ_1 + r^2Q_2$$

$$\begin{aligned} Q_0 &= \tau\tilde{\nabla}^a F_{ar} + \frac{\tau}{2}\tilde{\nabla}^a(T-R)F_{ar} + v^a\tilde{\nabla}_a b_r + b_a\partial_r v^a \\ Q_1 &= 2b_r f \\ Q_2 &= f\partial_r b_r + b_r\partial_r f \end{aligned} \tag{4.97}$$

$$\begin{aligned} \tau\nabla^\mu F_{\mu a} + \mathrm{Lie}_\xi A_a &= Q_0 + re^{-R}Q_1 + r^2e^{-R}Q_2 \\ Q_0 &= \tau\tilde{\nabla}^b F_{ba} + \frac{\tau}{2}\tilde{\nabla}^b(T+R)F_{ba} + \mathrm{Lie}_v b_a \\ Q_1 &= 2\tau F_{ra} \\ Q_2 &= -\tau\partial_r F_{ra} + \frac{\tau}{2}\partial_r(T-R)F_{ra} + \frac{\tau}{2}KF_{ra} + \tau\gamma^{bc}K_{ba}F_{cr} \\ &\quad + e^R f\partial_r b_a + e^R b_r\tilde{\nabla}_a f \end{aligned} \tag{4.98}$$

with the t-component being trivial. The gauge fixing term $\partial_\mu\Lambda$ is determined by Λ which takes the form

$$\begin{aligned} \Lambda = \nabla_\mu A^\mu &= \Lambda_0 + re^{-R}\Lambda_1 + r^2e^{-R}\Lambda_2 \\ \Lambda_0 &= \tilde{\nabla}_a b^a + \frac{1}{2}\tilde{\nabla}^a(T+R)b_a \\ \Lambda_1 &= 2b_r \\ \Lambda_2 &= \frac{1}{2}(\partial_r(T-R)+K)b_r + \partial_r b_r \end{aligned} \tag{4.99}$$

so we see this is also a smooth function. It is then clear that the covector given by its gradient, namely $\partial_\mu\Lambda$, then preserves the form of the gauge field (4.96) with its contribution to the flow.
Now we turn to the contribution in metric flow equation, so the term $F_\mu{}^\alpha F_{\nu\alpha}$ gives

$$F_\mu{}^\alpha F_{\nu\alpha} = \begin{pmatrix} -r^2\hat{A}_{tt} & 0 & 0 \\ & \frac{1}{r^2}\hat{A}_{rr} & \hat{A}_a \\ & & \hat{A}_{ab} + r^2\hat{A}_a\hat{A}_b \end{pmatrix} \tag{4.100}$$

where

$$\begin{aligned} \hat{A}_{tt} &= 0 \\ \hat{A}_{rr} &= r^2\gamma^{ab}F_{ra}F_{rb} \\ \hat{A}_a &= \gamma^{bc}F_{rb}F_{ac} \\ \hat{A}_{ab} + r^2\hat{A}_a\hat{A}_b &= \gamma^{cd}F_{ac}F_{bd} + r^2e^{-R}F_{ra}F_{rb} \end{aligned} \tag{4.101}$$

with $F_{ra} = \partial_r b_a - \tilde{\nabla}_a b_r$ and $F_{ab} = \tilde{\nabla}_a b_b - \tilde{\nabla}_b b_a$. Because we have $\hat{A}_{tt} = 0$ and $\hat{A}_{rr} \sim O(r^2)$, the smoothness conditions in (4.65) are trivially fulfilled. Hence, the backreaction of the magnetic potential in the metric flow preserves smoothness of

the extremal horizon.
The near horizon limit of the magnetic gauge potential $A = b_r(r, x^b)dr + b_a(r, x^b)dx^a$ at $r = 0$ becomes the 2-vector potential

$$\begin{aligned} A^{NH} &= b_a^{NH}(x^b)dx^a \\ b_a^{NH}(x^b) &= b_a(0, x^b) \end{aligned} \tag{4.102}$$

which is defined over the 2-geometry γ_{ab} of the horizon.

Collecting Terms and the Near Horizon Limit

We have seen above that each term in the static EM flow equations preserves the smoothness of both the extremal horizon and the gauge field. Recall that to simplify the task of computing these terms we have chosen coordinates where the off-diagonal terms w_a vanish. However, we emphasize that having shown smoothness in these simpler coordinates, then guarantees smoothness in more general coordinates where the off-diagonal terms are present.
We will now consider the near horizon limit of the flow. We explicitly showed above that the transformation to remove these off-diagonal terms does not affect the near horizon form of smooth tensors. Thus, having computed the near horizon forms in coordinates, where w_a vanishes, gives their form for any (smooth) choice of coordinates with terms w_a, i.e. the near horizon limit is independent of w_a.
Using the results from before we may take the near horizon limit of the EM flow so that for $r = 0$ we have in the electric case

$$\begin{aligned} \frac{d}{d\lambda}T &= \tilde{\nabla}^2 T + v'^a \tilde{\nabla}_a T + 2e^{-2T}\left(e^T - (\Phi^{NH})^2\right) \\ \frac{d}{d\lambda}\gamma_{ab} &= -2R^{(\gamma)}_{ab} + 2\tilde{\nabla}_{(a}v'_{b)} + \tilde{\nabla}_a T \tilde{\nabla}_b T + 2\gamma_{ab}e^{-2T}(\Phi^{NH})^2 \end{aligned} \tag{4.103}$$

where

$$\begin{aligned} v'^a &= e^{\bar{T}-T}\bar{\gamma}^{ab}\tilde{\nabla}_b\bar{T} + \xi^{(\gamma)a} \\ \xi^{(\gamma)a} &= \gamma^{bc}\left(\tilde{\Gamma}^a{}_{bc} - \bar{\tilde{\Gamma}}^a{}_{bc}\right). \end{aligned} \tag{4.104}$$

In particular, v'^a generates a diffeomorphism along the near horizon flow and has a contribution from the near horizon 2d DeTurck vector $\xi^{(\gamma)a}$. We note that, following our discussion above, the near horizon electric potential Φ^{NH} is simply a constant that doesn't change with flow time. We further note that v'^a differs from the previous v^a above in equation (4.89).
In the magnetic case the near horizon limit of flow takes the following form

$$\frac{d}{d\lambda}T = \tilde{\nabla}^2 T + v'^a \tilde{\nabla}_a T + 2e^{-T} - (F^{NH})^2$$

$$\begin{aligned}\frac{d}{d\lambda}\gamma_{ab} &= -2R^{(\gamma)}_{ab} + 2\tilde{\nabla}_{(a}v'_{b)} + \tilde{\nabla}_a T\tilde{\nabla}_b T + 4F^{NH}_{ac}F^{NH\ c}_{b} - \gamma_{ab}(F^{NH})^2 \\ \frac{d}{d\lambda}b^{NH}_a &= \tilde{\nabla}^b F^{NH}_{ba} + \tilde{\nabla}_a \Lambda^{NH} + \mathrm{Lie}_{v'} b^{NH}_a \end{aligned} \tag{4.105}$$

where $F^{NH}_{ab} = \tilde{\nabla}_a b^{NH}_b - \tilde{\nabla}_b b^{NH}_a$, $\Lambda^{NH} = \tilde{\nabla}^a b_a$, and v'^a is defined as above in the electric case.
The two derivative terms on the right-hand side of both the electric and the magnetic metric flow equations have precisely the correct form to give a parabolic flow for the metric components

$$\begin{aligned}\frac{d}{d\lambda}T &= \gamma^{ab}\partial_a\partial_b T + \dots \\ \frac{d}{d\lambda}\gamma_{ab} &= \gamma^{cd}\partial_c\partial_d\gamma_{ab} + \dots \end{aligned} \tag{4.106}$$

where ... represent lower derivative terms. Thus, the metric components obey coupled diffusion equations governed by the near horizon (inverse) metric γ^{ab}, which is Riemannian and hence gives parabolic flows. We note that it is the 2d near horizon limit of the DeTurck vector that ensures this parabolic flow for the near horizon metric.
For the electric flow the electric potential remains constant. In the magnetic case we see that the principle part of the potential flow is

$$\frac{d}{d\lambda}b_a = \gamma^{cd}\partial_c\partial_d b_a + \dots \tag{4.107}$$

so that it also yields a parabolic flow, due to the gauge fixing term $\tilde{\nabla}_a\Lambda^{NH}$ in equation (4.105).
Away from the horizon we know that the EM flow has a parabolic character. It also preserves the smooth static extremal horizon structure. Thus, we may construct this near horizon flow and then regard its solution as Dirichlet data for the parabolic flow in the exterior of the horizon. This gives a heuristic argument for well-posedness in the presence of an extremal horizon but it would be interesting to develop a rigorous mathematical proof of well-posedness.

4.4 EM Flows about non-extremal RN

Here we want to determine the stability of the electric and magnetic RN black holes which are fixed points of the EM flow, namely they obey $\dot{g}_{\mu\nu} = \dot{A}_\mu = 0$. In order to check that, we need to slightly perturb these solutions and observe whether the evolve back to the fixed point. If they do so, then they are stable fixed points, whereas if they don't, they are unstable fixed points. In the latter case we also want to know were the flow evolves to. Moreover, we will only consider

spherically symmetric perturbations since we strongly expect that these results extrapolate to the general case.
But first, let's setup the flow. We can write a general smooth static spherically symmetric metric as

$$ds^2 = -\rho^2 T(\lambda,\rho)dt^2 + 4r(\rho)^4 A(\lambda,\rho)d\rho^2 + r(\rho)^2 S(\lambda,\rho)d\Omega^2 \tag{4.108}$$

where $d\Omega^2 = d\theta^2 + \sin^2\theta d\phi^2$, ρ is the compactified radial coordinate introduced in section 4.1 related to the usual coordinate as $r = 1/(1-\rho^2)$. Then T, A, S specify the geometry and will depend on flow time λ. Following the discussion in section 4.3.1 they should be smooth functions of ρ^2 at the horizon $\rho = 0$. Flat spacetime in this radial variable ρ takes the form,

$$ds^2_{flat} = -dt^2 + 4r(\rho)^4 d\rho^2 + r(\rho)^2 d\Omega^2 \tag{4.109}$$

and thus we require $T, A, S \to 1$ as $\rho \to 1$ for our metric above to impose the boundary condition that it is asymptotically flat. Please note that (4.109) only covers flat space for $r \geq 1$. Further we require that

$$\left(T - 4\kappa^2 A\right)\Big|_{\rho=0} = 0. \tag{4.110}$$

Then, this spacetime has a smooth non-extremal horizon at $\rho = 0$ with surface gravity κ and, as discussed before, this surface gravity is preserved by the EM flow. Choosing

$$\begin{aligned} T &= F(\rho) \\ A &= F^{-1}(\rho) \\ S &= 1 \\ F(\rho) &= 1 - r_- + r_-\rho^2 \end{aligned} \tag{4.111}$$

then yields the RN metric from section 4.1. Here we have taken $r_+ = 1$ which we will use for the rest of this section. We now make this choice for the reference metric.
Due to static spherical symmetry the most general gauge field must take the form,

$$\begin{aligned} A &= \rho^2\Phi(\lambda,\rho)dt + \rho A_\rho(\lambda,\rho)d\rho + A^{(\Omega)} \\ A^{(\Omega)} &= A_\theta d\theta + A_\phi d\phi \end{aligned} \tag{4.112}$$

where Φ and A_ρ depend on flow time and are smooth functions of ρ^2. Here $A^{(\Omega)}$ is a one-form living on the 2-sphere (so only having $d\theta$ and $d\phi$ components). In order for the field strength of $A^{(\Omega)}$ to preserve the static spherical symmetry, its components A_θ and A_ϕ must have no time or radial dependence. Then, the only choice compatible with spherical symmetry is the potential, $A^{(\Omega)} = -q_B\cos\theta d\phi$ for a constant q_B (or an $SO(3)$ rotation of this). As mentioned previously, in

spherical symmetry we may consistently have both an electric and magnetic field, as both the electric and magnetic field are radial so there is no Poynting energy flux. However, following our previous discussion we will restrict to either, namely the purely electric or the purely magnetic cases. Noting that the radial component is pure gauge, we thus restrict to the forms

$$\begin{aligned} A_{elec} &= \rho^2 \Phi(\lambda, \rho) dt \\ A_{mag} &= -q_B \cos\theta d\phi. \end{aligned} \tag{4.113}$$

with q_B a constant. In the magnetic case we observed previously that the charge is fixed along the flow by boundary conditions and here we see it is given by q_B. In the electric case we require $\Phi(\rho) \to \mu$ as $\rho \to 1$, and then $G \cdot \mu$ gives the electric potential difference between the horizon and infinity (since the potential $A_t \sim \rho^2$ vanishes at the horizon).

4.4.1 Linear Perturbations about RN

We now consider linear perturbations to both these fixed points. To proceed, we expand around the fixed point RN geometry, given by $g_{\mu\nu}^{(RN)}$ and $A_\mu^{(RN)}$, and look for EM flow solutions of the form

$$\begin{aligned} g_{\mu\nu} &= g_{\mu\nu}^{(RN)} + \epsilon e^{\Omega\lambda} \delta g_{\mu\nu} \\ A_\mu &= A_\mu^{(RN)} + \epsilon e^{\Omega\lambda} \delta A_\mu \end{aligned} \tag{4.114}$$

where we linearized in ϵ, Ω is a complex constant and $\delta g_{\mu\nu}$, δA_μ preserve the static spherical symmetry. We expect all such linear "mode" solutions with this exponential flow time dependence provide a basis for the general flow solution and we may regard finding these solutions as an eigenvalue problem, where Ω is the eigenvalue. Mode solutions with $\mathrm{Re}(\Omega) \leq 0$ are stable in flow time and unstable modes have $\mathrm{Re}(\Omega) > 0$. The existence of such unstable modes would indicate the RN fixed point is an unstable fixed point of the static EM flow, in the sense that a generic initial perturbation to the RN fixed point will contain some component of the unstable mode and this will take the flow away from the fixed point as it exponentially grows in flow time.

We have chosen the reference metric to be the same RN solution as that of the fixed point metric and hence $\xi^\mu = 0$ at the fixed point. In both the electric and magnetic cases we also have $\Lambda = 0$ for the RN solution with the gauge potentials discussed previously. Thus, perturbing the RN solution as above we will have

$$\begin{aligned} \xi^\mu &= \epsilon e^{\Omega\lambda} \delta\xi^\mu \\ \Lambda &= \epsilon e^{\Omega\lambda} \delta\Lambda. \end{aligned} \tag{4.115}$$

We may then separate such eigenmodes into those with $\delta\xi^\mu, \Lambda = 0$ and those with $\delta\xi^\mu, \Lambda \neq 0$. The former case will be an eigenmode on the original Einstein-Maxwell flow equation (4.35), whilst the latter is an eigenmode up to a flow time

dependent diffeomorphism and gauge transformation.
More explicitly we take the metric components to be of the form

$$T(\rho) = \left(1 - r_- + r_-\rho^2\right)\left(1 + \epsilon e^{\Omega\lambda}\delta T(\rho)\right) \quad (4.116)$$

$$A(\rho) = \left(1 - r_- + r_-\rho^2\right)^{-1}\left(1 + \epsilon e^{\Omega\lambda}\delta A(\rho)\right) \quad (4.117)$$

$$S(\rho) = 1 + \epsilon e^{\Omega\lambda}\delta S(\rho). \quad (4.118)$$

Moreover, in the electric case we take the electric potential as

$$\Phi(\rho) = \sqrt{r_-} + \epsilon e^{\Omega\lambda}\delta\Phi(\rho) \quad (4.119)$$

while in the magnetic case, as discussed above, the gauge potential is simply fixed with magnetic charge $q_B = \sqrt{r_-}$. The functions, $\delta T, \delta A, \delta S$, and in the electric case $\delta\Phi$ too, are all smooth functions of ρ^2 (so even functions) on $\rho \in [0, 1)$. We further impose the asymptotically flat boundary condition that $\delta T = \delta A = \delta S = \delta\Phi = 0$ at $\rho = 1$.
In order to find the stable and unstable modes of the flow equations, we numerically solve them over the interval $\rho \in [0, 1)$ by discretizing spacetime into N points. Hence, our flow equation is then schematically of the form

$$Ov = \Omega v \quad (4.120)$$

where due to the discretization O and v are a $N \times N$ matrix and a N-vector respectively and v represents the values of the functions $\delta T, \delta A, \delta S$, and in the electric case $\delta\Phi$, at the discrete points. From this system we can then numerically determine the eigenmodes Ω and the eigenfunctions v. If we find at least one positive mode, we know that the fixed point is unstable.

4.4.2 Magnetic non-extremal RN Linear Stability

Here we consider linearized flow about magnetic RN. The work of Monteiro and Santos [115] shows that Euclidean magnetic RN has a negative mode for $|Q| < \sqrt{3}GM/2$, which for us implies $r_- < 1/3$ (remember $r_+ = 1$). This mode involves the metric and not the gauge potential which is simply the unperturbed magnetic solution $A_{mag} = -\sqrt{r_-}\cos\theta d\phi$. Continuing back to Lorentzian signature these negative modes precisely yield $\delta\xi = 0$ unstable eigenmodes of the linearized static EM flow equations for the metric, i.e. with $\mathrm{Re}(\Omega) > 0$, signifying an exponentially growing instability. The fact that $\delta\xi = 0$ for these modes originates from the statement that the tensor and vector perturbations decouple in this magnetic case [115]. One might naively then think that the magnetic RN solution becomes a stable fixed point for larger charges and up to extremality. However, it isn't clear that unstable modes cannot exist outside the sector $\delta\xi = 0$, as this has not previously been studied. We emphasize that, while such modes would not have

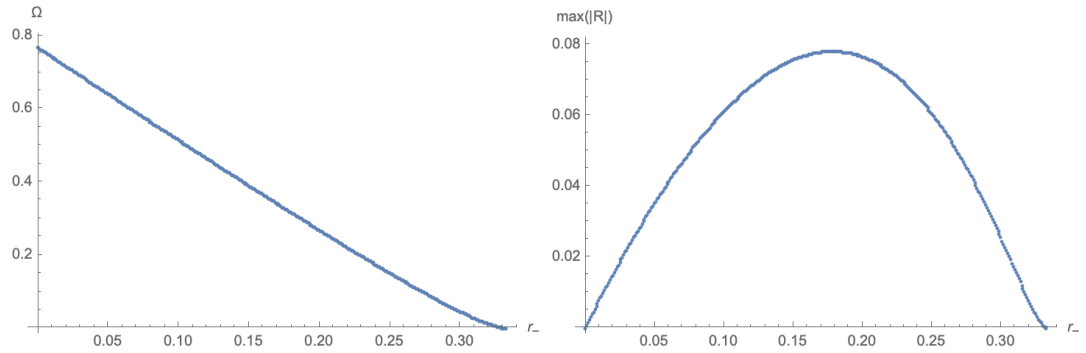

Figure 4.3: The left panel shows the eigenvalue Ω of the one unstable mode for the flow of the non-extremal magnetically charged RN solution against r_- which controls its charge. For $r_- = 0$ this is the Gross-Perry-Yaffe negative mode of the Schwarzschild solution. For charges $0 < r_- < 1/3$ this unstable mode persists, disappearing at $r_- = 1/3$, when it becomes a zero-mode which is generated by a perturbation within the RN family of solutions. For greater charges the fixed point is stable (within this spherically symmetric setting). ξ remains zero for all these unstable modes. In the right panel the maximum value of the perturbation to the Ricci scalar for the mode is shown.

a clear interpretation in terms of the Euclidean action studied in [115], they, if present, would certainly affect the stability of the fixed point of the static EM flow and that what we will investigate here.

In figure 4.3 we plot the unstable mode determined numerically against varying charge, i.e. against different values r_-. We find that there is only one unstable mode for $r_- < 1/3$ and we find none for $r_- > 1/3$. To be more precise, the unstable mode becomes a zero-mode at $r_- = 1/3$. The numerical wavefunctions $\delta T, \delta A, \delta S$ are extracted from the eigenvector v corresponding to the negative mode for a given r_- or the zero-mode at $r_- = 1/3$. We explicitly check that these wavefunctions are compatible with $\delta\xi = 0$ in all cases. Also shown in that figure is the maximum value of the perturbation to the Ricci scalar plotted against r_-. For the unstable mode of the Schwarzschild solution, so for $r_- = 0$, this vanishes as the Euclidean negative mode is traceless. The perturbation is non-vanishing for a finite charge range but vanishes again when the unstable mode disappears and becomes a zero-mode at $r_- = 1/3$. As it turns out, at that point the mode is a static perturbation of the unique RN solution. Thus, it fulfills the Einstein-Maxwell equations and must have a vanishing Ricci scalar.[5]

In figure 4.4 we plot the wavefunctions δT, δA, δS for $r_- = 0$, $r_- = 1/6$ and $r_- = 1/3$, normalized such that $\delta S = 1$ at the horizon. Moreover, in the bottom plot we include the wavefunctions determined from a static perturbation to the

[5]This was not explicitly discussed in [115].

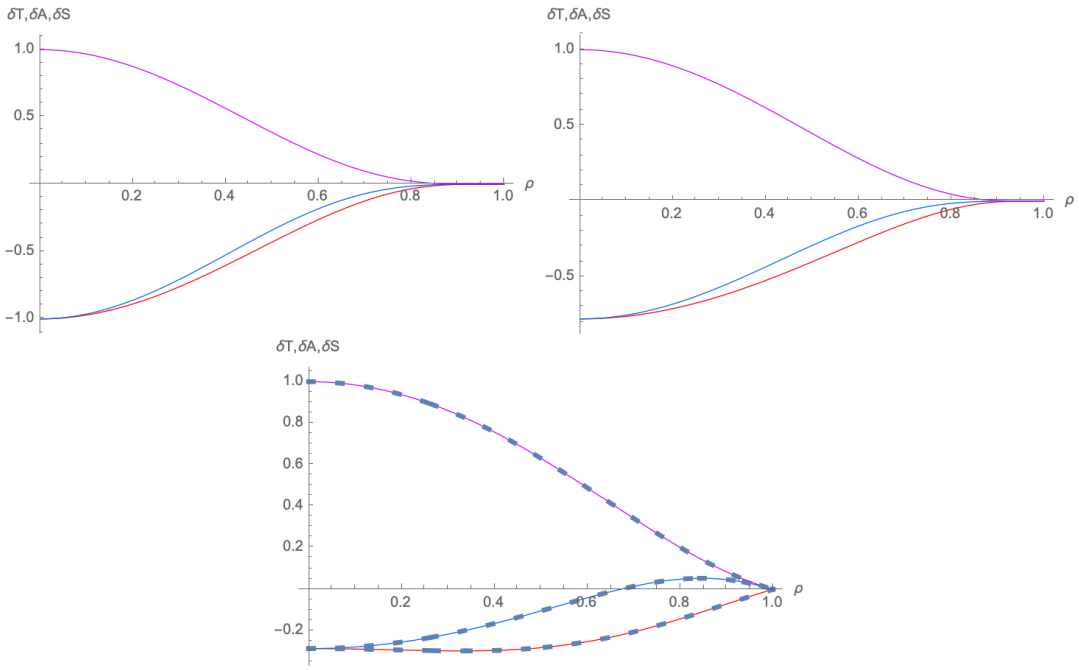

Figure 4.4: The numerically generated wavefunctions δT (Red), δA (Blue) and δS (Purple) are plotted against the radial coordinate ρ for the unstable modes corresponding to $r_- = 0$ (top left) and $r_- = 1/6$ (top right) and for the zero-mode at $r_- = 1/3$ (bottom). The instability becomes a static perturbation of RN for $r_- = 1/3$ and may be computed independently. These independently computed wavefunctions are shown as dashed curves in the bottom plot which perfectly agree with the numerically constructed wavefunctions in solid lines.

magnetic RN solution as dashed lines. These lie perfectly on top of the solid lines of the numerically generated wavefunctions confirming the zero-mode is indeed a perturbation within the RN family.
Thus, we conclude that the only unstable mode in the static spherically symmetric sector is the continuation of the Euclidean mode described by Monteiro and Santos which precisely has $\delta\xi = 0$. It is possible that one exists without spherical symmetry, but we believe it to be very unlikely.

4.4.3 Electric non-extremal RN Linear Stability

Now we consider the fixed point given by the electrically charged non-extremal RN solution. As discussed above, there is no decoupling of the metric flow from that of the gauge field electric potential. In particular, one cannot perturb the metric and consistently have the gauge field fixed – it will be forced to flow. Furthermore, in this electric case there is no straightforward Euclidean continuation, and therefore no prior results from considering Euclidean negative modes.

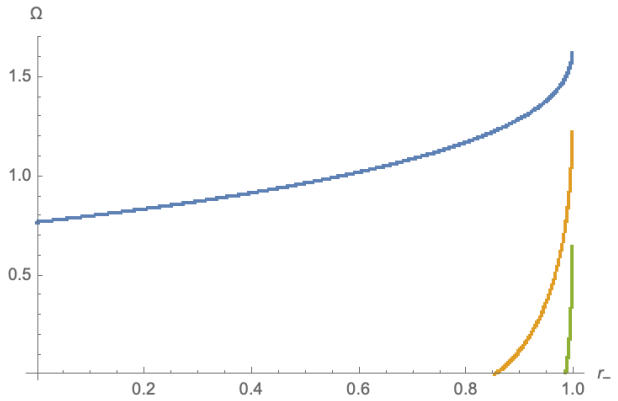

Figure 4.5: This figure shows the eigenvalues Ω for the unstable modes for the flow of the electrically charged RN solution against r_- for $r_- \leq 0.999$. The Gross-Perry-Yaffe negative mode at $r_- = 0$ continues to an unstable mode of the electrically charged solutions. However, additional negative modes appear as the charge is increased. For $r_- \leq 0.999$ up to three unstable modes may exist but very near extremality (not shown in the plot), for $0.999 < r_- < 1$, more unstable modes appear. It therefore appears that electrically charged RN is an unstable fixed point of the EM flow near extremality, unlike the magnetically charged RN solution which is stable.

It appears that at least one unstable mode is present up until extremality. Perhaps more surprisingly new unstable modes appear at specific values of the electric charge. At the numerical resolutions we use, it is difficult to see the behaviour very near extremality but it appears that an increasing number of unstable modes appear in the limit that $r_- \to 1$ (remember $r_+ = 1$).[6] In figure 4.5 we plot the eigenvalues with positive real part, noting that in fact we find all these eigenvalues are purely real. Their wavefunctions are also real. All the unstable modes here, except in the zero charge $r_- = 0$ case which corresponds to the Schwarzschild solution, have non-vanishing $\delta\xi$ and non-trivial gauge potential $\delta\Phi$. We have checked that they all have a non-vanishing perturbation to the Ricci scalar confirming that they are not simply a pure diffeomorphism on the metric but physically change the geometry as well as the gauge field.
In figure 4.6 and 4.4.3 we show the wavefunctions for values $r_- = 0.5, 0.9, 0.99, 0.999$ of the two most unstable modes present for those values (the second unstable mode only emerges for $r_- > 0.854$). We note that the number of nodes increases with each new branch of unstable modes. In the limit $r_- \to 1$ the wavefunctions appear to tend only to have non-trivial δS with the other components and gauge field apparently vanishing in this limit. We also observe that the curvature of

[6]It also could be that all these negative modes merge into a single mode in the extremal limit.

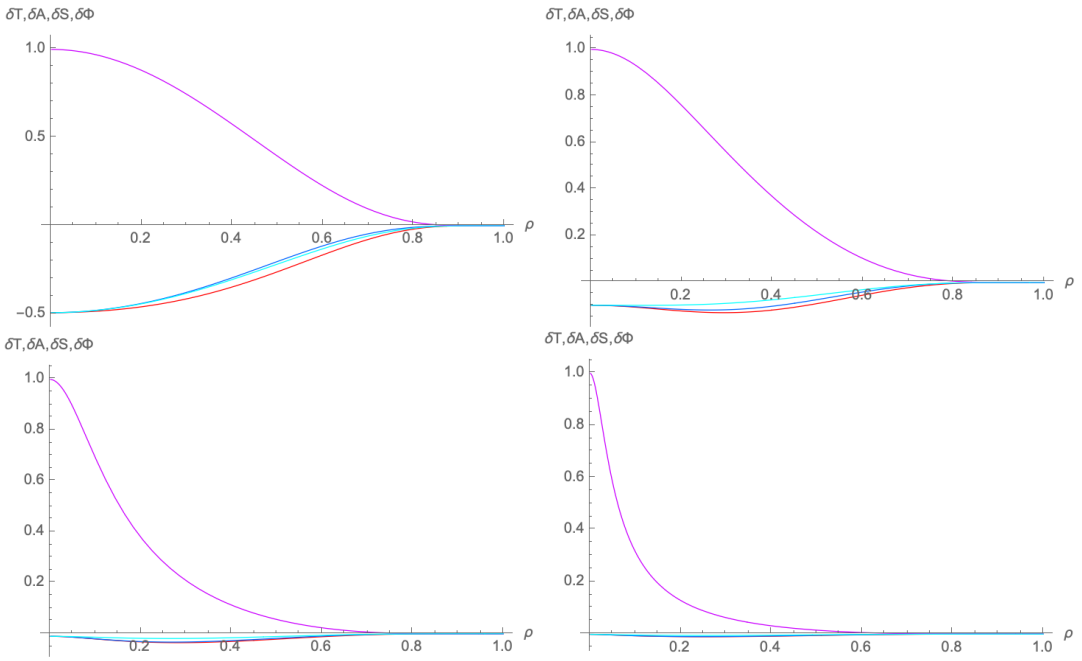

Figure 4.6: This figure shows the most unstable mode wavefunctions for the EM flow of perturbations of electrically charged RN for charges $r_- = 1/2$ (top left), $r_- = 0.9$ (top right), $r_- = 0.99$ (bottom left) and $r_- = 0.999$ (bottom right). The wavefunction δT is shown in red, δA in blue, δS in purple, and the potential perturbation $\delta\Phi$ is in light blue. The modes are normalized to have $\delta S = 1$ at the horizon and we see δS dominates the near horizon behaviour as extremality is approached, i.e. it becomes increasingly localized there.

the function δS at the horizon appears to increase as $r_- \to 1$, with δS becoming increasingly localized at the horizon $\rho = 0$, indicating the perturbation may not be smooth in the limit of extremality.

Finally we comment that the emergence of new unstable modes with increasing charge indicates that at special values of charge, there are static zero-modes, i.e. linear perturbations that don't flow. This occurs in the magnetic case when the unstable mode disappears but there we had $\delta\xi = 0$ and hence this zero mode is just a perturbation tangent to the RN space of solutions, as just discussed. Here, however, $\delta\xi \neq 0$ and we believe that these zero modes are not associated to perturbations that are tangent to the RN solution. Instead they should be tangent to new branches of "soliton" solutions of the Einstein-Maxwell system that presumably merge with the RN solutions at particular values of charge. We have not attempted to directly construct these soliton solutions as non-linear solutions to the Einstein-Maxwell soliton equation, but it should be possible to do so.

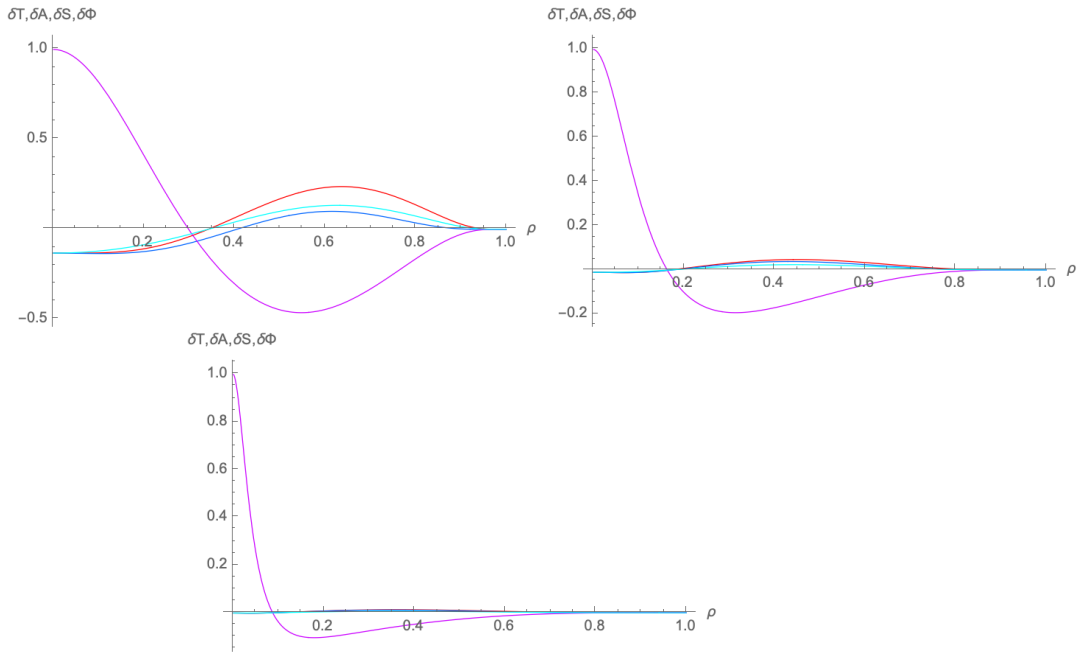

Figure 4.7: S
imilar to the previous figure, the wavefunctions (same color-coding as in figure 4.6) for the second most unstable mode are shown for perturbations of electrically charged RN with charges $r_- = 0.9$ (top left), $r_- = 0.99$ (top right) and $r_- = 0.999$ (bottom). We see that the wavefunctions have one node compared to figure 4.6. But δS grows again relative to the other component functions at the horizon as extremality is approached.

4.4.4 End Points of unstable RN Flows

In the case of the uncharged asymptotically flat Schwarzschild solution in static spherical symmetry the single unstable mode of Ricci flow generates two flows, one that leads the horizon to shrink to zero size in finite flow time and the other that expands the horizon "eating up" the whole spacetime [102]. In both the magnetic case for subcritical charge and in the electric case for all charges we have instabilities and we now ask where these flow.
In order to address this we solve the non-linear flow described at the start of this section 4.4. We numerically evolve the full metric functions T, A, S and for the electric case also the potential Φ by discretizing the ρ coordinate on the interval $[0, 1)$. We impose a Neumann boundary condition for the functions T, A, S and Φ at $\rho = 0$ in order to enforce the smooth horizon boundary condition (which requires these functions to be smooth in ρ^2). The asymptotic flatness is imposed as a Dirichlet boundary condition, namely $T, A, S \to 1$ at $\rho = 1$. In the electric case the potential has the boundary condition $\Phi \to \sqrt{r_-}$ at $\rho = 1$, fixing the potential difference to the horizon. As mentioned previously, the horizon smoothness and the value of the surface gravity are correctly preserved by the numerical flows.
We discuss the electrostatic EM flow first. We begin by perturbing the RN fixed point taking initial data

$$\begin{aligned} T &= 1 - (1 - \rho^2) r_- \\ A &= 1/T \\ S &= 1 \pm 0.01 \cdot (1 - \rho^2)^4 \\ \Phi &= \sqrt{r_-} \end{aligned} \tag{4.121}$$

such that we are perturbing only the sphere part of the metric via the function S, i.e. this corresponds to a spherical symmetric perturbation. Whilst obviously finite, this deformation to S is sufficiently small in amplitude that its initial evolution is well described by linear perturbation theory about the electric RN solution. It preserves the boundary conditions and, depending on the sign, either initially decreases ($-$ sign) or increases ($+$ sign) the horizon size a tiny bit. We expect it to have overlap with the linear unstable mode (or modes) of the electric RN fixed point and thus to generate flows driven by these unstable modes.
In figure 4.8 we show the evolution of the geometry by plotting the invariants $\sqrt{-g_{tt}} = \rho\sqrt{T}$ against $\sqrt{g_{\theta\theta}} = r(\rho)\sqrt{S}$ at a sequence of flow times λ. These are invariants in the sense that they transform as scalars under a coordinate transformation $\rho \to f(\rho)$. The curve of $\sqrt{-g_{tt}}$ against $\sqrt{g_{\theta\theta}}$ is then gauge invariant and illustrates how g_{tt} varies with the radius. In the figure we show the two evolutions started with the negative and positive initial perturbations to the horizon radius for a reasonably large charge, corresponding to $r_- = 0.8$. We see the perturbation that initially shrinks the horizon flows in finite flow time to a singularity (here occurring at $\lambda \simeq 3.9$), whereas the perturbation that initially expands the horizon

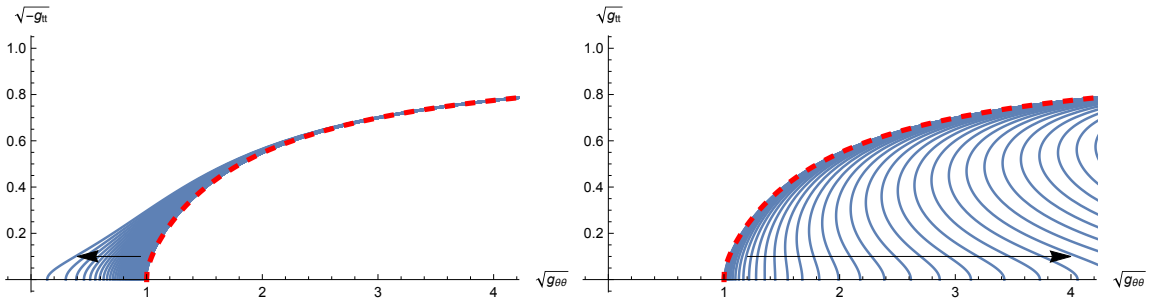

Figure 4.8: This figure shows curves of $\sqrt{-g_{tt}}$ plotted against $\sqrt{g_{\theta\theta}}$ at constant intervals of electric EM flow time $\Delta\lambda$ for a small initial perturbation of an electric RN solution with reasonably large charge corresponding to $r_- = 0.8$ (recall $r_+ = 1$). The left-hand frame shows the flow where the horizon is initially reduced in size and we see that it flows to a singularity at $\lambda \simeq 3.9$ (here $\Delta\lambda = 0.05$). The right-hand frame shows the situation where the horizon is perturbed initially to be larger than that of the electric RN solution and we see it apparently expands forever (here the curves are shown for flow intervals $\Delta\lambda = 0.25$). The geometry of the RN fixed point is shown by the red dashed curve and the arrows indicate the sense of change of the geometry for increasing flow time. Both these behaviours are qualitatively similar to the Schwarzschild fixed point under Ricci flow. We see analogous behaviour for all charges of the electric RN fixed point.

leads to it growing in flow time in an apparently unbounded manner. In the latter case the horizon accelerates in its expansion and we can only follow it numerically for a finite period, before time gradients become too large to resolve accurately. This behaviour is qualitatively the same behaviour as for the Schwarzschild solution. Moreover, we see precisely the same qualitative behaviour for smaller and larger charges, although as one approaches near extremal charges it becomes more challenging to perform the simulations. For large charges, where the linear theory tells us multiple unstable modes exist, presumably one may seed the initial flows by these different unstable modes to generate different flows. However, we expect that without fine tuning it is the dominant unstable mode that determines the final behaviour. Hence, we may regard our perturbation above, which is not chosen to coincide with the unstable modes but just overlaps them, as giving the generic evolution. It would be interesting to explore whether more exotic behaviours could be found in the case of large charges where there are multiple unstable modes which may be tuned initially in the seed perturbation.

This similar qualitative behaviour to the uncharged case is perhaps to be expected. Our electric EM flow preserves surface gravity and electric potential difference to the horizon. At fixed electric potential and surface gravity, i.e. temperature, there is only one infilling RN solution which is precisely the initially perturbed fixed point. Thus, as in the uncharged case, there is no natural end state solution

to flow to, except flat spacetime (with a constant electric potential). While we haven't explored this in detail here, one may resolve the singularity formed by the shrinking horizon case and presumably this then flows to flat spacetime after the topology is suitably changed, as it happens in the uncharged case [102]. We may understand the other growing horizon as the flow "searching" for a larger stable black hole. If one puts the flow in a box, then, as in the uncharged case, a new large black hole solution exists [122] and this expanding horizon flow would presumably settle down to that solution. The reader is here reminded of the figure 4.2 which precisely describes the situation.
Now let us discuss the case of the magnetic flow and recall that the magnetic charge is preserved by the flow. Analogous plots of $\sqrt{-g_{tt}}$ against $\sqrt{g_{\theta\theta}}$ are shown in figure 4.9 for two situations, one below the critical charge and one above. Above the critical charge our linear analysis has shown no negative modes and, indeed, we see that large initial deformations of the magnetic RN solution flow back to it. The figure shows the example of $r_- = 0.4$ (recall that $r_- > 1/3$ gives charges larger than the critical one) for an initially large deformation of the form

$$\begin{aligned} T &= 1 - (1-\rho^2) r_- \\ A &= 1/T \\ S &= 1 \pm 0.5 \cdot (1-\rho^2)^4. \end{aligned} \tag{4.122}$$

which is again a spherically symmetric perturbation. The lower plot in 4.9 shows both the positive and negative initial deformations on the same axes and both flow back to the RN fixed point. We observe this same behaviour for all charges greater than the critical one, so $r_- > 1/3$ and for a variety of non-linear initial deformations to the geometry.
The case of sub-extremal charge, so $r_- < 1/3$, is much more interesting. In this case we expect from [115] one unstable mode of the flow which was confirmed by our linear analysis. There is now an important difference compared to the electric case. While there is only one black hole solution at fixed surface gravity and electric potential, we have now in the magnetic case an additional fixed point. This new solution is stable, has $r_+ < 1$ and has the same surface gravity and charge as the unstable magnetic RN fixed point which has $r_+ = 1$. These two solutions were called small and large black hole before and we refer back to figure 4.1 in which this situation is depicted. Thus, for an initial perturbation that reduces the horizon size, rather than flowing to zero size and a singularity, another option is to flow to this second stable fixed point, namely the small black hole. This is precisely what occurs in our simulations. For an initial perturbation similar to that in the electric case

$$\begin{aligned} T &= 1 - (1-\rho^2) r_- \\ A &= 1/T \end{aligned}$$

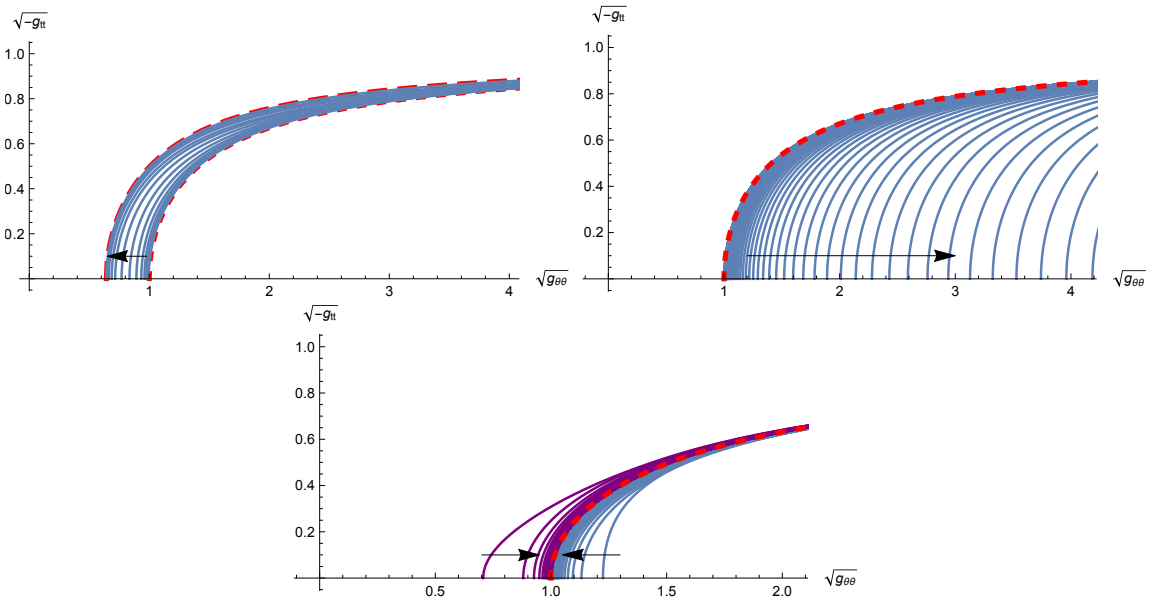

Figure 4.9: Here we now plot curves of $\sqrt{-g_{tt}}$ against $\sqrt{g_{\theta\theta}}$ at constant intervals for the magnetic EM flow. The top left- and right-hand frames are similar to those of the previous figure 4.8, being for an unstable magnetic RN solution with $r_- = 0.2$ perturbed initially to have smaller horizon size (left) or larger horizon size (right). The latter gives the same expanding horizon behaviour as that of the electric case. We have $\Delta\lambda = 0.5$ for this plot. The red dashed curve again shows the geometry of the initial magnetic RN fixed point that is perturbed. In the initially contracting case a new stable magnetic RN solution exists for the same surface gravity and charge and the flow asymptotes to this. Here it has $r_+ = 0.64$ (remember the starting point was at $r_+ = 1$) and we show the new stable fixed point geometry using longer red dashes. The flow curves in this case are plotted for $\lambda = 0, 10, 12, \ldots, 22, 24, 30, 50$ and 1000. The lower frame shows flows from a non-linear deformation of a fixed point with larger charge $r_+ = 0.4$, so it is stable. Two flows are shown, one with larger horizon initially (blue curves) and one with smaller (purple curves). Both quickly return to the stable fixed point (shown by the red dashed curve) under the flow (both curves are shown at intervals $\Delta\lambda = 0.5$). Arrows indicate the sense of change of the geometry under increasing flow time.

$$S = 1 \pm 0.01 \cdot (1 - \rho^2)^4 \tag{4.123}$$

we observe that the case with the negative sign flows to the stable small black hole solution. This is shown in the top left plot of figure 4.9 for the case $r_- = 0.2$. But we see the same behaviour for all initial charges $r_- < 1/3$ that we have studied. Unlike the uncharged or electric cases, where by a change of topology, that removes the horizon, we may have an infilling flat spacetime fixed point (with constant potential in the electric case), in this magnetic setting, where the magnetic charge is fixed by the asymptotic boundary conditions, this is not possible. With a flat spacetime topology there is no way to infill the geometry smoothly to a give a fixed point and yet carry the magnetic charge.
Therefore, it intuitively makes sense that in this magnetic case we see the horizon shrinking flow go to the stable charged small black hole, rather than a flow singularity corresponding to the collapse of the horizon. While this singularity could be resolved in principle, we won't flow to a flat spacetime fixed point afterwards due to the flow preserving magnetic charge. Another way to understand this different behaviour is that the charge enclosed at any radius is the same, as there is no charged matter, so the horizon carries the fixed magnetic charge. When the horizon shrinks, the backreaction from the fixed charge becomes larger, and its contribution to the stress tensor would diverge if the horizon shrinks to zero size. Hence, this trapped magnetic flux acts to prevent the horizon from shrinking to 0.
Lastly, as we see in the figure 4.9 on the top right, the flow, that initially increases the horizon size of the unstable fixed point, appears to continue to do so in an accelerated manner as in the uncharged or electric cases. We see this same behaviour for all $r_- < 1/3$ as we perturb the unstable RN fixed point in a manner initially expanding the horizon. As mentioned above for the electric case, presumably if we placed this system in a spherical box, a new stable "larger" black hole fixed point (meaning a third even larger black hole solution) would exist and this horizon expanding flow would asymptote to this. In the asymptotically flat setting we consider here, the flow expands the horizon forever, always searching, but not finding, a larger stable black hole to settle on.

4.5 EM Flows about extremal RN

For static extremal black hole spacetimes with pure electric or magnetic charge we have argued above that we may perform static EM flows and further that the flow of the near horizon geometry decouples from the exterior. Following our discussion of the stability of static EM flows in the spherically symmetric case about non-extremal RN, it is natural to extend this to the extremal case. To do this, we consider the general spherically symmetric metric using the coordinates

introduced earlier in equation (4.16), taking

$$ds^2 = -\rho'^2 T dt^2 + r(\rho')^4 A \frac{d\rho'^2}{\rho'^2} + r(\rho')^2 S d\Omega^2. \tag{4.124}$$

From our earlier discussion, in order to have a smooth extremal horizon located at $\rho' = 0$ we should have T, A, S being smooth functions of ρ' and further satisfying

$$\begin{aligned} (T-A)|_{\rho'=0} &= 0 \\ \left.\frac{\partial_{\rho'}(T-A)}{T}\right|_{\rho'=0} - 4 &= \psi' \end{aligned} \tag{4.125}$$

for some constant ψ'. Now considering the static EM flow, T, A, S become also functions of flow time λ. For the pure magnetic case, we simply have

$$A_{mag} = -\cos\theta d\phi \tag{4.126}$$

as this is preserved by the flow. Remember that we have performed the extremal limit $r_- \to 1$ for $r_+ = 1$. In the electric case, instead, we take

$$A_{elec} = \rho' \Phi dt \tag{4.127}$$

which is smooth provided Φ is a smooth function of ρ' and of λ. One may check explicitly that the spherically symmetric static EM flow equations preserve the smoothness conditions (4.125), following our general analysis earlier. From our discussion in section 4.1, using our choice of units, the extremal RN fixed point is given by $T = A = S = 1$, with $\Phi = 1$ in the electric case, so that $\psi' = -4$.
First, we may explicitly solve the near horizon non-linear flow equations in both the electric and magnetic cases. Specializing our general discussion in section 4.3.3 to our spherically symmetric Ansatz, the near horizon form of the metric is

$$ds^2_{NH} = T_0 \left(-\rho'^2 dt^2 + \frac{d\rho'^2}{\rho'^2} \right) + S_0 d\Omega^2 \tag{4.128}$$

and in the electric case

$$A^{NH}_{elec} = \rho' \Phi_0 dt \tag{4.129}$$

with T_0 and S_0 being functions of only flow time λ. As discussed in section 4.3.3, for the electric near horizon flow the potential Φ_0 is a constant in flow time. As one might expect from the non-extremal case above, solving this near horizon flow we will find that the magnetic RN solution is a stable fixed point of the magnetic flow but the electric solution is unstable.
In either the magnetic or electric case we may fix the near horizon metric to be that of extremal RN and then consider the flow in the exterior. We will simulate these flows numerically and fully non-linearly. In the magnetic case the flows approach magnetic RN at late times. However in the electric case, even with the horizon fixed to be that of extremal RN, we see generic initial data, even that corresponding to small initial perturbations, seem to develop to a singularity.

4.5.1 Near horizon Electric flow

The electrostatic near horizon flow is determined by the flow equations

$$\begin{aligned} T_0'(\lambda) &= 2 - 2\frac{\Phi_0^2}{T_0} \\ S_0'(\lambda) &= -2 + \frac{2\Phi_0^2 S_0(\lambda)}{T_0(\lambda)^2}. \end{aligned} \tag{4.130}$$

where the prime denotes a flow time derivative, i.e. $' = d/d\lambda$. The RN near horizon fixed point is given by $T_0(\lambda) = S_0(\lambda) = \Phi_0$. We will choose units such that $\Phi_0 = 1$. We may expand about this fixed point perturbatively and solve (4.130), giving

$$\begin{aligned} T_0(\lambda) &= 1 + \epsilon e^{2\lambda} a \\ S_0(\lambda) &= 1 + \epsilon e^{2\lambda}\,(b - 4\lambda a) \\ \Phi_0 &= 1 \end{aligned} \tag{4.131}$$

to first order in ϵ, where a and b are integration constants. Note that we do not perturb Φ_0, as it is constant in flow time. Moreover, a perturbation of Φ_0 would simply correspond to changing the charge of the fixed point solution which can be mapped back to one by a change of units. We thus see the fixed point is unstable and there are two relevant deformations of it, parameterized by ϵa and ϵb. Starting with the RN near horizon solution as $\lambda \to -\infty$, adding these relevant deformations will then flow the near horizon geometry away from near horizon extremal RN solution for finite λ.
The simplest class of non-linear solutions, which tend to the RN solution for $\lambda \to -\infty$, is that corresponding to T_0 being constant, namely $T_0(\lambda) = 1$. The flow equation for S_0 consequently linearizes, such that the non-linear solution for S_0 is simply

$$S_0(\lambda) = 1 + \epsilon\, e^{2\lambda}. \tag{4.132}$$

for a constant ϵ. We see that for $\epsilon < 0$ the horizon sphere shrinks to zero size at finite flow time λ. Alternatively for $\epsilon > 0$ it expands forever. Thus, the extremal electric RN black hole is an unstable fixed point of the EM near horizon flow with behaviour reminiscent of the non-extremal Schwarzschild black hole under Ricci flow [102].
The general near horizon solution has non-constant T_0 and can is given by

$$\begin{aligned} T_0(\lambda) &= (1 + P_\pm(\lambda)) \\ S_0(\lambda) &= \frac{(1 + (c - 4(\lambda - \lambda_0))\, P_\pm(\lambda) + P_\pm(\lambda)^2)}{1 + P_\pm(\lambda)} \end{aligned} \tag{4.133}$$

where we have defined

$$P_{\pm}(\lambda) = W_0\left(\pm e^{2(\lambda-\lambda_0)}\right) \tag{4.134}$$

with $W_0(x)$ being the Lambert W-function that gives the principle solution of y for the relation $x = ye^y$. The constant λ_0 arises from translation invariance of the equations in λ and c is the remaining constant of integration that determines the different behaviours. Asymptotically as $\lambda \to -\infty$ we have

$$P_{\pm}(\lambda) \to \pm e^{2(\lambda-\lambda_0)} \tag{4.135}$$

and the function $W_0(x)$ exists for all $x > -1/e$ and is monotonically increasing. At $x = -1/e$ it takes the value minus one.
The analytic behaviour of the near horizon flow is captured in Figure (4.10). The sign in the definition (4.135) of $P_{\pm}(\lambda)$ defines two distinct branches for evolutions away from the fixed point. For these the various trajectories in the (S_0, T_0)-plane are then labelled by the value of c. For the $P_+(\lambda)$ branch (shown as blue curves in the figure) we get $S_0 \to 0$ in finite flow time with T_0 remaining finite. For the $P_-(\lambda)$ branch with $c > 0$ (shown as orange curves) the same behaviour occurs. However, taking instead $c < 0$ (shown as red curves) then we have $S_0 \to \infty$ and $T_0 \to 0$ in a finite flow time. In the special case $c = 0$ for the $P_-(\lambda)$ branch (shown as the black curve), which separates these two behaviours, both T_0 and S_0 go to zero at the same finite flow time. Finally taking the limit $c \to \pm\infty$ for the $P_{\pm}(\lambda)$ branches results in the two $T_0 = 1$ behaviours in (4.132) above, one with S_0 that shrinks to zero in finite flow time (purple in the figure) and the other with growing S_0 (green in the figure) so that the horizon expands forever. The only behaviour which exists for all flow times is this last one.
The Ricci scalar of the near horizon geometry, which is the Ricci scalar of the full spacetime restricted to $\rho = 0$, is simply given by

$$R|_{\rho=0} = -\frac{2}{T_0} + \frac{2}{S_0}. \tag{4.136}$$

For all finite values of c then either $S_0 \to 0$ at a finite flow time with finite T_0 or, alternatively, $T_0 \to 0$ with $S_0 \to \infty$ at a finite flow time. In both cases the Ricci scalar diverges, showing that the geometry encounters a curvature singularity at finite flow time. The special case $c = 0$ where $T_0 \to 0$ and $S_0 \to 0$ could allow a cancellation between the two terms in the Ricci scalar but calculation reveals it is still singular. The only exception to a finite flow time singularity is the flow $T_0 = 1$ with expanding horizon, where the flow exists for all time, and the scalar curvature tends to $R|_{r=0} \to -2/T_0$. We note that any solution to the Einstein-Maxwell equations has vanishing Ricci scalar (since the stress tensor is traceless) and hence the asymptotic geometry that this flow tends to cannot be the near horizon geometry to an Einstein-Maxwell solution due to its non-vanishing Ricci scalar.

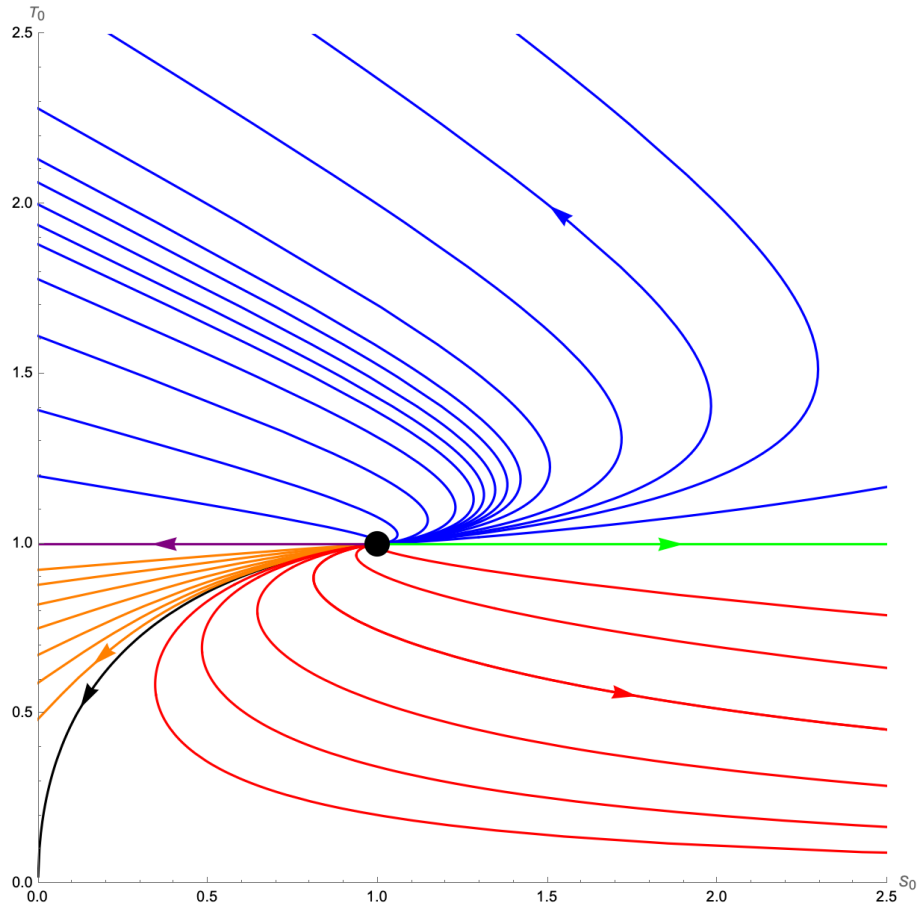

Figure 4.10: Analytic behaviour of the near horizon electric flow for small perturbations of the RN fixed point with $\Phi_0 = 1$. The various colors correspond to different choices for c and the branches $P_\pm$ and are detailed in the main text. The arrows point in the direction of the flow, while the black dot highlights the fixed point. The near horizon magnetic flow can be obtained by reversing the arrows and swapping S_0 and T_0.

4.5.2 Near horizon Magnetic flow

Now we consider the magnetic case where the near horizon flow equations are

$$\begin{aligned} T_0'(\lambda) &= 2 - 2\frac{T_0}{S_0^2} \\ S_0'(\lambda) &= -2 + \frac{2}{S_0(\lambda)}. \end{aligned} \tag{4.137}$$

Then, introducing functions $\bar{T}_0(\lambda) \equiv S_0(-\lambda)$ and $\bar{S}_0(\lambda) \equiv T_0(-\lambda)$, the above flow equations become

$$\begin{aligned} \bar{T}_0'(\lambda) &= 2 - \frac{2}{\bar{T}_0} \\ \bar{S}_0'(\lambda) &= -2 + 2\frac{\bar{S}_0}{\bar{T}_0^2} \end{aligned} \tag{4.138}$$

which are precisely the near horizon electric equations (4.130) taking $S_0 \to \bar{S}_0$ and $T_0 \to \bar{T}_0$. Hence, the near horizon magnetic flow is equivalent to the electric one, after exchanging T_0 and S_0 and flipping the sign of the flow time λ. This implies that the unstable near horizon RN fixed point that lies in the infinite past of the electric near horizon flow translates into a stable fixed point of the magnetic near horizon flow.

4.5.3 Flows of the full extremal spacetimes

Finally, we numerically investigate the non-linear spherically symmetric flows starting with a deformation of the extremal electric and magnetic RN solution that preserves extremality. We solve the full non-linear flow for the metric functions T, A, S, and in the electric case Φ too, by discretizing in the spacetime coordinates, as for the non-extremal case discussed earlier. In the non-extremal setting we needed a Neumann boundary condition at the horizon for our metric functions. However, in the extremal case the flow equations are simply imposed at the horizon and, as we have discussed above, decouple from the exterior flow as they involve no radial derivatives. While we have the analytic solution for any initial data for the near horizon flow, it is convenient here to simply evolve the near horizon flow numerically. We then check if it correctly reproduces the analytic solutions.

Our expectation is that deformations of the magnetic RN solution should return to it under the flow and, indeed, this is what we see. An example is shown in figure 4.11 where we start with a non-linear deformation of the magnetic solution, initially deforming the metric functions as

$$T = A = 1 + 2(1 - \rho'^2)^4$$

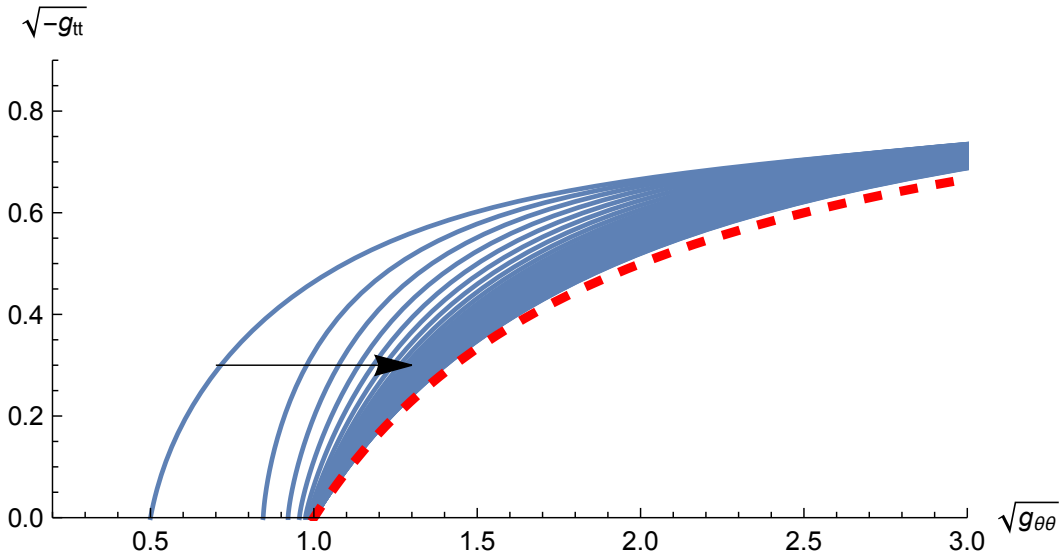

Figure 4.11: This figure shows curves of $\sqrt{-g_{tt}}$ plotted against $\sqrt{g_{\theta\theta}}$ at constant intervals of flow time, namely $\Delta\lambda = 0.25$, for a non-linear initial deformation of the extremal magnetic RN solution. The RN fixed point is shown in dashed red and we see that the initially deformed geometry asymptotes back towards extremal RN as the flow proceeds.

$$S = 1 - \frac{3}{4}(1 - \rho'^2)^4. \tag{4.139}$$

We note that these are compatible with smoothness of the horizon, as in equation (4.125), and preserve $\psi' = -4$. We already know that the near horizon flow, i.e. the behaviour at $\rho' = 0$, must return to the magnetic near horizon RN geometry. In figure 4.11 we display the geometric invariant $\sqrt{-g_{tt}}$ plotted against $\sqrt{g_{\theta\theta}}$. These curves are shown at intervals of flow time $\Delta\lambda = 0.25$ and we see that they asymptote back towards the magnetic RN fixed point. This behaviour is generic for other non-linear deformations we have implemented, provided they are not too large (when they can potentially give rise to singularities away from the horizon). Thus, at least in the spherically symmetric setting, the extremal magnetic RN solution appears to be a stable fixed point of the non-linear flow for the full extremal horizon spacetime.

Now let us consider the electrically charged RN fixed point. Our near horizon analysis already indicates it is unstable and in figure 4.12 we follow two flows (corresponding to the two signs) where the fixed point is initially perturbed by taking

$$S = 1 \pm 0.01 \cdot (1 - \rho'^2)^2 \tag{4.140}$$

with $T = A = \Phi = 1$. From our near horizon analysis for the negative sign above we know that the horizon behaviour is $T = 1$ and $S = 1 - 0.01e^{2\lambda}$ at $\rho' = 0$

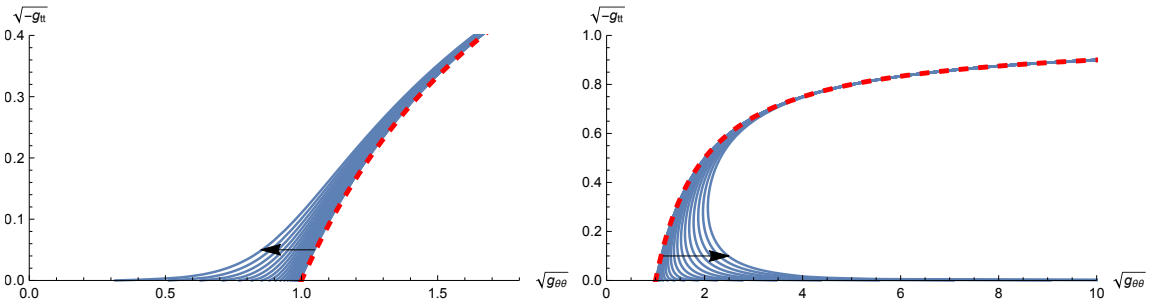

Figure 4.12: Here we show flows that begin with a small perturbation of the electrically charged extremal RN solution. The perturbation is subtracted and added to initially decrease and increase the horizon size, giving the left- and right-hand frames plotted for flow time intervals $\Delta\lambda = 0.1$ and 0.25 respectively. The flow behaviour at the extremal horizon decouples and follows the near horizon flow, leading to a collapse in finite flow time or exponential horizon expansion. We see that the exterior of the geometry follows this near horizon behaviour in a smooth manner. In the collapsing case the singularity occurs at $\lambda = 2.30$. In the expanding case curves are shown for flow times up to $\lambda = 5$, when gradients near the horizon become too difficult to numerically resolve.

and so the horizon sphere will shrink to zero size at time $\lambda = 2.30$. For the positive sign the horizon behaviour is $T = 1$ and $S = 1 + 0.01e^{2\lambda}$ by the near horizon analysis and so the horizon sphere exponentially expands in flow time. Simulating the full flows we again plot the invariant $\sqrt{-g_{tt}}$ against $\sqrt{g_{\theta\theta}}$ for both cases in the figure 4.12. Indeed, we see exactly these behaviours at the horizon, with the geometry away from the horizon responding but remaining smooth. In the expanding case the simulation is run until flow time $\lambda \simeq 5$ when the function S becomes too large ($S \sim O(10^2)$) at the horizon to properly resolve gradients there. In the case where the sphere shrinks to zero size we expect that one can resolve the singularity by a surgery, as done in [102], to continue the flow through to flat spacetime.
Finally, we can consider the case where we do not initially perturb the horizon geometry which means our perturbation is vanishing at the horizon, namely at $\rho' = 0$. We show here the example deformation

$$S = 1 \pm 0.5 \cdot \rho'^4 (1 - \rho'^2)^2 \tag{4.141}$$

with $T = A = \Phi = 1$ and again note this preserves smoothness of the extremal horizon with $\psi' = -4$. The near horizon analysis then implies $T = S = 1$ for all flow time at the horizon $\rho' = 0$. The plethora of unstable modes of the non-extremal flow suggests that, while the horizon geometry is pinned to that of the extremal electric RN, the exterior spacetime may be unstable. Indeed, this appears to be the case. In figure 4.13 we plot the same invariants as in the previous figures

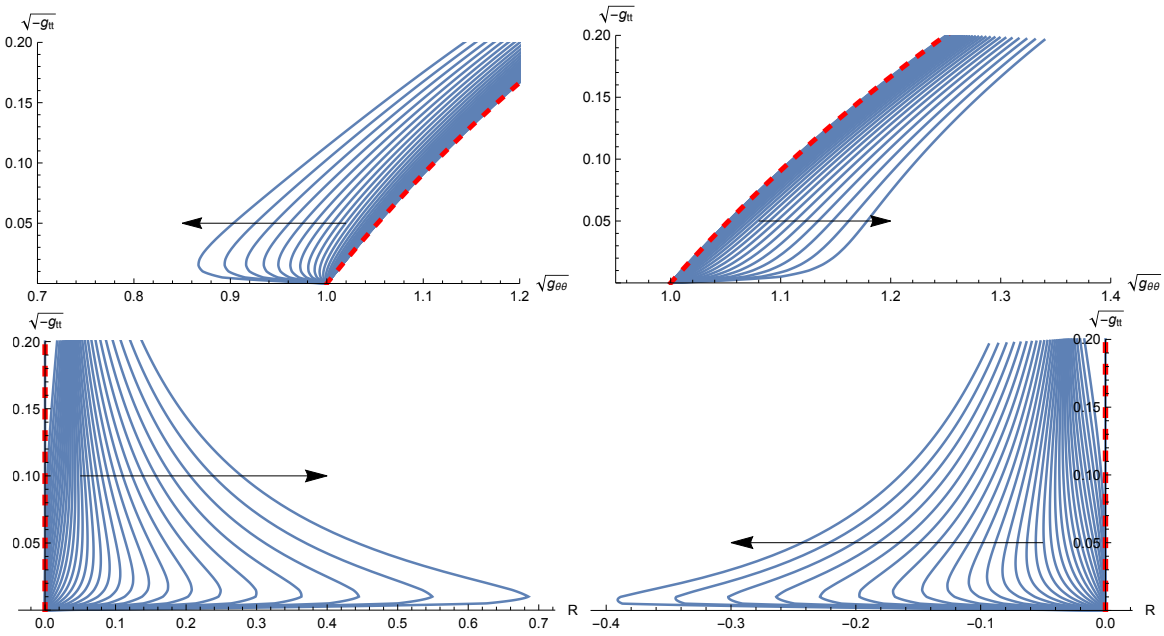

Figure 4.13: The top panels are similar to the previous figure but now the two flows depicted are for an initial small perturbation of extremal electrically charged RN that preserve the horizon geometry so that the near horizon geometry remains that of extremal RN throughout the flow. The same perturbation is both added and subtracted to RN, generating the top left and right panels respectively. In both cases the flow time interval between the curves is $\Delta\lambda = 0.1$. While the horizon geometry is fixed, we still see that extremal RN is unstable, as the perturbation grows in the exterior. This appears to build up curvature near, but not at the horizon. This is confirmed in the bottom two panels, where the Ricci scalar is plotted against $\sqrt{-g_{tt}}$ for the same perturbations respectively. This is zero for the RN solutions and hence is fixed to zero at the horizon as the near horizon geometry is unperturbed here. But we see the curvature appears to grow in the vicinity of the horizon. The curves are plotted up to a flow time $\lambda = 3$ when gradients become too large to accurately resolve. While it appears a singularity forms, it remains unclear whether this occurs in a finite flow time.

for both these flows, now zooming in on the region near the horizon. The horizon size indeed remains fixed and the flow away from the horizon remains smooth for some time. We show the flow at time steps $\Delta\lambda = 0.1$ up to a flow time of $\lambda = 3$ when in both cases the gradients near the horizon become very large. In the same figure we show the Ricci scalar R plotted against $\sqrt{-g_{tt}}$ near the horizon and see that it becomes large and localized just outside the horizon. Recall that for a RN solution we have $R = 0$ and for these flows it is fixed to have its vanishing RN value at the horizon as the near horizon geometry is pinned to that of extremal RN. The maximum absolute value of the Ricci scalar appears to grow in an unbounded way as the flow proceeds. The maximum also becomes closer to the horizon, making it difficult to numerically resolve at late flow times. The same qualitative behaviour occurred for other perturbations that we have tested for the electric extremal RN solution and that kept the near horizon geometry fixed.

These results appear to confirm that the extremal electric RN solution is unstable to all deformations. Deformations, that perturb the horizon, obviously flow away governed by the unstable near horizon flows discussed earlier. More interestingly, if the near horizon geometry is not perturbed and thus stays that of extremal RN, the exterior solution then appears to flow away from RN, developing increasing curvature that is more and more localized in the vicinity of the horizon as the flow proceeds.

Chapter 5

Cosmic Acceleration and Turns in the Swampland

This whole chapter is based on a collaboration with Marco Scalisi and Guoen Nian [3]. As the paper was only published after this thesis was handed in, this chapter differs slightly from [3]. But the general results are the same.

Cosmic acceleration plays a fundamental role in the current understanding of our universe. A variety of experiments operating at different scales, such as supernovae [123, 124] and cosmic microwaves background (CMB) [125, 126, 127] experiments, have provided very compelling evidence of a phase of accelerating expansion both in the early and in the current universe. While we have a good understanding of how this phase can be realized in terms of an effective scalar field theory, we still struggle to agree on a full-fledged embedding of it into String Theory.
The presence of several light scalar fields, active during the acceleration phase,[1] is a natural expectation for such an embedding (see [128] for a recent review on string cosmology). String Theory comes in fact with many moduli, often spanning non-trivial field geometries, and giving them a mass is definitely a complex task. Unlike scenarios with one single scalar field, multi-field models typically feature *non-geodesic trajectories* in field space.[2] Deviations from geodesics can be sourced by a non-zero scalar potential and they are usually quantified by the so called *turning rate* Ω. Strong non-geodesic motion, characterized by rapid turns in field space with $\Omega \gg 1$ (in Hubble units), can lead to intriguing and rich phenomenology. Examples have been provided in the context of inflation (see

[1] Here we consider only time-dependent acceleration phase, such as inflation or quintessence, with certain displacements in field space.

[2] It should be noted that the most common strategy to construct an effective (supergravity) model is to stabilize all fields except one, which drives the acceleration phase. However, despite its simplicity, this approach may not be the most natural and often demands precise control over the effective theory.

e.g.[129, 130, 131, 132, 133, 134, 135, 136, 137, 138]) and also for quintessence models (see e.g. [139, 140, 141, 142, 143, 144, 145, 146]). These can be modifications of the inflationary power spectrum [131, 133], production of primordial black holes [147, 148], possibility to inflate on a steep potential [136, 141, 143] (namely with large potential gradient) and also enhanced growth of large-scale structure. Despite the great attention this topic gained in the research community, the results are mainly model-dependent and so we lack a general principle of what a consistent Quantum Gravity embedding allows for (see [137] for some work in this direction in the context of supergravity).
An alternative route to (string) model building is given by the the Swampland Program, which suggests that one can employ a bottom-up approach to restrict the set of EFTs consistent with quantum gravity, as it was already explained earlier in this thesis. Especially the SDC can be quite helpful in this scenario, since we are usually dealing with several scalar fields in a non-trivial field space. Also remember that the Swampland Program can lead to possible observational predictions. For instance, implications of the SDC for cosmic inflation were first studied in [20] (see also [149]), where a universal upper bound on the inflaton range was found (see also [150, 151] for some variations of it with fixed decay rate).
Moreover, the SDC finds a natural test around the *boundary of moduli space*. These asymptotic regions are located at an infinite distance from any other point, hence they are also referred to as "infinite-distance singularities". Around these regions, the geometry exhibits negative curvature and non-compactness[3], while maintaining a finite volume [5]. The effective theory becomes simple and can be expressed as a perturbative expansion on a certain parameter. Additionally, there is evidence suggesting that the scalar potential approaches zero in this limit [158]. These factors have led to serious considerations of the boundary of moduli space as a promising framework for embedding models of cosmic acceleration [159, 145, 146], often referred to as "asymptotic acceleration".
Here we study the implications of the SDC for multi-field models of cosmic acceleration at the boundary of moduli space. As a main result, we find that the ratio between the turning rate Ω and the Hubble parameter H is constrained by

$$\frac{\Omega}{H} < c\,\sqrt{\epsilon} \tag{5.1}$$

with $\epsilon \equiv -\dot{H}/H^2$ being the acceleration parameter and c being a $\mathcal{O}(1)$ quantity, depending on the curvature of the moduli space and on the decay rate of the tower mass scale. Since $\epsilon < 1$ by definition, this result implies that asymptotic

[3]In the context of inflationary cosmology, it has been shown [152, 153, 154, 155, 156, 157] that non-compact symmetries and negative curvature of the field space are key features for an excellent fit to the observational data. The relation between the SDC and such a cosmological scenario has in fact been investigated in [20].

acceleration is incompatible with rapid turns or any strong non-geodesic motion. Thus, at the boundary of moduli space QG imposes predominantly geodesic motion. We argue that this result should be valid also in the more conservative case of super-Planckian excursions for which one can consistently apply the SDC.
One direct implication of (5.1) is a clear tension between asymptotic acceleration and the de Sitter conjecture [24, 160, 158]. In fact, a distinct characteristic of multi-field models is that the acceleration phase is not solely determined by the gradient of the scalar potential but rather by the interplay of this and the turning rate, as given by the following formula[4]

$$\epsilon = \frac{1}{2}\frac{|\nabla V|^2}{V^2}\left(1+\frac{\Omega^2}{9H^2}\right)^{-1}. \tag{5.2}$$

It has been previously highlighted in the literature [136] that, when $\Omega \gg H$, this formula allows for the fulfillment of the de Sitter conjecture (i.e. $|\nabla V| > \mathcal{O}(1)\cdot V$) while also enabling an acceleration phase with $\epsilon \ll 1$. However, our result (5.1) significantly limits this possibility within the context of asymptotic acceleration since it implies that the second term in the bracket of (5.2) is sub-leading. Given the current observational bounds, we conclude that models of early/late-time acceleration, near the boundary of moduli space, typically exhibit tension with the de Sitter conjecture.

5.1 SDC, Mass Decay Rate and Non-Geodesics

As it is beneficial for the rest of this chapter, we briefly review previously introduced concepts and elaborate further on them because here some more details are required.
The SDC implies the existence of at least one infinite tower of states with mass scale exponentially decreasing in field space in the infinite distance limit, namely

$$m = m_0 \exp(-\lambda\Delta) \qquad \text{as} \qquad \Delta \to \infty \tag{5.3}$$

where m_0 is the typical mass scale of the tower before any displacement, Δ is the traversed distance in moduli space and λ is the *decay rate*, namely the parameter regulating how fast the mass of the tower decreases in field space. It has been argued that λ is order one [51], in reduced Planck mass units, and lower bounds have also been pointed out in different contexts [46, 47, 48, 161, 150]. The existence of a lower bound is very important as it defines the validity of the EFT. Namely,

[4]Let us remark that (5.2) relies on a slow-roll approximation, which assumes that the second derivative of the fields is sub-dominant compared to the friction term in the equations of motion. The full formula, as discussed later, reveals that relaxing this condition can potentially aid in satisfying the de Sitter conjecture in an accelerating background.

it indicates how fast/slow one can approach the infinite distance singularity in field space and therefore how much field distance can be traversed, before the EFT completely breaks down due to genuine QG effects. It happens, in fact, that the QG cut-off $\Lambda_{\rm swamp}$, which is more precisely given by the species scale $\Lambda_{\rm s}$ [49, 50, 162, 163, 164], decreases exponentially in field space together with the mass scale of the tower. While a finite small number of light states can always be integrated in such to define a new EFT, the presence of an *infinite* number of light states necessarily drives the cut-off to zero with exponential rate α which is in general different from the rate λ of the tower [5]. In the case of states equally spaced, such as Kaluza-Klein modes, one can show that $\Lambda_{\rm s} = m^{1/3}$ (assuming $M_{\rm P} = 1$), thus yielding $\alpha = \lambda/3$ [15, 20, 30, 165]. This is consistent with the fact that, in the infinite distance limit, the QG cut-off lies still above the typical mass scale of the tower. While traversing a distance in field space, some states of the tower can enter the EFT and produce observational effects, while the QG cut-off remains still above the typical energy scale of the EFT. This explains how it is possible for the SDC to have an impact on observations in low-energy physics.
The exponential rate of the tower λ can in general depend on the *path* followed in moduli space while approaching the infinite-distance point. A first example of this situation was given in [20] for the hyperbolic half-plane where it was shown that trajectories, with the axion and saxion linear to each other[6], yield an effective reduction of the decay rate. This translates also into the possibility of engineering a larger field excursion. A more general analysis is given in [32]. In fact, one can reverse (5.3) and express the *mass decay rate* of the tower as

$$\lambda(\Delta) = -\frac{d\log m}{d\Delta} = -T^i \partial_i \log m \tag{5.4}$$

that is the scalar product between the normalized tangent vector T^i, along the trajectory that we follow to reach the point at infinity, and the gradient of the (logarithm of the) mass of the tower. In the most general case, the gradient of the mass can be aligned along any direction in moduli space [32]. However, in most of the String Theory examples, $\partial_i \log m$ is aligned along geodesics. This implies that λ becomes a measure to quantify the *non-geodicity* of the trajectory. In this case we can write

$$\lambda = -|\partial \log m| \cos\theta = \lambda_{\rm g} \cos\theta \tag{5.5}$$

where θ is the angle between the trajectory we are following in field space and the geodesic [7]. Both paths will reach the infinite-distance singularity but with

[5] Here we are more precise compared to the toy model in the previous chapter where we directly identified the $\Lambda_{\rm swamp}$ with the first tower state.

[6] Situations where the axion has a typical linear backreaction with the saxion, for large field displacements, have been observed in string theory models such as in [166, 52, 86, 167]. Moreover, this corresponds the critical case from section 2.3.3 where a 2-dimensional hyperbolic plane was discussed.

[7] More on the definition of the angle θ soon.

different angles. In fact, as mentioned before, the tangent vector T^i has to be constant in the full infinite-distance limit such that we are compatible with the SDC. The parameter $\lambda_{\rm g}$ represents the highest value of λ and it corresponds to the decay rate for a geodesic trajectory. Moving along a non-geodesic trajectory can be the result of introducing a scalar potential for the moduli (see section 5.2). Now (5.5) seems to suggest that λ could even become zero, if one moves along a trajectory, which is orthogonal to a geodesic (i.e. $\theta = \pi/2$) [8]. This would mean that arbitrary distances could be traversed without the mass scale of a tower dropping-off. The EFT would be valid for arbitrary long distances, and one could easily avoid the drastic implication of the SDC.[9] However, as mentioned above, we have clear indication that String Theory sets a lowest possible value for such a decay rate [46, 47, 48, 161, 150]. If we generically indicate the existence of such a lower bound with

$$\lambda \geq \lambda_0, \tag{5.6}$$

then we can translate this into a maximum deviation angle from the geodesic trajectory allowed by the SDC, namely

$$\cos\theta \geq -\frac{\lambda_0}{|\partial \log m|} = \frac{\lambda_0}{\lambda_{\rm g}}. \tag{5.7}$$

A bound on the angle θ means that not all the trajectories in moduli space are allowed by the SDC and we can deviate by a maximum angle from the geodesic. In the next section we recall how the introduction of a scalar potential can lead to a departure from a moduli space geodesic equation.

At this juncture, it is important to emphasize that our focus will now be solely on *infinite-distance trajectories* in the subsequent discussion. These trajectories are characterized by distances that can extend infinitely, providing a robust framework to apply the SDC. Specifically, we will first examine deviations from geodesics with a constant angle $\theta = \text{const}$ (section 5.3), which is nothing else than the critical case from section 2.3.3, and then trajectories with a time-dependent deviation angle $\theta = \theta(t)$ (section 5.4). On the one hand, we will refer to the former case henceforth as the critical case. And, on the other hand, let us emphasize that, given (5.5), the latter case corresponds to a time-dependent, or rather Δ-dependent, decay rate of the tower mass $\lambda = \lambda(\Delta)$. This will effectively induce field-dependent corrections such that the mass formula (5.3) will deviate from its the exponential form when moving away from the moduli space boundary (which is placed at $\Delta \to \infty$). Therefore, a time-dependent decay rate can serve as a convenient mean to parameterize a departure from the boundary.

[8] This was previously termed the swampy case, see section 2.3.3

[9] Models with highly curved trajectories and large field ranges have in fact been proposed in literature [133, 136, 168, 169, 140, 141, 170]. Whether these effective scenarios could be realized in a consistent string theory embedding is still unclear. Recent work [137] seems in fact to restrict such a possibility (see also [171]).

5.2 Multi-field Setup and Trajectories in Moduli Space

String Theory comes naturally with many moduli, namely massless scalar fields. The internal field geometry, defined by their kinetic terms, is generically non-flat, with a typical curvature, as the result of the compactification process. It is also characterized by a set of geodesics. However, the introduction of a scalar potential (e.g. by means of fluxes) can lead to a deviation from the original geodesic trajectories and a consequent change of dynamics.[10]
In this section we present a pedagogical introduction to a convenient framework for studying multi-scalar field systems [136]. This is based on projecting the equations of motion along the tangent and normal directions of the trajectory along which the system evolves. By employing this approach, we demonstrate how the system can be described using an equation resembling the equation of motion for a single scalar field, as well as another equation involving the turning rate Ω. We emphasize the relationship between the equations of motion and the trajectories (geodesic or non-geodesic) in field space. We progressively delve into increasing levels of complexity. We begin by considering the case of free massless scalar fields in a flat Minkowski background. Next, we introduce a scalar potential and demonstrate how it leads to deviations from geodesic motion. Subsequently, we incorporate gravity and investigate the effects of a Friedmann-Lemaître-Robertson-Walker (FLRW) background. Finally, we describe the equations governing a scalar multi-field system that gives rise to cosmic acceleration.

5.2.1 Scalar Fields in Minkowski Spacetime

Let us consider the Lagrangian of n free massless homogeneous scalar fields $\Phi^a = \Phi^a(t)$, thus depending just on the time variable t

$$\mathcal{L} = -\frac{1}{2}\eta^{\mu\nu} G_{ab}\, \partial_\mu \Phi^a \partial_\nu \Phi^b \tag{5.8}$$

where $\eta^{\mu\nu}$ is the Minkowski spacetime metric, $G_{ab} = G_{ab}(\Phi^a)$ is the internal field space metric and Latin indices a, b run from 1 to n. The equations of motion then take the form

$$\ddot{\Phi}^a + \Gamma^a_{bc}\dot{\Phi}^b\dot{\Phi}^c = 0, \tag{5.9}$$

where the dot $\dot{}$ is indicating a time derivative, and

$$\Gamma^a_{bc} = \frac{1}{2}G^{ad}\left(\frac{\partial G_{bd}}{\partial \Phi^c} + \frac{\partial G_{cd}}{\partial \Phi^b} - \frac{\partial G_{bc}}{\partial \Phi^d}\right) \tag{5.10}$$

[10] There are instead situations where the dynamics remain quite insensitive to a great variety of scalar potentials and is instead mainly determined by the geometric properties of the internal manifold. In the context of inflationary cosmology, the α-attractor scenario [152, 153, 156] is a primary example of such a circumstance.

are the Christoffel symbols of the moduli space. Note that (5.9) has precisely the form of a *geodesic equation*. It describes, in fact, the set of (geodesic) trajectories along which the scalar fields Φ^a evolve in time. Notice that the time t is not a preferred parameter for the geodesic and we can shift and rescale it as the result of the shift-symmetry of the Lagrangian (5.8) and scale-symmetry of the equations of motion (5.9).
Let us introduce the covariant derivative D_t, which is defined as

$$D_t A^a \equiv \dot{A}^a + \Gamma^a_{bc} A^b \dot{\Phi}^c \tag{5.11}$$

for a given vector A^a. Having $D_t A^a = 0$ means that the vector A^a is parallel transported along the trajectory Φ^a, i.e. A^a always "points at the same direction" along Φ^a. Moreover, D_t acting on a field scalar reduces to an ordinary time derivative. With this definition the above set of equations (5.9) reduces to

$$D_t \dot{\Phi}^a = 0, \tag{5.12}$$

which is consistent with the fact that the equations of motion are just geodesic equations and a geodesic is a trajectory which is autoparallel transported along itself.
We now introduce the tangent and the normal vector to the trajectory Φ^a, respectively, as

$$\begin{aligned} T^a &= \frac{\dot{\Phi}^a}{\dot{\Phi}} \\ N^a &= -\frac{1}{|D_t T|} D_t T^a \end{aligned} \tag{5.13}$$

where $\dot{\Phi}$ is the speed along the trajectory, defined as

$$\dot{\Phi} = \sqrt{G_{ab} \dot{\Phi}^a \dot{\Phi}^b}. \tag{5.14}$$

Both vectors T^a and N^a are normalised and orthogonal to each other, namely $G_{ab} T^a T^b = G_{ab} N^a N^b = 1$ and $G_{ab} T^a N^b = 0$. Now we can project the equations of motion along the tangent and normal vectors. This just means contracting the equations of motion with T^a and N^a. The tangential projection yields

$$\ddot{\Phi} = 0 \tag{5.15}$$

where we have used the product rule for D_t and the orthogonality property of T^a and N^a. Instead, the normal projection gives

$$\Omega \dot{\Phi} = 0 \tag{5.16}$$

where we have introduced the *turning rate* as

$$\Omega = |D_t T| \tag{5.17}$$

and used again orthogonality of the two vectors together with the fact that

$$D_t \dot{\Phi}^a = \dot{\Phi} D_t T^a + \ddot{\Phi} T^a. \tag{5.18}$$

Excluding the trivial case $\dot{\Phi} = 0$, (5.16) implies that we need $\Omega = 0$ in order to fulfill the geodesic equation. That is the reason why Ω is also called non-geodesicity factor. Furthermore, let us note that if T^a gets parallel transported along Φ^a, i.e. $D_t T^a = 0$, we immediately get $\Omega = 0$ and the equation of motion just reduces to the equation $\ddot{\Phi} = 0$. Since we are dealing with positive definite Riemannian field manifolds, the statement $\Omega = 0$ is equivalent to $D_t T^a = 0$. Geometrically, Ω measures the failure of T^a being parallel transported along Φ^a.

5.2.2 Scalar Fields with Potential in Minkowski Spacetime

As the next step, we now introduce a potential $V(\Phi^a)$ for the scalar fields. We still consider a flat Minkowski background such that the Lagrangian $\mathcal{L}$ becomes

$$\mathcal{L} = -\frac{1}{2}\eta^{\mu\nu} G_{ab} \partial_\mu \Phi^a \partial_\nu \Phi^b - V(\Phi^a)\,. \tag{5.19}$$

The equations of motion hence read

$$D_t \dot{\Phi}^a + G^{ab} V_b = 0 \tag{5.20}$$

where we define $V_b \equiv \partial V / \partial \Phi^b$. Projecting again the set of equations in the tangential and normal direction we get

$$\ddot{\Phi} + V_T = 0 \tag{5.21}$$

$$\Omega \dot{\Phi} = V_N \tag{5.22}$$

where we have introduced $V_T \equiv T^a V_a$ and $V_N \equiv N^a V_a$, i.e. the corresponding projections of the gradient of the potential V. It is interesting to understand what happens in the case $D_t T^a = 0$, which is, as explained earlier, equivalent to $\Omega = 0$. Rearranging the relation (5.18) we get

$$D_t T^a = \frac{1}{\dot{\Phi}} \left(D_t \dot{\Phi}^a - T^a \ddot{\Phi} \right). \tag{5.23}$$

In the case of zero potential, as seen before, both terms in the bracket of the last equation vanish, thus automatically leading to $\Omega = 0$. Instead, in the presence of a non-zero potential the situation is slightly more involved. The two terms

can in fact cancel each other, so that the trajectory will follow a geodesic path in field space. However, the acceleration along the trajectory will still be determined by the tangential projection of V, as expressed in (5.21). We can get more insight about this situation by using the equations of motion (5.20) and (5.21) and rewriting (5.23) as

$$D_t T^a = -\frac{1}{\dot{\Phi}} \left(G^{ab} V_b - T^a V_T \right). \tag{5.24}$$

In order to have $\Omega = 0$, we immediately see that the gradient of the potential V_a and the tangent vector T_a have to be aligned. This means that geodesic trajectories are always characterized by a zero normal component of the gradient of the scalar potential, namely $V_N = 0$. Intuitively, the trajectory corresponds to a valley of the scalar potential. If there is no normal force, the tangent vector gets parallel transported along the trajectory. This is an approach used very often in string/supergravity model building as it hugely simplifies the analysis of the system. In a typical saxion-axion system it corresponds to stabilizing one of the two fields and leaving the other very light to drive the acceleration phase. On the other hand, the multi-field framework allows, in principle, also for very sharp turns, $\Omega \gg 1$, which means a great misalignment between the potential gradient flow and the tangent vector T^a.

5.2.3 Scalar Fields with Potential in FLRW Spacetime

We further generalise our setup by taking the 4-dimensional spacetime to be a FLRW metric $g_{\mu\nu}$ with line element of the form

$$ds^2 = -dt^2 + a^2(t) d\vec{x}^2. \tag{5.25}$$

Then, given the action

$$S = \int d^4x \sqrt{-g} \left(\frac{1}{2} R - \frac{1}{2} g^{\mu\nu} G_{ab} \partial_\mu \Phi^a \partial_\nu \Phi^b - V(\Phi^a) \right) \tag{5.26}$$

with g being the determinant of $g_{\mu\nu}$ and R the Ricci scalar, we get the following equations

$$D_t \dot{\Phi}^a + 3H\dot{\Phi}^a + G^{ab} V_b = 0. \tag{5.27}$$

These contain an additional friction term [11], proportional to the Hubble expansion rate $H \equiv \dot{a}/a$. The projections work completely analogous to the previous cases, namely we get

$$\ddot{\Phi} + 3H\dot{\Phi} + V_T = 0 \tag{5.28}$$

$$\Omega \dot{\Phi} = V_N. \tag{5.29}$$

[11] In fact, the friction term can be eliminated by an appropriate affine reparametrisation.

We note that the set of equations (5.27) just reduce to two simple equations. The first, namely (5.28), has the form of the equation for a single scalar field in a FLRW spacetime. The second, i.e. (5.29), involves the turning rate Ω and it is not affected by the friction term. Since only the first equation is altered, we can draw the same conclusions about the case $D_t T^a = 0$, as discussed in the previous part.

5.2.4 Multi-field Cosmic Acceleration

As final step, we consider the coupled system and include the backreaction of the scalar dynamics on the FLRW background. We will explicitly state the conditions required to achieve cosmic acceleration. The action we consider is as before (5.26). Therefore, the background dynamics of the full system is given by

$$3H^2 - \frac{1}{2}\dot{\Phi}^2 - V = 0 \tag{5.30}$$

$$\ddot{\Phi} + 3H\dot{\Phi} + V_T = 0 \tag{5.31}$$

$$\Omega\dot{\Phi} = V_N. \tag{5.32}$$

where the first equation is the Friedmann equation associated to the FLRW metric while the last two equations refer to the dynamics of the scalar fields and are already in the projected form, as introduced before.
Cosmic acceleration happens when $\ddot{a} > 0$. One can show that this is equivalent to requiring

$$\epsilon < 1 \tag{5.33}$$

with ϵ being the *acceleration parameter* defined and equal to

$$\epsilon \equiv -\frac{\dot{H}}{H^2} = \frac{\dot{\Phi}^2}{2H^2}. \tag{5.34}$$

To ensure that the acceleration phase lasts for a sufficient number of Hubble times[12], one can require

$$\eta \equiv \frac{\dot{\epsilon}}{H\epsilon} = 2\epsilon + 2\frac{\ddot{\Phi}}{H\dot{\Phi}} < 1. \tag{5.35}$$

Note that the latter expressions are exact and do not assume any slow-roll condition. They can be obtained simply by differentiating (5.30) with respect to the cosmic time t and combining this with (5.31), once we observe that $V_T\dot{\Phi} =$

[12]This condition is particularly relevant in the case of cosmic inflation to solve the horizon problem. There it is necessary for ϵ to remain small for a minimum of around 60 e-foldings, whereas in the case of quintessence dark energy this condition can be relaxed.

$T^a V_a \dot{\Phi} = \dot{\Phi}^a V_a = \dot{V}$ by the chain rule.
Using these definitions one can rewrite the Friedmann equation (5.30) simply as

$$H^2 = \frac{V}{3-\epsilon}. \tag{5.36}$$

Finally, one can derive an expression which relates the fractional gradient of V and the acceleration parameter ϵ in a multi-field setup. Let us note that

$$\frac{|\nabla V|^2}{V^2} = \frac{V_T^2 + V_N^2}{V^2} \tag{5.37}$$

where we have used that $V^a = T^a V_T + N^a V_N$. We can obtain an expression for the tangential derivative of V as

$$V_T^2 = \frac{1}{2}\epsilon \left(6 - (2\epsilon - \eta)\right)^2 H^4 \tag{5.38}$$

by combining (5.31), (5.34) and the expression for η given in (5.35). Similarly, we can obtain an expression for the normal derivative of V, namely

$$V_N^2 = 2\Omega^2 H^2 \epsilon. \tag{5.39}$$

By combining the last four numbered equations, one finally obtains

$$\frac{|\nabla V|^2}{V^2} = 2\epsilon \left(\left(1 + \frac{\eta}{2(3-\epsilon)}\right)^2 + \frac{\Omega^2}{H^2(3-\epsilon)^2} \right). \tag{5.40}$$

If we demand a phase of cosmic acceleration, namely $\epsilon < 1$, then one has

$$\frac{|\nabla V|^2}{V^2} \simeq 2\epsilon \left(\left(1 + \frac{\eta}{6}\right)^2 + \frac{\Omega^2}{9H^2} \right). \tag{5.41}$$

The latter expression shows that one may fulfill the de Sitter conjecture [24] in an accelerating background, either by having a large turning rate Ω (namely, a misalignment between the tangent vector and the gradient flow of V) or a large η parameter (see [172] for a recent analysis of this regime in the context of single field inflation). One example of the latter situation is given by the so-called "scaling cosmologies" as recently analysed in [145, 146]. If one instead insists on $\eta \ll 1$, then one effectively requires a slow roll condition, namely $\ddot{\Phi} \ll H\dot{\Phi}$. In this regime, one obtains

$$\frac{|\nabla V|^2}{V^2} \simeq 2\epsilon \left(1 + \frac{\Omega^2}{9H^2}\right) \tag{5.42}$$

which was already displayed in the introduction section of this work as (5.2).

5.3 Asymptotic Acceleration and Turning Rate for constant θ

The boundary of moduli space provides an ideal testing ground to examine the predictions of the SDC. It allows for trajectories that extend infinitely, enabling the identification of a tower of states with exponentially decreasing mass along such paths.[13] Around these asymptotic regions, effective field theories exhibit significant simplifications and possess distinct features. Recent investigations [159, 145, 146] have therefore focused on studying cosmic acceleration in these limits.
In this section we examine the implications of the SDC on a multi-field system that leads to "asymptotic acceleration", referring to cosmic acceleration occurring at the boundary of moduli space. We consider *infinite-distance trajectories*, namely paths in field space that can approach such asymptotic regions. These trajectories can either follow geodesics or deviate from them by a certain angle θ, as already discussed. The SDC imposes a strict constraint on this deviation angle, requiring it to approach a constant value in the full infinite-distance limit [32]. In this section we stick to the case of (infinite-distance) trajectories with constant deviation angle from a geodesic.[14] Moreover, we focus on *hyperbolic spaces* as prototype geometries of infinite distance limits of Calabi-Yau compactifications.
As main result, we find that the turning rate of such infinite-distance trajectories is negligible during the acceleration phase since it takes the form

$$\frac{\Omega}{H} = F(\theta, R)\ \sqrt{\epsilon}. \tag{5.43}$$

Here F is a function of the deviation angle θ and of the (sectional) curvature R of the field manifold and it is upper bounded by

$$F(\theta, R) < F(\theta_0, R) \tag{5.44}$$

with θ_0 being the maximum deviation angle allowed which is related to the lower bound on the tower mass decay rate λ, see (5.7). The exact form of F will depend on the specific case and dimensionality of the hyperbolic space and the trajectory followed therein.
We will proceed as follows. First, we begin by considering the simplest case of a single hyperbolic plane, which corresponds to a typical saxion-axion system. Next, we move on to a more complex scenario by considering a product of two hyperbolic planes. We will explore the diverse trajectory possibilities that arise

[13] According to the Emergence String Conjecture [55], the tower of states can be represented by either Kaluza-Klein modes or tensionless strings. However, for the purposes of our discussion, the specific nature of the tower is not relevant.

[14] Moving away from the boundary allows to have more freedom, such as path-dependent deviations from geodesic trajectories. We will consider this case in the following section.

in this setup. Finally, we extend our analysis to the case of N hyperbolic planes and generalise our derived formulas.

5.3.1 Computation for one Hyperbolic Plane

As already introduced in section 2.3.3, the metric of a single hyperbolic upper half-plane is given by

$$d\Delta^2 = G_{ab} d\Phi^a d\Phi^b = \frac{n^2}{s^2}\left(ds^2 + d\phi^2\right) \tag{5.45}$$

for $s > 0$. For completeness let us reiterate some of its features at this point. For instance, the parameter $n > 0$ controls the curvature of the hyperbolic plane, namely the Ricci scalar reads $R = -2/n^2$. We are dealing with two scalar fields: the saxion s and the axion ϕ, i.e. $\Phi^a = (s, \phi)$. The saxion s is assumed to take large values since we are interested in infinite distance limits which correspond to $s \to \infty$. Furthermore, the axion ϕ is usually periodic with some identification even for large s, but this symmetry is in general broken in the presence of a potential [32]. Hence, we assume that ϕ can take any real value. We will make these assumptions throughout the rest of this chapter, i.e. also for products of hyperbolic planes with several saxions and axions.
To be consistent with the Scalar Distance Conjecture, we impose a mass tower scaling as

$$M_s \sim s^{-a} \tag{5.46}$$

where $a > 0$. This ensures a massless tower of states, which drops exponentially down, when traversing an infinite field distance along a geodesic, i.e. along the s-direction.
Now we can apply the techniques introduced in Section 5.2, namely the turning rate Ω is given by

$$\Omega^2 = \frac{n^2}{s^2}(D_t T^s)^2 + (D_t T^\phi)^2 \tag{5.47}$$

where

$$\begin{aligned} D_t T^s &= \dot{T}^s + \Gamma^s_{bc} T^b \dot{\Phi}^c = \dot{T}^s - \frac{1}{s} T^s \dot{s} + \frac{1}{s} T^\phi \dot{\phi} \\ D_t T^\phi &= \dot{T}^\phi + \Gamma^\phi_{bc} T^b \dot{\Phi}^c = \dot{T}^\phi - \frac{1}{s} T^s \dot{\phi} - \frac{1}{s} T^\phi \dot{s}. \end{aligned} \tag{5.48}$$

For the single hyperbolic plane the non-vanishing Christoffel symbols are

$$\Gamma^s_{ss} = -\frac{1}{s} = \Gamma^\phi_{s\phi}, \quad \Gamma^s_{\phi\phi} = \frac{1}{s}. \tag{5.49}$$

Next, to get an upper bound on the turning rate Ω, we choose a trajectory which enjoys maximal non-geodesicity compatible with the SDC. This precisely amounts

to the critical case introduced in section 2.3.3 for the single hyperbolic plane. Also recall that in this case the distance and, more importantly, the decay rate are modified by a constant factor compared to the geodesic case. For instance, recalling section 2.3.3 we have the following critical case condition here

$$\frac{d\phi}{ds} = \frac{\dot{\phi}}{\dot{s}} = \beta = const \tag{5.50}$$

where the first equality holds in general by the chain rule. Interestingly, the condition (5.50) makes the velocity along the trajectory a constant multiple of the speed experienced on a geodesic, i.e. along the s-direction. This is not surprising because, if the distance changes by a constant factor, then the speed, i.e. the time-derivative of the distance, also does. This results in

$$\dot{\Phi}^2 = \frac{n^2}{s^2}(\dot{s}^2 + \dot{\phi}^2) = n^2(1+\beta^2)\frac{\dot{s}^2}{s^2} \tag{5.51}$$

and the tangent vector to the trajectory reads

$$\begin{aligned} T^s &= \frac{1}{\dot{\Phi}}\dot{s} \\ T^\phi &= \frac{1}{\dot{\Phi}}\dot{\phi} = \frac{1}{\dot{\Phi}}\beta\dot{s}. \end{aligned} \tag{5.52}$$

Thus, we get

$$\begin{aligned} D_t T^s &= \frac{1}{\dot{\Phi}}\left(\ddot{s} - \frac{\dot{s}}{\dot{\Phi}}\ddot{\Phi} - \frac{\dot{s}^2}{s}(1-\beta^2)\right) \\ D_t T^\phi &= \frac{1}{\dot{\Phi}}\beta\left(\ddot{s} - \frac{\dot{s}}{\dot{\Phi}}\ddot{\Phi} - 2\frac{\dot{s}^2}{s}\right). \end{aligned} \tag{5.53}$$

Using

$$\frac{\dot{s}}{\dot{\Phi}}\ddot{\Phi} = \ddot{s} - \frac{\dot{s}^2}{s}, \tag{5.54}$$

which can be verified by explicit computation, the above becomes

$$\begin{aligned} D_t T^s &= \frac{\beta^2}{\dot{\Phi}}\frac{\dot{s}^2}{s} = \frac{\beta^2}{n\sqrt{1+\beta^2}}\dot{s} \\ D_t T^\phi &= -\frac{\beta}{\dot{\Phi}}\frac{\dot{s}^2}{s} = -\frac{\beta}{n\sqrt{1+\beta^2}}\dot{s}. \end{aligned} \tag{5.55}$$

Then, the turning rate Ω is finally given by

$$\Omega^2 = \beta^2\frac{\dot{s}^2}{s^2} = \frac{\beta^2}{n^2(1+\beta^2)}\dot{\Phi}^2. \tag{5.56}$$

A non-vanishing Ω immediately tells us that the path defined by (5.50) is not a geodesic of the hyperbolic plane, unless we have $\beta = 0$. In particular, more on the consistency of the critical case with the geodesic equation can be found in appendix C which provides a complementary picture. However, the above also implies that we need to apply a normal force V_N in order to be moving in a straight line, given by a linear relation between s and ϕ, on a hyperbolic plane. Since our intuition is usually built on Euclidean geometry, this is rather strange and one of the unusual properties of hyperbolic spaces.
Now a very natural question is, whether there is an interpretation of β in terms of the deviation angle θ such that we connect to the statements in the previous sections. To answer that, we use the following standard formula from Riemannian geometry

$$\cos\theta = \frac{v^a u_a}{|v||u|} \tag{5.57}$$

which defines an angle (between two vectors v^a and u^a) via the inner product for curved spaces. We are interested in the angle between the tangent to the trajectory T^a and the vertical axis, i.e. the s-axis. But, more generally, we are interested in the angle between the tangent to the geodesic trajectory T_g^a corresponding to the mass tower in question and the tangent to the non-geodesic trajectory T^a. The latter can be found above and the former is given by

$$\begin{aligned} \dot{\Phi}_g^2 &= n^2 \frac{\dot{s}^2}{s^2} \\ T_g^s &= \frac{1}{\dot{\Phi}_g}\dot{s} \\ T_g^\phi &= 0. \end{aligned} \tag{5.58}$$

We arrive at these expressions by setting $\beta = 0$ because on the geodesic trajectory the axion ϕ is just a constant. Also note that both tangent vectors are normalised such that the denominator in the angle formula (5.57) is just 1 such that

$$\cos\theta = G_{ab} T_g^a T^b = \frac{1}{\sqrt{1+\beta^2}}. \tag{5.59}$$

It is very obvious now that $\beta = \tan\theta$. However, this isn't a big surprise because there is the well-known relation

$$\frac{d\phi}{ds} = \frac{\dot{\phi}}{\dot{s}} = \tan\theta \tag{5.60}$$

which gives the angle between a curve $\phi(s)$ and the s-axis. This expression holds for conformally flat manifolds (as the hyperbolic plane is) because angles on a conformally flat manifold are the same angles as in Euclidean flat space, i.e. a

conformal transformation is angle-preserving. But let us emphasise that this second approach is only sensible here, because we are conformally flat, whereas the first method works for any curved space.
Furthermore, the quantity in (5.59) is precisely the factor from (5.5) which reduces the geodesic decay rate on a non-geodesic trajectory. At this point let us mention that negative θ have the same influence on the decay rate as positive θ. In fact, β can also be negative because we have a symmetry of $\phi \to -\phi$ in the equations of motion (also including a potential). This is also pointed out in appendix B for the geodesic equation. Moreover, this holds also for all the later cases.
Finally, using (5.75) the velocity along the trajectory and the turning rate can be written in terms of this angle θ as

$$\begin{aligned} \dot{\Phi}^2 &= \frac{n^2}{\cos^2\theta}\frac{\dot{s}^2}{s^2} \\ \Omega^2 &= \frac{\sin^2\theta}{n^2}\dot{\Phi}^2. \end{aligned} \tag{5.61}$$

By invoking (5.34) we arrive at the promised form for Ω/H, namely

$$\frac{\Omega^2}{H^2} = \frac{2\sin^2\theta}{n^2}\epsilon \tag{5.62}$$

where the prefactor clearly is an $\mathcal{O}(1)$ quantity, unless we have a very large curvature.

5.3.2 Computations for two Hyperbolic Planes

Once we include a second hyperbolic plane the situation gets more complicated. In a product of two hyperbolic planes we have two saxions s, u and two axions ϕ, ψ and the field space metric, as introduced in section 2.3.3, reads

$$d\Delta^2 = G_{ab}d\Phi^a d\Phi^b = \frac{n^2}{s^2}\left(ds^2 + d\phi^2\right) + \frac{m^2}{u^2}\left(du^2 + d\psi^2\right) \tag{5.63}$$

where $\Phi^a = (s, \phi, u, \psi)$. At this point we make the same assumptions about both the saxions and the axions as in the previous part. Moreover, we associate a mass tower with each saxionic direction, namely

$$\begin{aligned} M_s &\sim s^{-a} \\ M_u &\sim u^{-b} \end{aligned} \tag{5.64}$$

where a, b are again some positive constants. Keep in mind that this is just the bare minimum of the mass towers required by consistency with the SDC. In

general, there is an abundance of towers in a realistic string theory setup.
The turning rate Ω gets now contributions from both hyperbolic planes

$$\Omega^2 = \frac{n^2}{s^2}\left((D_t T^s)^2 + (D_t T^\phi)^2\right) + \frac{m^2}{u^2}\left((D_t T^u)^2 + (D_t T^\psi)^2\right) \tag{5.65}$$

where

$$\begin{aligned}
D_t T^s &= \dot{T}^s + \Gamma^s_{bc} T^b \dot{\Phi}^c = \dot{T}^s - \frac{1}{s} T^s \dot{s} + \frac{1}{s} T^\phi \dot{\phi} \\
D_t T^\phi &= \dot{T}^\phi + \Gamma^\phi_{bc} T^b \dot{\Phi}^c = \dot{T}^\phi - \frac{1}{s} T^s \dot{\phi} - \frac{1}{s} T^\phi \dot{s} \\
D_t T^u &= \dot{T}^u + \Gamma^u_{bc} T^b \dot{\Phi}^c = \dot{T}^u - \frac{1}{u} T^s \dot{u} + \frac{1}{u} T^\psi \dot{\psi} \\
D_t T^\psi &= \dot{T}^\psi + \Gamma^\psi_{bc} T^b \dot{\Phi}^c = \dot{T}^\psi - \frac{1}{u} T^u \dot{\psi} - \frac{1}{u} T^\psi \dot{u}.
\end{aligned} \tag{5.66}$$

For the product of two hyperbolic planes the non-vanishing Christoffel symbols are

$$\Gamma^s_{ss} = -\frac{1}{s} = \Gamma^\phi_{s\phi}, \quad \Gamma^s_{\phi\phi} = \frac{1}{s}, \quad \Gamma^u_{uu} = -\frac{1}{u} = \Gamma^\psi_{s\psi}, \quad \Gamma^u_{\psi\psi} = \frac{1}{u}. \tag{5.67}$$

Please note that there are no non-vanishing Christoffel symbols which mix between the two hyperbolic planes because the coordinates are independent of each other (only in the next step we assume some relations between them).
So far not much has changed in the product case. We have just extended all the quantities by two new entries. However, the differences are coming in now, namely in the choice of the trajectory. For now we will focus on a saxionic direction, the s-direction. However, this isn't a restriction in any form because the situation is symmetric. So, if we pick the u-direction, we would acquire exactly the same results. This means we are investigating how the mass tower M_s behaves under different trajectories in moduli space. For a product of two hyperbolic planes we can have up to four scalar fields moving at the same time. But we will keep it slow and start with trajectories only involving the saxion s and one other field.

Saxion-Axion Trajectories

In the first case we keep u and ψ fixed, i.e. $u = u_0 = const$, $\psi = \psi_0 = const$ and hence $T^u = 0 = T^\psi$. However, here we immediately recover the result from the single hyperbolic plane (5.61) because we keep everything fixed on the other hyperbolic plane.
Next, we assume that $u = u_0$ and $\phi = \phi_0$ are constant such that $T^u = 0 = T^\phi$. Effectively, we are just considering the saxion from one hyperbolic plane which evolves together with the axion from the other hyperbolic plane. We have to establish now a relation between s and ψ which maximizes the non-geodesicity

whilst respecting the SDC. As already seen in section 2.3.3, it turns out that the condition

$$\frac{\dot{\psi}}{\frac{\dot{s}}{s}} = \gamma = const \tag{5.68}$$

has the desired effect. Unlike the last case, the above relation isn't directly equal to $\frac{d\psi}{ds}$ because we have the extra $\frac{1}{s}$ term (we could use some logarithmic coordinate for s but there will be more on the interpretation later). The geodesic trajectory can be recovered by setting $\gamma = 0$.
Now (5.68) produces the following velocity along the trajectory

$$\dot{\Phi}^2 = \frac{n^2}{s^2}\dot{s}^2 + \frac{m^2}{u_0^2}\dot{\psi}^2 = n^2\frac{\dot{s}^2}{s^2}\left(1 + \frac{m^2\gamma^2}{u_0^2 n^2}\right), \tag{5.69}$$

which is again a constant multiple of the geodesic velocity, and the tangent vector to the trajectory reads

$$\begin{aligned} T^s &= \frac{1}{\dot{\Phi}}\dot{s} \\ T^\phi &= 0 \\ T^u &= 0 \\ T^\psi &= \frac{1}{\dot{\Phi}}\dot{\psi} = \frac{1}{\dot{\Phi}}\gamma\frac{\dot{s}}{s}. \end{aligned} \tag{5.70}$$

Thus, we get

$$\begin{aligned} D_t T^s &= \frac{1}{\dot{\Phi}}\left(\ddot{s} - \frac{\dot{s}}{\dot{\Phi}}\ddot{\Phi} - \frac{\dot{s}^2}{s}\right) \\ D_t T^\phi &= 0 \\ D_t T^u &= \frac{1}{u_0}\frac{\dot{\psi}^2}{\dot{\Phi}} \\ D_t T^\psi &= \frac{1}{\dot{\Phi}}\left(\ddot{\psi} - \frac{\dot{\psi}}{\dot{\Phi}}\ddot{\Phi}\right). \end{aligned} \tag{5.71}$$

Using

$$\begin{aligned} \frac{\dot{s}}{\dot{\Phi}}\ddot{\Phi} &= \ddot{s} - \frac{\dot{s}^2}{s} \\ \ddot{\psi} &= \gamma\left(\frac{\ddot{s}}{s} - \frac{\dot{s}^2}{s^2}\right) \\ \frac{\dot{\psi}}{\dot{\Phi}}\ddot{\Phi} &= \frac{\gamma}{s}\left(\ddot{s} - \frac{\dot{s}^2}{s}\right), \end{aligned} \tag{5.72}$$

which can be again verified by explicit computation, the above reduces dramatically to

$$\begin{aligned} D_t T^s &= 0 \\ D_t T^\phi &= 0 \\ D_t T^u &= \frac{1}{u_0}\frac{1}{\dot\Phi}\dot\psi^2 = \frac{1}{u_0}\frac{1}{\dot\Phi}\gamma^2\frac{\dot s^2}{s^2} \\ D_t T^\psi &= 0. \end{aligned} \tag{5.73}$$

It is quite interesting that the contribution to the turning rate Ω is concentrated along the u-direction which will be important soon. All in all, these computations work out quite similar to the single hyperbolic plane. The turning rate then finally reads

$$\Omega^2 = \frac{m^2\gamma^4}{u_0^4}\frac{1}{\dot\Phi^2}\left(\frac{\dot s^2}{s^2}\right)^2 = \frac{\frac{m^2\gamma^4}{u_0^4 n^4}}{\left(1+\frac{m^2\gamma^2}{u_0^2 n^2}\right)^2}\dot\Phi^2. \tag{5.74}$$

We immediately recognise the same quadratic scaling with the speed $\dot\Phi$ as in (5.61).

Analogous to the previous section, we also employ an angle formulation. By (5.57) we can again compute the angle θ between the geodesic tangent vector T_g^a corresponding to the mass tower M_s (this is the same vector as in the single plane case, we just add two zero components T^u and T^ψ) and the non-geodesic tangent vector T^a which is given above for this trajectory. Again both tangent vectors are normalised, so we get

$$\cos\theta = G_{ab}T_g^a T^b = \frac{1}{\sqrt{1+\frac{m^2\gamma^2}{u_0^2 n^2}}}. \tag{5.75}$$

This immediately implies the identification $\tan\theta = \frac{m\gamma}{u_0 n}$. But we can't directly apply the second method from the previous section here because we aren't conformally flat. Moreover, this is again the expression for $\cos\theta$ in (5.5).

As an alternative approach to the above angle definition, we can consider the effective metric of the trajectory which is given by

$$d\Delta_{eff}^2 = \frac{n^2}{s^2}ds^2 + \frac{m^2}{u_0^2}d\psi^2. \tag{5.76}$$

Please remember that n, m, u_0 are constants here. Then, we can redefine our coordinates

$$d\Delta_{eff}^2 = d(n\ln s)^2 + d\left(\frac{m}{u_0}\psi\right)^2 = d\tilde s^2 + d\tilde\psi^2 \tag{5.77}$$

which gives us a flat manifold in which we can use normal angle definitions. For instance, these coordinates enable us to apply the formula from the previous

section, namely (5.60), work our way back to the original coordinates and use (5.68)

$$\tan\theta = \frac{d\tilde{\psi}}{d\tilde{s}} = \frac{\frac{d\tilde{\psi}}{dt}}{\frac{d\tilde{s}}{dt}} = \frac{\frac{m}{u_0}\dot{\psi}}{n\frac{\dot{s}}{s}} = \frac{m\gamma}{u_0 n}. \tag{5.78}$$

Hence, the angle θ can be interpreted as the angle between $\tilde{\psi}(s)$ and the $\tilde{s}$-axis in the usual sense known from flat space, whereas the angle defined by (5.75) came from a more generalised angle notion which goes beyond flat space. We just wanted to provide both formulations, but when in doubt the general formulation (5.57) is more robust.

Finally, if we employ this angle formulation, the above results become quite similar to the single hyperbolic plane results, namely

$$\begin{aligned} \dot{\Phi}^2 &= \frac{n^2}{\cos^2\theta}\frac{\dot{s}^2}{s^2} \\ \Omega^2 &= \frac{\sin^4\theta}{m^2}\dot{\Phi}^2. \end{aligned} \tag{5.79}$$

In particular, the velocity $\dot{\Phi}$ is formally given by the same expression as for the single hyperbolic plane. But the prefactor for the turning rate is slightly altered to before which isn't really surprising because the saxion and axion came from different hyperbolic planes in contrast to the previous case.

Furthermore, let us comment some more about this effective metric (5.76). If we would repeat the computation of the turning rate Ω using the effective metric with coordinates s and ψ or using the effective flat metric (5.77) with coordinates $\tilde{s}$ and $\tilde{\psi}$, we get immediately 0. The mindful reader might wonder at this point, if Ω isn't coordinate invariant. This would imply that Ω behaves like a pseudo-force which depends on the given coordinate frame and can be transformed away. However, that is a wrong conclusion. The root of the problem here is the fact that we toss away the ϕ- and u- coordinate. Looking back at (5.73) we see that the only contribution to Ω comes from $D_t T^u$. In a sense the non-geodesicity is fully concentrated in a coordinate which is absent in the effective system (5.77). So it isn't surprising that the result becomes 0 in the flat effective coordinates. A little bit more on that can be also found in appendix C. In conclusion we can say that the effective formulation (5.77) is very useful in providing some intuition to the angle definition. But, as we just showed, there are some clear limitations to the formulation and one has to treat such simplifications with great care since the coordinate truncation might not be consistent.

In the end the result can be expressed in the desired form

$$\frac{\Omega^2}{H^2} = \frac{2\sin^4\theta}{m^2}\epsilon \tag{5.80}$$

where we used (5.34). The prefactor is again $\mathcal{O}(1)$ for a moderate curvature. It is perhaps slightly interesting that the relevant curvature corresponds to the

hyperbolic plane of the axion, namely $1/m^2$.

Saxion-Saxion Trajectories

Finally, there is another possible two-field trajectory, namely we keep the two axions ϕ and ψ fixed and let the two saxions s and u evolve together. Then we follow our recipe by determining the critical case relation first which turns out to be

$$\frac{\frac{\dot{u}}{u}}{\frac{\dot{s}}{s}} = \delta = const. \tag{5.81}$$

This can directly inferred by demanding a constant change of the distance. Therefore, the speed along the trajectory becomes

$$\dot{\Phi}^2 = \frac{n^2}{s^2}\dot{s}^2 + \frac{m^2}{u^2}\dot{u}^2 = n^2\frac{\dot{s}^2}{s^2}\left(1 + \frac{m^2}{n^2}\delta^2\right) \tag{5.82}$$

and the tangent vector to the trajectory reads

$$\begin{aligned} T^s &= \frac{1}{\dot{\Phi}}\dot{s} \\ T^\phi &= 0 \\ T^u &= \frac{1}{\dot{\Phi}}\dot{u} = \frac{u}{\dot{\Phi}}\delta\frac{\dot{s}}{s} \\ T^\psi &= 0. \end{aligned} \tag{5.83}$$

The covariant time derivatives become

$$\begin{aligned} D_t T^s &= \frac{1}{\dot{\Phi}}\left(\ddot{s} - \frac{\dot{s}}{\dot{\Phi}}\ddot{\Phi} - \frac{\dot{s}^2}{s}\right) \\ D_t T^\phi &= 0 \\ D_t T^u &= \frac{1}{\dot{\Phi}}\left(\ddot{u} - \frac{\dot{u}}{\dot{\Phi}}\ddot{\Phi} - \frac{\dot{u}^2}{u}\right) \\ D_t T^\psi &= 0. \end{aligned} \tag{5.84}$$

We immediately recognise that the only two non-vanishing components have the same structure. Again we can show by explicit calculation that

$$\begin{aligned} \frac{\dot{s}}{\dot{\Phi}}\ddot{\Phi} &= \ddot{s} - \frac{\dot{s}^2}{s} \\ \frac{\dot{u}}{\dot{\Phi}}\ddot{\Phi} &= \ddot{u} - \frac{\dot{u}^2}{u}. \end{aligned} \tag{5.85}$$

Here the symmetry of the situation, namely $s \leftrightarrow u$, becomes even more evident. Ultimately, the above leads to

$$D_t T^s = 0$$

$$\begin{aligned} D_t T^{\phi} &= 0 \\ D_t T^{u} &= 0 \\ D_t T^{\psi} &= 0 \end{aligned} \tag{5.86}$$

which directly implies

$$\Omega^2 = 0. \tag{5.87}$$

Hence, a critical trajectory involving only two saxions (related by (5.81)) is geodesic. The explanation for that can be found in appendix C where the situation is analyzed on the level of the geodesic equation. Let us emphasise that this is a geodesic for any δ.

At this point we need make some further comments regarding the mass towers. For instance, observe that the bigger δ is, the more we move away from the s-axis into the direction of the u-axis. At first this seems to be a problem because we can apparently delay the mass tower M_s as long as we want by increasing δ, which would be in tension with the SDC. But here we have two saxionic directions and both of them have a mass tower associated to them, as stated before. Intuitively, if we move away from the s-axis, i.e. the mass tower M_s, the mass tower M_u along the u-axis might come to the rescue. To be more precise, once we include several saxions, we have to go beyond our minimal model that states that we only have mass towers along the saxionic directions. These tower generally combine in some ways, in fact, there are usually a lot of combined mass towers in a realistic String Theory setting. These combined towers are, however, heavily model-dependent, i.e. we would have to specify how the different saxionic mass towers interact and combine. So it is hard to make general bottom-up statements if we include more than one saxion in the trajectory. Moreover, if we need to consider a more general tower structure for this case, it is also not compatible with the previous results, where we only had the single mass tower M_s. On top of that, a saxion-saxion critical trajectory can't make a significant impact on the magnitude of Ω/H because it is geodesic. Thus, henceforth we only focus on trajectories involving a single saxion, which means we fix a single mass tower, together with one or more axions.

Saxion-Axion-Axion Trajectories

That leaves one final combination to investigate for a product of two hyperbolic planes. The situation in question is the one where only the second saxion u is constant, i.e. $u = u_0 = const$. This is the first trajectory involving three fields, which brings another new feature with it. The critical case condition connects here all three fields in general, namely

$$\left(\frac{\dot{\phi}}{\dot{s}}\right)^2 + \frac{m^2}{n^2 u_0^2}\left(\frac{\dot{\psi}}{\frac{\dot{s}}{s}}\right)^2 = const \tag{5.88}$$

will result in the desired maximal deviation from a geodesic at the boundary of moduli space. But we won't treat this case in full generality [15]. We instead focus on a subset fulfilling the above constraint. For instance, we will assume that both terms are separately constant which allows us to make direct contact to the previous calculations and results

$$\begin{aligned} \frac{\dot{\phi}}{\dot{s}} &= \beta = const \\ \frac{\dot{\psi}}{\frac{\dot{s}}{s}} &= \gamma = const. \end{aligned} \tag{5.89}$$

Here we dropped the squares and the other constants m/nu_0 from the second term. Furthermore, we reuse the constants as before, to better illustrate the similarities and differences, although this here is a completely separate case. Also we don't expect anything to change qualitatively in the fully general situation where just the sum is constant.
Now we are ready to give the velocity along the trajectory

$$\dot{\Phi}^2 = \frac{n^2}{s^2}(\dot{s}^2 + \dot{\phi}^2) + \frac{m^2}{u_0^2}\dot{\psi}^2 = n^2\frac{\dot{s}^2}{s^2}\left(1 + \beta^2 + \frac{m^2\gamma^2}{u_0^2 n^2}\right) \tag{5.90}$$

and the tangent vector to the trajectory

$$\begin{aligned} T^s &= \frac{1}{\dot{\Phi}}\dot{s} \\ T^\phi &= \frac{1}{\dot{\Phi}}\dot{\phi} = \frac{1}{\dot{\Phi}}\beta\dot{s} \\ T^u &= 0 \\ T^\psi &= \frac{1}{\dot{\Phi}}\dot{\psi} = \frac{1}{\dot{\Phi}}\gamma\frac{\dot{s}}{s}. \end{aligned} \tag{5.91}$$

Following the procedure of the previous calculations we continue by determining the covariant derivatives

$$\begin{aligned} D_t T^s &= \frac{1}{\dot{\Phi}}\left(\ddot{s} - \frac{\dot{s}}{\dot{\Phi}}\ddot{\Phi} - \frac{\dot{s}^2}{s}(1-\beta^2)\right) \\ D_t T^\phi &= \frac{1}{\dot{\Phi}}\beta\left(\ddot{s} - \frac{\dot{s}}{\dot{\Phi}}\ddot{\Phi} - 2\frac{\dot{s}^2}{s}\right) \\ D_t T^u &= \frac{1}{u_0}\frac{\dot{\psi}^2}{\dot{\Phi}} \\ D_t T^\psi &= \frac{1}{\dot{\Phi}}\left(\ddot{\psi} - \frac{\dot{\psi}}{\dot{\Phi}}\ddot{\Phi}\right). \end{aligned} \tag{5.92}$$

[15] It might be possible to treat the case fully general by employing a suitable parametrisation for (5.88).

Although we have a different prefactor in $\dot{\Phi}$, we recover again similar relations to the prior calculations

$$\begin{aligned} \frac{\dot{s}}{\dot{\Phi}}\ddot{\Phi} &= \ddot{s} - \frac{\dot{s}^2}{s} \\ \ddot{\psi} &= \gamma\left(\frac{\ddot{s}}{s} - \frac{\dot{s}^2}{s^2}\right) \\ \frac{\dot{\psi}}{\dot{\Phi}}\ddot{\Phi} &= \frac{\gamma}{s}\left(\ddot{s} - \frac{\dot{s}^2}{s}\right) \end{aligned} \tag{5.93}$$

such that we arrive at

$$\begin{aligned} D_t T^s &= \frac{\beta^2}{\dot{\Phi}}\frac{\dot{s}^2}{s} \\ D_t T^\phi &= -\frac{\beta}{\dot{\Phi}}\frac{\dot{s}^2}{s} \\ D_t T^u &= \frac{1}{u_0}\frac{1}{\dot{\Phi}}\gamma^2\frac{\dot{s}^2}{s^2} \\ D_t T^\psi &= 0. \end{aligned} \tag{5.94}$$

Finally, the turning rate Ω becomes

$$\Omega^2 = \frac{\dot{\Phi}^2}{\left(1+\beta^2+\frac{m^2\gamma^2}{u_0^2 n^2}\right)^2}\left(\frac{\beta^2}{n^2}(1+\beta^2) + \frac{m^2\gamma^4}{u_0^4 n^4}\right). \tag{5.95}$$

It is interesting that the result here isn't just the sum of the separate cases since the prefactor is different. But, when setting either $\beta = 0$ or $\gamma = 0$, we recover the previous cases which is a nice consistency check. Most importantly, the turning rate Ω scales again with $\dot{\Phi}$. As already firmly stated, this is the key property when relating the results to cosmic acceleration.
Although there are three fields evolving now, the angle formula from before can still be applied. Then, the geodesic tangent vector T_g^a along the tower M_s is given as in the preceding cases (or it is recovered from T^a here by setting $\beta = 0 = \gamma$), whereas the non-geodesic tangent vector T^a was defined above. Again both vectors are normalised, so by (5.57) we find

$$\cos\theta = G_{ab}T_g^a T^b = \frac{1}{\sqrt{1+\beta^2+\frac{m^2\gamma^2}{u_0^2 n^2}}} \tag{5.96}$$

such that $\tan\theta = \sqrt{\beta^2 + \frac{m^2\gamma^2}{u_0^2 n^2}}$. As probably expected, $\cos\theta$, which modifies the geodesic decay rate due to (5.5), depends on both β and γ. Furthermore, we can

define the angle θ_ϕ as the projection of θ to the (s,ϕ)-plane by setting $\gamma = 0$ in T^a and analogously the angle θ_ψ as the projection to the (s,ψ)-plane by setting $\beta = 0$, resulting in

$$\begin{aligned} \tan\theta_\phi &= \beta \\ \tan\theta_\psi &= \frac{m\gamma}{nu_0}. \end{aligned} \tag{5.97}$$

These are also precisely the angles defined in the trajectories with only two fields, a single saxion and axion. This enables us to express everything in terms of these angles which gives a very similar result to the previous instances

$$\begin{aligned} \dot\Phi^2 &= \frac{n^2}{\cos^2\theta}\frac{\dot s^2}{s^2} \\ \Omega^2 &= \cos^4\theta\left(\frac{1}{n^2}\frac{\tan^2\theta_\phi}{\cos^2\theta_\phi} + \frac{1}{m^2}\tan^4\theta_\psi\right)\dot\Phi^2. \end{aligned} \tag{5.98}$$

In this formulation the connection to the previous findings becomes even more apparent. If we set $\gamma = 0$, we get $\theta = \theta_\phi$ and $\theta_\psi = 0$ and we immediately recover the result from the single hyperbolic plane. As expected, the same consistency check works for setting $\beta = 0$, where we recover (5.79). Let us also point out the structurally different contributions from the axion on the same hyperbolic plane compared to the one from the other hyperbolic plane.
By (5.34) this yields the desired form

$$\frac{\Omega^2}{H^2} = 2\epsilon\cos^4\theta\left(\frac{1}{n^2}\frac{\tan^2\theta_\phi}{\cos^2\theta_\phi} + \frac{1}{m^2}\tan^4\theta_\psi\right) \tag{5.99}$$

where the prefactor is again $\mathcal{O}(1)$ for moderate curvatures. At this point we are ready to extend the results to an arbitrary amount of hyperbolic planes.

5.3.3 Computations for N Hyperbolic Planes

In this section we extend our computations to an arbitrary amount of hyperbolic planes. Since we have treated already all possible caveats, this generalisation is quite straightforward. Basically, one just gets more components and equations, but each one of them falls into one of the categories discussed before. So the calculation for an arbitrary N is just built up from the two possible base cases: saxion with axion from the same hyperbolic plane and saxion with an axion from another hyperbolic plane. And it was shown how these cases combine. In fact, the generalisation to N hyperbolic planes just amounts to adding copies of the same equations/terms, as we will see shortly. For the reasons discussed before we won't include more than a single saxion here.

First, the metric now is given by

$$d\Delta^2 = G_{ab} d\Phi^a d\Phi^b = \sum_{i=1}^{N} \frac{n_i^2}{s_i^2} \left(ds_i^2 + d\phi_i^2 \right). \tag{5.100}$$

This is a product of N hyperbolic planes where the saxions s_i and the axions ϕ_i are combined in $\Phi^a = (s_1, \phi_1, ..., s_N, \phi_N)$. Moreover, each hyperbolic plane has its own parameter n_i which is related to the scalar curvature R_i of the i-th hyperbolic plane like $R_i = -2/n_i^2$. As demanded by the SDC we assign to each saxionic direction a mass tower

$$M_{s_i} \sim s^{-a_i} \tag{5.101}$$

for some constants $a_i > 0$. The object we seek to determine is the turning rate Ω which reads here

$$\Omega^2 = \sum_{i=1}^{N} \frac{n_i^2}{s_i^2} \left((D_t T^{s_i})^2 + (D_t T^{\phi_i})^2 \right). \tag{5.102}$$

From here on we fix a saxionic direction we want to investigate. Without loss of generality we pick s_1 because one can always rearrange the indices such that the desired direction carries the index 1. Moreover, we drop the index 1 from all quantities of the first hyperbolic plane, i.e. $s_1 \equiv s$, $\phi_1 \equiv \phi$ and $n_1 \equiv n$.
Next, we fix the critical trajectory. Except s_1 the trajectory doesn't contain any other saxionic directions which means all $s_i = s_{0i} = const$ for $i \geq 2$. In order to avoid a clumsy notation, we drop the 0-label here, which normally indicates a constant quantity, i.e. we just write s_i instead of s_{0i}. The critical case condition turns out to be

$$\left(\frac{\dot{\phi}}{\dot{s}} \right)^2 + \sum_{i=2}^{N} \frac{n_i^2}{n^2 s_i^2} \left(\frac{\dot{\phi}_i}{\frac{\dot{s}}{s}} \right)^2 = const \tag{5.103}$$

which is completely analogous to the previous cases. But again we simplify the situation by assuming that all terms are individually constant. Here we also don't expect that this simplification has a major impact on the key results. Hence, we demand

$$\frac{\dot{\phi}}{\dot{s}} = \beta = const \tag{5.104}$$

$$\frac{\dot{\phi}_i}{\frac{\dot{s}}{s}} = \beta_i = const \quad \text{for } i \geq 2. \tag{5.105}$$

Following along the procedure of the previous instances the velocity of the trajectory is readily given by

$$\dot{\Phi}^2 = \frac{n^2}{s^2}(\dot{s}^2 + \dot{\phi}^2) + \sum_{i=2}^{N} \frac{n_i^2}{s_i^2} \dot{\phi_i}^2 = n^2 \frac{\dot{s}^2}{s^2} \left(1 + \beta^2 + \sum_{i=2}^{N} \frac{n_i^2 \beta_i^2}{s_i^2 n^2} \right). \tag{5.106}$$

This allows us to write down the tangent vector T^a to the trajectory as

$$\begin{aligned} T^s &= \frac{1}{\dot{\Phi}}\dot{s} \\ T^\phi &= \frac{1}{\dot{\Phi}}\dot{\phi} = \frac{1}{\dot{\Phi}}\beta\dot{s} \\ T^{s_i} &= 0 \\ T^{\phi_i} &= \frac{1}{\dot{\Phi}}\dot{\phi}_i = \frac{1}{\dot{\Phi}}\beta_i\frac{\dot{s}}{s} \end{aligned} \tag{5.107}$$

for $i \geq 2$. Since the further calculation works out in same way as the previous ones, we can just piece it together. For instance, we then get

$$\begin{aligned} D_t T^s &= \frac{\beta^2}{\dot{\Phi}}\frac{\dot{s}^2}{s} \\ D_t T^\phi &= -\frac{\beta}{\dot{\Phi}}\frac{\dot{s}^2}{s} \\ D_t T^{s_i} &= \frac{1}{s_i}\frac{1}{\dot{\Phi}}\beta_i^2\frac{\dot{s}^2}{s^2} \\ D_t T^{\phi_i} &= 0 \end{aligned} \tag{5.108}$$

where $i \geq 2$. For a general N here the last two equations just get copied $N-1$ times. Therefore, it's no surprise that the turning rate Ω amounts to

$$\Omega^2 = \frac{\dot{\Phi}^2}{\left(1+\beta^2+\sum_{i=2}^N \frac{n_i^2\beta_i^2}{s_i^2 n^2}\right)^2}\left(\frac{\beta^2}{n^2}(1+\beta^2)+\sum_{i=2}^N \frac{n_i^2\beta_i^4}{s_i^4 n^4}\right). \tag{5.109}$$

which is a straightforward generalisation of the prior findings. Let us emphasise the important part here, namely $\Omega \sim \dot{\Phi}$ for a general critical trajectory involving up to N axions on top of the saxion associated with the mass tower in question. Then it's again possible to define the total angle θ between the geodesic tangent vector T_g^a, which corresponds to setting $\beta = 0 = \beta_i$, and the tangent vector to the trajectory T^a which is defined at the beginning of the section, yielding

$$\cos\theta = G_{ab}T_g^a T^b = \frac{1}{\sqrt{1+\beta^2+\sum_{i=2}^N \frac{n_i^2\beta_i^2}{s_i^2 n^2}}}. \tag{5.110}$$

Moreover, there are also the angles of the projection onto the (s,ϕ)-plane and onto the (s,ϕ_i)-plane. The former is defined by setting $\beta_i = 0$ for $i \geq 2$, whereas the latter is given by setting $\beta = 0 = \beta_j$ for $j \neq i$ in the above angle formula. These then read

$$\tan\theta_\phi = \beta$$

$$\tan\theta_{\phi_i} = \frac{n_i\beta_i}{ns_i}. \tag{5.111}$$

That allows us to express the results in terms of these angles such that we get

$$\begin{aligned}\dot{\Phi}^2 &= \frac{n^2}{\cos^2\theta}\frac{\dot{s}^2}{s^2} \\ \Omega^2 &= \cos^4\theta\left(\frac{1}{n^2}\frac{\tan^2\theta_\phi}{\cos^2\theta_\phi}+\sum_{i=2}^{N}\frac{1}{n_i^2}\tan^4\theta_{\phi_i}\right)\dot{\Phi}^2\end{aligned} \tag{5.112}$$

which is perfectly consistent with all previous results, in the sense that all the prior turning rates were just special cases of this general formula.
In the end we recover, even for an arbitrary amount of hyperbolic planes, by (5.2) the promised expression

$$\frac{\Omega^2}{H^2} = 2\epsilon\cos^4\theta\left(\frac{1}{n^2}\frac{\tan^2\theta_\phi}{\cos^2\theta_\phi}+\sum_{i=2}^{N}\frac{1}{n_i^2}\tan^4\theta_{\phi_i}\right). \tag{5.113}$$

Unless we have high curvature or an unnaturally high number N of hyperbolic planes (in a typical String Theory construction we can only have up to 3 hyperbolic planes), this prefactor is again $\mathcal{O}(1)$.

5.4 Asymptotic Acceleration and Turning Rate for non-constant θ

As seen in the previous section 5.3, it is impossible to achieve a large turning rate for asymptotic acceleration with a constant deviation from a geodesic, i.e. a constant deviation angle θ. However, this condition was only forced upon us in the full limit to the boundary of moduli space since the limiting tangent vector has to be constant [32]. Once we are just near the boundary, but still close enough such that the geometry is hyperbolic, we can relax this condition and allow for a non-constant tangent vector corresponding to a varying θ. In particular, it is enough for consistency with the SDC to assume that we only approach a constant tangent vector. Then we can get additional contributions to the turning rate from (possibly) large turns in field space. Moreover, the existence of a lower bound λ_0 on the decay rate (which translates to an upper bound θ_0 for the angle) restricts the movement to a cone which is very reminiscent of a light-cone in Special Relativity. This cone will be termed *swamp cone*. Under these assumptions a general expression for the turning rate is derived which could in principle get large due to contributions from rapid turns. But as it turns out, very close to the boundary these turns are very limited such that we recover again the relation

$$\frac{\Omega}{H} < c\sqrt{\epsilon} \tag{5.114}$$

for an $\mathcal{O}(1)$ constant c. To be more precise, this is inferred by an asymptotic expansion around the boundary of moduli space. Such an asymptotic expansion was previously proposed in [20].
In this section we will restrict our analysis to a single hyperbolic plane given by (5.45), as the results directly translate to the more general cases. So we first introduce the swamp cone as a mean to construct an infinite-distance trajectory with non-constant deviation angle θ from a geodesic consistent with the SDC. Using that we then derive a general formula for the turning rate Ω, where we indeed get new terms proportional to the turning of the trajectory, i.e. proportional to $\dot{\theta}$. After that an asymptotic expansion in terms of $1/s$ is performed around the boundary of moduli space (corresponding to $s = \infty$). This will yield $\dot{\theta} \sim \dot{\Phi} \sim \sqrt{\epsilon}$ for large s in the context of asymptotic acceleration. Thus, even the new contributions to the turning rate Ω can't become arbitrarily large which then implies again the above bound on Ω/H.

5.4.1 Swamp Cone and the general Turning Rate

Before we begin, let's recall the definitions and assumptions for the single hyperbolic plane in section 5.3.1 which will again apply here.
The first step is then to relax the critical case condition (5.50) which is supposed to hold for limiting tangent vectors. This is possible, if we are not fully at the boundary of moduli space, meaning we only consider large s here. Let us emphasise that (5.50) can also be extended into the bulk of moduli space away from the boundary. However, once we allow for a non-constant tangent vector, we gain more freedom in the choice of our trajectory and that is precisely what we exploit now. This is achieved by replacing the proportionality constant β with a general function $f(t)$, namely

$$\beta = const \quad \rightarrow \quad f(t). \tag{5.115}$$

By the previously employed angle notion this can be translated into a non-constant angle $\theta(t)$ via

$$f(t) = \tan\theta(t) \tag{5.116}$$

which is completely harmless since we are dealing with a conformally flat hyperbolic plane. To develop intuition, it is usually better to use the formulation in terms of the angle. Let us emphasise that, up to this point, we are still fully general for infinite-distance trajectories. We have just reparametrised the field $\phi(t)$ in terms of the function $f(t)$, namely

$$\dot{\phi} = f(t)\dot{s}. \tag{5.117}$$

For a given $s(t)$ and $\phi(t)$ one can determine $f(t)$ or, the other way round, we can integrate this expression for a given $f(t)$ and $s(t)$ to find $\phi(t)$. Of course, there might be some extreme functions which might give some problems, but we will

assume, that every function involved here has a sufficiently nice behavior. Then, it turns out that this parametrisation is very well suited for our purposes.
Moreover, the function $f(t)$ has to be bounded because there exists a maximum deviation angle θ_0 (coming from the lower bound on the decay rate λ_0) which may not be exceeded to be consistent with the SDC. As argued earlier, it is also allowed to have negative angles, which then translates into a lower bound on the angle $-\theta_0$, such that we get

$$-\tan\theta_0 \leq f(t) = \tan\theta(t) \leq \tan\theta_0. \tag{5.118}$$

This holds due to the montonicity of $\tan\theta$ on the interval $[-\pi/2, \pi/2]$. One direct implication of the above is that a trajectory now given by

$$\begin{aligned} \dot{\Phi}^2 &= n^2 \frac{\dot{s}^2}{s^2}\left(1 + f(t)^2\right) \\ T^s &= \frac{1}{\dot{\Phi}}\dot{s} \\ T^\phi &= \frac{1}{\dot{\Phi}} f(t)\dot{s} \end{aligned} \tag{5.119}$$

is completely contained in a cone in the $(\dot{s}, \dot{\phi})$-plane which extends from $-\theta_0$ to θ_0. We name this cone the *swamp cone* because everything outside the cone is inconsistent with the SDC and therefore in the Swampland. In the previous section the trajectories were restricted to straight lines within this cone, but here the trajectory may do whatever it wants, as long as it doesn't reach out of the swamp cone. In order to translate this idea to the (s, ϕ)-plane, we have to integrate. Keep in mind, that so far it has been trivial to integrate the fields because $\dot{s}$ and $\dot{\phi}$ have been just related by a constant factor β. The situation with a general $f(t)$ is more involved. For instance, the trajectory in (s, ϕ)-plane has a swamp cone associated at each point such that the slope of the trajectory stays within the cone. To the mindful reader, this should be very reminiscent of Special Relativity and the light-cone. This is illustrated in figure 5.1.
At this point one might worry that this is a very strong interpolation of statements, which are supposed to hold at the boundary of moduli space. But this isn't a problem here because we will take a modest approach and just assume that these principles also apply near the boundary of moduli space, i.e. just for very large s. This will be made manifest in the next section. For now we continue with a general function $f(t)$.
The main reason for this generalisation was to investigate, whether this enables us to generate a larger turning rate Ω. The calculation of Ω works in complete analogy to the previous section. The tangent vector and the speed of the trajectory were already given in (5.119) such that we arrive at

$$D_t T^s = \frac{1}{\dot{\Phi}}\left(\ddot{s} - \frac{\dot{s}}{\dot{\Phi}}\ddot{\Phi} - \frac{\dot{s}^2}{s}(1 - f^2)\right)$$

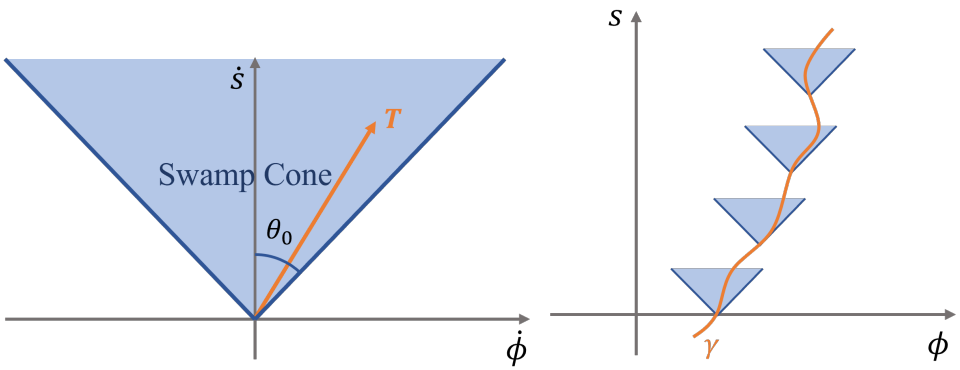

Figure 5.1: This figure shows an illustration of the swamp cone. For instance, on the left-hand side we have the swamp cone (indicated by the blue shading) on the $(\dot{s}, \dot{\phi})$-plane where a trajectory, given by its tangent vector T^a, is just restricted to stay inside the blue-shaded area. Although the orange tangent vector is depicted as a straight line, as it was the case previously, it isn't constrained to that. In fact, the trajectory can turn as sharply as it wants, as long as it stays consistent with an infinite distance limit. Moreover, on the right-hand side we have the (s, ϕ)-plane. Here the orange trajectory has a swamp cone (again indicated by the blue shading) associated at each point along it, meaning that the slope has to stay within it. This is clearly reminiscent of the light-cone from Special Relativity.

$$D_t T^\phi = \frac{1}{\dot{\Phi}}\left(\ddot{\phi} - \frac{\dot{\phi}}{\dot{\Phi}}\ddot{\Phi} - 2\frac{\dot{s}\dot{\phi}}{s}\right) \tag{5.120}$$

which turns out to be formally identical with the result for a constant tangent vector. But now the differences start to come in, namely all the second derivative terms, which implicitly involve $f(t)$, get extra contributions. The relevant terms work out to be

$$\begin{aligned} \frac{\dot{s}}{\dot{\Phi}}\ddot{\Phi} &= \ddot{s} - \frac{\dot{s}^2}{s} + \frac{\dot{s}}{1+f^2} f\dot{f} \\ \ddot{\phi} &= \ddot{s} f + \dot{s}\dot{f} \\ \frac{\dot{\phi}}{\dot{\Phi}}\ddot{\Phi} &= f\left(\ddot{s} - \frac{\dot{s}^2}{s}\right) + \frac{f^2}{1+f^2}\dot{s}\dot{f}. \end{aligned} \tag{5.121}$$

Thus, the covariant derivative of the tangent vector also changes

$$\begin{aligned} D_t T^s &= \frac{f^2}{n\sqrt{1+f^2}}\dot{s} - \frac{sf}{n\,(1+f^2)^{\frac{3}{2}}}\dot{f} \\ D_t T^\phi &= -\frac{f}{n\sqrt{1+f^2}}\dot{s} + \frac{s}{n\,(1+f^2)^{\frac{3}{2}}}\dot{f}. \end{aligned} \tag{5.122}$$

Let us emphasise that everything is consistent with the previous findings upon setting $\dot{f} = 0$. But these expressions are quite cumbersome, so we switch directly to the formulation in terms of the angle $\theta(t)$ by virtue of (5.116). Then, the covariant derivatives $D_t T^a$ become

$$\begin{aligned} D_t T^s &= \frac{1}{n} \tan^2\theta \cos\theta \ \dot{s} - \frac{s}{n} \sin\theta \ \dot{\theta} \\ D_t T^\phi &= -\frac{1}{n} \sin\theta \ \dot{s} + \frac{s}{n} \cos\theta \ \dot{\theta} \end{aligned} \tag{5.123}$$

where we used $\dot{f} = \dot{\theta}/\cos^2\theta$. From this point it is straightforward to determine the turning rate which turns out to be

$$\Omega^2 = \left(\tan\theta \ \frac{\dot{s}}{s} - \dot{\theta} \right)^2 . \tag{5.124}$$

For the last step please note that the velocity along the trajectory takes the following familiar form

$$\dot{\Phi} = \frac{n}{\cos\theta} \frac{\dot{s}}{s}. \tag{5.125}$$

Then, we arrive at the final result

$$\Omega = \left| \frac{\sin\theta}{n} \dot{\Phi} - \dot{\theta} \right| . \tag{5.126}$$

First of all, this result is still fully consistent with (5.61). Since it was already argued that the first term here is bounded by $\mathcal{O}(1) \cdot \sqrt{\epsilon}$, we would require a large angular velocity $\dot{\theta}$ to achieve a significant turning rate Ω. Without making further model-dependent specifications we can't really infer something quantitative from here. But, as we will see shortly, there are some implications for $\dot{\theta}$ near the boundary of moduli space where the constraints of the SDC become stronger. Before we move on, let us point out that (5.126) is the fully general expression for the turning rate of an infinite-distance trajectory on a hyperbolic plane.

5.4.2 Asymptotic Expansion of θ

As argued before, the function $f(t)$ is in principle capable to describe the full trajectory up to $s = \infty$. However, we can't make any quantitative statements without assuming a specific trajectory. Hence, instead of using the full function $f(t)$ we make an expansion around $s = \infty$ because we know how $f(t)$ has to behave in the limit, in order to respect the SDC, namely it has to stay within the swamp cone and it has to approach a constant

$$f(t) \overset{t\to\infty}{\longrightarrow} \beta = const \tag{5.127}$$

which is precisely the constant we have introduced for the critical case (5.50). Or, equivalently, the angle hast to behave as

$$\theta(t) \overset{t\to\infty}{\longrightarrow} \theta_\infty = const \tag{5.128}$$

where $\theta_\infty = \tan^{-1}\beta$. One could expand either $f(t) = \tan\theta(t)$ or directly $\theta(t)$, but it turns out that the latter connects better to the previous calculations, although both are perfectly fine. Because for our setup s is always monotonically increasing with t (otherwise we would certainly leave the swamp cone), we can also parametrise θ in terms of s instead of t. This enables us to directly expand $\theta(s)$ like

$$\theta(s) = \theta_\infty + \sum_{n>0} \frac{c_n}{s^n} \tag{5.129}$$

around $s = \infty$, which represents the boundary of moduli space, and θ_∞ is given as above. The sum only runs over positive integers such that the expression converges to a certain value in the limit $s \to \infty$ [16]. Moreover, it was already established that $\theta(s) \leq \theta_0$ as required by consistency with the SDC. Since we also allow for negative θ, there is also the lower bound $\theta(s) \geq -\theta_0$. However, this leads to exactly the same conclusions so we just stick to the upper bound.
Now we take s to be large enough that the sum in (5.129) is very well approximated by the first non-zero term, which we assume to be the k-th term, so we get

$$\theta(s) \approx \theta_\infty + \frac{c_k}{s^k}. \tag{5.130}$$

Using $\theta(s) \leq \theta_0$ we can find the following estimate

$$\frac{c_k}{s^k} \leq \theta_0 - \theta_\infty \leq 2\theta_0 \tag{5.131}$$

where in the last step we used that θ_∞ could at most be equal to $-\theta_0$. Ultimately, the angular velocity $\dot\theta$ is the object we are after. Thus, performing the derivative of (5.130) leads to

$$\dot\theta(s) \approx -k\frac{c_k}{s^k}\frac{\dot s}{s} \tag{5.132}$$

by the chain rule. Furthermore, the derivative vanishes for $s \to \infty$ which is required to approach a finite value. Now let's turn to the absolute value of $\dot\theta$ because we are only interested in the magnitude of $\dot\theta$. Hence, using (5.131) and (5.125) we can get an upper bound for the absolute value of the angular velocity

$$\left|\dot\theta(s)\right| \leq \frac{2k}{n}\theta_0 \cos\theta(s)\ \dot\Phi. \tag{5.133}$$

[16] This excludes expansions like $\sum_n c_n \sin(ns)$ because these would have an indeterminate limit $s \to \infty$. Furthermore, there is another class of functions which is not captured by the above expansion. These functions don't admit a polynomial expansion but rather a "non-perturbative" one using exponentials like $\sum_n c_n e^{-ns}$.

where every quantity on the right-hand side is positive. Here $\cos\theta(s)$ could also be expanded according to (5.130), but this isn't necessary here, since the cosine is a bounded $\mathcal{O}(1)$ function anyway. The question is now, how large can this be? If we again assume moderate curvature, meaning $1/n \sim \mathcal{O}(1)$, then only k could make the above big. Now recall that k is the first non-vanishing contribution in the sum in (5.129), so a large k would be very unnatural. But, most importantly, the angular velocity $\dot{\theta}$ is proportional to the speed along the trajectory like the other contribution to the turning rate Ω.
So have seen that $|\dot{\theta}|$ cannot become arbitrarily large near the boundary of moduli space and that it comes at the same order in ϵ as the other contribution. By using (5.34) we have thus found that, even including turns, the turning rate Ω is generally bounded by

$$\frac{\Omega}{H} < c\,\sqrt{\epsilon} \tag{5.134}$$

around the boundary of moduli space where c is an $\mathcal{O}(1)$ constant. The precise value of c depends on the interplay between $\sin\theta/n$ and $\dot{\theta}$ in the absolute value. But this isn't really important as c is just $\mathcal{O}(1)$ for generic Quantum Gravity setups.

Chapter 6

Summary and Outlook

6.1 Summary

Before going into more detail, let us reiterate the main results of this thesis:

1. A novel geometric flow for the number of spacetime dimensions D was derived from a refined version of Ricci flow.

2. An extension to Ricci flow, the so called Einstein-Maxwell flow, was constructed, which includes the backreaction of the matter content, namely given by a Maxwell field, onto the spacetime metric.

3. In the setting of cosmic acceleration the non-geodesicity Ω allowed by the SDC near the boundary of moduli space is restricted to be $\Omega < \mathcal{O}(1) \cdot \sqrt{\epsilon}$ (in Hubble units).

Now a more complete summary of the findings is presented.

Geometric Flow Equation for the Number of Spacetime Dimensions

Starting from the expression for the graviton β-function, which is derived from the String Theory worldsheet σ-model, a two-loop refined version of the Ricci flow equation was stated. Then the associated flow equation for the volume $\mathcal{V}$ of the manifold, on which the flow takes place, was explicitly constructed. Exploiting its suitable form, namely it having its D-dependence factored out, the spacetime dimension D was generalised to a continuous parameter and provided with an analogous flow, the so called D-flow. It must be stressed that the geometric evolution equation for D only corresponds to the one for $\mathcal{V}$, when it is non-singular. In this sense, the equation for D can be regarded as a generalisation of the framework from which we started. Thereafter, D-flow was applied to maximally symmetric Einstein spaces, for instance a family of D-spheres and D-dimensional AdS spacetime, highlighting the interesting behaviour around fixed and singular points. In

both cases the attractive or repulsive behaviour of the singled-out values of D was studied in detail. Lastly, the physically relevant example of Freund-Rubin compactification, which is a product manifold of the previous cases, i.e. $AdS_d \times S^{d'}$, was analysed extensively, finding some remarkable similarities with the behaviour one would expect from the SDC. In particular, D-flow restricted to the internal dimension d' lead to an infinite KK-tower becoming light with an induced distance Δ along the flow which scales as $\Delta \sim \ln d'$ for large d'.

Gradient Flow of Einstein-Maxwell Theory

The natural geometric flow for Einstein gravity coupled to a Maxwell field in the asymptotically flat setting was explored. It arises as the gradient flow of the Einstein-Maxwell action. Then, we have shown that for static geometries and Maxwell fields this flow, the so called EM flow, is well-posed taking either purely electric or magnetic potentials, when it is parabolic in character. It was also argued that EM flow preserves smooth non-extremal and extremal horizons, hence making it suitable for the application to charged black hole geometries. For geometries with an extremal horizon the near horizon flow decouples from the exterior, as one might expect. Moreover, the surface gravity of a horizon is preserved by the flow. In the electric case the potential difference between infinity and the horizon is fixed by the natural asymptotic boundary conditions which fix the gauge potential at infinity. In the magnetic case the natural boundary condition of fixing the asymptotic magnetic potential results in a conserved magnetic charge under the EM flow. Thus, we may regard the electric and magnetic flows as being conjugate to each other in the sense that the electric flow preserves the potential (difference), while the magnetic one preserves charge. Furthermore, EM flow was applied to non-extremal and extremal Reissner-Nordström solutions. Although these are fixed points of the flow, one could induce a non-trivial flow by perturbing the geometry. As the geometric flow behavior for black holes is generally very complicated, we resorted to a numerical evaluation. However, for extremal Reissner-Nordström the near horizon flow could be solved analytically.

Cosmic Acceleration and Turns in the Swampland

As it turned out, the Swampland Distance Conjecture can be consistent with non-geodesic paths, as long as the limiting tangent vector of the trajectory is constant. In particular, this ensures a non-vanishing decay rate of the mass tower in the limit to the boundary of moduli space. Since cosmic acceleration, which is characterised by $\epsilon < 1$, usually involves several scalar fields on non-geodesic trajectories, it serves as a natural application of this feature. For instance, it was previously observed in the literature that a highly turning, i.e. highly non-geodesic, motion could resolve the tension between the dS conjecture and cosmic acceleration. However, for infinite-distance trajectories with a constant tangent vector in a hyperbolic

geometry, which is the typical asymptotic limit of Calabi-Yau compactifications, the turning rate or non-geodesicity factor Ω is bounded by $\Omega < \mathcal{O}(1) \cdot \sqrt{\epsilon}$ (in Hubble units). This holds for very general trajectories and severely restricts a large turning rate. Away from the boundary of moduli space the condition of a constant tangent vector can be relaxed which results in additional contributions to the turning rate Ω. However, as we show by an asymptotic expansion around the the boundary of moduli space, these new terms are again $\mathcal{O}(1) \cdot \sqrt{\epsilon}$ such that the previous bound persists. Moreover, a new concept for the analysis with infinite-distance trajectories consistent with the SDC was developed, namely the swamp cone.

6.2 Outlook

In this part some possible future directions of the results in this thesis are suggested. After that some final remarks are made.

Geometric Flow Equation for the Number of Spacetime Dimensions

First of all, the limit $d' \to \infty$ in the Freund-Rubin compactification corresponds to large curvatures which might lead to problems, as it is a regime where the geometric formulation breaks down due to the KK-tower becoming super-Planckian. A possible solution to this is the inclusion of even higher-loop corrections from the graviton β-function in String Theory. In fact, this inclusion might further influence the structure of fixed points and singular points, possibly giving new ones at finite dimensions. Moreover, D-flow applied to general D-dimensional black hole solutions, like the generalisation of the Schwarzschild black hole, might yield some intriguing results. This could also open up a possibility to relate D-flow to other Swampland Conjectures. Finally, it would interesting to construct a proper notion of distance for the context of D-flow beyond the large D limit since the standard formulas, like Δ_g for the metric distance, can't be directly applied.

Gradient Flow of Einstein-Maxwell Theory

There are a lot of possible future directions here. First, one could consider EM flow in the context of the Swampland Program. For instance, it would be expected that the Ricci Flow Conjecture also applies here since EM flow is a direct generalisation of Ricci flow. Moreover, EM flow can also be applied to extremal black holes, which are a very natural test object within QG. A very welcomed property here is the analytical control in the near horizon flow of the geometry. Then, the flow could be easily extended to also include scalar fields which would provide a direct connection to the SDC. In a preliminary study into this direction it seemed that the attractor formalism was preserved by a flow of an extremal dilatonic black hole

including a scalar field. Furthermore, if a geometric flow of a black hole ends up at flat space after a resolution of a flow singularity, the black hole "disappears" along the flow which closely resembles the effect of Hawking radiation. Thus, black hole evaporation could be modelled by geometric flow equations. The resolution of a flow singularity is done by hand and is called surgery. As Ricci flow and also EM flow are closely related to the string β-functions, the inclusion of higher-loop corrections might provide a mechanism for the surgery. However, there are still a lot more future directions, e.g. an extension from static to stationary spacetimes, a proper investigation of the parameter τ characterising the relative speed between the metric and the Maxwell field flow, a systematic exploration of the unstable modes in the electric Reissner-Nordström EM flow or the construction of the analogue to Ricci solitons for EM flow.

Cosmic Acceleration and Turns in the Swampland

Since a non-geodesic trajectory typically is realized by the addition of a potential, the bound on Ω induced by the SDC should translate into a constraint on the potential, or at least a constraint on the valleys, i.e. the flat directions, of the potential. Moreover, the bound on Ω doesn't release the tension between the dS conjecture and cosmic inflation but it further hints at a delicate interplay between Ω, ϵ, η which is required to satisfy the dS conjecture. In particular, the parameter η was recently of growing interest within the community. As more investigations are conducted, we should get closer and closer to a resolution of this problem. Furthermore, if the moduli fields are inhomogeneous instead of homogeneous, the extra spacetime dependence can be understood as introducing extra forces in moduli space providing another mechanism for non-geodesic trajectories. It would be interesting to see whether this approach yields a similar bound on the turning rate near the boundary of moduli space.

Final Remarks

The current time is truly exciting, as more and more significant breakthroughs are made within the Swampland Program. The theoretical understanding becomes better and the observational implications more frequent and more precise. Hence, I believe that it is only a matter of time until we have a real observational test for String Theory at the energy scale accessible to us. Then we know, if String Theory is a "mistake", relating back to the quote by Lee Smolin. But it was hopefully firmly established throughout this thesis that String Theory, as a consistent theory of Quantum Gravity, certainly isn't trivial either way.

Appendix A

Decomposition of R_D

The metric is given as

$$ds^2 = G_{MN}dX^M dX^N = e^{2\alpha\phi}g_{\mu\nu}dX^\mu dX^\nu + e^{2\beta\phi}\left(dX^d\right)^2 \tag{A.1}$$

where $M = 0, \ldots, d$ and $\mu = 0, \ldots, d-1$. Furthermore, $g_{\mu\nu}$ and ϕ only depend on the external coordinates X^μ. Introducing

$$\tilde{g}_{\mu\nu} = e^{2(\alpha-\beta)\phi}g_{\mu\nu} \tag{A.2}$$

the metric (A.1) becomes

$$ds^2 = e^{2\beta\phi}\left(\tilde{g}_{\mu\nu}dX^\mu dX^\nu + \left(dX^d\right)^2\right). \tag{A.3}$$

Now we can further define

$$G_{MN} = e^{2\beta\phi}\tilde{G}_{MN}. \tag{A.4}$$

The above is a Weyl rescaling of the metric such that we can apply the standard transformation behavior of the Ricci scalar under Weyl rescalings, namely in general it holds for a n-dimensional metric

$$\begin{aligned} G_{MN} &\to \Omega^2 G_{MN} \\ R &\to \Omega^{-2}\left(R - 2(n-1)\nabla^2 \ln\Omega - (n-2)(n-1)(\partial \ln\Omega)^2\right). \end{aligned} \tag{A.5}$$

Thus, we get

$$R_D = e^{-2\beta\phi}\left(\tilde{R}_D - 2\beta(D-1)\tilde{\Box}\phi - \beta^2(D-2)(D-1)(\tilde{\partial}\phi)^2\right) \tag{A.6}$$

where

$$\tilde{\Box}\phi = \tilde{G}^{MN}\tilde{\nabla}_M\tilde{\nabla}_N\phi$$

$$(\tilde{\partial}\phi)^2 = \tilde{G}^{MN}\partial_M\phi\partial_N\phi.$$

Furthermore, $\tilde{R}_D$ is the Ricci scalar with respect to $\tilde{G}_{MN}$ and $\tilde{\nabla}_M$ is the covariant derivative with respect to $\tilde{G}_{MN}$. The above quantities need to be further decomposed as follows

$$\tilde{\Box}\phi = e^{-2(\alpha-\beta)\phi}\left(\Box\phi + (d-2)(\alpha-\beta)(\partial\phi)^2\right) \tag{A.7}$$

$$(\tilde{\partial}\phi)^2 = e^{-2(\alpha-\beta)\phi}(\partial\phi)^2 \tag{A.8}$$

where the quantities on the right-hand side are purely defined in terms of $g_{\mu\nu}$, namely

$$\Box\phi = \partial^\mu\partial_\mu\phi$$
$$(\partial\phi)^2 = \partial_\mu\phi\partial^\mu\phi.$$

Lastly, we need to take care of $\tilde{R}_D$. Because nothing depends on X^d, it is not hard to show by using the explicit formulas that

$$\tilde{R}_D = \tilde{R}_d. \tag{A.9}$$

Here $\tilde{R}_d$ is determined by $\tilde{g}_{\mu\nu}$. Thus, one can apply the above Weyl rescaling formula (A.5) once more

$$\tilde{R}_d = e^{-2(\alpha-\beta)\phi}\left(R_d - 2(d-1)(\alpha-\beta)\Box\phi - (d-1)(d-2)(\alpha-\beta)^2(\partial\phi)^2\right). \tag{A.10}$$

All these results can be plugged into (A.6) and, when the dust settles, we arrive at

$$R_D = e^{-2\alpha\phi}\left(R_d - C_1\partial_\mu\phi\partial^\mu\phi - C_2\partial^\mu\partial_\mu\phi\right) \tag{A.11}$$

with

$$C_1 = (d-1)(d-2)(\alpha-\beta)^2 + 2\beta d(d-2)(\alpha-\beta) + d(d-1)\beta^2 \tag{A.12}$$

$$C_2 = 2\left((d-1)(\alpha-\beta) + \beta d\right). \tag{A.13}$$

Appendix B

Geodesics of Hyperbolic Planes

Here we will derive the geodesics for a single hyperbolic plane and a product of two hyperbolic planes. Let's first recall the geodesic equation

$$\ddot{\Phi}^a + \Gamma^a_{bc}\dot{\Phi}^a\dot{\Phi}^b = 0 \tag{B.1}$$

where the dot indicates a derivative with respect to ξ, i.e. $\dot{} = d/d\xi$, which parametrises the geodesic. Also note that we used Φ^a instead of ϕ^a to collectively label the fields in order to avoid confusion with the axion ϕ. Thus, we slightly differ here from the notation in section 2.2.1.
We begin by examining the single hyperbolic plane whose metric we state here again for completeness

$$d\Delta^2 = g_{ab}d\Phi^a d\Phi^b = \frac{n^2}{s^2}\left(ds^2 + d\phi^2\right) \tag{B.2}$$

where $\Phi^a = (s, \phi)$. This parametrises the upper half of the hyperbolic plane, i.e. $s > 0$. The non-vanishing Christoffel symbols are

$$\Gamma^s_{ss} = -\frac{1}{s} = \Gamma^\phi_{s\phi}, \quad \Gamma^s_{\phi\phi} = \frac{1}{s} \tag{B.3}$$

such that the geodesic equation (B.1) becomes

$$\begin{aligned} \ddot{s} - \frac{1}{s}\dot{s}^2 + \frac{1}{s}\dot{\phi}^2 &= 0 \\ \ddot{\phi} - \frac{2}{s}\dot{s}\dot{\phi} &= 0. \end{aligned} \tag{B.4}$$

First of all, we note that these equations are invariant under the transformation $\phi \to -\phi$. Then, it is easy to see that a solution to these equations is given by a vertical line along the s-direction with $\phi = \phi_0 = const.$ Moreover, there is a second class of solutions, namely semi-circles with centers along $s = 0$ [32].

But because we are interested in the region of large s with trajectories trending towards $s = \infty$, we will focus only on the first class. Assuming $\phi = \phi_0 = const$ the second geodesic equation becomes trivial, whereas the first reads

$$\ddot{s} - \frac{1}{s}\dot{s}^2 = 0. \tag{B.5}$$

We can safely divide by s, since it is positive, such that we get

$$\begin{aligned} \frac{\ddot{s}}{s} - \frac{\dot{s}^2}{s^2} &= 0 \\ \frac{d^2}{d\xi^2} \ln s &= 0 \\ \ln s &= a\xi + b \\ \Rightarrow s(\xi) &= C\ e^{a\xi} \end{aligned} \tag{B.6}$$

where $C \equiv e^b$. This also implies $C > 0$ which is required by $s > 0$. Furthermore, the integration constant a is also positive to be consistent with $s \to \infty$. Please note that we are always able to reparametrise this such that we can get almost any behavior for s, i.e. s doesn't have to be necessarily exponential.
Next, we turn to the product of two hyperbolic planes. In that case the metric reads

$$d\Delta^2 = g_{ab} d\Phi^a d\Phi^b = \frac{n^2}{s^2}\left(ds^2 + d\phi^2\right) + \frac{m^2}{u^2}\left(du^2 + d\psi^2\right) \tag{B.7}$$

where $\Phi^a = (s, \phi, u, \psi)$. This again holds for $s, u > 0$. The non-vanishing Christoffel symbols for this metric are

$$\Gamma^s_{ss} = -\frac{1}{s} = \Gamma^\phi_{s\phi}, \quad \Gamma^s_{\phi\phi} = \frac{1}{s}, \quad \Gamma^u_{uu} = -\frac{1}{u} = \Gamma^\psi_{s\psi}, \quad \Gamma^u_{\psi\psi} = \frac{1}{u}. \tag{B.8}$$

Therefore, we arrive at the following geodesic equations

$$\begin{aligned} \ddot{s} - \frac{1}{s}\dot{s}^2 + \frac{1}{s}\dot{\phi}^2 &= 0 \\ \ddot{\phi} - \frac{2}{s}\dot{s}\dot{\phi} &= 0 \\ \ddot{u} - \frac{1}{u}\dot{u}^2 + \frac{1}{u}\dot{\psi}^2 &= 0 \\ \ddot{\psi} - \frac{2}{u}\dot{u}\dot{\psi} &= 0. \end{aligned} \tag{B.9}$$

In analogy to the above, these equations enjoy an invariance under axion reflection, i.e. $\phi \to -\phi$ and $\psi \to -\psi$. Moreover, it is pretty evident from these equations that a geodesic for the product of two hyperbolic planes consists of two geodesics of the single hyperbolic plane combined in one vector. Due to the same reasons

as above, we reject all the semi-circle solutions and just focus on the case with constant axions, namely $\phi = \phi_0 = const$ and $\psi = \psi_0 = const$. Hence, the axion equations become again trivial and we get twice the same saxion equation which precisely has the same form as above

$$\begin{aligned} \ddot{s} - \frac{1}{s}\dot{s}^2 &= 0 \\ \ddot{u} - \frac{1}{u}\dot{u}^2 &= 0. \end{aligned} \tag{B.10}$$

Similarly to the case before, the solution to these equations works out to be

$$\begin{aligned} \Rightarrow s(\xi) &= Ce^{a\xi} \\ u(\xi) &= De^{b\xi} \end{aligned} \tag{B.11}$$

where $a, b, C, D > 0$ due to the same consistency arguments. Note that we could also choose either a or b to be 0 such that one hyperbolic plane is completely constant and we just have a geodesic, i.e. a vertical line, on the other one. Furthermore, as above, this solution can also be reparametrised to give a behavior different from the exponential one.
Finally, one has to emphasise that all the constants introduced in this appendix have no relation to the main part of the text, they are merely integration constants.

Appendix C

Geodesicity of Critical Trajectories

Here we check, if the critical trajectories from section 5.3.1 and 5.3.2 fulfill the geodesic equation. This is meant as a complementary point of view to the analysis in the just mentioned sections, 5.3.1 and 5.3.2, where the geodesicity was determined by the computation of Ω.
Now recall the geodesic equations for a single hyperbolic plane which has already been introduced in appendix B, namely we have

$$\begin{aligned} \ddot{s} - \frac{1}{s}\dot{s}^2 + \frac{1}{s}\dot{\phi}^2 &= 0 \\ \ddot{\phi} - \frac{2}{s}\dot{s}\dot{\phi} &= 0 \end{aligned} \tag{C.1}$$

where the dot indicates a derivative with respect to ξ, i.e. $\dot{} = d/d\xi$, which parametrizes the given trajectory.
Inspired by section 5.3.1 we explore now what is happening in the critical case characterized by

$$\dot{\phi} = \beta \dot{s} \tag{C.2}$$

where β is a real constant. Intuitively, we would immediately say that this isn't a geodesic unless $\beta = 0$ because we have seen in appendix B that a geodesic (trending towards $s = \infty$) has to have $\dot{\phi} = 0$. For the critical case the geodesic equations above become

$$\begin{aligned} \ddot{s} - \frac{1}{s}\dot{s}^2(1-\beta^2) &= 0 \\ \beta\left(\ddot{s} - \frac{2}{s}\dot{s}^2\right) &= 0. \end{aligned} \tag{C.3}$$

It turns out this can only be consistently solved for $\beta = 0$ and then we recover the geodesic solution from appendix B which is what we anticipated from the

start. However, we also see that the critical condition $\dot{\phi} = \beta\dot{s}$ makes the system of equations overdetermined, i.e. we have two equations for a single function s. Overdetermined systems aren't guaranteed to have a solution which is precisely the case here. They are usually only solvable, if some equations are linearly dependent. Here we could only make that happen with $\beta^2 = -1$ (after multiplying the second equation by β) which would imply a complex β. So, we reject that possibility. Besides, we want a solution for an arbitrary β and not only for some special value. That explains what happens on the level of the geodesic equation in the critical case which is in perfect agreement with the result of a non-vanishing turning rate Ω in section 5.3.1.
Now we turn to the product of two hyperbolic planes. Again, recall the geodesic equations from appendix B which read

$$\begin{aligned} \ddot{s} - \frac{1}{s}\dot{s}^2 + \frac{1}{s}\dot{\phi}^2 &= 0 \\ \ddot{\phi} - \frac{2}{s}\dot{s}\dot{\phi} &= 0 \\ \ddot{u} - \frac{1}{u}\dot{u}^2 + \frac{1}{u}\dot{\psi}^2 &= 0 \\ \ddot{\psi} - \frac{2}{u}\dot{u}\dot{\psi} &= 0. \end{aligned} \tag{C.4}$$

Now it is very interesting to see what happens in the critical case for two saxions from section 5.3.2, which is governed by constant axions ($\phi = \phi_0 = const$ and $\psi = \psi_0 = const$) and the condition

$$\frac{\dot{u}}{u} = \delta\frac{\dot{s}}{s} \tag{C.5}$$

for some $\delta = const$. Since the axions are kept constant, it's quite reasonable to expect that this should also solve the geodesic equations. And, indeed, we get

$$\begin{aligned} \ddot{s} - \frac{1}{s}\dot{s}^2 &= 0 \\ \delta\left(\ddot{s} - \frac{1}{s}\dot{s}^2\right) &= 0. \end{aligned} \tag{C.6}$$

Unlike above these two equations are compatible in the sense that the two equations are linear dependent. And we can solve this overdetermined system of equations consistently for an arbitrary non-vanishing δ. In particular, the solution for s is given by

$$s(\xi) = Ce^{a\xi} \tag{C.7}$$

where $C, a > 0$, as in appendix B. As another cross check, we can integrate the critical case condition (C.5) to

$$\ln u = \delta \ln s + k \tag{C.8}$$

where k is some integration constant. Plugging the solution for s, i.e. (C.7), into that we arrive at

$$\ln u = \delta \ln s + k = (\delta a)\, \xi + (\delta \ln C + k) \tag{C.9}$$

which is obviously also a solution to the geodesic equation for constant axions. Therefore, the critical case here turns out to be a geodesic trajectory for the product of two hyperbolic planes which is again in perfect agreement with the corresponding result $\Omega = 0$ from chapter 5.
Moreover, it is also worthwhile to explore what happens in the case involving the saxion and the axion from the other hyperbolic plane, which was also introduced in section 5.3.2. In that case we set $\phi = \phi_0 = const$ and $u = u_0 = const$. This makes the geodesic equation associated with ϕ trivial again. But this time the equation for the other constant coordinate u isn't trivial, which is very crucial. Omitting the ϕ-equation, we get

$$\begin{aligned} \ddot{s} - \frac{1}{s}\dot{s}^2 &= 0 \\ \frac{1}{u_0}\dot{\psi}^2 &= 0 \\ \ddot{\psi} &= 0. \end{aligned} \tag{C.10}$$

We can already read off some implications from this set of equations, for instance, ψ has to be constant. But let's employ the critical case condition first. In this setting it is given by

$$\dot{\psi} = \gamma \frac{\dot{s}}{s} \tag{C.11}$$

for $\gamma = const$. Hence, the above equations turn into

$$\begin{aligned} \ddot{s} - \frac{1}{s}\dot{s}^2 &= 0 \\ \frac{1}{u_0}\gamma^2 \left(\frac{\dot{s}}{s}\right)^2 &= 0 \\ \gamma \left(\ddot{s} - \frac{1}{s}\dot{s}^2\right) &= 0. \end{aligned} \tag{C.12}$$

Without the second equation we would be in the same situation as in the previous case which would imply a geodesic trajectory with $\Omega = 0$. However, precisely this second equation spoils the situation since it forces upon us the uninteresting case $s = const$. Besides the fact that this case is uninteresting, we have also demanded that we want our trajectory to approach $s = \infty$. So there is no solution to the geodesic equation in this case. In agreement with the findings of section 5.3.2 we conclude that $\Omega \neq 0$ and that we have to include all the coordinates in order to get a proper result. Hence, this is another point of view to the argument, why we have to be careful with these effective metrics, which was also presented in section 5.3.2.

Bibliography

[1] D. De Biasio, J. Freigang and D. Lüst, *Geometric Flow Equations for the Number of Space-Time Dimensions*, *Fortschritte der Physik* **70** (2022) 2100171 [2104.05621].

[2] D. De Biasio, J. Freigang, D. Lust and T. Wiseman, *Gradient flow of Einstein-Maxwell theory and Reissner-Nordström black holes*, *J. High Energ. Phys.* (2023) [2210.14705].

[3] J. Freigang, D. Lust, G.-E. Nian and M. Scalisi, *Cosmic Acceleration and Turns in the Swampland*, 2306.17217.

[4] C. Vafa, *The String Landscape and the Swampland*, *arXiv e-prints* (2005) hep [hep-th/0509212].

[5] H. Ooguri and C. Vafa, *On the Geometry of the String Landscape and the Swampland*, *Nucl. Phys. B* **766** (2007) 21 [hep-th/0605264].

[6] N. Arkani-Hamed, L. Motl, A. Nicolis and C. Vafa, *The String landscape, black holes and gravity as the weakest force*, *JHEP* **06** (2007) 060 [hep-th/0601001].

[7] W. Lerche, D. Lust and A.N. Schellekens, *Chiral Four-Dimensional Heterotic Strings from Selfdual Lattices*, *Nucl. Phys. B* **287** (1987) 477.

[8] M.R. Douglas, *The Statistics of string / M theory vacua*, *JHEP* **05** (2003) 046 [hep-th/0303194].

[9] S. Ashok and M.R. Douglas, *Counting flux vacua*, *JHEP* **01** (2004) 060 [hep-th/0307049].

[10] R. Blumenhagen, F. Gmeiner, G. Honecker, D. Lust and T. Weigand, *The Statistics of supersymmetric D-brane models*, *Nucl. Phys. B* **713** (2005) 83 [hep-th/0411173].

[11] J. McNamara and C. Vafa, *Cobordism Classes and the Swampland*, 1909.10355.

[12] E. Palti, *The Swampland: Introduction and Review*, *Fortschritte der Physik* **67** (2019) 1900037 [1903.06239].

[13] M. van Beest, J. Calderón-Infante, D. Mirfendereski and I. Valenzuela, *Lectures on the Swampland Program in String Compactifications*, *Phys. Rept.* **989** (2022) 1 [2102.01111].

[14] E. Fermi, *An attempt of a theory of beta radiation. 1.*, *Z. Phys.* **88** (1934) 161.

[15] N. Cribiori, D. Lust and M. Scalisi, *The gravitino and the swampland*, *JHEP* **06** (2021) 071 [2104.08288].

[16] M. Montero, C. Vafa and I. Valenzuela, *The dark dimension and the Swampland*, *JHEP* **02** (2023) 022 [2205.12293].

[17] L.A. Anchordoqui, I. Antoniadis, N. Cribiori, D. Lust and M. Scalisi, *The Scale of Supersymmetry Breaking and the Dark Dimension*, *JHEP* **05** (2023) 060 [2301.07719].

[18] L.A. Anchordoqui, I. Antoniadis and D. Lust, *Dark dimension, the swampland, and the dark matter fraction composed of primordial black holes*, *Phys. Rev. D* **106** (2022) 086001 [2206.07071].

[19] D. Klaewer, D. Lüst and E. Palti, *A Spin-2 Conjecture on the Swampland*, *Fortsch. Phys.* **67** (2019) 1800102 [1811.07908].

[20] M. Scalisi and I. Valenzuela, *Swampland distance conjecture, inflation and α-attractors*, *JHEP* **08** (2019) 160 [1812.07558].

[21] T. Banks and N. Seiberg, *Symmetries and Strings in Field Theory and Gravity*, *Phys. Rev. D* **83** (2011) 084019 [1011.5120].

[22] D. Harlow and H. Ooguri, *Symmetries in quantum field theory and quantum gravity*, *Commun. Math. Phys.* **383** (2021) 1669 [1810.05338].

[23] D. Harlow and H. Ooguri, *Constraints on Symmetries from Holography*, *Phys. Rev. Lett.* **122** (2019) 191601 [1810.05337].

[24] G. Obied, H. Ooguri, L. Spodyneiko and C. Vafa, *De Sitter Space and the Swampland*, 1806.08362.

[25] D. Lüst, E. Palti and C. Vafa, *AdS and the Swampland*, *Phys. Lett. B* **797** (2019) 134867 [1906.05225].

[26] A. Bedroya and C. Vafa, *Trans-Planckian Censorship and the Swampland*, *JHEP* **09** (2020) 123 [1909.11063].

[27] A. Kehagias, D. Lüst and S. Lüst, *Swampland, Gradient Flow and Infinite Distance*, *JHEP* **04** (2020) 170 [1910.00453].

[28] Q. Bonnefoy, L. Ciambelli, D. Lüst and S. Lüst, *Infinite Black Hole Entropies at Infinite Distances and Tower of States*, *Nucl. Phys. B* **958** (2020) 115112 [1912.07453].

[29] Q. Bonnefoy, L. Ciambelli, D. Lüst and S. Lüst, *The Swampland at Large Number of Space-Time Dimensions*, 2011.06610.

[30] T.W. Grimm, E. Palti and I. Valenzuela, *Infinite Distances in Field Space and Massless Towers of States*, *JHEP* **08** (2018) 143 [1802.08264].

[31] E. Palti, *The Swampland: Introduction and Review*, *Fortsch. Phys.* **67** (2019) 1900037 [1903.06239].

[32] J. Calderón-Infante, A.M. Uranga and I. Valenzuela, *The Convex Hull Swampland Distance Conjecture and Bounds on Non-geodesics*, *JHEP* **03** (2021) 299 [2012.00034].

[33] M.B. Green, J.H. Schwarz and E. Witten, *Superstring Theory. VOL. 1: Introduction*, Cambridge Monographs on Mathematical Physics (7, 1988).

[34] M.B. Green, J.H. Schwarz and E. Witten, *Superstring Theory. VOL. 2: Loop Amplitudes, Anomalies and Phenomenology* (7, 1988).

[35] R. Blumenhagen, D. Lüst and S. Theisen, *Basic concepts of string theory*, Theoretical and Mathematical Physics, Springer, Heidelberg, Germany (2013), 10.1007/978-3-642-29497-6.

[36] J. Polchinski, *String theory. Vol. 1: An introduction to the bosonic string*, Cambridge Monographs on Mathematical Physics, Cambridge University Press (12, 2007), 10.1017/CBO9780511816079.

[37] J. Polchinski, *String theory. Vol. 2: Superstring theory and beyond*, Cambridge Monographs on Mathematical Physics, Cambridge University Press (12, 2007), 10.1017/CBO9780511618123.

[38] B. Zwiebach, *A first course in string theory*, Cambridge University Press (7, 2006).

[39] Y. Nambu, *DUALITY AND HADRODYNAMICS*, in *Winter School in Theoretical Particle Physics*, pp. 573–596, 1986.

[40] T. Goto, *Relativistic quantum mechanics of one-dimensional mechanical continuum and subsidiary condition of dual resonance model*, *Prog. Theor. Phys.* **46** (1971) 1560.

[41] A.M. Polyakov, *Quantum Geometry of Bosonic Strings*, *Phys. Lett. B* **103** (1981) 207.

[42] A.M. Polyakov, *Quantum Geometry of Fermionic Strings*, *Phys. Lett. B* **103** (1981) 211.

[43] S. Deser and B. Zumino, *A complete action for the spinning string*, *Physics Letters B* **65** (1976) 369.

[44] L. Brink, P. Di Vecchia and P. Howe, *A locally supersymmetric and reparametrization invariant action for the spinning string*, *Physics Letters B* **65** (1976) 471.

[45] L. Brink and J.H. Schwarz, *Local Complex Supersymmetry in Two-Dimensions*, *Nucl. Phys. B* **121** (1977) 285.

[46] N. Gendler and I. Valenzuela, *Merging the weak gravity and distance conjectures using BPS extremal black holes*, *JHEP* **01** (2021) 176 [2004.10768].

[47] D. Andriot, N. Cribiori and D. Erkinger, *The web of swampland conjectures and the TCC bound*, *JHEP* **07** (2020) 162 [2004.00030].

[48] T. Rudelius, *Asymptotic observables and the swampland*, *Phys. Rev. D* **104** (2021) 126023 [2106.09026].

[49] G. Dvali, *Black Holes and Large N Species Solution to the Hierarchy Problem*, *Fortsch. Phys.* **58** (2010) 528 [0706.2050].

[50] G. Dvali and D. Lust, *Evaporation of Microscopic Black Holes in String Theory and the Bound on Species*, *Fortsch. Phys.* **58** (2010) 505 [0912.3167].

[51] D. Klaewer and E. Palti, *Super-Planckian Spatial Field Variations and Quantum Gravity*, *JHEP* **01** (2017) 088 [1610.00010].

[52] F. Baume and E. Palti, *Backreacted Axion Field Ranges in String Theory*, *JHEP* **08** (2016) 043 [1602.06517].

[53] T. Kaluza, *Zum Unitätsproblem der Physik*, *Sitzungsber. Preuss. Akad. Wiss. Berlin (Math. Phys.)* **1921** (1921) 966 [1803.08616].

[54] O. Klein, *Quantum Theory and Five-Dimensional Theory of Relativity. (In German and English)*, *Z. Phys.* **37** (1926) 895.

[55] S.-J. Lee, W. Lerche and T. Weigand, *Emergent strings from infinite distance limits*, *JHEP* **02** (2022) 190 [1910.01135].

[56] E. Gonzalo, L.E. Ibáñez and A.M. Uranga, *Modular symmetries and the swampland conjectures*, *JHEP* **05** (2019) 105 [1812.06520].

[57] A. Font, A. Herráez and L.E. Ibáñez, *The Swampland Distance Conjecture and Towers of Tensionless Branes*, *JHEP* **08** (2019) 044 [1904.05379].

[58] S.-J. Lee, W. Lerche and T. Weigand, *Tensionless Strings and the Weak Gravity Conjecture*, *JHEP* **10** (2018) 164 [1808.05958].

[59] S.-J. Lee, W. Lerche and T. Weigand, *A Stringy Test of the Scalar Weak Gravity Conjecture*, *Nucl. Phys. B* **938** (2019) 321 [1810.05169].

[60] P. Corvilain, T.W. Grimm and I. Valenzuela, *The Swampland Distance Conjecture for Kähler moduli*, *JHEP* **08** (2019) 075 [1812.07548].

[61] R. Blumenhagen, D. Kläwer, L. Schlechter and F. Wolf, *The Refined Swampland Distance Conjecture in Calabi-Yau Moduli Spaces*, *JHEP* **06** (2018) 052 [1803.04989].

[62] D. Erkinger and J. Knapp, *Refined swampland distance conjecture and exotic hybrid Calabi-Yaus*, *JHEP* **07** (2019) 029 [1905.05225].

[63] D. Klaewer, S.-J. Lee, T. Weigand and M. Wiesner, *Quantum corrections in 4d $N = 1$ infinite distance limits and the weak gravity conjecture*, *JHEP* **03** (2021) 252 [2011.00024].

[64] B.S. DeWitt, *Quantum theory of gravity. i. the canonical theory*, *Phys. Rev.* **160** (1967) 1113.

[65] O. Gil-Medrano and P.W. Michor, *The Riemannian manifold of all Riemannian metrics*, *arXiv Mathematics e-prints* (1991) math/9201259 [math/9201259].

[66] R.S. Hamilton, *Three-manifolds with positive Ricci curvature*, *Journal of Differential Geometry* **17** (1982) 255 .

[67] B. Chow and D. Knopf, *The Ricci Flow: An Introduction: An Introduction*, vol. 1, American Mathematical Soc. (2004).

[68] P.M. Topping, *Lectures on the ricci flow*, 2006.

[69] G. Perelman, *The Entropy formula for the Ricci flow and its geometric applications*, math/0211159.

[70] G. Perelman, *The entropy formula for the Ricci flow and its geometric applications*, *arXiv Mathematics e-prints* (2002) math/0211159 [math/0211159].

[71] G. Perelman, *Ricci flow with surgery on three-manifolds*, *arXiv Mathematics e-prints* (2003) math/0303109 [math/0303109].

[72] J.P. Bourguignon, *Ricci curvature and einstein metrics*, in *Global Differential Geometry and Global Analysis*, D. Ferus, W. Kühnel, U. Simon and B. Wegner, eds., (Berlin, Heidelberg), pp. 42–63, Springer Berlin Heidelberg, 1981.

[73] C. Mantegazza, G. Catino, L. Cremaschi, Z. Djadli and L. Mazzieri, *The ricci-bourguignon flow*, *Pacific Journal of Mathematics* **287** (2015) .

[74] E. Calabi, *Extremal kÄhler metrics*, in *Seminar on Differential Geometry. (AM-102), Volume 102*, S. tung Yau, ed., (Princeton), pp. 259–290, Princeton University Press (1982), DOI.

[75] I. Bakas, *Geometric flows and (some of) their physical applications*, *Bulg. J. Phys.* **33** (2006) 091 [hep-th/0511057].

[76] I. Bakas, *Renormalization group equations and geometric flows*, *Ann. U. Craiova Phys.* **16** (2006) 20 [hep-th/0702034].

[77] C. Gómez, *Gravity as Universal UV Completion: Towards a Unified View of Swampland Conjectures*, *Fortsch. Phys.* **69** (2021) 2000096 [1907.13386].

[78] D. De Biasio, *On-Shell Flow*, 2211.04231.

[79] R. Emparan, R. Suzuki and K. Tanabe, *The large D limit of General Relativity*, *JHEP* **06** (2013) 009 [1302.6382].

[80] R. Emparan and C.P. Herzog, *Large D limit of Einstein's equations*, *Rev. Mod. Phys.* **92** (2020) 045005 [2003.11394].

[81] D. Lust, *Toroidal & Orbifold Compactifications at Large D and D-Duality*, *Fortsch. Phys.* **70** (2022) 2100172 [2107.09780].

[82] N. Seiberg, *Notes on quantum Liouville theory and quantum gravity*, *Prog. Theor. Phys. Suppl.* **102** (1990) 319.

[83] R.C. Myers, *New Dimensions for Old Strings*, *Phys. Lett. B* **199** (1987) 371.

[84] A. Chamseddine, *A study of non-critical strings in arbitrary dimensions*, *Nuclear Physics B* **368** (1992) 98.

[85] J. Teschner, *Liouville theory revisited*, *Class. Quant. Grav.* **18** (2001) R153 [hep-th/0104158].

[86] I. Valenzuela, *Backreaction Issues in Axion Monodromy and Minkowski 4-forms*, *JHEP* **06** (2017) 098 [1611.00394].

[87] R. Blumenhagen, I. Valenzuela and F. Wolf, *The Swampland Conjecture and F-term Axion Monodromy Inflation*, *JHEP* **07** (2017) 145 [1703.05776].

[88] T.W. Grimm, C. Li and E. Palti, *Infinite Distance Networks in Field Space and Charge Orbits*, *JHEP* **03** (2019) 016 [1811.02571].

[89] T.W. Grimm, C. Li and I. Valenzuela, *Asymptotic Flux Compactifications and the Swampland*, *JHEP* **06** (2020) 009 [1910.09549].

[90] E. Silverstein and A. Westphal, *Monodromy in the CMB: Gravity Waves and String Inflation*, *Phys. Rev. D* **78** (2008) 106003 [0803.3085].

[91] N. Kaloper and L. Sorbo, *A Natural Framework for Chaotic Inflation*, *Phys. Rev. Lett.* **102** (2009) 121301 [0811.1989].

[92] F. Marchesano, G. Shiu and A.M. Uranga, *F-term Axion Monodromy Inflation*, *JHEP* **09** (2014) 184 [1404.3040].

[93] L. McAllister, E. Silverstein, A. Westphal and T. Wrase, *The Powers of Monodromy*, *JHEP* **09** (2014) 123 [1405.3652].

[94] C.G. Callan, Jr., E.J. Martinec, M.J. Perry and D. Friedan, *Strings in Background Fields*, *Nucl. Phys. B* **262** (1985) 593.

[95] C.G. Callan, Jr., I.R. Klebanov and M.J. Perry, *String Theory Effective Actions*, *Nucl. Phys. B* **278** (1986) 78.

[96] A.P. Foakes and N. Mohammedi, *An Explicit Three Loop Calculation for the Purely Metric Two-dimensional Nonlinear σ Model*, *Nucl. Phys. B* **306** (1988) 343.

[97] E.S. Fradkin and A.A. Tseytlin, *Quantum String Theory Effective Action*, *Nucl. Phys. B* **261** (1985) 1.

[98] S.J. Graham, *Three Loop Beta Function for the Bosonic Nonlinear σ Model*, *Phys. Lett. B* **197** (1987) 543.

[99] M.T. Grisaru and D. Zanon, *σ Model Superstring Corrections to the Einstein-hilbert Action*, *Phys. Lett. B* **177** (1986) 347.

[100] D.J. Gross and E. Witten, *Superstring Modifications of Einstein's Equations*, *Nucl. Phys. B* **277** (1986) 1.

[101] I. Jack, D.R.T. Jones and N. Mohammedi, *A Four Loop Calculation of the Metric Beta Function for the Bosonic σ Model and the String Effective Action*, *Nucl. Phys. B* **322** (1989) 431.

[102] M. Headrick and T. Wiseman, *Ricci flow and black holes*, *Class. Quant. Grav.* **23** (2006) 6683 [hep-th/0606086].

[103] A.A. Tseytlin, *On sigma model RG flow, 'central charge' action and Perelman's entropy*, *Phys. Rev. D* **75** (2007) 064024 [hep-th/0612296].

[104] J.W. York, Jr., *Black hole thermodynamics and the Euclidean Einstein action*, *Phys. Rev. D* **33** (1986) 2092.

[105] S.W. Hawking and D.N. Page, *Thermodynamics of Black Holes in anti-De Sitter Space*, *Commun. Math. Phys.* **87** (1983) 577.

[106] D.J. Gross, M.J. Perry and L.G. Yaffe, *Instability of Flat Space at Finite Temperature*, *Phys. Rev. D* **25** (1982) 330.

[107] B.F. Whiting and J.W. York, Jr., *Action Principle and Partition Function for the Gravitational Field in Black Hole Topologies*, *Phys. Rev. Lett.* **61** (1988) 1336.

[108] B.F. Whiting, *Black Holes and Thermodynamics*, *Class. Quant. Grav.* **7** (1990) 15.

[109] T. Prestidge, *Dynamic and thermodynamic stability and negative modes in Schwarzschild-anti-de Sitter*, *Phys. Rev. D* **61** (2000) 084002 [hep-th/9907163].

[110] H.S. Reall, *Classical and thermodynamic stability of black branes*, *Phys. Rev. D* **64** (2001) 044005 [hep-th/0104071].

[111] D. Marolf and J.E. Santos, *The canonical ensemble reloaded: the complex-stability of Euclidean quantum gravity for black holes in a box*, *JHEP* **08** (2022) 215 [2202.11786].

[112] D.H. Friedan, *Nonlinear Models in Two + Epsilon Dimensions*, *Annals Phys.* **163** (1985) 318.

[113] A. Adam, S. Kitchen and T. Wiseman, *A numerical approach to finding general stationary vacuum black holes*, *Class. Quant. Grav.* **29** (2012) 165002 [1105.6347].

[114] T. Wiseman, *Numerical construction of static and stationary black holes*, in *Black holes in higher dimensions*, G.T. Horowitz, ed., pp. 233–270 (2012) [1107.5513].

[115] R. Monteiro and J.E. Santos, *Negative modes and the thermodynamics of Reissner-Nordstrom black holes*, *Phys. Rev. D* **79** (2009) 064006 [0812.1767].

[116] R. Monteiro, M.J. Perry and J.E. Santos, *Thermodynamic instability of rotating black holes*, *Phys. Rev. D* **80** (2009) 024041 [0903.3256].

[117] L.D. Landau and E.M. Lifshitz, *Statistical Physics Part I*, Elsevier, Amsterdam, 3rd ed. (1980).

[118] T. Prestidge, *PhD Thesis*, University of Cambridge (2000).

[119] D. DeTurck, *Deforming metrics in the direction of their ricci tensors*, *Journal of Differential Geometry* **18** (1983) 157.

[120] T.A. Oliynyk and E. Woolgar, *Asymptotically Flat Ricci Flows*, *Communications in Analysis and Geometry* **15** (2007) 535 [math/0607438].

[121] P. Figueras, J. Lucietti and T. Wiseman, *Ricci solitons, Ricci flow, and strongly coupled CFT in the Schwarzschild Unruh or Boulware vacua*, *Class. Quant. Grav.* **28** (2011) 215018 [1104.4489].

[122] H.W. Braden, J.D. Brown, B.F. Whiting and J.W. York, Jr., *Charged black hole in a grand canonical ensemble*, *Phys. Rev. D* **42** (1990) 3376.

[123] Supernova Search Team collaboration, *Observational evidence from supernovae for an accelerating universe and a cosmological constant*, *Astron. J.* **116** (1998) 1009 [astro-ph/9805201].

[124] A.G. Riess et al., *A Comprehensive Measurement of the Local Value of the Hubble Constant with 1 km/s/Mpc Uncertainty from the Hubble Space Telescope and the SH0ES Team*, 2112.04510.

[125] Boomerang collaboration, *Cosmology from MAXIMA-1, BOOMERANG and COBE / DMR CMB observations*, *Phys. Rev. Lett.* **86** (2001) 3475 [astro-ph/0007333].

[126] SDSS collaboration, *Cosmological parameters from SDSS and WMAP*, *Phys. Rev. D* **69** (2004) 103501 [astro-ph/0310723].

[127] Planck collaboration, *Planck 2018 results. VI. Cosmological parameters*, 1807.06209.

[128] M. Cicoli, J.P. Conlon, A. Maharana, S. Parameswaran, F. Quevedo and I. Zavala, *String Cosmology: from the Early Universe to Today*, 2303.04819.

[129] S. Dimopoulos, S. Kachru, J. McGreevy and J.G. Wacker, *N-flation*, *JCAP* **08** (2008) 003 [hep-th/0507205].

[130] D. Wands, *Multiple field inflation*, *Lect. Notes Phys.* **738** (2008) 275 [astro-ph/0702187].

[131] S. Cremonini, Z. Lalak and K. Turzynski, *Strongly Coupled Perturbations in Two-Field Inflationary Models*, *JCAP* **03** (2011) 016 [1010.3021].

[132] I.-S. Yang, *The Strong Multifield Slowroll Condition and Spiral Inflation*, *Phys. Rev. D* **85** (2012) 123532 [1202.3388].

[133] A.R. Brown, *Hyperbolic Inflation*, *Phys. Rev. Lett.* **121** (2018) 251601 [1705.03023].

[134] P. Christodoulidis, D. Roest and E.I. Sfakianakis, *Angular inflation in multi-field α-attractors*, *JCAP* **11** (2019) 002 [1803.09841].

[135] M. Dias, J. Frazer, A. Retolaza, M. Scalisi and A. Westphal, *Pole N-flation*, *JHEP* **02** (2019) 120 [1805.02659].

[136] A. Achúcarro and G.A. Palma, *The string swampland constraints require multi-field inflation*, *JCAP* **02** (2019) 041 [1807.04390].

[137] V. Aragam, R. Chiovoloni, S. Paban, R. Rosati and I. Zavala, *Rapid-turn inflation in supergravity is rare and tachyonic*, *JCAP* **03** (2022) 002 [2110.05516].

[138] S. Renaux-Petel, *Inflation with strongly non-geodesic motion: theoretical motivations and observational imprints*, *PoS* **EPS-HEP2021** (2022) 128 [2111.00989].

[139] M. Cicoli, G. Dibitetto and F.G. Pedro, *New accelerating solutions in late-time cosmology*, *Phys. Rev. D* **101** (2020) 103524 [2002.02695].

[140] M. Cicoli, G. Dibitetto and F.G. Pedro, *Out of the Swampland with Multifield Quintessence?*, *JHEP* **10** (2020) 035 [2007.11011].

[141] Y. Akrami, M. Sasaki, A.R. Solomon and V. Vardanyan, *Multi-field dark energy: Cosmic acceleration on a steep potential*, *Phys. Lett. B* **819** (2021) 136427 [2008.13660].

[142] L. Anguelova, J. Dumancic, R. Gass and L.C.R. Wijewardhana, *Dark energy from inspiraling in field space*, *JCAP* **03** (2022) 018 [2111.12136].

[143] J.R. Eskilt, Y. Akrami, A.R. Solomon and V. Vardanyan, *Cosmological dynamics of multifield dark energy*, *Phys. Rev. D* **106** (2022) 023512 [2201.08841].

[144] M. Brinkmann, M. Cicoli, G. Dibitetto and F.G. Pedro, *Stringy multifield quintessence and the Swampland*, *JHEP* **11** (2022) 044 [2206.10649].

[145] G. Shiu, F. Tonioni and H.V. Tran, *Accelerating universe at the end of time*, 2303.03418.

[146] G. Shiu, F. Tonioni and H.V. Tran, *Late-time attractors and cosmic acceleration*, 2306.07327.

[147] G.A. Palma, S. Sypsas and C. Zenteno, *Seeding primordial black holes in multifield inflation*, *Phys. Rev. Lett.* **125** (2020) 121301 [2004.06106].

[148] J. Fumagalli, S. Renaux-Petel, J.W. Ronayne and L.T. Witkowski, *Turning in the landscape: A new mechanism for generating primordial black holes*, *Phys. Lett. B* **841** (2023) 137921 [2004.08369].

[149] R. Bravo, G.A. Palma and S. Riquelme, *A Tip for Landscape Riders: Multi-Field Inflation Can Fulfill the Swampland Distance Conjecture*, *JCAP* **02** (2020) 004 [1906.05772].

[150] M. Etheredge, B. Heidenreich, S. Kaya, Y. Qiu and T. Rudelius, *Sharpening the Distance Conjecture in diverse dimensions*, *JHEP* **12** (2022) 114 [2206.04063].

[151] D. van de Heisteeg, C. Vafa, M. Wiesner and D.H. Wu, *Bounds on Field Range for Slowly Varying Positive Potentials*, 2305.07701.

[152] D. Roest, M. Scalisi and I. Zavala, *Kähler potentials for Planck inflation*, *JCAP* **11** (2013) 007 [1307.4343].

[153] R. Kallosh, A. Linde and D. Roest, *Superconformal Inflationary α-Attractors*, *JHEP* **11** (2013) 198 [1311.0472].

[154] C.P. Burgess, M. Cicoli, F. Quevedo and M. Williams, *Inflating with Large Effective Fields*, *JCAP* **11** (2014) 045 [1404.6236].

[155] C. Burgess and D. Roest, *Inflation by Alignment*, *JCAP* **06** (2015) 012 [1412.1614].

[156] D. Roest and M. Scalisi, *Cosmological attractors from α-scale supergravity*, *Phys. Rev. D* **92** (2015) 043525 [1503.07909].

[157] C.P. Burgess, M. Cicoli, D. Ciupke, S. Krippendorf and F. Quevedo, *UV Shadows in EFTs: Accidental Symmetries, Robustness and No-Scale Supergravity*, *Fortsch. Phys.* **68** (2020) 2000076 [2006.06694].

[158] H. Ooguri, E. Palti, G. Shiu and C. Vafa, *Distance and de Sitter Conjectures on the Swampland*, *Phys. Lett. B* **788** (2019) 180 [1810.05506].

[159] J. Calderón-Infante, I. Ruiz and I. Valenzuela, *Asymptotic Accelerated Expansion in String Theory and the Swampland*, 2209.11821.

[160] S.K. Garg and C. Krishnan, *Bounds on Slow Roll and the de Sitter Swampland*, *JHEP* **11** (2019) 075 [1807.05193].

[161] A. Castellano, A. Font, A. Herraez and L.E. Ibáñez, *A gravitino distance conjecture*, *JHEP* **08** (2021) 092 [2104.10181].

[162] G. Dvali and M. Redi, *Black Hole Bound on the Number of Species and Quantum Gravity at LHC*, *Phys. Rev. D* **77** (2008) 045027 [0710.4344].

[163] G. Dvali and C. Gomez, *Species and Strings*, 1004.3744.

[164] G. Dvali, C. Gomez and D. Lust, *Black Hole Quantum Mechanics in the Presence of Species*, *Fortsch. Phys.* **61** (2013) 768 [1206.2365].

[165] A. Hebecker and T. Wrase, *The Asymptotic dS Swampland Conjecture - a Simplified Derivation and a Potential Loophole*, *Fortsch. Phys.* **67** (2019) 1800097 [1810.08182].

[166] R. Blumenhagen, A. Font, M. Fuchs, D. Herschmann and E. Plauschinn, *Towards Axionic Starobinsky-like Inflation in String Theory*, *Phys. Lett. B* **746** (2015) 217 [1503.01607].

[167] R. Blumenhagen, *Large Field Inflation/Quintessence and the Refined Swampland Distance Conjecture*, *PoS* **CORFU2017** (2018) 175 [1804.10504].

[168] T. Bjorkmo and M.C.D. Marsh, *Hyperinflation generalised: from its attractor mechanism to its tension with the 'swampland conditions'*, *JHEP* **04** (2019) 172 [1901.08603].

[169] V. Aragam, S. Paban and R. Rosati, *Multi-field Inflation in High-Slope Potentials*, *JCAP* **04** (2020) 022 [1905.07495].

[170] V. Aragam, S. Paban and R. Rosati, *The Multi-Field, Rapid-Turn Inflationary Solution*, *JHEP* **03** (2021) 009 [2010.15933].

[171] S. Bhattacharya and I. Zavala, *Sharp turns in axion monodromy: primordial black holes and gravitational waves*, *JCAP* **04** (2023) 065 [2205.06065].

[172] G. Tasinato, *A large $|\eta|$ approach to single field inflation*, 2305.11568.